RADIOLOGY AND ONCOLOGY

vol.58 no.4
december 2024

RADIOLOGY AND ONCOLOGY

December 2024
Vol. 58 No. 4
Pages 459-587
ISSN 1318-2099
UDC 616-006
CODEN: RONCEM
eISSN: 1581-3207

Publisher
Association of Radiology and Oncology

Aims and Scope
Radiology and Oncology (ISSN 1318-2099) is a multidisciplinary journal devoted to the publishing original and high-quality scientific papers and review articles, pertinent to oncologic imaging, interventional radiology, nuclear medicine, radiotherapy, clinical and experimental oncology, radiobiology, medical physics, and radiation protection. Papers on more general aspects of interest to the radiologists and oncologists are also published (no case reports).

Editorial office

Radiology and Oncology
Zaloška cesta 2
P. O. Box 2217
SI-1000 Ljubljana
Slovenia
Phone: +386 1 5879 369
Phone/Fax: +386 1 5879 434
E-mail: gsersa@onko-i.si

Reader for English
Vida Kološa

Secretary
Mira Klemenčič, Zvezdana Vukmirović, Vijoleta Kaluža, Uroš Kuhar

Design
Monika Fink-Serša, Samo Rovan, Ivana Ljubanović

Layout
Matjaž Lužar

Printed by
Tiskarna Ozimek, Slovenia

Published quarterly in 300 copies

Beneficiary name: DRUŠTVO RADIOLOGIJE IN ONKOLOGIJE
Zaloška cesta 2
1000 Ljubljana
Slovenia

Beneficiary bank account number: SI56 02010-0090006751
IBAN: SI56 0201 0009 0006 751
Our bank name: Nova Ljubljanska banka, d.d.,
Ljubljana, Trg republike 2,
1520 Ljubljana; Slovenia

SWIFT: LJBASI2X

Subscription fee for institutions EUR 100, individuals EUR 50

The publication of this journal is subsidized by the Slovenian Research Agency.

Indexed and abstracted by:

- *Baidu Scholar*
- *Case*
- *Chemical Abstracts Service (CAS) - CAplus*
- *Chemical Abstracts Service (CAS) - SciFinder*
- *CNKI Scholar (China National Knowledge Infrastructure)*
- *CNPIEC - cnpLINKer*
- *Dimensions*
- *DOAJ (Directory of Open Access Journals)*
- *EBSCO (relevant databases)*
- *EBSCO Discovery Service*
- *Embase*
- *Genamics JournalSeek*
- *Google Scholar*
- *Japan Science and Technology Agency (JST)*
- *J-Gate*
- *Journal Citation Reports/Science Edition*
- *JournalGuide*
- *JournalTOCs*
- *KESLI-NDSL (Korean National Discovery for Science Leaders)*
- *Medline*
- *Meta*
- *Microsoft Academic*
- *Naviga (Softweco)*
- *Primo Central (ExLibris)*
- *ProQuest (relevant databases)*
- *Publons*
- *PubMed*
- *PubMed Central*
- *PubsHub*
- *QOAM (Quality Open Access Market)*
- *ReadCube*
- *Reaxys*
- *SCImago (SJR)*
- *SCOPUS*
- *Sherpa/RoMEO*
- *Summon (Serials Solutions/ProQuest)*
- *TDNet*
- *Ulrich's Periodicals Directory/ulrichsweb*
- *WanFang Data*
- *Web of Science - Current Contents/Clinical Medicine*
- *Web of Science - Science Citation Index Expanded*
- *WorldCat (OCLC)*

This journal is printed on acid- free paper

On the web: ISSN 1581-3207
https://content.sciendo.com/raon
http://www.radioloncol.com

contents

clinical oncology

slovenian abstracts

review

Characteristics of exposure to radioactive iodine during a nuclear incident

Katja Zaletel[1,2], Anamarija Mihovec[2], Simona Gaberscek[1,2]

[1] Division of Nuclear Medicine, University Medical Centre Ljubljana, Ljubljana, Slovenia
[2] Faculty of Medicine, University of Ljubljana, Ljubljana, Slovenia

Radiol Oncol 2024; 58(4): 459-468.

Received 17 June 2024
Accepted 12 August 2024

Correspondence to: Assoc. Prof. Katja Zaletel, M.D., Ph.D., Division of Nuclear Medicine, University Medical Centre Ljubljana, Zaloška c 2, SI-1000 Ljubljana, Slovenia. E-mail: katja.zaletel@kclj.si

Disclosure: No potential conflicts of interest were disclosed.

Background. During a nuclear accident, numerous products of nuclear fission are released, including isotopes of radioactive iodine. Among them is iodine-131, with a half-life of 8.02 days, which emits β radiation. For decades, it has been effectively and safely used in medicine. However, in the event of a nuclear accident, uncontrolled exposure can have harmful biological effects. The main sources of internal contamination with iodine-131 are contaminated air, food and water. The most exposed organ is the thyroid gland, where radioactive iodine accumulates via the Na+/I- symporter (NIS). NIS does not distinguish between radioactive iodine isotopes and the stable isotope iodine-127, which is essential for the synthesis of thyroid hormones. Exposure to radioactive iodine during a nuclear accident is primarily associated with papillary thyroid cancer, whose incidence begins to increase a few years after exposure. Children and adolescents are at the highest risk, and the risk is particularly significant for individuals living in iodine-deficient areas.

Conclusions. Ensuring an adequate iodine supply is therefore crucial for lowering the risk of the harmful effects of exposure to radioactive iodine at the population level. Protecting the thyroid with potassium iodide tablets significantly reduces radiation exposure, as stable iodine prevents the entry of radioactive iodine into the thyroid. Such protection is effective only within a narrow time window - a few hours before and after the exposure and is recommended only for those under 40 years of age, as the risks of excessive iodine intake outweigh the potential benefits in older individuals.

Key words: thyroid; radioactive iodine; nuclear accident; thyroid cancer; potassium iodide

Introduction

Various sources of ionizing radiation play a crucial role in nuclear medicine, industry, the military, as well as in science and research. Nuclear power plants, significant sources of electrical energy, exploit the nuclear fission reaction of enriched uranium-235 or plutonium-239. Risks associated with radioactive contamination in the event of a nuclear reactor accident have been the subject of numerous public debates, especially in the last few decades following the catastrophic consequences of the accidents in Chernobyl in 1986 and Fukushima in 2011.[1,2]

The nuclear fission reaction was also characteristic of nuclear weapons used in the Second World War. A representative of the newer generation of nuclear weapons is the hydrogen bomb, which utilizes the process of nuclear fusion in combination with nuclear fission and can be up to 1000 times more powerful than a fission bomb.[3] In addition to the threat of nuclear warfare, nuclear terrorism poses one of the major threats to international security today. It involves the illegal and intention-

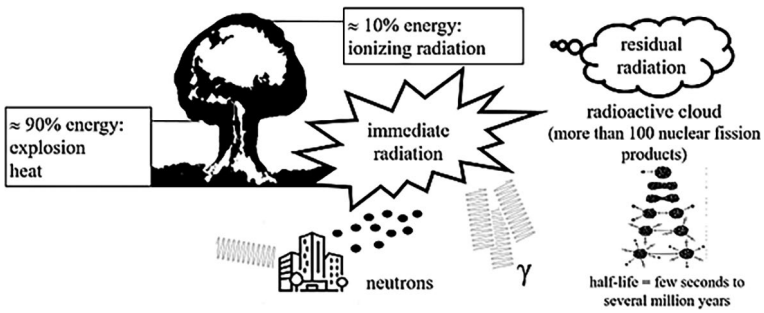

FIGURE 1. Sources of ionizing radiation during a nuclear accident.

al use of radioactive material to achieve various harmful objectives. This includes terrorist attacks on nuclear power plants and the use of nuclear weapons, as well as the use of "dirty bombs" that disperse radioactive substances into the environment without a nuclear explosion.[4]

According to the definition provided by the International Atomic Energy Agency, nuclear and radiation accidents involve exposure to radioactive radiation, resulting in significant consequences for individuals, the environment, or objects.[5] In contrast to radiation incidents, where exposure to radioactive radiation is not linked to nuclear fission, nuclear accidents are distinguished by their association with an explosion that involves nuclear fission. This can be observed in events such as a nuclear bomb detonation or a nuclear reactor incident.[4,6] Such accidents are characterized by a substantial release of energy, with approximately 90% being released in the form of explosion and heat, and about 10% being released in the form of ionizing radiation. Additionally, a variety of nuclear fission products are released, including isotopes of radioactive iodine (Figure 1).[7]

Sources of ionizing radiation in a nuclear incident

In a nuclear accident, energy in the form of ionizing radiation is predominantly released immediately within the first minute after the explosion. The risks associated with immediate radiation primarily relate to the harmful effects of gamma and neutron radiation, which have the highest penetration capability.[8,9] Neutron radiation, in addition to its direct effects on living organisms, destabilizes stable atoms of materials (such as iron and concrete) in objects surrounding the explosion, transforming them into new sources of ionizing radiation. Over an extended period following the explosion, residual radiation is emitted into the atmosphere in the form of a radioactive cloud, traveling several hundred kilometers from the accident site, and depositing radioactive substances gradually onto the Earth (Figure 1).[9]

In the immediate vicinity of the explosion site, larger radioactive particles settle locally, with the most intense settling occurring within the first 24 hours. Smaller particles reaching the troposphere continue to settle for several months after the accident, particularly in the broader vicinity of the nuclear explosion. The smallest particles, especially in powerful nuclear weapon explosions, can reach the stratosphere, settling on the entire surface of the Earth for several years after the explosion.[4,9]

During a nuclear accident, a broad spectrum of different radioactive fission products can be produced, with half-lives ranging from a few seconds to several million years.[7,10] Their total radioactivity is initially extremely high, but it decreases relatively rapidly due to radioactive decay.[11] Only those radioactive isotopes with appropriate physical properties (small particles reaching higher atmospheric layers, water-soluble particles, etc.) and a sufficiently long half-life can represent a long-term source of radiation exposure in the broader vicinity of a nuclear incident. Examples of such radioactive isotopes that are a source of harmful β radiation include cesium-137, strontium-90, and iodine-131.[12,13] Similar to the mentioned isotopes, xenon-133 is also a source of β radiation, easily entering the atmosphere due to its gaseous form. Although its physical half-life is approximately 5 days, its biological half-life is only 30 seconds. After entering the body, it is exhaled within a few minutes, thus having no significant harmful effects.[10]

Cesium-137, with a half-life of approximately 30 years, has a relatively low boiling point and is water-soluble. Consequently, it travels effectively in the air, spreading even after deposition from the atmosphere to the soil, causing radioactive contamination of land, water, and living organisms. Once absorbed into the body, it accumulates in tissues, constituting a source of prolonged exposure to radiation.[12] Strontium-90, with a half-life of 28 years, chemically resembles calcium. As a result, it accumulates in bones and teeth, representing a source of radiation exposure for the bone marrow.[14] Iodine-131 is water-soluble and emits both β radiation and, to a lesser extent, γ radiation. Compared to cesium-137 and strontium-90, it has a significantly shorter half-life, causing no long-term

environmental contamination. It accumulates in the thyroid gland, where it has harmful biological effects.[10,15]

Characteristics of iodine isotopes

There are 37 known isotopes of iodine, ranging from iodine-108 to iodine-144. The only stable isotope is iodine-127, which is essential for the synthesis of thyroid hormones and is commonly consumed in the form of iodized salt in everyday life. All other iodine isotopes exhibit radioactive decay with half-lives, mostly shorter than 60 days. Only iodine-129 has a long half-life of 1.57×10^7 years.[16]

In medicine, radioactive iodine has been used for several decades, particularly for diagnosing and treating thyroid diseases.[17] Various isotopes of iodine, including iodine-123, iodine-124, iodine-125, and iodine-131 play important roles today. Iodine-123 is a cyclotron-produced isotope with a half-life of 13.2 hours. It emits low-energy γ radiation with a long range, causing no tissue destruction. It is suitable for diagnostic purposes, as the γ radiation detected by a gamma camera provides valuable information about the uptake of iodine in the thyroid.[18] Similarly, iodine-124 is a cyclotron-produced isotope with a half-life of 4.18 days. Due to the emission of positrons during radioactive decay, it is suitable for imaging with positron emission tomography.[19] Iodine-125, obtained in nuclear reactors, has a long half-life of 59.4 days and emits low-energy γ radiation. It is used in brachytherapy[20] and serves as a tracer in radioimmunoassays for the laboratory determination of various analytes.[19]

Iodine-131, also obtained in nuclear reactors, has a half-life of 8.02 days. Upon decay, it emits high-energy β radiation of 0.61 MeV with a short tissue range of up to 0.8 mm.[19,21] Iodine-131 is the treatment of choice for patients with autonomous thyroid tissue and a second-line treatment for patients with Graves' disease. In both patient groups, the goal of treatment is to alleviate hyperthyroidism. Iodine-131 is an effective medication for ablating residual thyroid tissue after thyroid cancer surgery, and it can also be used to treat euthyroid nodular goiter with the goal of reducing thyroid volume.[21] The activity required for the successful treatment of thyroid diseases must be sufficiently high to expose the target tissue to the deterministic effects of iodine-131. Our study involving patients with Graves' disease, for example, indicates that iodine-131 treatment successfully eliminated hyperthyroidism in over 90% of patients with an average received dose of 144 Gy or 164 Gy, whereas in patients with an average received dose of 105 Gy, success was achieved in only 64% of patients.[22]

Iodine and the thyroid

Non-radioactive or stable iodine is a fundamental constituent element of thyroid hormones thyroxine (T_4) and triiodothyronine (T_3), which are essential for metabolism in all age groups and for the develpoment and brain maturation in foetuses and young children. According to World Health Organisation (WHO) recommendations, the daily iodine intake for adults should be around 150 μg, while pregnant and lactating women should aim for around 250 μg.[23]

A healthy adult body contains 15–20 mg of iodine, 70–80% of which is stored in the thyroid gland.[24] As reported, serum concentration of free iodide (I^-), however, is only 50 nM to 300 nM.[25] The thyroid cells have evolved an extremely efficient mechanism to accumulate iodine. The glycoprotein responsible for active iodine transport into the thyroid cell was identified in 1996 as Na^+/I^- symporter (NIS), localized in the basolateral membrane of thyroid epithelial cells, facing the bloodstream.[26,27] NIS facilitates Na^+/I^- symport with a 2:1 stoichiometry, driven by the Na^+ electrochemical gradient established by the basolateral Na^+/K^+ ATPase. As a result, I^- is actively concentrated in the thyroid cells. NIS cannot differentiate between stable and radioactive iodine, making it a powerful tool for diagnostics and treatment with radioiodine, as it rapidly concentrates in the thyroid.[27] Upon entering the thyroid cell, I^- passes transcellularly to reach the apical membrane. Here, it undergoes oxidation catalysed by the enzyme thyroid peroxidase (TPO) in the presence of H_2O_2, followed by iodination of tyrosine residues on thyroglobulin (Tg) and synthesis of thyroid hormones.[28]

The regulation of NIS is primarily influenced by thyroid stimulating hormone (TSH), a pituitary hormone. TSH, a key regulator of thyroid function and size, stimulates thyroid gland by promoting NIS transcription, upregulating the expression of TPO and Tg, as well as facilitating Tg endocytosis. Moreover, TSH also regulates NIS localization and is necessary for targeting NIS to the plasma membrane, as well as its retention there.[29]

In addition to TSH, iodine content in the thyroid cell itself regulates the I^- uptake. If iodine content

is low, the expression of NIS is increased and vice versa. A mechanism, known as autoregulation, enables the normal synthesis of thyroid hormones irrespective of iodine supply.[30] Exposure to high concentrations of I^- inhibits thyroid hormone synthesis and secretion, likely by supressing H_2O_2 production and reducing the expression of TPO and Tg. This phenomenon was named the Wolff-Chaikoff effect.[30,31] However, despite ongoing excess of I^-, its inhibitory effect diminishes after approximately 48 hours, allowing for the restoration of thyroid hormone synthesis. This escape from the Wolff-Chaikoff effect is enabled by an intrinsic autoregulatory mechanism, wherein NIS is downregulated by high intracelluar I^- leading to the intracellular iodine concentration below critical inhibitory threshold.[31] This downregulation occurs through several mechanisms, including inhibition of NIS transcription and increased degradation of NIS mRNA and NIS protein as well as translocation of NIS molecules from the basolateral membrane into the thyroid cell.[27,30]

Radioactive iodine contamination in a nuclear accident

During a nuclear accident, the by-products of nuclear fission released into the environment include various isotopes of radioactive iodine. Notably, iodine-131, with its relatively long half-life and high energy, poses the most significant biological risks.[32] Released in the form of a radioactive cloud, radioactive iodine contaminates air, water, soil, vegetation, and surfaces, thereby constituting a source of external contamination. Inhalation of contaminated air and ingestion of tainted food and water result in internal contamination of both humans and animals.[33] For infants of exposed mothers, breastfeeding is also a risk factor for iodine-131 ingestion, since NIS expression in breast occurs during lactation enabling I^- secretion into the milk as the sole source of this nutrient for the newborn.[27] During internal contamination, the thyroid is the most exposed organ, as approximately 10–30% of the incorporated amount accumulates in it within 24 hours, facilitated by the action of NIS. Most of the remaining radioactive iodine is excreted from the body with urine.[34]

Experiences from Chernobyl reveal that contaminated cow's milk was the primary source of iodine-131 internal contamination for residents, while the contaminated air affected exposed workers at the power plant. Factors such as age, place of residence, and milk consumption habits during the first 8 weeks after the accident had the greatest impact on the doses received by residents.[35] They estimate that residents in exposed areas of Belarus and Ukraine received an average thyroid dose of about 0.65 Gy, with the maximum dose reaching 42 Gy. Workers at the power plant exposed to radioactive iodine received an average dose of 0.18 Gy. In the most affected region of Belarus, children received an average dose of 0.75 Gy, with a maximum estimated dose of 8.7 Gy.[36] According to the largest study on in utero exposure to iodine-131 from Chernobyl fallout in selected regions of Ukraine, the mean estimated fetal thyroid dose was 0.072 Gy, with a range of 0–3.23 Gy.[37] Higher thyroid doses in children and adolescents compared to adults are attributed to factors such as a higher iodine uptake, smaller thyroid glands, and greater milk consumption.[38] A 5-year-old child at the time of the accident received a thyroid dose approximately four times larger than that of an adult.[39]

In Fukushima, only approximately 10% of radioactivity compared to Chernobyl was released.[40] Early public notification prevented the majority of residents from ingesting contaminated water and food, making inhalation of iodine-131 the primary route of internal contamination.[41] According to one of the earliest reports, the median thyroid dose was estimated at 0.0042 Gy for exposed children and 0.0035 Gy for adults.[42] A recent assessment of children who were 1 year old at the time of the accident in the most affected areas around the Fukushima power plant showed that their thyroid glands were exposed to an average dose of 0.015 Gy, with the maximum received dose being 0.029 Gy.[43] These values appear to be lower than earlier estimates, where average thyroid doses at 1 year ranged from 0.033 to 0.083 Gy.[44] Among workers 0.7% exceeded thyroid dose of 0.1 Gy, while the majority received less than 0.1 Gy.[45] Unlike the Chernobyl accident, where residents' thyroids were primarily exposed to iodine-131, in Fukushima, internal contamination with iodine-131 contributed to thyroid dose in 40–50%, with other short-lived isotopes of radioactive iodine (iodine-132, iodine-133, iodine-135) contributing 5–20%, and external irradiation due to radionuclides in the radioactive cloud and on surfaces in 40–50%.[41]

Among atomic bomb survivors from Hiroshima and Nagasaki exposed as children under 10 years, the mean thyroid radiation dose was 0.182 Gy, ranging from 0–4 Gy[46], whereas the mean mater-

nal uterine radiation dose was 0.256 Gy.[47] After atmospheric nuclear weapons tests conducted in the second half of the last century in Arizona, Kazakhstan, China and French Polynesia, the mean estimated thyroid doses were up to 4 Gy due to radioactive fallout and external thyroid irradiation, whereas they were several times higher during experiments on the Marshall Islands.[44]

Harmful effects of radioactive iodine in nuclear accident

The harmful effects of I-131 in a nuclear accident are primarily stochastic in nature, meaning they are random, with their likelihood proportional to the received dose, while the level of harm is not dependent on the dose size.[43] They are usually associated with a higher incidence of papillary thyroid cancer and benign thyroid nodules, as well as a higher prevalence of autoimmune thyroid diseases.[33,44] Low doses are typically classified as those under 0.1 Gy, while moderate doses fall within the range of 0.1 to 1 Gy.[47] Exposure to high I-131 doses results in deterministic effects, where the frequency and severity increase with the dose after a threshold dose is reached, potentially resulting in hypothyroidism.[48] Unlike the effects of uncontrolled exposure to I-131, in medicine we safely utilize its deterministic effects through the targeted, controlled use of higher activities of I-131 (Table 1).

The most vulnerable to the harmful effects of radioactive iodine are the thyroids of children, especially those under 5 years of age.[10] Additionally, research has shown a significant inverse correlation between age at radiation exposure and thyroid cancer risk, with this correlation diminishing to statistical insignificance by age of 15.[49] The increased cancer risk is attributed to rapid tissue growth and smaller thyroid sizes, resulting in higher radiation doses.[37,45] Moreover, this elevated risk persists for at least four decades after exposure.[10,48,49] Even doses as low as 0.05–0.1 Gy have been linked to higher thyroid cancer risk in children, with a linear dose-response up to about 10–20 Gy, beyond which the risk stabilizes.[44,48,49] In individuals with radiation exposure in utero the risk of cancer is comparable to that of those exposed during childhood.[50] The ability of the fetal thyroid to take up iodine increases from the third month, reaching the maximum at around the sixth month of pregnancy. During this period, the fetal thyroid receives the highest dose in cases of iodine-131 exposure.[51] In early pregnancy, the fetal exposure originates from the iodine-131 activity in the mother's thyroid, peaking at one month of gestation and then gradually decreasing during gestation.[52]

TABLE 1. Differences in exposure to iodine-131 in medicine and during nuclear accident

Parameter	In medicine	In nuclear accident
Radioactivity	High	Low
Average received dose (Gy)	> 100	< 10
Effects	Deterministic	Stochastic
The source	Controlled production in a nuclear reactor	Uncontrolled release during a nuclear accident (nuclear reactor, nuclear bomb)
Form	Capsule Solution	Radioactive cloud
Body intake	Ingestion Intravenously	Ingestion Inhalation

Experiences from Chernobyl indicate that the incidence of thyroid cancer began to increase only 4–5 years after exposure. In the population under 18 years of age in 1986 residing in contaminated areas of Belarus, Ukraine and Russia, nearly 20,000 new cases of thyroid cancer were detected between 1991 and 2015.[35] In individuals younger than 15 years who received a thyroid dose of ≥ 0.3 Gy, the risk of thyroid cancer was 5 times higher than in individuals with a received dose < 0.3 Gy.[39] The Belarus data reveal distinctions in radiation-related pediatric thyroid cancers compared to radiation-nonrelated cases, including a higher incidence in boys, in children of the youngest age, a dominant follicular structural component, extrathyroidal tumor extension, and greater risk of distant metastases.[53,54] However, the 15-year overall survival rate in radiation-related cases is excellent, exceeding 95%, despite recurrences occurring in 28% of cases.[53] Childhood exposure of Belarus residents was also associated with benign thyroid nodules larger than 10 mm and the risk significantly increased with thyroid dose.[55] In a cohort of exposed Ukrainian subjects with an estimated mean prenatal thyroid dose of 0.073 Gy, a markedly increased risk of thyroid cancer and a strong, significant dose-response relationship for large (≥ 10 mm) benign thyroid nodules were found three decades after the Chernobyl nuclear accident.[56]

After the Fukushima accident, a 10-year follow-up of individuals exposed before the age of 18, using ultrasound screening, confirmed a 10-fold increase in the prevalence of thyroid cancer, pre-

dominantly the papillary variant.[57,58] Some believe that this observation might reflect overdiagnosis due to the use of highly sensitive ultrasound equipment during screening.[44,59] However, analysis of a substantial number of operated patients revealed cervical lymph node metastases in 79% and extrathyroidal spread in 46%.[58] Furthermore, a strong positive correlation was observed between the incidence rate of thyroid cancer among exposed children and thyroid dose, underscoring the necessity for close monitoring in high-risk individuals.[44,59]

During the follow-up of Japanese atomic bomb survivors, the increased thyroid cancer risk persisted for more than 50 years after childhood exposure, with about 36% of thyroid cancer cases being attributable to radiation exposure before age of 20.[60]

Hypothyroidism can be directly related to the deterministic effects of radiation, or it can be a result of autoimmunity induced by radiation exposure.[40] After the Chernobyl accident, hypothyroidism was observed in 4.8% of emergency workers and in 3–6.2% of children under 18 years of age at the time of the accident.[40,61,62] The risk of hypothyroidism increased with thyroid dose, decreased with increasing age at exposure and was similar for both genders.[62] In Fukushima, where thyroid doses were much lower, the association between thyroid dose and hypothyroidism was not confirmed.[40] More than six decades after the bombing, observations in atomic bomb survivors exposed as children, who had a mean thyroid radiation dose of 0.182 Gy, confirmed hypothyroidism in 7.8% and positive thyroid antibodies in 21.5%. None of these observations were associated with radiation dose.[45]

The impact of iodine deficiency on the effects of exposure to radioactive iodine

One of the key factors regulating the uptake of iodine by the thyroid is the iodine supply. Adequate iodine supply for populations is ensured through national iodine fortification programs, with the iodization of table salt being the easiest and most effective method.[23,63] Iodine deficiency is indeed associated with health complications, such as goitre and hypothyroidism. It leads to increased secretion of TSH, which stimulates the expression of NIS to maximize iodine uptake into thyrocytes.[64]

It was shown that after the improvement in iodine supply, thyroid uptake decreases.[65-68] In Poland, an approximately 40% decrease in 24-hour iodine uptake was observed in euthyroid patients following a 30% increase in salt iodization.[65] In Graves' patients a 40% decrease in radioiodine uptake was associated with a 74% increase in iodine intake.[66] Twice the urinary iodine excretion was associated with a 25% lower iodine intake.[67] Ten years after the 2.5-fold increase in mandatory salt iodization in Slovenia, the early and late thyroid uptake of iodine were significantly lower (37% and 32%, respectively) than before the increase.[68] Most likely, the decrease in early thyroid uptake reflects decreased expression and activity of NIS.[69] The mechanism for the decrease in late thyroid uptake could be increased intracellular iodine content, which decreases the incorporation of diagnostic radiopharmaceuticals into thyroid hormones.[68]

In accordance with thyroid uptake research findings, studies demonstrate that the improvement of iodine supply is also associated with a higher activity of iodine-131, needed for the successful treatment of thyroid diseases. In patients with Graves' disease, 40% higher iodine-131 activity was required to cure hyperthyroidism after a 74% increase in iodine intake.[66] In Slovenia, around 11% higher iodine-131 activity was needed to eliminate hyperthyroidism after the change from mild iodine deficiency to adequate iodine supply.[68]

Iodine deficiency is associated with an increased susceptibility of the thyroid gland to nuclear radiation and with an increased risk of developing radiation-related thyroid cancer.[32,33,64] Although data on iodine intake at the time of the Chernobyl catastrophe are not available, the region had historically been known as an area of iodine deficiency.[70] Additionally, research conducted in the affected territories during the first decade after the disaster also pointed to the problem of iodine deficiency, with some areas placed even in the category of severe iodine deficiency.[71] An epidemiological study in the Russian Federation confirmed that the risk of thyroid cancer was significantly associated with thyroid radiation dose and inversely associated with urinary excretion levels.[72] In severely iodine-deficient areas, the risk of radiation-related thyroid cancer was approximately 2–3 times higher than in areas with adequate iodine intake.[72,73] Ensuring an adequate supply of iodine is therefore an important measure to reduce the risk of exposure to the harmful effects of radioactive iodine at the population level.[64]

TABLE 2. Influential factors on the risk of harmful effects from iodine-131 in nuclear accidents

Parameter	Higher risk	Lower risk
Exposure	Late public notification Accompanying accident (earthquake, fire ...) Exposed workers	Early public notification Preventing contaminated food and water intake Indoor sheltering
Received dose (Gy)	> 0.05	< 0.05
Age	Children (especially < 5) Exposure in utero	Adults
Iodine intake before exposure	Deficient	Sufficient
Thyroid blocking (KI tablets)	No blocking Inappropriate timing	Appropriate timing (less than 24 hours before and up to 2 hours after exposure)
Pre-existent thyroid disease	Iodine deficiency disorders No pre-existent thyroid disease	After thyroidectomy Hormone replacement therapy for other reasons
Medical surveillance	No surveillance	Close surveillance in high-risk individuals

In the Fukushima nuclear disaster, long-term dietary habits with high iodine content, mostly from seaweeds, certainly contributed to a lower radiation burden on the thyroid glands of the exposed population.[33,74] Based on available data from dietary records, food surveys, urine iodine analysis, and seaweed iodine content, it was estimated in 2011 that the average iodine intake in Japan exceeded 1000 μg/day.[75] Additionally, a study of children performed over a 5-year period after the accident confirmed sufficient iodine intake, with urine iodine content being twice the limit recommended by the WHO.[74]

Thyroid blocking with potassium iodide administration

Timely administration of stable iodine is highly effective in reducing radiation exposure to the thyroid.[32] It saturates the thyroid, inhibiting NIS activity, and consequently blocking the uptake of radioactive iodine into the thyroid.[33] Inhibition of I^- uptake appears to occur within a few hours after exposure to I^- excess.[76] Early animal and *in vitro* studies demonstrated that after acute I^- exposure, NIS mRNA levels decreased within 6 hours, while NIS protein levels decreased only after 24 hours, indicating that the reduced NIS expression does not account for the initial I^- uptake inhibition.[31,69,76] Subsequent research demonstrated that acute excess of I^- leads to NIS inactivation at the plasma membrane, caused by reactive oxygen species generated in response to elevated I^- levels.[76] An excess of stable iodine also leads to the displacement of radioiodine at the carrier site on the basolateral membrane, inhibiting its entry into the cells.[77] In human investigations, it was found that single doses of sodium iodide exceeding 10 mg suppressed 24-hour thyroid radioiodine uptake to approximately 1%, while continued daily intake of 15 mg or more consistently yielded values below 2%.[78]

For thyroid protection in nuclear emergencies, the most commonly used form of stable iodine is potassium iodide (KI) tablets, where 130 mg of KI contains 100 mg of iodine.[32,79] The WHO recommends thyroid blocking when the estimated thyroid radiation dose exceeds 0.05 Gy. This protection is suitable for adults under 40, given the higher prevalence of thyroid diseases in older individuals, where the risks of excessive iodine intake outweigh the potential benefits. WHO advises a single administration of 130 mg of KI for adults, adolescents, as well as pregnant and breastfeeding women. For children aged 3–12 years, the recommended dose is 65 mg, for children aged 1 month to 3 years it is 32 mg, and for infants under 1 month old it is 16 mg.[79] Iodine is quickly and almost entirely absorbed in the stomach and duodenum.[24] KI tablets offer protection for approximately 24 hours. If exposure persists beyond this timeframe, repeated administrations for up to 7 consecutive days may be required for certain groups, excluding neonates, pregnant or breastfeeding women.[79,80]

KI tablets offer effective protection only within a narrow time window less than 24 hours before and up to 2 hours after exposure.[32,79] They are 99% effective when administered at the time of exposure, at least 85% effective within 24 hours before or 2 hours after, but ineffective 96 hours before and only 50% effective 3–4 hours after.[32] However, administration later than 24 hours following exposure can even be harmful, as it can lead to the trap-

ping of radioactive iodine in the thyroid, thereby prolonging its biological half-life and increasing its harmful effects.[79] Due to the narrow time window, pre-distribution of KI tablets in exposed areas, such as the vicinity of nuclear reactors, is important.[34]

During the Chernobyl accident, administering KI to 95% of Polish children and 23% of the total population was estimated to reduce their projected thyroid dose by approximately 40%.[34,81] In Belarus and Russian children under 15 years of age, administering lower doses of KI primarily to prevent goiter reduced the risk of radiation-related cancer by 3-fold.[73] However, Japan did not implement KI prophylaxis for the general public after Fukushima accident, acknowledging its unpreparedness for such measures.[32]

Thyroid blocking with KI may be associated with adverse events. Based on observations from Poland, mild reactions, such as skin rash, vomiting, or abdominal discomfort were experienced in less than 4% of children and less than 3% of adults.[32,33] In neonates, the concern can be iodine-induced hypothyroidism, which can occur even with iodine administration exceeding twice the recommended amount.[81] In adults, however, excess iodine exposure can induce thyroid dysfunction in patients with thyroid autoimmune diseases or goiter.[34,82] Since these thyroid diseases are prevalent in the population and their incidence rises with age, the administration of KI tablets is associated with health risks, particularly after the age of 40.[34,83] Finally, it is important to note that patients who have had a thyroidectomy or are undergoing hormone replacement therapy for other reasons do not need protection with KI tablets.[34]

Conclusions

Given the threat of nuclear accidents, good preparedness is crucial for effectively managing critical events. One of the many products of nuclear fission is radioactive iodine, which, due to its properties, can contaminate the broader area surrounding the accident. Adverse effects from exposure to I-131 depend on several factors, including national-level emergency preparedness and response, the thyroid dose received, the age of the exposed person, iodine intake prior to exposure, the adequacy of KI tablet administration, and any pre-existing thyroid disorder (Table 2). Experience from past accidents indicates that children's thyroids are the most vulnerable. The risk of thyroid cancer starts to increase a few years after exposure and is related to the thyroid dose received, with higher risks observed even many years later. However, in older adults, the risk of adverse effects from I-131 is lower, yet the prevalence of thyroid diseases is high. Therefore, the use of KI tablets for thyroid blockade could pose health risks. The most effective measure to reduce the consequences of exposure to radioactive iodine at the population level is ensuring adequate iodine intake, which is achieved in several countries through the consumption of iodized salt.

References

1. Konoplev A. Fukushima and Chernobyl: similarities and differences of radiocesium behavior in the soil-water environment. *Toxics* 2022; **10:** 578. doi: 10.3390/toxics10100578
2. Barquinero JF, Chumak V, Ohba T, Della Monaca S, Nuccetelli C, Akahane K, et al. Lessons from past radiation accidents: critical review of methods addressed to individual dose assessment of potentially exposed people and integration with medical assessment. *Environ Int* 2021; **146:** 106175. doi: 10.1016/j.envint.2020.106175
3. Prăvălie R. Nuclear weapons tests and environmental consequences: a global perspective. *Ambio* 2014; **43:** 729-44. doi: 10.1007/s13280-014-0491-1
4. Gale RP, Armitage MD. Are we prepared for nuclear terrorism? *N Engl J Med* 2018; **378:** 1246-54. doi: 10.1056/NEJMc1805627
5. IAEA, AEN/NEA. *International Nuclear and Radiological Events Scale users' manual;* 2008 Edition. Vienna, Austria: International Atomic Energy Agency; 2008.
6. Bomanji JB, Novruzov F, Vinjamuri S. Radiation accidents and their management: emphasis on the role of nuclear medicine professionals. *Nucl Med Commun* 2014; **35:** 995-1002. doi: 10.1097/MNM.0000000000000156
7. Christodouleas JP, Forrest RD, Ainsley CG, Tochner Z, Hahn SM, Glatstein E. Short-term health risks of nuclear-power-plant accidents. *N Engl J Med* 2011; **364:** 2334-41. doi: 10.1056/NEJMra1103676
8. Foster CRM. Emergency preparedness: losing radiation incidents and medical management. *BMJ Mil Health* 2020; **166:** 21-8. doi: 10.1136/jramc-2018-000958
9. Buddemeier BR, Dillon MB. *Key response planning factors for the aftermath of a nuclear terrorism*. LLNL-TR-410067; 2009.
10. Dewyi SA, Bales K, Asano E, Veinot K, Eckerman K, Hart S, et al. Estimation of external contamination and exposure rates due to Fission product release. *Health Phys* 2022; **119:** 163-75. doi: 10.1097/HP.0000000000001168
11. Długosz-Lisiecka M. Public health decision making in the case of the use of a nuclear weapon. *Int J Environ Res Public Health* 2022; **6:** 19:12766. doi: 10.3390/ijerph191912766
12. Taniguchi K, Onda Y, Smith HG, Blake W, Yoshimura K, Yamashiki Y, et al. Transport and redistribution of radiocesium in Fukushima fallout through rivers. *Environ Sci Technol* 2019; **53:** 12339-47. doi: 10.1021/acs.est.9b02890
13. Ishikawa T. Radiation doses and associated risk from the Fukushima nuclear accident: a review of recent publications. *Asia Pac J Public Health* 2017; **29(2 Suppl):** 18S-28S. doi: 10.1177/1010539516675703
14. Drozdovitch V, Kukhta T, Trofimik S, Melo DR, Viarenich K, Podgaiskaya M, et al. Doses from external irradiation and ingestion of ^{134}Cs, ^{137}Cs and ^{90}Sr of the population of Belarus accumulated over 35 years after the Chernobyl accident. *Radiat Environ Biophys* 2022; **61:** 445-64. doi: 10.1007/s00411-022-00979-1
15. Drozdovitch V. Radiation exposure to the thyroid after Chernobyl accident. *Front Endocrinol* 2021; **11:** 569041. doi: 10.3389/fendo.2020.569041

16. Lin CC, Chao JH. Radiochemistry of iodine: relevance to health and disease. In: Preedy VR, Burrow GN, Watson R, editors. *Comprehensive handbook of iodine: nutritional, biochemical, pathological and therapeutic aspects*. Academic Press; 2009, p. 171-82. doi: 10.1016/B978-0-12-374135-6.00017-0

17. Fahey FH. Celebrating eighty years of radionuclide therapy and the work of Saul Hertz. *J APPL Clin Med Phys* 2021; **22:** 4-10. doi: 10.1002/acm2.13175

18. Kim PD, Tran HD. *I-123 uptake*. In: *StatPearls* [Internet]. Treasure Island (FL): StatPearls Publishing; 2023. [cited 2024 May 15]. Available at: https://www.ncbi.nlm.nih.gov/books/NBK559314/

19. Kumar K, Ghosh A. Radiochemistry, production processes, labeling methods, and immunoPET imaging pharmaceuticals of iodine-124. *Molecules* 2021; **26:** 414. doi: 10.3390/molecules26020414

20. Wei S, Li C, Li M, Xiong Y, Jiang Y, Sun H, et al. Radioactive Iodine-125 in tumor therapy: advances and future directions. *Front Oncol* 2021; **11:** 717180. doi: 10.3389/fonc.2021.717180

21. Bonnema SJ, Hegedüs L. Radioiodine therapy in benign thyroid diseases: effects, side effects, and factors affecting therapeutic outcome. *Endocr Rev* 2012; **33:** 920-80. doi: 10.1210/er.2012-1030

22. Pirnat E, Zaletel K, Gaberšček S, Hojker S. The outcome of 131I treatment in Graves' patients pretreated or not with methimazole. *Hell J Nucl Med* 2011; **14:** 25-9. PMID: 21512661

23. WHO. *Assessment of iodine deficiency disorders and monitoring their elimination: a guide for programme managers*. 3rd edition. Geneva: World Health Organization; 2007.

24. Zimmermann MB. Iodine deficiency. *Endocr Rev 2009;* **30:** 376-408. doi: 10.1210/er.2009-0011

25. Carrasco N. Iodide transport in the thyroid gland. *Biochim Biophys Acta* 1993; **1154:** 65-82. doi: 10.1016/0304-4157(93)90017-i

26. Dai G, Levy O, Carrasco N. Cloning and characterization of the thyroid iodide transporter. *Nature* 1996; **379:** 458-60. doi: 10.1038/379458a0

27. Portulano C, Paroder-Belenitsky M, Carrasco N. The Na^+/I^- symporter (NIS): mechanism and medical impact. *Endocr Rev* 2014; **35:** 106-49. doi: 10.1210/er.2012-1036

28. Ravera S, Reyna-Neyra A, Ferrandino G, Amzel LM, Carrasco N. The sodium/iodide symporter (NIS): molecular physiology and preclinical and clinical applications. *Annu Rev Physiol* 2017; **79:** 261-89. doi: 10.1146/annurev-physiol-022516-034125

29. Riedel C, Levy O, Carrasco N. Post-transcriptional regulation of the sodium/iodide symporter by thyrotropin. *J Biol Chem* 2001; **276:** 21458-63. doi: 10.1074/jbc.M100561200

30. Jing L, Zhang Q. Intrathyroidal feedforward and feedback network regulating thyroid hormone synthesis and secretion. *Front Endocrinol* 2022; **13:** 992883. doi: 10.3389/fendo.2022.992883

31. Eng PHK, Cardona GR, Fang AL, Previti M, Alex S, Carrasco N, et al. Escape from the acute Wolff-Chaikoff effect is associated with a decrease in thyroid sodium/iodide symporter messenger ribonucleic acid and protein. *Endocrinology* 1999; **140:** 3404-10. doi: 10.1210/endo.140.8.6893

32. Braverman ER, Blum K, Loeffke B, Baker R, Kreuk F, Yang SP, et al. Managing terrorism or accidental nuclear errors, preparing for iodine-131 emergencies: a comprehensive review. *Int J Environ Res Public Health* 2014; **11:** 4158-200. doi: 10.3390/ijerph110404158

33. Calcaterra V, Mameli C, Rossi V, Massini G, Gambino M, Baldassarre, et al. The iodine rush: over- or under-iodination risk in the prophylactic use of iodine for thyroid blocking in the event of a nuclear disaster. *Front Endocrinol* 2022; **13:** 901620. doi: 10.3389/fendo.2022.901620

34. Yoshida S, Ojino M, Ozaki T, Hatanaka T, Nomura K, Ishii M, et al. Guidelines for iodine prophylaxis as a protective measure: information for physicians. *Japan Med Assoc* J 2014; **57:** 113-23. PMID: 25784824

35. Sharifi A, Dinparastisaleh R, Kumar N, Mirsaeidi M. Health effects of radioactive contaminated dust in the aftermath of potential nuclear accident in Ukraine. *Front Public Health* 2022; **10:** 959668. doi: 10.3389/fpubh.2022.959668

36. Drozdovitch V. Radiation exposure to the thyroid after Chernobyl accident. *Front Endocrinol* 2021; **11:** 569041. doi: 10.3389/fendo.2020.569041

37. Hatch M, Brenner A, Bogdanova T, Derevyanko A, Kuptsova N, Likhtarev I, et al. A screening study of thyroid cancer and other thyroid diseases among individuals exposed in utero to iodine-131 from Chernobyl fallout. *J Clin Endocrinol Metab* 2009; **94:** 899-906. doi: 10.1210/jc.2008-2049

38. Lewis EB. Thyroid radiation doses from fallout. *Proc Natl Acad Sci USA* 1959; **45:** 894-7. doi: 10.1073/pnas.45.6.894

39. Ron E. Thyroid cancer incidence among people living in areas contaminated by radiation from the Chernobyl accident. *Health Phys* 2007; **92:** 502-11. doi: 10.1097/01

40. Reiners C, Drozd C, Yamashita S. Hypothyroidism after radiation exposure: brief narrative review. *J Neural Transm* 2020; **127:** 1455-66. doi: 10.1007/s00702-020-02260-5

41. Shinkarev SM. Comparison of thyroid doses to the public from radioiodine following the Chernobyl and Fukushima accidents. *Ann ICRP* 2021; **50(Suppl 1):** 174-80. doi: 10.1177/01466453211006816

42. Tokonami S, Hosoda M, Akiba S, Sorimachi A, Kashiwakura I, Balonov M. Thyroid doses for evacuees from the Fukushima nuclear accident. *Sci Rep* 2012; **2:** 507. doi: 10.1038/srep00507

43. Suzuki G, Ishikawa T, Ohba T, Hasegawa A, Nagai H, Miyatake H, et al. Estimation of children's thyroid equivalent doses in 16 municipalities after the Fukushima Daiichi nuclear power station accident. *J Radiat Res* 2022; **63:** 796804. doi: 10.1093/jrr/rrac058

44. Saenko V, Mitsutake N. Radiation-related cancer. *Endocr Rev* 2024; **45:** 1-29. doi: 10.1210/endrev/bnad022

45. Tatsuzaki H, Kishimoto R, Kurihara O, Tominaga T, Yamashita S. No evidence of thyroid consequences in seven nuclear workers at the Tokyo Electric Power Company Fukushima Daiichi Nuclear Power Plant accident: 10-year follow-up results of thyroid status. *J Radiat Res* 2023; **64:** 294-9. doi: 10.1093/jrr/rrac092

46. Imaizumi M, Ohishi W, Nakashima E, Sera N, Neriishi K, Yamada M, et al. Thyroid dysfunction and autoimmune thyroid diseases among atomic bomb survivors exposed in childhood. *J Clin Endocrinol Metab* 2017; **102:** 2516-24. doi: 10.1210/jc.2017-00102

47. Imaizumi M, Ashizawa K, Neriishi K, Akahoshi M, Nakashima E, Usa T, et al. Thyroid diseases in atomic bomb survivors exposed in utero. *J Clin Endocrinol Metab* 2008; **93:** 1641-8. doi: 10.1210/jc.2008-0042

48. Sinnot B, Ron E, Schneider AB. Exposing the thyroid to radiation: a review of its current extent, risks, and implications. *Endocr Rev* 2010; **31:** 756-73. doi: 10.1210/er.2010-0003

49. Ron E, Lubin JH, Shore RE, Mabuchi K, Modan B, Pottern LM, et al. Thyroid cancer after exposure to external radiation: a pooled analysis of seven studies. *Radiat Res* 1995; **141:** 259-77. PMID: 7871153

50. Ozasa K. Epidemiological research on radiation-induced cancer in atomic bomb survivors. *J Radiat Res* 2016; **57(Suppl 1):** i112-17. doi: 10.1093/jrr/rrw005

51. Evans TC, Kretzschmar RM, Hodges RE, Song CW. Radioiodine uptake studies of the human fetal thyroid. *J Nucl Med* 1967; **8:** 157-65. PMID: 6024129

52. Stabin MG, Watson EE, Marcus CS, Salk RD. Radiation dosimetry for the adult female and fetus from iodine-131 administration in hyperthyroidism. *J Nucl Med* 1991; **32:** 808-13. PMID: 2022987

53. Fridman M, Savva N, Krasko O, Mankovskaya S, Branovan DI, Schmid KW, et al. Initial presentation and late results of treatment of post-Chernobyl papillary thyroid carcinoma in children and adolescents of Belarus. *J Clin Endocrinol Metab* 2014; **99:** 2932-41. doi: 10.1210/jc.2013-3131

54. Drozd V, Saenko V, Branovan DI, Brown K, Yamashita S, Reiners C. A search for causes of rising incidence of differentiated thyroid cancer in children and adolescents after Chernobyl and Fukushima: comparison of the clinical features and their relevance for treatment and prognosis. *Int J Environ Res Public Health* 2021; **18:** 3444. doi: 10.3390/ijerph18073444

55. Cahoon EK, Nadyrov EA, Polyanskaya ON, Yauseyenka VV, Veyalkin IV, Yeudachkova TI, et al. Risk of thyroid nodules in residents of Belarus exposed to Chernobyl fallout as children and adolescents. *J Clin Endocrinol Metab* 2017; **102:** 2207-17. doi: 10.1210/jc.2016-3842: 10.1210/jc.2016-3842

56. Hatch M, Brenner A, Cahoon EK, Drozdovitch V, Little MP, Bogdanova T, et al. Thyroid cancer and benign nodules after exposure *in utero* to fallout from Chernobyl. *J Clin Endocrinol Metab* 2019; **104:** 41-8. doi: 10.1210/jc.2018-00847

57. Shimura H, Suzuki S, Yokoya S, Iwadate M, Suzuki S, Matsuzuka T, et al. A comprehensive review of the progress and evaluation of the thyroid ultrasound examination program, the Fukushima health management survey. *J Epidemiol* 2022; **32(Suppl XII):** S23-S35. doi: 10.2188/jea.JE20210271

58. Iwadate M, Mitsutake N, Matsuse M, Fukushima T, Suzuki S, Matsumoto Y, et al. The clinicopathological results of thyroid cancer with BRAFV600E mutation in the young population of Fukushima. *J Clin Endocrinol Metab* 2020; **105:** dgaa573. doi: 10.1210/clinem/dgaa573

59. Kato T, Yamada K, Hongyo T. Area dose-response and radiation origin of childhood thyroid cancer in Fukushima based on thyroid dose in UNSCEAR 2020/2021: high ^{131}I exposure comparable to Chernobyl. *Cancers 2023*; **15:** 4583. doi: 10.3390/cancers15184583

60. Furukawa K, Preston D, Funamoto S, Yonehara S, Ito M, Tokuoka S. Long-term trend of thyroid cancer risk among Japanese atomic-bomb survivors: 60 years after exposure. *Int J Cancer* 2013; **132:** 1222-26. doi: 10.1002/ijc.27749

61. Ostroumova E, Brenner A, Oliynyk V, McConnell R, Robbins J, Terekhova G, et al. Subclinical hypothyroidism after radioiodine exposure: Ukrainian-American cohort study of thyroid cancer and other thyroid diseases after the Chornobyl accident (1998–2000). *Environ Health Perspect* 2009; **117:** 745-50. doi: 10.1289/ehp.080018

62. Ostroumova E, Rozhko A, Hatch M, Furukawa K, Polyanskaya O, McConnell RJ, et al. Measures of thyroid function among Belarusian children and adolescents exposed to iodine-131 from the accident at the Chernobyl nuclear plant. *Environ Health Perspect* 2013; **121:** 865-71. doi: 10.1289/ehp.12057 83

63. Ittermann T, Albrecht D, Arohonka P, Bilek R, de Castro JJ, Dahl L, et al. Standardized map of iodine status in Europe. *Thyroid* 2020; **30:** 1346-54. doi: 10.1089/thy.2019.0353

64. Zimmermann MB, Boelaert K. Iodine-deficiency disorders and thyroid disorders. *Lancet* 2015; **3:** 286-95. doi: 10.1016/S2213-8587(14)70225-6

65. Huszno B, Hubalewska-Hoła A, Bałdys-Waligórska A, Sowa-Staszczak A, Szybiński Z. The impact of iodine prophylaxis on thyroid 131-iodine uptake in the region of Krakow, Poland. *J Endocrinol Invest* 2003; **26(Suppl 2):** 7-10. PMID: 12762633

66. Bączyk M, Junik R, Ziemnicka K, Sowiński J. Iodine prophylaxis intensification. Influence on radioiodine uptake and activity of 131I in the treatment of hyperthyroid patients with Graves' disease. *Nuklearmedizin* 2005; **44:** 197-9. PMID: 16395495

67. Meller B, Hasse A, Seyfarth M, Wenzel BE, Richter E, Baehre M. Reduced radioiodine uptake at increased iodine intake and I-131-induced release of "cold" iodine stored in thyroid. *Nuklearmedizin* 2005; **44:** 137-42. doi: 10.1267/nukl05040137

68. Gaberšček S, Bajuk V, Zaletel K, Pirnat E, Hojker S. Beneficial effects of adequate iodine supply of thyroid autonomy. *Clin Endocrinol* 2013; **79:** 867-3. doi: 10.1111/cen.12215

69. Eng PHK, Cardona GR, Previtti MC, Chin WW, Braverman LE. Regulation of the sodium iodide symporter by iodide in FRTL-5 cells. *Eur J Endocrinol* 2001; **144:** 139-44. doi: 10.1530/eje.0.1440139

70. Drozd VM, Saenko VA, Brenner AV, Drozdovitch V, Pashkevich VI, Kudelsky AV, et al. Major factors affecting incidence of childhood thyroid cancer in Belarus after the Chernobyl accident: do nitrates in drinking water play a role? *PLoS One* 2015; **10:** e0137226. doi: 10.1371/journal.pone.0137226

71. Gembicki M, Stozharov AN, Arinchin AN, Moschik KV, Petrenko S, Khmara IM, et al. Iodine deficiency in Belarusian children as a possible factor stimulating the irradiation of the thyroid gland during the Chernobyl catastrophe. *Environ Health Perspect* 1997; **105 (Suppl 6):** 1470-90. doi: 10.1289/ehp.97105s61487

72. Shakhtarin VV, Tsyb AF, Stepanenko VF, Orlov MY, Kopecky KJ, Davis S. Iodine deficiency, radiation dose, and the risk of thyroid cancer among children and adolescents in the Bryansk region of Russia following the Chernobyl power station accident. *Int J Epidemiol* 2003; **32:** 584-91. doi: 10.1093/ije/dyg205

73. Cardis E, Kesminiene A, Ivanov V, Malakhova I, Shibata Y, Khrouch V, et al. Risk of thyroid cancer after exposure to 131 I in childhood. *J Natl Cancer Inst* 2005; **97:** 724-32. doi: 10.1093/jnci/dji129

74. Tsubokura M, Nomura S, Watanobe H, Nishikawa Y, Sutuki C, Ichi S, et al. Assessment of nutritional status of iodine through urinary iodine screening among local children and adolescents after the Fukushima Daiichi nuclear power plant accident. *Thyroid* 2016; **26:** 1778-85. doi: 10.1089/thy.2016.0313

75. Zava TT, Zava DT. Assessment of Japanese iodine intake based on seaweed consumption in Japan: a literature-based analysis. *Thyroid Res* 2011; **4:** 14. doi: 10.1186/1756-6614-4-14

76. Arrigada AA, Albornoz E, Opazo MC, Bacerra A, Vidal G, Fardella C, et al. Excess iodide induces an acute inhibition of the sodium/iodide symporter in thyroid male rat cells by increasing reactive oxygen species. *Endocrinology* 2015; **156:** 1540-51. doi: 10.1210/en.2014-1371

77. Rump A, Eder S, Hermann C, Lamkowski A, Kinoshita M, Yamamoto T, et al. Modeling principles of protective thyroid blocking. *Int J Radiat Biol* 2022; **98:** 831-42. doi: 10.1080/09553002.2021.1987570

78. Sternthal E, Lipworth, L, Stanley B, Abreau C, Fang SL, Braverman LE. Suppression of thyroid radioiodine uptake by various doses of stable iodide. *N Engl J Med* 1980; **303:** 1083-88. doi: 10.1056/NEJM198011063031903

79. World Health Organization (WHO). *Iodine thyroid blocking: guidelines for use in planning and responding to radiological and nuclear emergencies*. Geneva: World Health Organization; 2017.

80. Martin JC, Pourcher T, Phan G, Guglielmi J, Crambes C, Caire-Maurisier F, et al. Review of the PRIODAC project on thyroid protection from radioactive iodine by repeated iodide intake in individuals aged 12+. *Eur Thyroid J* 2024; **13:** e230139. doi: 10.1530/ETJ-23-0139

81. Becker DV, Zanzonico P. Potassium iodide for thyroid blockade in a reactor accident: Administrative policies that govern its use. *Thyroid* 1997; **7:** 193-7. doi: 10.1089/thy.1997.7.193

82. Leung AM, Braverman LE. Consequences of excess iodine. *Nat Rev Endocrinol* 2014; **10:** 136-42. doi: 10.1038/nrendo.2013.251

83. Gaberšček S, Gaberšček B, Zaletel K. Incidence of thyroid disorders in the second decade of adequate iodine supply in Slovenia. *Wien Klin Wochenschr* 2021; **133:** 182-7. doi: 10.1007/s00508-020-01662-5

review

Current Operating Procedure (COP) for Bleomycin ElectroScleroTherapy (BEST) of low-flow vascular malformations

Tobian Muir[1], Walter A Wohlgemuth[2], Maja Cemazar[3,4], Giulia Bertino[5], Ales Groselj[6,7], Lakshmi A Ratnam[8,9], Ian McCafferty[10], Moritz Wildgruber[11,12], Bernhard Gebauer[13], Francesca de Terlizzi[14], Alessandro Zanasi[14], Gregor Sersa[3,15]

[1] South Tees NHS Foundation Trust, Middlesbrough TS4 3BW, United Kingdom
[2] Clinic and Policlinic of Radiology, Martin-Luther University Halle-Wittenberg, Halle (Saale), Germany
[3] Department of Experimental Oncology, Institute of Oncology Ljubljana, Ljubljana, Slovenia
[4] Faculty of Health Sciences, University of Primorska, Isola, Slovenia
[5] Department of Otolaryngology Head Neck Surgery, University of Pavia, Istituto di Ricovero e Cura a Carattere Scientifico (IRCCS) Policlinico San Matteo Foundation, Pavia, Italy
[6] Department of Otorhinolaryngology and Cervicofacial Surgery, University Medical Centre Ljubljana, Ljubljana, Slovenia
[7] Faculty of Medicine, University of Ljubljana, Ljubljana, Slovenia
[8] St George's University Hospitals NHS Foundation Trust, London, United Kingdom
[9] City St George's University of London, School of Health & Medical Sciences, London, United Kingdom
[10] Birmingham Women's and Children's Hospital NHS Foundation Trust, Birmingham, United Kingdom
[11] Department of Radiology, University Hospital, LMU Munich, München, Germany
[12] Interdisziplinäres Zentrum für Gefäßanomalien (IZGA), University Hospital, LMU Munich, München, Germany
[13] Diagnostic and Interventional Radiology, Charité Universitätsmedizin Berlin, Germany
[14] IGEA S.p.A., Clinical Biophysics Lab. Carpi, Modena, Italy
[15] Faculty of Health Sciences, University of Ljubljana, Ljubljana, Slovenia

Radiol Oncol 2024; 58(4): 469-479.

Received 23 September 2024
Accepted 17 October 2024

Correspondence to: Prof. Gregor Serša, Ph.D., Institute of Oncology Ljubljana, Department of Experimental Oncology, Zaloška 2, SI-1000 Ljubljana, Slovenia. E-mail: gsersa@onko-i.si

Dr. Tobian Muir and Prof. Walter A Wohlgemuth contributed equally to preparation of the manuscript and share first authorship.

Disclosure: AZ and FdT are IGEA employees. The other authors do not declare potential conflicts of interest.

Background. Bleomycin ElectroScleroTherapy (BEST) is a new approach in the treatment of vascular malformations. After bleomycin is administered to the malformation, electric pulses are applied to the target area to enhance the effectiveness of bleomycin. The mode of action is comparable to the effect of electrochemotherapy on tumour vasculature. For the wider and safer use of BEST in the clinical treatment of low-flow vascular malformations, this Current Operating Procedure (COP) is being prepared. It is a proposal for the clinical standardisation of BEST using the Cliniporator® as the electrical pulse generator with its associated electrodes. The electrical parameters considered in this protocol are those validated by the European Standard Operating Procedures for Electrochemotherapy (ESOPE) with the Cliniporator®.

Conclusions. General requirements are proposed, and, depending on the type of lesion, local skills and the availability of radiological equipment, two technical approaches of BEST are described based on ultrasound guided intervention or combined ultrasound and fluoroscopic guided intervention.

Key words: low-flow vascular malformations; bleomycin sclerotherapy, bleomycin electrosclerotherapy; BEST

Introduction

Reversible electroporation has several biomedical applications. By enhancing the delivery of drugs or nucleic acids to normal or tumour tissues, it can be used in oncology for tumour treatment, for vaccination or, as recently described, for Bleomycin ElectroScleroTherapy (BEST) of vascular malformations. There are several clinical reports published on the use of BEST in the treatment of low-flow and high-flow vascular malformations.[1-10] This approach has gained interest because bleomycin is already widely used in conventional sclerotherapy of vascular malformations and the application of electrical pulses potentiates its effectiveness.[11-15] Therefore, in BEST treatment, the dose of bleomycin and number of sessions needed could be reduced as compared to conventional bleomycin sclerotherapy, contributing to the safety of the treatment approach. Several case series have been published in adults and children in the last few years, showing that BEST could increase the efficacy of bleomycin and reduce the number of treatments required when treating vascular malformations.[2,4-6] Furthermore, the effectiveness is significant even in patients presenting with therapy-resistant venous malformations.[3] A recently published paper by Schmidt et al. has demonstrated the safety and effectiveness of BEST in a very large population of 233 children and adults, demonstrating greater efficacy in children.[7]

Why is BEST effective especially on abnormal vasculature? The principle of BEST can be related to the vascular disruption and vascular locking effects of electrochemotherapy. Electrochemotherapy is based on the application of electric pulses to tumours after intravenous or intratumoral bleomycin injection. A substantial portion of the antitumor effectiveness of electrochemotherapy is attributed to its vascular effects.[16] The application of electric pulses acts on the blood vessels, among other things inducing temporary vasoconstriction. This causes a temporary cessation of blood flow, the so-called **vascular lock effect**. This results in a prolonged retention of injected bleomycin in the region where the electric pulses have been applied, contributing to the effectiveness of electrochemotherapy and BEST. Another feature is the **vascular disrupting effect** due to the increased uptake of bleomycin in endothelial cells to the reversible electroporation. These cells die slowly by apoptosis due to bleomycin-induced G2M-arrest when proliferating. The applied electric pulses temporarily permeabilize the endothelial cell lining, which may further increase bleomycin uptake. The vascular disrupting effect was shown to be predominantly confined to abnormal vasculature in tumours, due to the higher proliferation rate of endothelial cells, compared to normal vasculature.[17-21] The same could be assumed for the atypical vasculature of low-flow vascular malformations, which are caused by mosaic mutations in the same cellular pathways as in tumour endothelial cells.[22] The clinical results of BEST are compelling[1], but its cellular and immunological mechanisms on the dysplastic vasculature need to be explored in further detail to support increased use of BEST in clinical practice and also to provide rationale for its refinement.

The group of clinicians within the InspECT consortium, in collaboration with other experts in the field of vascular malformations treatment, have prepared this document, a Current Operating Procedure (COP). It is a proposal for the clinical standardisation of BEST using the Cliniporator® as the electrical pulse generator with its associated electrodes. The electrical parameters considered in this protocol are those validated by the European Standard Operating Procedures for Electrochemotherapy (ESOPE) with the Cliniporator®.[23] After validation of these COP in the clinical application, a standard operating procedure would need to be prepared.

Current Operating Procedure (COP)

Requirements for performing a safe procedure

- Experience or training in the technique of image-guided sclerotherapy.
- Experience or training in the electroporation technique using a Cliniporator® pulse generator.
- Agreed local protocol for the safe administration, use and disposal of a cytotoxic chemotherapeutic agent (bleomycin).
- Agreed local protocol for respiratory monitoring of patients receiving BEST (may be different in children and adults).

Patient referral and suitability

- Patient referral by a vascular-malformation multidisciplinary team (MDT) or experienced centre.

Indications for BEST of vascular malformations

- Patients with a low-flow vascular malformation (venous, lymphatic, capillary, mixed type) suitable for BEST, i.e.: injection of bleomycin and safe placement of electrodes into the vascular malformation are technically feasible.
- Patients with a low-flow vascular malformation poorly responding or recurring after previous treatment(s).

Contraindications for BEST of vascular malformations

- Pregnancy and lactation.
- In adults, previous bleomycin exposure with a cumulative dose greater than 100 000 IU.
- In children, previous bleomycin exposure greater than 1300 IU/kg (taking into account the increasing weight of the child).
- In case of abnormal respiratory results/chest pathology (including previous severe or long COVID) in consultation with a pulmonologist, special care is required, and bleomycin exposure may be contraindicated.
- In patients with impaired renal function, the dose of bleomycin should be reduced at least by 1/3.
- Known allergy or hypersensitivity to bleomycin.
- Presence of significant central venous drainage precluding sclerotherapy.

Pre-treatment investigations

- **Respiratory surveillance**
  - Follow local procedure.

- **Recommendations for treatment of adults**
  - Agreed protocol for respiratory monitoring.
  - Pre-treatment pulmonary function test and diffusing capacity for carbon monoxide (DLCO) according to local protocol.
  - In the event of abnormal pre-treatment lung function test or DLCO, or known chest pathology (excluding controlled asthma), the patient should be assessed by a pulmonologist.
  - Post-treatment assessment and protocol if patient develops respiratory symptoms need to be established.

- **Recommendations for treatment of children**
  - Further caution is mandatory as in children lungs are still developing. Patients are suggested to be assessed by a paediatric pulmonologist or as per local protocol before BEST treatment. Preassessment for general anaesthesia or sedation.
  - Follow local procedure.

- **Pre-treatment imaging investigation**
  - Ultrasound imaging to determine characteristics, extent and flow status.
  - Magnetic Resonance Imaging (MRI) in most cases prior to interventional treatments to fully define and assess the low flow malformation (extent, deeper parts, drainage, differential diagnosis, multifocal lesion, etc.)
  - Magnetic Resonance Angiography (MRA)/ Magnetic Resonance Venography (MRV) may be added.
- If there are concerns about medical history or any abnormal/atypical findings on clinical examination or imaging: Perform an open biopsy or core ultrasound needle-guided biopsy for differential diagnosis.
- For large-volume venous malformations, assess coagulation profile (D-Dimer; fibrinogen) to exclude Localized / Disseminated Intravascular Coagulopathy (LIC/DIC); assess the need for preoperative Low Molecular Weight Heparin treatment (LMWH).

Patient information

- Discuss the BEST procedure and any possible alternatives.
- Clearly state that bleomycin for vascular malformations is an off-label use as it is in conventional sclerotherapy.
- Provide full information on all possible risks and benefits for the patient to consider (letter/ website).
- Discuss the possibility that bleomycin carries a potential risk of pulmonary toxicity.
- Provide information about possible effects of bleomycin on fertility and pregnancy.
- Discuss the potential risk of air embolism if bleomycin is foamed.
- Discuss risks of skin hyperpigmentation.
- Provide contact details in case the patient requires further information.
- Sign informed consent of the patient for the BEST procedure.

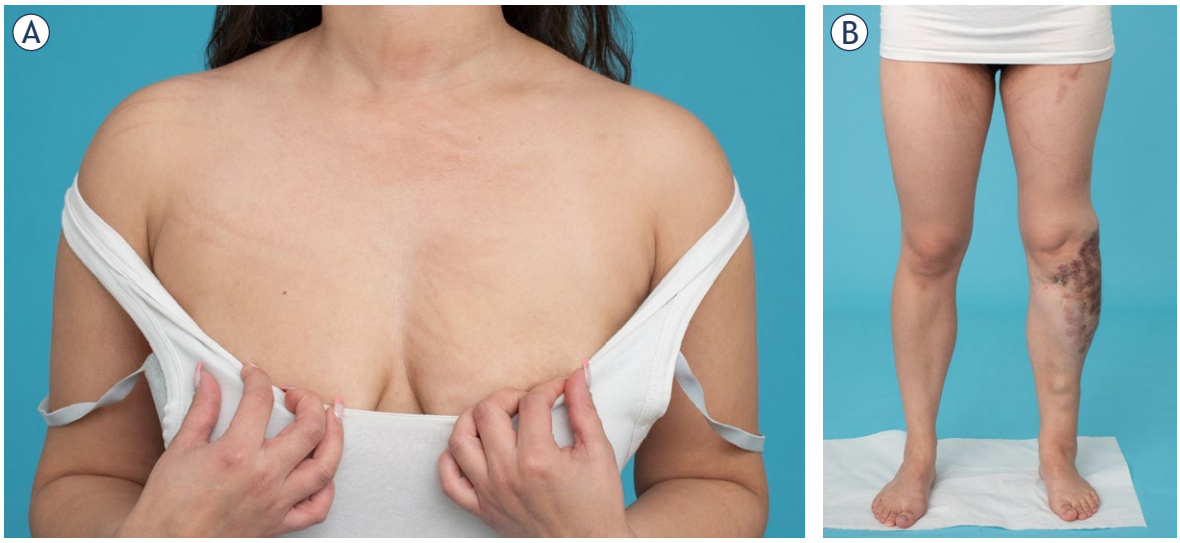

FIGURE 1. After Bleomycin ElectroScleroTherapy (BEST) flagellate dermatitis can occur on the sites of skin. **(A)** Scratching can cause permanent hyperpigmentation due to bleomycin. **(B)** Marks of the electrode insertion are visible at the site of the treatment.

Anaesthesia (follow local procedure)

- Most cases are performed under general anaesthesia due to the painful electric pulse sensation.
- Selected cases may be performed under sedation or local anaesthesia/block.
- Put ECG stickers on the sole of the foot and in axillae. ECG stickers have been associated with hyperpigmentation (Figure 1).
- Other skin fixations or their removal from the skin, such as eye taping, tube fixation or blood pressure cuff etc., may be associated with hyperpigmentation but are not contraindicated. Care should be taken to limit the amount of skin taping if possible. Endotracheal tubes can be tied, Blood Pressure (BP) cuffs should be placed over cotton wool. Removal should be undertaken with great care to avoid skin trauma (and thus hyperpigmentation). This can be facilitated by using a silicone-based spray to reduce the stickiness of the tape or plasters.
- ECG synchronisation system should be used when treating the left chest wall or close to the heart.
- After bleomycin administration keep FiO2 less than 30% if possible or as per local anaesthetic protocol. However, if there is any concern at any stage, oxygen should be administered as high as required but as low as needed.
- May consider ultrasound-guided analgesia injection of e.g. levobupivacaine or block, being aware of possible systemic drainage to reduce post-treatment pain.

Route of bleomycin injection

- Direct percutaneous injection into the low-flow vascular malformation under ultrasound or other imaging guidance.
- In rare cases with multiple or extensive lesions, intravenous infusion can be considered. This requires a careful risk-benefit assessment in this scenario of treating a benign disease with a cancer drug.

Preparations for the operative procedure

- Informed consent signed by the patient.
- Treatment area and laterality clearly marked (using US and marking the lesion on the skin).
- Pre-treatment urine pregnancy test in fertile female patients.
- WHO surgical safety checklist.
- Relevant imaging available in the theatre.

BEST procedure

- Anaesthesia – as suggested.
- Bleomycin preparation and injection.
  - *Bleomycin has confusing unit nomenclature* and care should be taken to ensure predictable dosing. Historically, bleomycin dosage

TABLE 1. Recommended preparation and dosing of intralesional injection (neat or foamed) of bleomycin for Bleomycin ElectroScleroTherapy (BEST)

	Concentration	Preparation for injection	Maximal dose per session	Cumulative dose in all sessions
Bleomycin and contrast	1 000 IU/ml in NaCl solution	1 part of solution in 3 parts of Contrast Medium (250 IU/ml)	10 000 IU in adults 200 IU/kg in children Divide the total dose into anticipated number of sessions The interval between sessions should be at least 8 weeks	100 000 IU in adults 1 300 IU/kg in children -divided by number of sessions
Foamed bleomycin	1 000 IU/ml in NaCl solution	1 ml albumin; 1 ml plain 1% lidocaine; 8 000 IU bleomycin; contrast agent may be added; orthogonal 3 way tap connection; 5 ml air- or according to local practice	As above	As above

is described in terms of mg potency, where 1 mg-potency corresponds to 1 Unit or 1 000 International Units. Because 1 mg potency is not always equivalent to 1 mg weight, the International Unit measure is preferred.[24]

- Take care: 1 mg potency translates nowadays to 0.56 - 0.66 mg weight of bleomycin sulphate, depending on local pharmacy preparation.
- *The suggested concentration of bleomycin for injection is 1 000 IU/ml.* Bleomycin prepared as a solution at a concentration of 1 000 IU/ml dissolved in 0.9% NaCl. Bleomycin and other drugs should be clearly marked and distinguished on the operative tray.
  - For injection of the prepared bleomycin, dilute 1 part of this bleomycin solution with 3 parts of contrast medium (CM) providing a solution with a bleomycin concentration of 250 IU/ml for intralesional injection. When ultrasound guided injection only is performed, contrast is not needed. Bleomycin can be injected neat or foamed.
  - Bleomycin may be used foamed depending on local practice, e.g.: 1 ml albumin; 1 ml plain 1% lidocaine; 8 000 IU bleomycin; contrast agent may be added; orthogonal 3 way tap connection; 5 ml air- or according to local practice. It is also possible to dilute the mixture or bleomycin itself with normal saline to reduce the administered dose.
- *Assessment of the extent of the vascular malformation.*
  - Prior to bleomycin injection assess the anatomy and extent of the vascular malformation either with ultrasound or fluoroscopy.
  - In bigger low-flow malformations (more than 5 cm in largest diameter) prior to bleomycin application, ultrasound-guided access to the vascular malformation should be obtained by positioning needles in all of the intended area: contrast agent injection through the needles and fluoroscopy or ultrasound should be performed to document the needle position, to assess the extent of punctured areas, to assess possible major venous drainage, and to assess the required volume of diluted bleomycin solution per areas. The aim is to fill the whole intended volume to be treated.
  - If necessary, drainage can be limited by compression, tourniquet or intravascular occlusion techniques (Lesion Puig type 3 to 4).
- *Injected amount of bleomycin* depends on the size (longest diameter) of the malformation, drainage pattern, and dilution with contrast or other agents. Suggested doses for different longest diameters of malformations are:
  - Longest diameter below 1 cm - bleomycin dose up to 500 IU.
  - Longest diameter 1 - 3 cm – bleomycin dose between 500 – 1 000 IU.
  - Longest diameter 3 - 5 cm – bleomycin dose between 1 000 – 2 000 IU.
  - Longest diameter > 5 cm - bleomycin dose > 2 000 IU (maximum 5 000 – 10 000 IU).

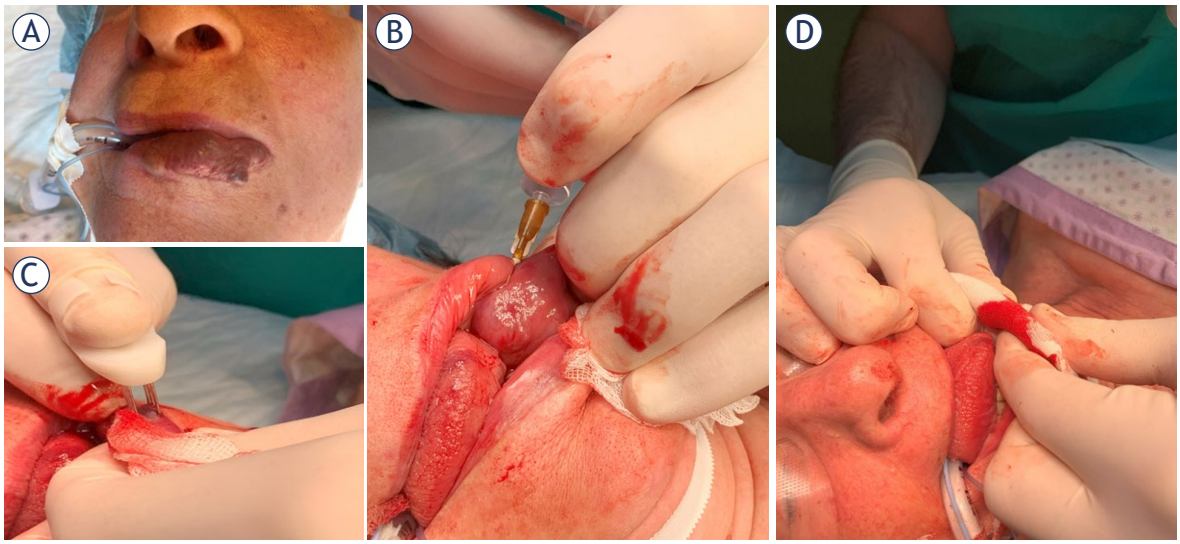

FIGURE 2. Procedure of Bleomycin ElectroScleroTherapy (BEST) in the treatment of low-flow vascular malformation on the lip. **(A)** Patient pre-treatment. **(B)** After the injection of bleomycin solution, the **(C)** electric pulses were applied on several areas with the finger electrode, avoiding overlap of the electric field. Procedure was completed in 10 minutes. The treated malformation was compressed **(D)** for several minutes to stop bleeding. Due to the vascular effects of BEST, the bleeding stopped spontaneously.

  - *Maximal doses:* The cumulative dose in all treatments (lifetime dose) should normally not exceed 100 000 IU in an adult. In children, a cumulative total dose more than 1300 IU/kg, should not be exceeded.
  - *Maximal dose of bleomycin per session* delivered locally should normally not exceed 10 000 IU in adults, in children 200 IU/kg body weight
- *Direct injection of bleomycin* into the malformation is verified by ultrasound, fluoroscopy or other imaging modalities. The bleomycin solution should be applied through the verified needle accesses in venous malformations and in macrocystic lymphatic malformations. Several needles or repeated injections could be used to ensure that the entire intended treatment area has been injected and filled. Interstitial or intravenous injection can be applied in microcystic lymphatic malformations.
- *Intravenous administration* of bleomycin only for very large and/or multiple lesions or when there are too many compartments, or generally when local application is not possible. Intravenous bleomycin is infused over 5 minutes with a dose of 200 IU bleomycin per kg body weight, not exceeding 15 000 IU in total.
- *Verification of the injection* either with ultrasound or fluoroscopy, possibly in 2 planes. If you see extravascular/interstitial contrast/bleomycin, you probably did not inject within the lesion and should repeat the treatment.
- Electroporation of the low-flow malformation as recommended below.

Electrode selection

- Electroporate the malformation, choosing the electrode according to the depth, extent and location of the malformation.
- Superficial cutaneous or subcutaneous malformations: Finger, linear or hexagonal electrodes.
- Deeper or larger surface area malformations: Single long needle electrodes (VGD) placed in a triangular geometry or other geometries with a maximum distance of 3 cm between them. The electric field should not exceed 1000 V per cm distance between the electrodes.

Electroporation method

- Start the electroporation as soon as possible after intralesional drug administration. After systemic drug administration start electroporation within 8 minutes.
- Apply electric pulses to the area to be treated. If the area is larger than the area covered by the electrode, reposition the electrode. Multiple intralesional applications are needed for large le-

sions. As opposed to oncological therapy, very strict coverage by electroporation of the malformation or safety margins around the malformation are not required. It is strongly recommended to avoid overlapping of the treated areas, because of possible side effects due to potential irreversible electroporation, like swelling, bleeding, necrosis or hyperpigmentation.
- In venous malformations, electroporation should start from the point of drainage of the lesion towards the inflow of blood, to prevent outflow of bleomycin. Needle for direct bleomycin injection should be removed before applying electric pulses. Macrocystic lymphatic malformations are first drained, and then treated. Microcystic lymphatic malformations are treated covering the entire lesion if possible.

Other considerations

- Careful consideration should be given to the possible risk of swelling after treatment, particularly in the head and neck area, airways, lips, eyelids, ears and genital areas. Significant swelling may occur with microcystic lymphatic malformations, particularly in the tongue.
- Patients must be advised to avoid skin trauma in the first 48 hours after the procedure (e.g. scratching, etc.) to avoid possible skin hyperpigmentation.

Post-operative

- After the procedure, hospitalization according to the local procedure.
- Tongue or airway involvement: admit with High Dependency Unit / Intensive Therapy Unit (HDU/ITU) support as needed. This might include a prophylactic (pre-procedure) tracheostomy, prolonged intubation or in extreme cases an emergency tracheostomy.
- LMWH at local protocol discretion.
- Post-operative compression therapy at the discretion of the local protocol.
- Pain after treatment might be more intense when using a hexagonal vs linear or finger electrode due to more pulses being delivered.
- Local cooling may alleviate post-operative pain and swelling depending on the extent of the procedure.
- In case of acute pneumonitis due to bleomycin, administer high-dose corticosteroids (30 mg/kg) as soon as possible after bleomycin injection and onset of lung toxicity.
- Consider periinterventional antibiotic treatment after 20 or more applications of electric pulses (loss of skin barrier to bacteria due to puncture related skin trauma).
- Pain management according to local procedure (As an example for adult patients):
  - Basic analgesia with oxycodone 10 mg or oxycodone 20 mg twice per day with 12 h interval.
  - You can add etoricoxib 90 mg (or paracetamol/metamizole) once after 12 h.
  - In case of persisting moderate to severe pain (numeric rating scale [NRS], 0 = no pain, 10 = unbearable pain) NRS ≥ 4 in spite of oxycodone, add oxygesic 5 mg per os for max. 4 times/day every 2-3 h.
  - In case of further persistent pain (NRS ≥ 4), despite 4 times added oxygesic/day, increase oxycodone dose for 10 mg, but you should not exceed 2 x 40 mg oxycodone/day).
  - In case of pain < NRS 4, do not add oxygesic. Continue oxycodone until second post-operative day, thereafter, reduce and stop.

Follow up

- 3-6 months unless a series of treatments are clearly going to be needed, then consider seeing earlier.

Treatment interval

- At least 8-12 weeks in-between treatments.

Discussion

The Current Operating Procedure (COP) for Bleomycin ElectroScleroTherapy (BEST), as outlined in this article, represents the first consensus-driven protocol for the treatment of low-flow vascular malformations. Multiple centers across Europe and the United Kingdom practice BEST, having acquired their skills either through treating tumours with electrochemotherapy—where standard operating procedures (SOPs) are already established—or by training under specialists in this field.[23] This article summarizes the collective experience in a concise list of steps recommended to maximize safety and clinical effectiveness based on current knowledge (Figure 3, 4) The COP was initially developed by a small group of authors and subsequently reviewed and refined by a broader community of co-authors, ensuring comprehensive

FIGURE 3. Example of Bleomycin ElectroScleroTherapy (BEST) treatment effectiveness on low-flow vascular malformation. After treatment, the treated area is oedematous, with a scab over the treated area after 3 weeks. The scab falls off in about 6 weeks with already visible treatment effectiveness. After 3 months, an excellent effect is visible after one treatment only.

consensus within the BEST community. As most BEST applications have so far focused on treating low-flow vascular malformations, this COP is specifically tailored to this type of malformation. We anticipate that future iterations of the COP will evolve into SOPs based on more extensive evidence, ultimately facilitating the wider use and acceptance of BEST for both low-flow and high-flow vascular malformations.

The current understanding of BEST's mechanism of action is derived from electrochemotherapy and its effects on the vascular system.[16] Studies in mice, pigs, and humans have shown that tumour vessels are more sensitive to electrochemotherapy than normal vessels, likely due to the higher proliferation rate of endothelial cells.[17,25,26] Bleomycin induces mitotic endothelial cell death, which may explain the differential effect observed between tumour and normal blood vessels.[27] This concept can be extended to vascular anomalies, where various mutations in molecular signalling pathways lead to a higher proliferation rate of endothelial cells.[28–32] Vascular malformations are influenced by several key molecular pathways. The PI3K/AKT/mTOR pathway is particularly significant, with mutations in PIK3CA commonly associated with venous and lymphatic malformations but can be also found in tumour endothelial cells. The RAS/MAPK pathway also plays a crucial role, with mutations in genes such as KRAS linked to various vascular anomalies.[33,34] Additionally, the TIE2/TEK pathway, involving mutations in the TEK gene, is also known to contribute to the development of venous malformations. Both mutated signalling pathways are also found in tumours.[33,35,36] Similarities in mutated genes between endothelial cells in tumour vessels and those in vascular malformations suggest a comparable phenotype and provide insights into the mechanisms of action of BEST in treating vascular malformations. Nevertheless, pathway activation in vascular malformations leads to localized, benign

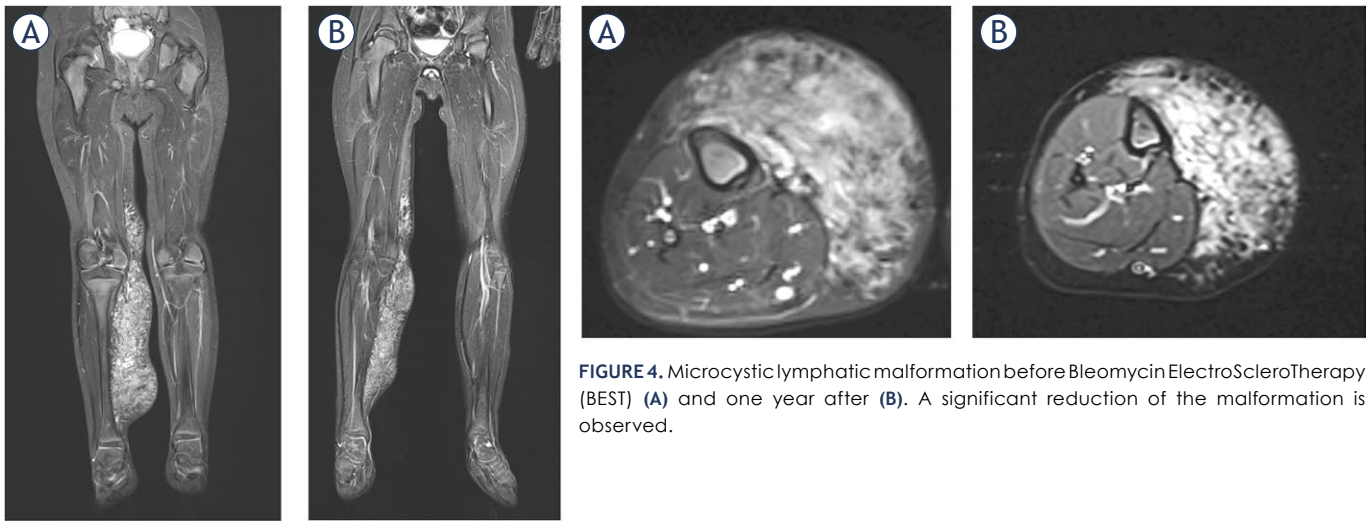

FIGURE 4. Microcystic lymphatic malformation before Bleomycin ElectroScleroTherapy (BEST) **(A)** and one year after **(B)**. A significant reduction of the malformation is observed.

overgrowths of blood vessels, without the invasive properties of cancer. In cancer, activations of these pathways are part of a broader oncogenic process that not only promotes angiogenesis, but also supports tumour growth, metastasis, and resistance to therapy. Thus, to support the broader application of BEST and the development of evidence-based SOPs, more basic research is needed. Establishing preclinical models of vascular malformations in vitro and in animal models would offer deeper insights into the mechanisms of action of BEST and its clinical response.

Currently, the BEST procedure is based on the experience of a few centres, leaving several critical questions unanswered. These include, among other things, determining the optimal bleomycin dosage and the optimal interval between drug injection and electric pulse application. Current experience suggests that the required bleomycin dose for BEST is much lower than for electrochemotherapy, but further research is needed to establish the minimum effective dose.[1] Additionally, the optimal number of applied electric pulses according to the area of vascular malformation and the coverage with the electric field to achieve a clinical response without over-treatment is still under investigation. Answering these questions requires preclinical models of vascular malformations and leveraging tools developed for electrochemotherapy, such as analytical methods for determining bleomycin concentration[37,38], numerical models for simulating electric field distribution[39], and modern radiological and molecular techniques for monitoring tissue and cellular changes.

When comparing BEST to other treatments for low-flow vascular malformations, several advantages and distinctive characteristics emerge. Surgical excision, while effective, often carries significant morbidity, including scarring and the risk of incomplete removal, leading to recurrence.[40] Conventional sclerotherapy involves injecting sclerosing agents to induce fibrosis and shrinkage of the malformation, but it can be less effective in larger or more complex lesions and may require multiple sessions.[11,13,41] Laser therapy is beneficial for superficial malformations but has limited efficacy in deeper or more extensive lesions and can cause skin discoloration or damage [42,43]. BEST, however, has so far demonstrated high effectiveness with fewer required sessions, leading to rapid and significant reduction in malformation size.[1]

As these questions are resolved, we will gain a clearer understanding of the fundamental principles of BEST. Subsequent steps will involve accumulating clinical data to assess the safety and effectiveness of BEST. This data will form the basis for developing SOPs, providing evidence-based guidelines enabling the safe and effective use of BEST to treat low-flow vascular malformations.

Acknowledgements

This research was funded by the Slovenian Research and Innovation Agency (ARIS) under the research program P3-0003.

Author contribution

Study concepts: GS, MC, FdT, TM, WW. Study design: GS, MC, FdT, AZ. Data acquisition: GS, MC, AZ. Manuscript preparation: GS, MC, TM, WW, FdT, AZ. Manuscript editing: GS, MC, TM, WW, FdT, AZ. Manuscript review: GB, AG, LR, IMC, MW, BG.

References

1. Muir T, Bertino G, Groselj A, Ratnam L, Kis E, Odili J, et al. Bleomycin Electrosclerotherapy (BEST) for the treatment of vascular malformations. An International Network for Sharing Practices on Electrochemotherapy (InspECT) study group report. *Radiol Oncol* 2023; **57:** 141-9. doi: 10.2478/raon-2023-0029
2. Horbach SER, Wolkerstorfer A, Jolink F, Bloemen PR, Van Der Horst CMAM. Electrosclerotherapy as a novel treatment option for hypertrophic capillary malformations: a randomized controlled pilot trial. *Dermatol Surg* 2020; **46:** 491-8. doi: 10.1097/DSS.0000000000002191
3. Wohlgemuth WA, Müller-Wille R, Meyer L, Wildgruber M, Guntau M, Heydt SVD, et al. Bleomycin electrosclerotherapy in therapy-resistant venous malformations of the body. *J Vasc Surg Venous Lymphat Disord* 2021; **9:** 731-9. doi: 10.1016/j.jvsv.2020.09.009
4. McMorrow L, Shaikh M, Kessell G, Muir T. Bleomycin electrosclerotherapy: new treatment to manage vascular malformations. *Br J Oral Maxillofac Surg* 2017; **55:** 977-9. doi: 10.1016/j.bjoms.2017.10.002
5. Kostusiak M, Murugan S, Muir T. Bleomycin electrosclerotherapy treatment in the management of vascular malformations. *Dermatol Surg* 2022; **48:** 67-71. doi: 10.1097/DSS.0000000000003220
6. Dalmády S, Csoma Z, Besenyi Z, Bottyán K, Oláh J, Kemény L, et al. New treatment option for capillary lymphangioma: bleomycin-based electrochemotherapy of an infant. *Pediatrics* 2020; **146:** e20200566. doi: 10.1542/peds.2020-0566
7. Schmidt VF, Cangir Ö, Meyer L, Goldann C, Hengst S, Brill R, et al. Outcome of bleomycin electrosclerotherapy of slow-flow malformations in adults and children. *Eur Radiol* 2024; **34:** 6425-34. doi: 10.1007/s00330-024-10723-6
8. Guntau M, Cucuruz B, Brill R, Bidakov O, Von Der Heydt S, Deistung A, et al. Individualized treatment of congenital vascular malformations of the tongue. *Clin Hemorheol Microcirc* 2023; **83:** 421-9. doi: 10.3233/CH-221683
9. Krt, A, Cemazar M, Lovric D, Sersa G, Jamsek C, Groselj A. Combining superselective catheterization and electrochemotherapy: a new technological approach to the treatment of high-flow head and neck vascular malformations. *Front Oncol* 2022; **12:** 1025270. doi: 10.3389/fonc.2022.1025270
10. Loeser JH, Kisser U, Dießel L, Von Der Heydt S, Bidakov O, Loberg C, et al. Interdisciplinary treatment of macroglossia due to a microcystic lymphatic malformation with bleomycin electrosclerotherapy followed by partial resection. *Cardiovasc Intervent Radiol* 2024; **47:** 852-4. doi: 10.1007/s00270-024-03693-1
11. Horbach SER, Rigter IM, Smitt JHS, Reekers JA, Spuls PI, Van Der Horst CMAM. Intralesional bleomycin injections for vascular malformations: a systematic review and meta-analysis. *Plast Reconstr Surg* 2016; **137:** 244-56. doi: 10.1097/PRS.0000000000001924
12. Horbach SER, Wolkerstorfer A, De Bruin DM, Van Der Horst CMAM. Electrosclerotherapy for capillary malformations: study protocol for a randomised within-patient controlled pilot trial. *BMJ Open* 2017; **7:** e016401. doi: 10.1136/bmjopen-2017-016401
13. Horbach SER, Lokhorst MM, Saeed P, De Goüyon Matignon De Pontouraude, CMF, Rothová A, Van Der Horst CMAM. Sclerotherapy for low-flow vascular malformations of the head and neck: a systematic review of sclerosing agents. *J Plast Reconstr Aesthet Surg* 2016; **69:** 295-304. doi: 10.1016/j.bjps.2015.10.045
14. Mir LM, Orlowski S, Belehradek J, Paoletti C. Electrochemotherapy potentiation of antitumour effect of bleomycin by local electric pulses. *Eur J Cancer Clin Oncol* 1991; **27:** 68-72. doi: 10.1016/0277-5379(91)90064-K
15. Orlowski S, Belehradek J, Paoletti C, Mir LM. Transient electropermeabilization of cells in culture. *Biochem Pharmacol* 1988; **37:** 4727-33. doi: 10.1016/0006-2952(88)90344-9
16. Jarm T, Cemazar M, Miklavcic D, Sersa G. Antivascular effects of electrochemotherapy: implications in treatment of bleeding metastases. *Expert Rev Anticancer Ther* 2010; **10:** 729-46, doi: 10.1586/era.10.43
17. Markelc B, Sersa G, Cemazar M. Differential mechanisms associated with vascular disrupting action of electrochemotherapy: intravital microscopy on the level of single normal and tumor blood vessels. *PLoS One* 2013; **8:** e59557. doi: 10.1371/journal.pone.0059557
18. Sersa G, Beravs K, Cemazar M, Miklavcic D, Demsar F. Contrast enhanced MRI assessment of tumor blood volume after application of electric pulses. *Electro Magnetobiol* 1998; **17:** 299-306. doi: 10.3109/15368379809022574
19. Sersa G, Cemazar M, Miklavcic D, Chaplin DJ. Tumor blood flow modifying effect of electrochemotherapy with bleomycin. *Anticancer Res* 1999; **19:** 4017-22. PMID: 10628347
20. Sersa G, Cemazar M, Parkins CS, Chaplin DJ. Tumour blood flow changes induced by application of electric pulses. *Eur J Cancer* 1999; **35:** 672-7. doi: 10.1016/S0959-8049(98)00426-2
21. Cemazar M, Parkins CS, Holder AL, Chaplin DJ, Tozer GM, Sersa G. Electroporation of human microvascular endothelial cells: evidence for an anti-vascular mechanism of electrochemotherapy. *Br J Cancer* 2001; **84:** 565-70. doi: 10.1054/bjoc.2000.1625
22. Al-Olabi L, Polubothu S, Dowsett K, Andrews KA, Stadnik P, Joseph AP, et al. Mosaic RAS/MAPK variants cause sporadic vascular malformations which respond to targeted therapy. *J Clin Invest* 2018; **128:** 1496-508. doi: 10.1172/JCI98589
23. Gehl J, Sersa G, Matthiessen LW, Muir T, Soden D, Occhini A, Quaglino P, et al. Updated standard operating procedures for electrochemotherapy of cutaneous tumours and skin metastases. *Acta Oncologica* 2018; **57:** 874-82. doi: 10.1080/0284186X.2018.1454602
24. Poole S. Bleomycin sulphate dosing nomenclature. *Aust J Hosp Pharm* 1998; **28:** 211-11. doi: 10.1002/jppr1998283211
25. Snoj M, Cemazar M, Srnovrsnik T, Kosir SP, Sersa G. Limb sparing treatment of bleeding melanoma recurrence by electrochemotherapy. *Tumori* 2009; **95:** 398-402. doi: 10.1177/030089160909500324
26. Lv Y, Feng Z, Chen S, Cheng X, Zhang J, Yao C. A fundamental theoretical study on the different effect of electroporation on tumor blood vessels and normal blood vessels. *Bioelectrochem* 2022; **144:** 108010. doi: 10.1016/j.bioelechem.2021.108010
27. Mir LM. Bases and rationale of the electrochemotherapy. *Eur J Cancer Suppl* 2006; **4:** 38-44. doi: 10.1016/j.ejcsup.2006.08.005
28. Kunimoto K, Yamamoto Y, Jinnin M. ISSVA classification of vascular anomalies and molecular biology. *Int J Mol Sci* 2022; **23:** 2358. doi: 10.3390/ijms23042358
29. Majesky MW. Vascular development. *Arterioscler Thromb Vasc Biol* 2018; **38:** e17-e24. doi: 10.1161/ATVBAHA.118.310223
30. Castel P, Carmona FJ, Grego-Bessa J, Berger MF, Viale A, Anderson, et al. Somatic *PIK3CA* mutations as a driver of sporadic venous malformations. *Sci Transl Med* 2016; **8:** 332ra42. doi: 10.1126/scitranslmed.aaf1164
31. Schonning MJ, Koh S, Sun RW, Richter GT, Edwards AK, Shawber CJ, et al. Venous malformation vessels are improperly specified and hyperproliferative. *PLoS One* 2021; **16:** e0252342. doi: 10.1371/journal.pone.0252342

32. Clapp A, Shawber CJ, Wu JK. Pathophysiology of slow-flow vascular malformations: current understanding and unanswered questions. *J Vasc Anom* 2023; **4:** e069, doi: 10.1097/JOVA.0000000000000069

33. Queisser A, Seront E, Boon LM, Vikkula M. Genetic basis and therapies for vascular anomalies. *Circ Res* 2021; **129:** 155-73. doi: 10.1161/CIRCRESAHA.121.318145

34. Zhang W, Chen G, Ren J, Zhao Y. Bleomycin induces endothelial mesenchymal transition through activation of m TOR pathway: a possible mechanism contributing to the sclerotherapy of venous malformations. *Br J Pharmacol* 2013; **170:** 1210-20. doi: 10.1111/bph.12355

35. Mansur A, Radovanovic I. The expansion of liquid biopsies to vascular care: an overview of existing principles, techniques and potential applications to vascular malformation diagnostics. *Front Genet* 2024; **15:** 1348096. doi: 10.3389/fgene.2024.1348096

36. Li D, Sheppard SE, March ME, Battig MR, Surrey LF, Srinivasan AS, et al. Genomic profiling informs diagnoses and treatment in vascular anomalies. *Nat Med* 2023; **29:** 1530-9. doi: 10.1038/s41591-023-02364-x

37. Kosjek T, Krajnc A, Gornik T, Zigon D, Groselj A, Sersa G, et al. Identification and quantification of bleomycin in serum and tumor tissue by liquid chromatography coupled to high resolution mass spectrometry. *Talanta* 2016; **160:** 164-71. doi: 10.1016/j.talanta.2016.06.062

38. Groselj A, Kranjc S, Bosnjak M, Krzan M, Kosjek T, Prevc A, et al. Vascularization of the tumours affects the pharmacokinetics of bleomycin and the effectiveness of electrochemotherapy. *Basic Clin Pharmacol Toxicol* 2018; **123:** 247-56. doi: 10.1111/bcpt.13012

39. Miklavcic D, Snoj M, Zupanic A, Kos B, Cemazar M, Kropivnik M, et al. Towards treatment planning and treatment of deep-seated solid tumors by electrochemotherapy. *BioMed Eng OnLine* 2010; **9:** 10. doi: 10.1186/1475-925X-9-10

40. Johnson AB, Richter GT. Surgical considerations in vascular malformations. *Tech Vasc Interv Radiol* 2019; **22:** 100635. doi: 10.1016/j.tvir.2019.100635

41. Heninger J, Cheon E, Green J, Hajduk J, Benzon H. Intralesional bleomycin injection and skin hyperpigmentation: a case series of a single-center experience with a standardized skin-protective protocol. *A A Pract* 2022; **16:** e01551. doi: 10.1213/XAA.0000000000001551

42. DeHart AN, Richter GT. Laser Treatment of vascular anomalies. *Dermatologic Clinics* 2022; **40:** 481-7. doi: 10.1016/j.det.2022.06.002

43. Mulligan PR, Prajapati HJS, Martin LG, Patel TH. Vascular anomalies: classification, imaging characteristics and implications for interventional radiology treatment approaches. *Br J Radiol* 2014; **87:** 20130392. doi: 10.1259/bjr.20130392

review

Posterior interosseous nerve lesion due to lipoma. Review of the literature and rare case presentation

Bojan Rojc[1,2], Peter Golob[1]

[1] General Hospital Izola, Izola, Slovenia
[2] Faculty of Mathematics, Natural Sciences and Information Technologies, University of Primorska, Koper, Slovenia

Radiol Oncol 2024; 58(4): 480-485.

Received 20 April 2024
Accepted 21 June 2024

Correspondence to: Assist. Prof. Bojan Rojc, M.D., General Hospital Izola, Slovenia. E-mail: bojan.rojc@sb-izola.si

Disclosure: No potential conflicts of interest were disclosed.

Background. Posterior interosseous nerve lesion is a rare mononeuropathy of the upper limb. Atraumatic posterior interosseous nerve lesions are commonly caused by lipomas of the forearm, manifesting as slow-progressing wrist and finger drop.

Patients and methods. In this review and case report study, we present a systematic review of the literature for patients presenting with posterior interosseous palsy due to lipomas and a rare case of patient with acute posterior interosseous nerve lesion caused by a lipoma. Our primary interest was in the timing of clinical presentation. For the review process, we followed the Preferred Reporting Items for Systematic Reviews and Meta-Analysis guidelines.

Results. After reviewing the literature, we identified thirty patients with posterior interosseous nerve lesions caused by lipomas. In 28 patients, the symptoms presented progressively, ranging from 1 month to a maximum of 240 months. We found only one case of a patient with acute presentation and another patient with acute worsening of chronic weakness due to trauma.

Conclusions. Atraumatic posterior interosseous nerve lesions are frequently secondary to forearm lipomas. In the majority of cases, the symptoms will develope progressively. However, in this study, we also report a rare case of a patient presenting with acute posterior interosseous nerve lesion due to a lipoma.

Key words: posterior interosseus nerve; lipoma; compression; acute

Introduction

Upper arm mononeuropathies are common pathologies, particularly entrapment neuropathies affecting median and ulnar nerves.[1] While radial nerve lesions are less frequent, but they still occur, often presenting as radial neuropathy at spiral groove due to extrinsic compression. In rare cases, a lesion of the radial nerve can occur at the forearm.[1]

At the lateral epicondyle level, the radial nerve bifurcates into two branches: the superficial radial sensory nerve and the deep radial motor branch. The motor branch enters the supinator muscle beneath the Arcade of Frohse, where it is known as the Posterior Interosseus Nerve (PIN). PIN is almost exclusively a motor nerve providing innervation to the extensor carpi ulnaris, extensor digitorum communis, extensor digiti quinti, abductor pollicis longus, extensor pollicis longus, extensor pollicis brevis, and extensor indicis proprius muscle.[2]

Nontraumatic PIN neuropathy at the elbow is a rare condition with an annual incidence of 0.003%.[1,3] However, some confusion and controversies exist regarding the nomenclature of nontraumatic PIN neuropathy in the elbow. Radial tunnel syndrome (RTS) is defined as a compressive neuropathy of the PIN, causing pain and tenderness

3–5 cm distal to the lateral epicondyle, without motor signs.[4,5] Despite the belief that RTS results from PIN compression, most cases do not show abnormalities on medical imaging or electrodiagnostic testing.[6] On the other hand, PIN lesion or PIN syndrome (PINS) presents most often with slow onset weakness of the muscles innervated by the PIN, without sensory findings.[2] PIN lesion can be further categorized in compressive and non-compressive (neuralgic amyotrophy, hourglass-like fascicular constriction).[7]

There are five potential sites of intrinsic compression of the PIN at the proximal forearm:

1. fibrous bands of tissue anterior to the radiocapitellar joint between the brachialis and brachioradialis muscle;
2. the recurrent radial vessels that fan out across the PIN ("leash of Henry");
3. the leading edge of the extensor carpi radialis brevis muscle;
4. arcade of Frohse;
5. and the distal edge of the supinator muscle.[1,7–9]

Occupations involving repetitive pronation and supination movements are considered to be a risk factor for PINS.[7] Extrinsic compression of the PIN can result from various pathologies, with as many as 30 different pathologies described.[7] Among these, lipoma is the most reported pathology causing extrinsic compression of PIN.[9–11]

Lipomas are slow-growing benign tumours composed of adipose cells encapsulated by a thin layer of fibrous tissue.[12] They can be classified based on their anatomical site into dermal, subcutaneous and sub-fascial lipomas, or tumours directly related to muscle, bone, synovium or nerve.[13] In the context of PINS, parosteal, intermuscular and intramuscular types of lipomas have been most often reported. Due to their slow growth, lipomas predominantly cause progressive PIN palsy.

Patients and methods

For the review process, we adhered to the Preferred Reporting Items for Systematic Reviews and Meta-Analysis (PRISMA) guidelines. The authors conducted searches on PubMed, MEDLINE and Google scholar using keywords: posterior interosseus nerve, palsy, and lipoma. Through this procedure, we identified 47 studies. Only full-text articles in English or translated versions were accepted for further screening. Our search encompassed studies published up to February 2024. Subsequently, we analysed these studies to identify those reporting patients with PINS due to lipoma. We included only studies where the manifestation of symptoms (whether progressive or acute) was clearly stated. Ultimately, we reviewed 24 studies, which collectively reported on 30 patients (Table 1).

Case

A 68-year-old female patient presented to the emergency room of our hospital with weakness of left wrist and fingers extension. In her past medical history, she reported having diabetes and arterial hypertension. The current symptoms had started 3 days prior to her visit. The patient mentioned strenuous work involving her arms due to cleaning, which included repetitive pronation and supination movements. A few hours after this activity she suddenly noticed weakness extending her fingers, without experiencing pain or paraesthesia. Clinical examination revealed weakness in left wrist extension accompanied by slight radial deviation (Muscle Power Scale - MRC 3) and more pronounced weakness in left fingers extension (MRC 2), the strength of other muscle groups of the left arm was preserved (MRC 5). There were no sensory deficits. To rule out possible brain vascular lesions brain computer tomography (CT) and CT angiography of cerebral arteries were performed, but the imaging did not show acute stroke or arterial narrowing. Based on these findings and patient's history a clinical diagnosis of left PIN palsy due to intrinsic entrapment caused by repetitive movements was made. Electromyography (EMG) performed a week after symptoms onset confirmed PIN lesion, showing denervation with fibrillations potentials and positive sharp waves (on scale 2 out of 3) and motor unit potential reduction in PIN innervated extensor indicis proprius muscle, brachioradial muscle did not show any signs of denervation. The superficial sensory radial nerve conduction study was normal. At the follow-up visit after 4 weeks, there was no improvement of muscle strength. Consequently, we decided to perform a magnetic resonance imaging (MRI) scan of the left elbow, which revealed a 50 x 40 x 25 mm lipoma as a probable cause of nerve compression (Figure 1). The patient included in this study provided written informed consent for the publication of anonymized data in accordance with the declaration of Helsinki.

Subsequently, after 2 months, surgery was performed on the left forearm to remove the lipoma.

TABLE 1. Twenty-four studies reported 30 patients with posterior interosseous palsy due to lipomas

Patient	Ref	Year	Age (years)	Sex	Onset	Duration (months)	Lipoma	Recovery
1	Vikas[14]	2020	54	F	Progressive	5	Parosteal	Complete
2	Allagui[15]	2014	28	F	Progressive	6	Intramuscular	Complete
3	Maldonado[16]	2017	78	M	Progressive	8	Parosteal	Incomplete
4	Maldonado[16]	2017	65	F	Progressive	30	Parosteal	Incomplete
5	Yamamoto[17]	2016	60	F	No symptoms	?	Intermuscular	Complete
6	Rishab[18]	2021	47	M	No symptoms	?	Intramuscular	Complete
7	Flores Robles[19]	2017	40	M	Progressive	1	?	Complete
8	Salama[20]	2010	83	F	Acute Trauma		Parosteal	Complete
9	Saaiq[21]	2017	53	M	Progressive	7	Parosteal	Complete
10	Patel[22]	2018	66	M	Progressive	4	Intraneural	Near Complete
11	Murphy[23]	2009	58	M	Progressive	<1	Intramuscular	Near Complete
12	Nishida[24]	1998	60	F	Progressive	2	Parosteal	Complete
13	Nishida[24]	1998	61	F	Progressive	?	Parosteal	Complete
14	Ganapathy[25]	2006	54	M	Progressive	144	Intramuscular	Near Complete
15	Colasanti[26]	2016	59	F	Progressive	6	Intermuscular	Complete
16	Avram[27]	2004	69	M	Progressive	4	Parosteal	Partial
17	Hamdi[28]	2010	59	M	Progressive	2	Parosteal	Complete
18	Matsuo[29]	2007	60	M	Progressive	240	Intraneural	Poor
19	Seki[30]	2012	67	F	Progressive	2	Parosteal	Complete
20	Eralp[31]	2006	45	M	Progressive	?	?	Complete
21	Fitzgerald[32]	2002	71	F	Progressive	1	?	No recovery
22	Fitzgerald[32]	2002	62	M	Progressive	2	?	Complete
23	Fitzgerald[32]	2002	64	M	Progressive	3	?	Complete
24	Fitzgerald[32]	2002	68	F	Progressive	5	?	Complete
25	Fitzgerald[32]	2002	63	F	Progressive	2	?	No recovery
26	Narayan[33]	2016	46	F	Progressive	6	Parosteal	?
27	El Hyaoui[34]	2014	68	F	Progressive	14	Parosteal	?
28	Borman[35]	2010	69	F	Progressive	6	Parosteal	Partial
29	Richmond[36]	1953	62	M	Progressive	3	Intramuscular	Near Complete
30	Bugnicourt[37]	2009	48	M	Acute		?	?

F = female; M = male; ? = no data

During the surgical procedure, the patient was placed in supine position arm resting on a side table. Our dissection began above the elbow, in the groove between brachialis/biceps muscles medially and brachioradialis muscle laterally, aiming to expose common radial nerve. We followed the nerve distally into the proximal forearm, where the brachioradialis muscle was retracted laterally, providing exposure to the tumorous mass. The tumour was situated between cutaneous branches on its lateral and anterior side and PIN on its medial and posterior side. Cutaneous branches were then dissected off the tumour and retracted laterally allowing for further dissection going from lateral to medial and anterior to posterior. This gave us exposure to the PIN lying below the tumour tethered to its pseudo-capsule at the point of PIN entry into the supinator muscle (Figure 2). We released the PIN and continued resection towards the neck of the radius, where the tumor reached into the depth and terminated. The tumour was removed en-bloc and sent to histopathological ex-

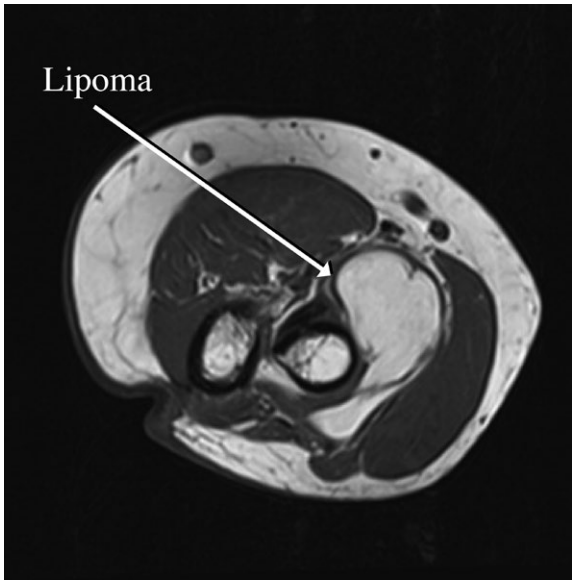

FIGURE 1. MRI of left elbow.

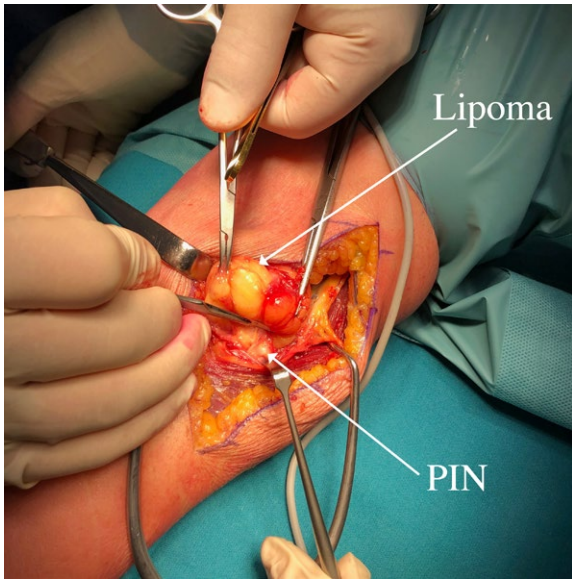

FIGURE 2. Lateral dissection along the common radial nerve and posterior interosseus nerve (PIN).

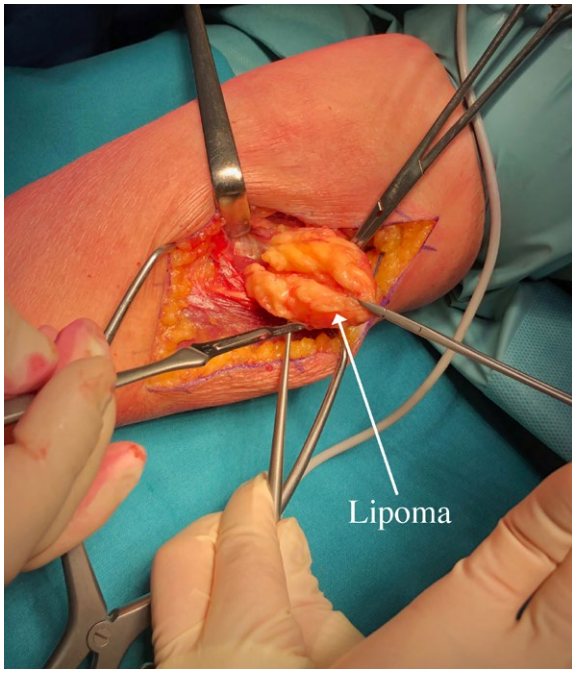

FIGURE 3. Medial dissection away from posterior interosseus nerve (PIN).

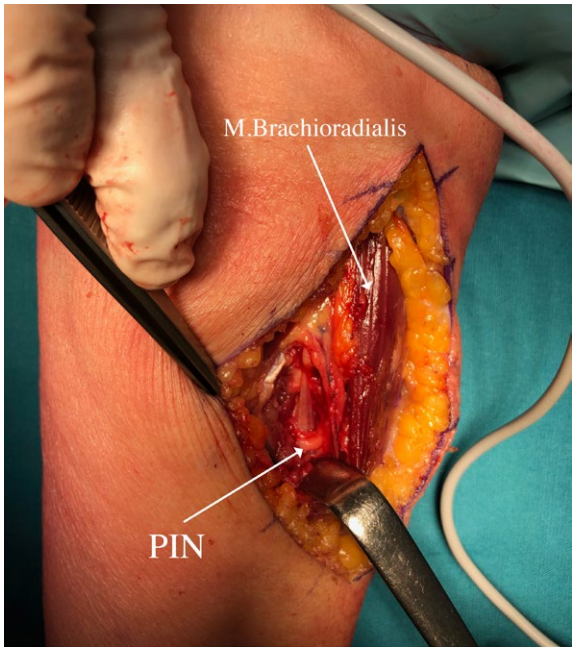

FIGURE 4. Local situation after lipoma removal

PIN = posterior interosseus nerve.

amination, which confirmed the diagnosis of lipoma (Figure 3 and 4).

At the follow-up visit after 11 months the patient demonstrated substantial clinical improvement. Remarkably after 24 months there was no weakness in left finger and wrist extension.

To our knowledge, this case represents a rare instance of acute nontraumatic PINS caused by a lipoma.

Results

We identified 30 patients with PIN palsy caused by lipoma compression. The median age of these patients was 59.6 years, ranging from 28 to 83 years. Among the 30 patients 28 experienced a progressive build-up of symptoms, which varied from less than a month to a maximum 240 months. Only one

patient was reported to have an acute manifestation of symptoms, while another patient had acute worsening of chronic weakness after trauma and immobilisation. Both female and male patients were equally represented, 15 females and 15 males. The most predominant type of lipoma observed was parosteal occurring in 13 patients. In most cases, the recovery was complete or near complete (Table 1).

Discussion

Entrapment neuropathies of upper arm are common conditions, primary manifesting as carpal tunnel or cubital tunnel syndrome.[3] In contrast, nontraumatic PIN palsy is a rare condition, with prevalence of only around 0.003 %.[1,3,38] Patients with PIN palsy present with motor symptoms due to weakness of PIN innervated muscles in the forearm.[1] Clinically, it can resemble the lesion of radial nerve at the spiral groove. Both conditions present with wrist and finger drop, sparing the elbow extension. However, two important differences set them apart. In a PIN lesion, the muscles innervated above the take-off of the PIN are spared, allowing these patients to weakly extend the wrist with radial deviation, and there are no sensory findings.

Atraumatic PIN lesions most commonly result from compressive pathology at the level of upper forearm.[2] There are 5 well-known sites at the elbow that can cause intrinsic compression - entrapment of the PIN, with repetitive pronation and supination movements being a well-established predisposing factor.[1,7] Conversely extrinsic compression of the PIN is most often due to lipoma.[9–11] In both cases a slow progressive build-up of symptoms is expected.[2]

Our patient presented with acute PIN lesion caused by a parosteal lipoma. She also reported repetitive pronation and supination movements in the preceding days. In the reviewed literature, we found only one case of acute PIN lesion caused by lipoma, mimicking stroke. In that case, the symptoms started suddenly, and no predisposing activities were reported.[37] Another case involved a 83-year-old woman who had a combination of chronic PIN lesion caused by a lipoma and an acute worsening after forearm immobilisation due to distal radius fracture.[20] We suggest that the acute presentation in our patient is most likely due to nerve traction caused by lipoma movement during repetitive arm pronation and supination. Based on EMG findings, showing denervation a week after symptoms onset, we can assume that there was some longstanding axonal nerve injury due to lipoma growth. We suppose that the acute manifestation of symptoms was caused by nerve demyelination block. This would also explain the good recovery. Unfortunately, we do not have motor conduction studies to prove this suggestion.

The recommended treatment for patients with PIN lesion due to lipoma is surgical excision.[1,7,39] Fortunately, most patients recover well and the symptom duration serves as a predictor for good recovery.[39] After surgery and removal of the lipoma, our patients showed complete restitution of function after 24 months.

PIN lesion due to lipoma is rarely encountered in clinical practice. The most common clinical scenario involves progressive weakness of wrist and finger extension, accompanied by a palpable mass at the proximal forearm. As presented in our review, the acute presentations are very rare. Nevertheless, it is advisable to perform imaging studies of elbow in all patients with PIN lesion, as a substantial proportion of cases are secondary to expansive masses surrounding the nerve. We propose as imaging method of choice nerve ultrasonography[8] or MR imaging. This recommendation holds true, especially considering the good prognosis associated with surgical removal.

References

1. Dang AC, Rodner CM. Unusual compression neuropathies of the forearm, Part I: Radial Nerve. *J Hand Surg* 2009; **34:** 1906-14. doi: 10.1016/j.jhsa.2009.10.016
2. Sigamoney KV, Rashid A, Ng CY. Management of atraumatic posterior interosseous nerve palsy. *J Hand Surg* 2017; **42:** 826-30. doi: 10.1016/j.jhsa.2017.07.026
3. Hohenberger GM, Schwarz AM, Grechenig P, Maier MJ, Schwarz U, Kuchling S, et al. Morphology of the posterior interosseous nerve with regard to entrapment syndrome. *Indian J Orthop* 2020; **54:** 188-92. doi:10.1007/s43465-020-00084-9
4. Levina Y, Dantuluri PK. Radial tunnel syndrome. *Curr Rev Musculoskelet Med* 2021; **14:** 205-13. doi: 10.1007/s12178-021-09703-w
5. Moradi A, Ebrahimzadeh MH, Jupiter JB. Radial tunnel syndrome, diagnostic and treatment dilemma. *Arch Bone Jt Surg* 2015; **3:**156-62. PMID: 26213698
6. Ang GG, Bolzonello DG, Johnstone BR. Radial tunnel syndrome: case report and comprehensive critical review of a compression neuropathy surrounded by controversy. *Hand (N Y)* 2023; **18:** 146S-53S. doi: 10.1177/15589447211029045
7. McGraw I. Isolated spontaneous posterior interosseous nerve palsy: a review of aetiology and management. *J Hand Surg Eur Vol* 2019; **44:** 310-6. doi: 10.1177/1753193418813788
8. Kim Y, Ha DH, Lee SM. Ultrasonographic findings of posterior interosseous nerve syndrome. *Ultrasonography* 2017; **36:** 363-9. doi: 10.14366/usg.17007
9. Anania P, Fiaschi P, Ceraudo M, Balestrino A, Zaottini F, Martinoli C, et al. Posterior interosseous nerve entrapments: review of the literature. Is the entrapment distal to the arcade of Frohse a really rare condition? *Acta Neurochir* 2018; **160:** 1857-64. doi: 10.1007/s00701-018-3615-8

10. Kim DH, Kline DG. Surgical treatment and outcomes in 45 cases of posterior interosseous nerve entrapments and injuries. *J Neurosurg* 2006; **104:** 766-77. doi: 10.3171/jns.2006.104.5.766

11. Martínez-Villén G, Badiola J, Alvarez-Alegret R, Mayayo E. Nerve compression syndromes of the hand and forearm associated with tumours of non-neural origin and tumour-like lesions. *J Plast Reconstr Aesthet Surg* 2014; **67:** 828-36. doi: 10.1016/j.bjps.2014.02.003

12. Kosztyuova T, Shim TN. Rapidly enlarging lipoma. *BMJ Case Rep* 2017; **23:** bcr-2017-221272. doi: 10.1136/bcr-2017-221272

13. Al-Qattan MM, Al-Lazzam AM, Al Thunayan A, Al Namlah A, Mahmoud S, Hashem F, et al. Classification of benign fatty tumours of the upper limb. *Hand Surg* 2005; **10:** 43-59. doi: 10.1142/S0218810405002541

14. Vikas V, Bhatia N, Garg J. Posterior interosseous nerve entrapment due to bilobed parosteal lipoma. *J Clin Orthop Trauma* 2020; **11:** S174-6. doi: 10.1016/j.jcot.2019.10.006

15. Allagui M, Maghrebi S, Touati B, Koubaa M, Hadhri R, Hamdi MF, et al. Posterior interosseous nerve syndrome due to intramuscular lipoma. *Eur Orthop Traumatol* 2014; **5:** 75-9. doi: 10.1007/s12570-013-0203-5

16. Maldonado AA, Howe BM, Spinner RJ. Posterior interosseous nerve discontinuity due to compression by lipoma: report of 2 cases. *J Neurosurg* 2017; **126:** 1698-701. doi: 10.3171/2016.2.JNS152810

17. Yamamoto D, Yamauchi D, Tsuchiya H. Intraneural lipoma of the posterior interosseous nerve. *J Hand Surg Eur Vol* 2016; **41:** 882-3. doi: 10.1177/1753193415594109

18. C R, Naidu D, Ravi S, S D. A case report on parosteal lipoma stretching the posterior interosseous nerve without causing palsy. *Cureus* 2021; **13:** e14776. doi: 10.7759/cureus.14776

19. Flores Robles BJ, Sanz Sanz J, Sanabria Sanchinel AA, Hualde Juvera A. Posterior interosseous nerve palsy secondary to deep lipoma. *Neurol Barc Spain* 2017; **32:** 57-8. doi: 10.1016/j.nrl.2015.12.020

20. Salama H, Kumar P, Bastawrous S. Posterior interosseous nerve palsy caused by parosteal lipoma: a case report. *Case Rep Med* 2010; **2010**: 1-3. doi: 10.1155/2010/785202

21. Saaiq M, Siddiui S. Posterior interosseous nerve syndrome resulting from parosteal lipoma of the proximal radius: an elusive diagnosis yet excellent outcome. *World J Plast Surg* 2017; **6:** 100-5.

22. Patel AP, Aoun SG, Al Tamimi M. Intraneural posterior interosseous nerve lipoma with complete paralysis: case report and review of the literature. *Cureus* 2018; **10:** e2689. doi: 10.7759/cureus.2689

23. Murphy A, Williams J. Posterior interosseous nerve palsy caused by lipoma: A case report. *Can J Plast Surg* 2009; **17:** e42-4.

24. Nishida J, Shimamura T, Ehara S, Shiraishi H, Sato T, Abe M. Posterior interosseous nerve palsy caused by parosteal lipoma of proximal radius. *Skeletal Radiol* 1998; **27:** 375-9. doi: 10.1007/s002560050401

25. Ganapathy K, Winston T, Seshadri V. Posterior interosseous nerve palsy due to intermuscular lipoma. *Surg Neurol* 2006; **65:** 495-6. doi: 10.1016/j.surneu.2005.06.035

26. Colasanti R. Delayed diagnosed intermuscular lipoma causing a posterior interosseous nerve palsy in a patient with cervical spondylosis: the "priceless" value of the clinical examination in the technological era. *G Chir* 2016; **37:** 42-5. doi: 10.11138/gchir/2016.37.1.042

27. Avram R, Hynes NM. Posterior interosseous nerve compression secondary to a parosteal lipoma: Case report and literature review. *Can J Plast Surg* 2004; **12:** 69-72. doi: 10.1177/229255030401200206

28. Hamdi M, Aloui I, Allagui M, Abid A. Paralysis of posterior interosseous nerve caused by parosteal lipoma. *Neurol India* 2010; **58:** 319. doi: 10.4103/0028-3886.63790

29. Matsuo T, Sugita T, Shimose S, Kubo T, Yasunaga Y, Ochi M. Intraneural lipoma of the posterior interosseous nerve. *J Hand Surg Am* 2007; **32:** 1530-2. doi: 10.1016/j.jhsa.2007.08.007

30. Seki Y, Hoshino Y, Kuroda H. Posterior interosseous nerve palsy due to parosteal lipoma. *Neurol India* 2012; **60:** 644-5. doi: 10.4103/0028-3886.105203

31. Eralp L, Ozger H, Ozkan K. [Posterior interosseous nerve palsy due to lipoma]. [Turkish]. *Acta Orthop Traumatol Turc* 2006; **40:** 252-4. PMID: 16905900

32. Fitzgerald A, Anderson W, Hooper G. Posterior interosseous nerve palsy due to parosteal lipoma. *J Hand Surg* 2002; **27:** 535-7. doi: 10.1054/jhsb.2002.0783

33. Narayan S, Ahluwalia VV, Saharan PS, Gupta AK. Intraosseous lipoma of the proximal radius with extra osseous extension leading to posterior interosseous nerve compression: HRUS diagnosis. J Orthop Case Rep 2016; **6:** 56-8. doi: 10.13107/jocr.2250-0685.506

34. El Hyaoui H, Hassoun J, Garch A, Kassimi EH, El Fatimi A. Compression of the posterior interosseous nerve by a deep lipoma. *Joint Bone Spine* 2014; **81:** 265. doi: 10.1016/j.jbspin.2014.01.016

35. Borman P, Tuncay F, Ulusoy G, Koçer U. Posterior interosseous nerve syndrome due to lipoma. *Neurophysiol Clin Neurophysiol* 2010; **40:** 189-91. doi: 10.1016/j.neucli.2010.01.004

36. Richmond DA. Lipoma causing a posterior interosseous nerve lesion. *J Bone Joint Surg Br* 1953; **35-B:** 83. doi: 10.1302/0301-620X.35B1.83

37. Bugnicourt JM, Peltier J, Merle PE, Le Gars D. Acute peripheral nerve compression by a lipoma mimicking stroke. *Clin Neurol Neurosurg* 2009; **111:** 395-6. doi: 10.1016/j.clineuro.2008.10.019

38. Rocks MC, Donnelly MR, Li A, Glickel SZ, Catalano LW 3rd, Posner M, et al. Demographics of common compressive neuropathies in the upper extremity. *Hand (N Y)* 2024; **19:** 217-23. doi: 10.1177/15589447221107701

39. Cheng C, Punjabi A, Gunther S, Chepla K. Forearm lipoma causing PIN compression: literature review and meta-analysis of predictors for motor recovery. *Hand (N Y)* 2024; **19:** 149-53. doi: 10.1177/15589447221096710

research article

[^{18}F]fluorocholine PET *vs*. [^{99m}Tc]sestamibi scintigraphy for detection and localization of hyperfunctioning parathyroid glands in patients with primary hyperparathyroidism: outcomes and resource efficiency

Sebastijan Rep[1,2], Klara Sirca[3], Ema Macek Lezaic[4], Katja Zaletel[1,5], Marko Hocevar[3,5], Luka Lezaic[1,5]

[1] Division of Nuclear Medicine, University Medical Centre Ljubljana, Ljubljana, Slovenia
[2] Medical Imaging and Radiotherapy Department, Faculty of Health Sciences, University of Ljubljana, Ljubljana, Slovenia
[3] Department of Oncological Surgery, Institute of Oncology Ljubljana, Ljubljana, Slovenia
[4] Charité Universitätsmedizin Berlin, Humboldt-Universität zu Berlin, Berlin, Germany
[5] Faculty of Medicine, University of Ljubljana, Ljubljana, Slovenia

Radiol Oncol 2024; 58(4): 486-493.

Received 6 September 2024
Accepted 24 September 2024

Correspondence to: Assist. Prof. Luka Ležaić, M.D., Ph.D., Division of Nuclear Medicine, University Medical Centre Ljubljana, Zaloška 7, 1525 Ljubljana, Slovenia. E-mail: luka.lezaic@kclj.si

Disclosure: No potential conflicts of interest were disclosed.

Background. Minimally invasive parathyroidectomy is the treatment of choice in patients with primary hyperparathyroidism (PHP), but it needs a reliable preoperative localization method to detect hyperfunctioning parathyroid tissue. Higher sensitivity and lower radiation exposure was demonstrated for [^{18}F]fluorocholine PET/CT (FCh-PET/CT) in comparison to [^{99m}Tc]sestamibi (MIBI) scintigraphy. However, data of its efficiency in resource use and patient outcomes is lacking. The aim of our study was to determine the resource efficiency and patient outcomes of FCh-PET/CT in comparison to conventional MIBI scintigraphy.

Patients and methods. A group of 234 patients who underwent surgery after MIBI scintigraphy was compared to a group of 163 patients who underwent surgery after FCh-PET/CT. The whole working process from the implementation of imaging to the completion of surgical treatment was analyzed. The economic burden was expressed in the time needed for the required procedures.

Results. The time needed to perform imaging was reduced by 83% after FCh-PET/CT in comparison to MIBI scintigraphy. The time needed to perform surgery was reduced by 41% when intraoperative parathyroid hormone monitoring was not used. There was no significant difference in the time of surgery between FCh-PET/CT and MIBI scintigraphy.

Conclusions. FCh-PET/CT reduces the time of imaging, the time of surgery and potentially reduces the number of reoperations for persistent disease.

Key words: hyperparathyroidism; surgery; parathyroidectomy; cost-effectiveness; [^{18}F]choline; [^{99m}Tc]sestamibi; PET/CT; SPECT/CT

Introduction

Primary hyperparathyroidism (PHP) is a condition that develops as a result of increased and uncontrolled production and secretion of parathyroid hormone (PTH) from hyperfunctioning parathyroid glands (HPG). The diagnosis of PHP is typically established through biochemical tests by

confirming elevated PTH levels in a patient with hypercalcemia and exclusion of alternative causes.[1] The therapy of choice in PHP is the surgical removal of the HPG. The traditional surgical approach in primary hyperparathyroidism involves bilateral neck exploration and evaluation of all four parathyroid glands. Due to the development of morphological and functional imaging diagnostics of HPG, a targeted approach has been established in the last decades in which only the area where imaging procedures indicate a solitary HPG is explored through a minimal 2 cm incision (minimally invasive parathyroidectomy, MIP). Accurate preoperative localization is crucial for optimal treatment results using MIP.[2,3]

Imaging procedures are performed only after biochemical confirmation of PHP and are used to plan the operative approach. Parathyroid scintigraphy with [^{99m}Tc]sestamibi (MIBI) using several recommended protocols (in particular single-photon emission computed tomography combined with computed tomography, SPECT/CT) in conjunction with neck ultrasound (US) is the reference method for the preoperative localization of HPG.[4-6]

In recent years, positron emission tomography/computed tomography (PET/CT) with [^{18}F]fluorocholine (FCh-PET/CT) emerged as the most accurate technique in preoperative localization of HPG.[7] Results from both early and later studies have shown that the sensitivity of FCh-PET/CT is superior to other molecular imaging approaches, including subtraction scintigraphy (SS) and single photon emission computer tomography/computed tomography (SPECT/CT) with MIBI. This is particularly evident in studies that directly compared scintigraphy protocols with FCh-PET/CT as a first-line approach.[8-13] Further advantage of FCh-PET/CT is markedly lower radiation exposure compared to MIBI SS and SPECT/CT.[14]

However, the outcomes and the economic impact of the use of FCh-PET/CT have not been extensively studied. The aim of our study was to compare the clinical outcomes and the resource efficiency of FCh-PET/CT versus MIBI SS combined with SPECT/CT in patients with PHP in the local setting.

Patients and methods

Clinical outcomes

This retrospective analysis (approval No. 0120-582/2021/4 by the Committee for Medical ethics of the Republic of Slovenia) covered the period from 2008 to 2016 and included 234 patients who underwent surgery after MIBI SS in combination with SPECT/CT and 163 patients who underwent surgery following FCh-PET/CT. Due to the retrospective nature of the analysis the request for patient consent was waived. We evaluated the success of surgery performed after MIBI SS and SPECT/CT imaging and after FCh-PET/CT imaging and the need for additional surgery in patients with persistent PHP.

Resource efficiency

As the cost of diagnostic imaging, surgery and hospitalization vary depending on the healthcare environment in which they are performed[15,16], we evaluated the burden of imaging and surgical procedures by measuring the time required to complete the procedure. This evaluation included the number of imaging procedures per day and/or in the number of hours required by the various occupational groups involved in the process. We assessed the workflow of radiopharmacists, nurses, radiographers (technologists) and physicians. A brief description of the working process for each professional profile is given in Table 1.

Diagnostic imaging

The SS was performed on a Siemens BasiCAM planar gamma camera at 10 and 90 minutes after the intravenous (i.v.) injection of 600 MBq of MIBI. After the completion of imaging at 90 minutes, the patient was left in the same position and 150 MBq of [^{99m}Tc]O_4^- was injected i.v. and identical imaging was performed after 10 minutes. After completion of imaging, a SS was generated by processing where the planar image obtained with [^{99m}Tc]O_4^- was subtracted from the planar image obtained with MIBI.

SPECT/CT imaging was performed on a SIEMENS Simbia® T2 gamma camera (Siemens Medical Solutions, Erlangen, Germany), SPECT/CT imaging of the neck and chest was performed 30 minutes after the i.v. injection of 600 MBq of MIBI. Typically, three patients per day were examined. The combination of dual-phase, SS and SPECT/CT is described as "hybrid" imaging protocol.

PET imaging was performed on a SIEMENS Biograph mCT® 128 system. PET imaging of the neck and chest was performed 5 and 60 minutes after i.v. injection of 100 MBq of FCh. The vial supplied by the manufacturer contains 2700 MBq FCh in the prescribed volume. The daily delivered ac-

TABLE 1. Workload of the profiles involved in the imaging process

	No. workers	SS + SPECT (hours)	No. patients/day	FCh PET (hours)	No. patients/day
Pharmacist	1		**3 (12)***		12
RP preparation		**0.7 (2.8)***		0,25	
Nurse	1				
Cannula placement		**0.75 (3)***		3	
Cannula removal		**0.3 (1.2)***		1,2	
Technologist	2				
RP application		**0.75 (3)***		1,2	
Imaging time		**6 (24)***		4	
QC dally test		**0.5 (2)***		0,5	
Physician	1				
PH&CE and writing a report		**3 (12)***		12	

* time required for 12 patients to perform SS + SPECT/CT

FCh PET = [18F]fluorocholine positron emission tomography; PH&CE = patient history and clinical examination; RP = radiopharmaceutical; QC = quality control; SS + SPECT/CT = subtraction scintigraphy and single-photon emission tomography/computed tomography

Time in minutes	120 min				240 min				360 min			
	0 - 20 min	30 - 60 min	90 min	100 - 120 min	0 - 20 min	30 - 60 min	90 min	100 - 120 min	0-20 min	30 - 60 min	90 min	100 - 120
Patient 1	RF application and first phase imaging	SPECT	Second phase imaging	RF application and subtraction scintigraphy								
Patient 2					RF application and first phase imaging	SPECT	Second phase imaging	RF application and subtraction scintigraphy				
Patient 3									RF application and first phase imaging	SPECT	Second phase imaging	RF application and subtraction scintigraphy

FIGURE 1. Time workflow/scheme of radiopharmaceutical (RP) application and imaging of subtraction scintigraphy (SS) and single-photon emission tomography/computed tomography (SPECT/CT) in a working day. Approximate times are taken into account for all procedures.

tivity typically allowed us to examine 12 patients per day, divided into two groups of 6 patients. The daily workflow and occupancy of imaging equipment for both examinations is shown in Figures 1 and 2.

Surgery

The time of the surgical procedure was recorded from the arrival of the patient in the operating room to the departure from it.

In patients with a solitary HPG on MIBI SS and SPECT/CT or FCh-PET/CT only a focused (lateral trapdoor approach) parathyroidectomy without intraoperative PTH (ioPTH) testing was performed. In patients with multiple lesions or nonlocalization a more extensive classical bilateral neck exploration with ioPTH testing was performed. PTH measurements (in pg/mL) were performed at the induction of general anesthesia and 10 min after the removal of the last enlarged parathyroid gland and the procedure was deemed successful if there was a ≥ 50% drop from baseline. For determination of ioPTH, blood samples were collected into K2-EDTA Vacutainer™ tubes (Becton-Dickinson, Plymouth, UK), centrifuged (2,500 g, 10 min, room temperature) and analysed using a commercially available kit (cobas PTH STAT) and analyzer (cobas e 411; both Roche Diagnostics, Mannheim, Germany).

Patients were discharged from the hospital on the next day and in all patient's serum values of Ca^{2+} and PTH were obtained on the morning before discharge. Normalization of Ca^{2+} and PTH values was considered to represent successful surgery.

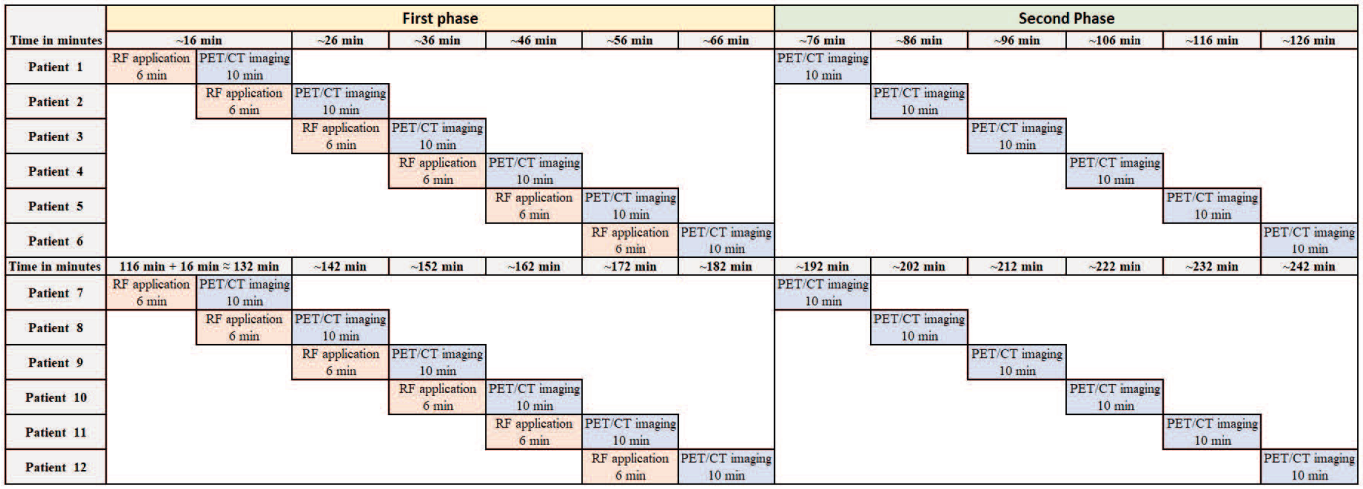

FIGURE 2. Time workflow/scheme of radiopharmaceutical (RP) application and imaging of [18F]fluorocholine positron emission tomography (FCh-PET) in a working day. Approximate times are taken into account for all procedures.

Statistical analysis

Differences in the required time to completion were expressed as percentages. The Kolmogorov-Smirnov test was used for the evaluation of the normality of data distribution and Mann-Whitney test to confirm the difference between the independent variables. A $p < 0.05$ was considered statistically significant.

Results

Clinical outcomes

For the evaluation of the surgical part, we reviewed the 4-year period before and after the implementation of FCh-PET/CT (2008 to 2016) for preoperative localization of HPG. The period before the implementation included 234 patients and the period after the implementation included 163 patients. All localized HPG were surgically removed. Persistent hypercalcemia was more often observed in patients who underwent MIBI SS and SPECT/CT prior to surgery (15.8%) in comparison to those who underwent FCh-PET/CT (2.4%) ($p < 0.001$). Reoperation was required in 12.3% of patients who underwent SS and SPECT/CT prior to the initial surgery, compared to 1.8% of patients who had FCh-PET/CT. Postoperative complications occurred in 5.3% of patients after SS and SPECT/CT and 4.7% of patients after FCh-PET/CT. Detailed data are presented in Table 2.

Resource efficiency

The time required for surgery based on the results of MIBI SS and SPECT/CT versus FCh-PET/CT was comparable (Table 3). However, the implementation of ioPTH monitoring significantly prolonged the time of surgery, while the duration of hospitalization did not differ significantly (Table 4).

Diagrams 1 and 2 (Figures 1 and 2) depict the workflow of the imaging process for SS and SPECT/CT and FCh-PET/CT, respectively. With MIBI SS and SPECT/CT imaging, up to three patients were typically imaged in a day, whereas up

TABLE 2. The most common causes (percentages) of postoperative complications

	SS and SPECT/CT	FCh PET
Tingling	4/234 (1.7%)	3/163 (1.8%)
Chvostek sign	1/234 (0.4%)	1/163 (0.6%)
Hungry bone syndrome	1/234 (0.4%)	2/163 (1.2%)
Malaise	1/234 (0.4%)	N/C
Hoarseness	1/234 (0.4%)	N/C
Postoperative Hypocalcemia	1/234 (0.4%)	N/C
Hematoma	1/234 (0.4%)	N/C
Deterioration of renal function	N/C	1/163 (0.6%)
Reoperation	29/234 (12.3%)*	3/163 (1.8%)*
All	39/234 (16.6%)**	10/163 (6.1%)**

*$p < 0.001$ for SS and SPECT/CT vs. FCh PET; **$p < 0.001$ for SS and SPECT/CT vs. FCh PET

FCh PET = [18F]fluorocholine positron emission tomography; N/C = no case; SS and SPECT/CT = subtraction scintigraphy and single-photon emission tomography/computed tomography

TABLE 3. The patient number and the required time of surgery expressed in minutes after subtraction scintigraphy (SS) and single-photon emission computed tomography/computed tomography (SPECT/CT) *vs.* [18F]fluorocholine positron emission tomography (FCh-PET)

	All pts	Mean	Median	SD	Min	Max
MIBI SS and SPECT/CT	234	67.37	60.00	36.88	20.00	280.00
FCh-PET	163	70.79	55.00	38.21	25.00	195.00
p		0.66				
	Solitary HPG	**Mean**	**Median**	**SD**	**Min**	**Max**
MIBI SS and SPECT/CT	195	63.56	50.00	33.04	20.00	235.00
FCh-PET	138	64.42	50.00	33.04	25.00	180.00
p		0.93				
	Multiple HPG	**Mean**	**Median**	**SD**	**Min**	**Max**
MIBI SS and SPECT/CT	39	94.26	100.00	43.65	25.00	235.00
FCh-PET	25	104.79	107.00	40.79	30.00	180.00
p		0.23				

HPG = hyperfunctioning parathyroid gland(s); Max = maximum; Min = minimum; pts = patients; SD = standard deviation

to 12 patients were imaged per day with FCh-PET/CT. Assuming a standard imaging workload of 12 patients, pure imaging time was reduced by 83%, radipharmaceutical (RP) preparation time by 89% and quality control (QC) procedures by 75% with the use of FCh-PET/CT (as derived from Table 1). There were no differences in the time required for cannula placement and removal, RP injection/application, the time needed for patient history and clinical examination (PH&CE), and for writing the report.

Discussion

Parathyroid scintigraphy for the preoperative localization of HPG in patients with PHP enabled the introduction of MIP as the optimal surgical approach in patients with solitary HPG (approximately 85% of all patients with PHP). The main advantages of MIP include the possibility of using local/regional anaesthesia, shorter operative time, better cosmetic results and a more favourable extent of initial surgery in patients requiring repeated surgical treatment due to persistent or recurrent disease.[15-19] A prerequisite for optimal treatment results using MIP is accurate preoperative localization.[3]

In recent years, various publications have described using FCh-PET/CT in the preoperative localization of HPG in patients with PHP. FCh-PET/CT has been shown to enhance the sensitivity for the localization of HPG in comparison to MIBI SS and SPECT/CT, especially in patients with multiglandular disease.[8, 10-13]

Despite excellent diagnostic performance as shown in meta-analyses[7,20] and lower radiation exposure[14] of FCh-PET/CT in comparison to conventional MIBI SS and SPECT/CT, the main drawback is the higher cost of the radiopharmaceutical compared to MIBI. Since the price of the radiopharmaceutical is only one aspect of the entire procedure, we evaluated and compared the workflow burden of FCh-PET/CT *vs.* MIBI SS combined with SPECT/CT expressed in the required time for different procedures from the implementation of imaging to the completion of surgical treatment.

The main difference was found in the number of imaging procedures that can be performed in a typical imaging day. While we were able to complete FCh-PET/CT imaging in 12 patients, we were able to complete MIBI SS and SPECT/CT in three patients, resulting in overall four-fold gain for FCh-PET/CT. The main reason is the short imaging time and imaging protocol for FCh PET/CT that allows overlap between patients (Figure 2). All other aspects of the imaging procedure (RP preparation, placement and removal of the cannula, RP injection, PH&CE and writing the report) differed significantly less, if at all, in terms of time requirements. The first reason for the shorter imaging time using PET *vs.* MIBI SS and SPECT/CT is significantly higher sensitivity of the PET detector system in comparison to conventional gamma

TABLE 4. Influence of probable prognostic factors on overall survival (OS) and deasise-free survival (DFS)

	All pts	Mean	Median	SD	Min	Max
No ioPTH	123	60.00	50.00	33.91	25.00	195.00
ioPTH	39	103.00	100.00	31.27	40.00	195.00
p		< 0.001				
	Solitary HPG	**Mean**	**Median**	**SD**	**Min**	**Max**
No ioPTH	113	57.30	50.00	31.05	25.00	180.00
ioPTH	25	96.60	90.00	29.71	40.00	155.00
p		< 0.001				
	Multiple HPG	**Mean**	**Median**	**SD**	**Min**	**Max**
No ioPTH	10	85.55	70.00	49.90	30.00	195.00
ioPTH	15	116.33	110.00	30.49	80.00	195.00
p		0.03				

HPG = hyperfunctioning parathyroid gland(s); ioPTH = intraoperative parathyroid hormone determination; Max = maximum; Min = minimum; pts = patients; SD = standard deviation

cameras.[21] The time requirement for a single phase of FCh-PET/CT imaging – the acquisition time (5 min) and the time needed for the patient to occupy and leave the examination table (5 min) – amounted to 10 minutes. Our routine dual-phase workflow allowed us to image 12 patients in a working day. In contrast, about 2 hours were required per patient to perform MIBI SS and SPECT/CT using the routine hybrid imaging protocol, limiting the number of patients to 3 daily; cumulatively, for a standard 12-patient workload higher burden was found for pure imaging time, RP preparation and QC procedures.

Alternative imaging protocols requiring substantially shorter imaging times are also in routine use.[6] Subtraction scintigraphy (including tomographic subtraction) can also be performed with Na[^{123}I]I, allowing for simultaneous imaging with MIBI due to differing energy windows. this approach can substantially reduce cumulative imaging times, potentially making them comparable to FCh PET, while single-RP protocols using solely dual-phase MIBI SPECT/CT further simplify the procedure; both approaches were shown to result in favourable clinical accuracy.[5] However, in our experience[8,12] and that of other groups[22], the hybrid protocol results in the optimal diagnostic performance when using conventional scintigraphic approaches. Nevertheless, FCh-PET/CT was unequivocally found to be diagnostically superior to conventional imaging.[7] In summary, FCh-PET/CT offers shorter acquisition times in comparison to MIBI SS and SPECT/CT.[6,23-25] Small additional gains may result from fewer required quality control procedures and reduced reporting times due to the superior image quality of FCh-PET/CT.

Further potential aspect of improved resource efficiency is the superior diagnostic accuracy of FCh-PET/CT which enables MIP without the need for ioPTH. As demonstrated by our group, ioPTH can be safely omitted in patients with solitary HPG on FCh-PET/CT, leading to the reduction of surgery time.[3] Our results suggest that the average time of surgery can be shortened by as much as 41% if ioPTH monitoring is not performed, which reduces the overall cost of the procedure. In the present analysis the difference in time requirement of the surgical procedure with and without ioPTH was evaluated only in patients operated on the basis of FCh-PET/CT imaging as the method of ioPTH determination was introduced in our institution(s) in 2012 (approximately the time of introduction of FCh-PET/CT). This was reflected in inferior results of MIP in patients operated based on MIBI SS and SPECT/CT imaging without ioPTH assessment in comparison to patients after FCh-PET/CT (reoperation for persistent PHP was required in 12.3% of patients after MIBI SS and SPECT/CT imaging in comparison to only 1.8% of surgeries after FCh-PET/CT imaging). With the use of ioPTH assessment in patients operated after MIBI SS and SPECT/CT imaging the number of reoperations for persistent PHP would probably be lower. However, in a large series comparing the diagnos-

tic accuracy of MIBI SS and SPECT/CT to FCh-PET/CT imaging in pHPT reported by our group, 47% of patients with multiglandular disease on FCh-PET/CT would undergo resection of a single gland detected of conventional scintigraphic imaging[12]; in several of those patients, removal of the largest offending gland would have resulted in the reduction of ioPTH levels above 50% and premature termination of surgery, an occurrence also reported by other groups.[26]

The superior diagnostic performance of FCh-PET/CT over conventional scintigraphic imaging resulted in the recommendation for the method in the current EANM guidelines on parathyroid imaging as an "alternative" first-line imaging approach to be used whenever possible, with the caveat of unclear cost-effectiveness.[6] Most recently, the superior diagnostic performance of FCh-PET/CT over MIBI SS and SPECT/CT already reported in direct comparison was confirmed in a randomized trial comparing the two methods as a first-line imaging approach: FCh-PET/CT was shown to be superior and safe imaging option.[27] As the social cost of the compared first-line imaging approaches was part of the study protocol[28], the additional results are awaited. Indeed, the main barrier for the introduction of FCh-PET/CT into routine clinical practice – in particular as a first-line imaging choice – is the limited availability of the method in many clinical environments, related to locally specific factors such as lack of equipment, prohibitive cost and/or legal limitations of off-label use of the radiopharmaceutical. These limitations are clearly recognized in detailed reviews, meta-analyses and existing guidelines, stating that a cost-effectiveness analysis of the method would be required if not crucial to promote its widespread use.[6-7,20] Few attempts to assess the cost-effectiveness of FCh-PET/CT in comparison to conventional scintigraphic and alternative radiological imaging methods reflect the significant local differences in availability and reimbursement strategies. In the United States, FCh-PET/CT was found to be a potentially economically viable imaging approach, but expensive with a narrow cost-effectiveness margin.[29] Conversely, in the EU setting, FCh-PET/CT was shown to be an effective sole, first-line imaging choice with negligible additional expenses.[30] With clearly superior diagnostic performance and comparable cost, FCh-PET/CT is expected to be promoted as a first-line imaging method of choice in primary hyperparathyroidism.

Conclusions

FCh-PET/CT reduces the time of imaging, the time of surgery and potentially reduces the number of reoperations for persistent disease. All these advantages may translate into lower overall costs of management of patients with pHP by using FCh-PET/CT in comparison to MIBI SS and SPECT/CT, confirming its appropriate role as a first-line imaging choice.

References

1. Bilezikian JP, Bandeira L, Khan A, Cusano NE. Hyperparathyroidism. *Lancet* 2018; **391:** 168-178. doi: 10.1016/S0140-6736(17)31430-7
2. Minisola S, Cipriani C, Diacinti D, Tartaglia F, Scillitani A, Pepe J, et al. Imaging of the parathyroid glands in primary hyperparathyroidism. *Eur J Endocrinol* 2016; **174:** D1-8. doi: 10.1530/EJE-15-0565
3. Hocevar M, Lezaic L, Rep S, Zaletel K, Kocjan T, Sever MJ, et al. Focused parathyroidectomy without intraoperative parathormone testing is safe after pre-operative localization with 18F-fluorocholine PET/CT. *Eur J Surg Oncol* 2017; **43:** 133-7. doi: 10.1016/j.ejso.2016.09.016
4. Wong KK, Fig LM, Gross MD, Dwamena BA. Parathyroid adenoma localization with 99mTc-sestamibi SPECT/CT: a meta-analysis. *Nucl Med Commun* 2015; **36:** 363-75. doi: 10.1097/MNM.0000000000000262
5. Treglia G, Trimboli P, Huellner M, Giovanella L. Imaging in primary hyperparathyroidism: focus on the evidence-based diagnostic performance of different methods. *Minerva Endocrinol* 2018; **43:** 133-43, doi: 10.23736/S0391-1977.17.02685-2
6. Petranović Ovčariček P, Giovanella L, Carrió Gasset I, Hindié E, Huellner MW, Luster M, et al. The EANM practice guidelines for parathyroid imaging. *Eur J Nucl Med Mol Imaging* 2021; **48:** 2801-22. doi: 10.1007/s00259-021-05334-y
7. Lee SW, Shim SR, Jeong SY, Kim SJ. Direct comparison of preoperative imaging modalities for localization of primary hyperparathyroidism: a systematic review and network meta-analysis. *JAMA Otolaryngol Head Neck Surg* 2021; **147:** 692-706. doi: 10.1001/jamaoto.2021.0915
8. Lezaic L, Rep S, Sever MJ, Kocjan T, Hocevar M, Fettich J. ^{18}F-Fluorocholine PET/CT for localization of hyperfunctioning parathyroid tissue in primary hyperparathyroidism: a pilot study. *Eur J Nucl Med Mol Imaging* 2014; **41:** 2083-9. doi: 10.1007/s00259-014-2837-0
9. Michaud L, Balogova S, Burgess A, Ohnona J, Huchet V, Kerrou K, et al. A pilot comparison of 18F-fluorocholine PET/CT, ultrasonography and 123I/99mTc-sestaMIBI dual-phase dual-isotope scintigraphy in the preoperative localization of hyperfunctioning parathyroid glands in primary or secondary hyperparathyroidism: influence of thyroid anomalies. *Medicine* 2015; **94:** e1701. doi: 10.1097/MD.0000000000001701
10. Thanseer N, Bhadada SK, Sood A, Mittal BR, Behera A, Gorla AKR, et al. Comparative effectiveness of ultrasonography, 99mTc-sestamibi, and 18F-fluorocholine PET/CT in detecting parathyroid adenomas in patients with primary hyperparathyroidism. *Clin Nucl Med* 2017; **42:** e491-7. doi: 10.1097/RLU.0000000000001845
11. Beheshti M, Hehenwarter L, Paymani Z, Rendl G, Imamovic L, Rettenbacher R, et al. (18)F-Fluorocholine PET/CT in the assessment of primary hyperparathyroidism compared with (99m)Tc-MIBI or (99m)Tc-tetrofosmin SPECT/CT: a prospective dual-centre study in 100 patients. *Eur J Nucl Med Mol Imaging* 2018; **45:** 1762-71. doi: 10.1007/s00259-018-3980-9
12. Cuderman A, Senica K, Rep S, Hocevar M, Kocjan T, Sever MJ, et al. 18F-fluorocholine PET/CT in primary hyperparathyroidism: superior diagnostic performance to conventional scintigraphic imaging for localization of hyperfunctioning parathyroid glands. *J Nucl Med* 2020; **61:** 577-83. doi: 10.2967/jnumed.119.229914

13. Imperiale A, Bani J, Bottoni G, Latgé A, Heimburger C, Catrambone U, et al. Does (18)F-Fluorocholine PET/CT add value to positive parathyroid scintigraphy in the presurgical assessment of primary hyperparathyroidism? *Front Med* 2023; **10:** 1148287. doi: 10.3389/fmed.2023.1148287

14. Rep S, Hocevar M, Vaupotic J, Zdesar U, Zaletel K, Lezaic L. 18F-choline PET/CT for parathyroid scintigraphy: significantly lower radiation exposure of patients in comparison to conventional nuclear medicine imaging approaches. *J Radiol Prot* 2018; **38:** 343-56. doi: 10.1088/1361-6498/aaa86f

15. Ahuja AT, Wong KT, Ching AS, Fung MK, Lau JY, Yuen EH, et al. Imaging for primary hyperparathyroidism--what beginners should know. *Clin Radiol* 2004; **59:** 967-76. doi: 10.1016/j.crad.2004.04.005

16. Díaz-Aguirregoitia FJ, Emparan C, Gaztambide S, Aniel-Quiroga MA, Busturia MA, Vázquez JA, et al. Intraoperative monitoring of kinetic total serum calcium levels in primary hyperparathyroidism surgery. *J Am Coll Surg* 2004; **198:** 519-24. doi: 10.1016/j.jamcollsurg.2003.12.006

17. Bergenfelz A, Lindblom P, Tibblin S, Westerdahl J. Unilateral versus bilateral neck exploration for primary hyperparathyroidism: a prospective randomized controlled trial. *Ann Surg* 2002; **236:** 543-51. doi: 10.1097/00000658-200211000-00001

18. Inabnet WB 3rd, Dakin GF, Haber RS, Rubino F, Diamond EJ, Gagner M. Targeted parathyroidectomy in the era of intraoperative parathormone monitoring. *World J Surg* 2002; **26:** 921-5. doi: 10.1007/s00268-002-6619-7

19. Dillavou ED, Cohn HE. Minimally invasive parathyroidectomy: 101 consecutive cases from a single surgeon. *J Am Coll Surg* 2003; **197:** 1-7. doi: 10.1016/S1072-7515(03)00113-3

20. Treglia G, Piccardo A, Imperiale A, Strobel K, Kaufmann PA, Prior JO, et al. Diagnostic performance of choline PET for detection of hyperfunctioning parathyroid glands in hyperparathyroidism: a systematic review and meta-analysis. *Eur J Nucl Med Mol Imaging* 2019; **46:** 751-65. doi: 10.1007/s00259-018-4123-z

21. Jansen FP, Vanderheyden JL. The future of SPECT in a time of PET. *Nucl Med Biol* 2007; **34:** 733-5. doi: 10.1016/j.nucmedbio.2007.06.013.

22. Nichols KJ, Tomas MB, Tronco GG, Rini JN, Kunjummen BD, Heller KS, et al. Preoperative parathyroid scintigraphic lesion localization: accuracy of various types of readings. *Radiology* 2008; **248:** 221-32. doi: 10.1148/radiol.2481071066

23. Broos WAM, Wondergem M, Knol RJJ, van der Zant FM. Parathyroid imaging with 18F-fluorocholine PET/CT as a first-line imaging modality in primary hyperparathyroidism: a retrospective cohort study. *EJNMMI Res* 2019; **9:** 72. doi: 10.1186/s13550-019-0544-3

24. Imperiale A, Taïeb D, Hindié E. 18F-fluorocholine PET/CT as a second line nuclear imaging technique before surgery for primary hyperparathyroidism. *Eur J Nucl Med Mol Imaging* 2018; **45:** 654-7. doi: 10,1007/s00259-017-3920-0

25. Evangelista L, Ravelli I, Magnani F, Iacobone M, Giraudo C, Camozzi V, et al. 18F-choline PET/CT and PET/MRI in primary and recurrent hyperparathyroidism: a systematic review of the literature. *Ann Nucl Med* 2020; **34:** 601-19. doi: 10.1007/s12149-020-01507-1

26. Hindié E, Zanotti-Fregonara P, Tabarin A, Rubello D, Morelec I, Wagner T, et al. The role of radionuclide imaging in the surgical management of primary hyperparathyroidism. *J Nucl Med* 2015; **56:** 737-44. doi: 10.2967/jnumed.115.156018

27. Quak E, Lasne-Cardon A, Cavarec M, Lireux B, Bastit V, Roudaut N, et al. F18-Choline PET/CT or MIBI SPECT/CT in the surgical management of primary hyperparathyroidism: a diagnostic randomized clinical trial. *JAMA Otolaryngol Head Neck Surg* 2024; **150:** 658-65. doi: 10.1001/jamaoto.2024.1421

28. Quak E, Lasne Cardon A, Ciappuccini R, Lasnon C, Bastit V, Le Henaff V, et al. Upfront F18-choline PET/CT versus Tc99m-sestaMIBI SPECT/CT guided surgery in primary hyperparathyroidism: the randomized phase III diagnostic trial APACH2. *BMC Endocr Disord* 2021; **21:** 3. doi: 10.1186/s12902-020-00667-5

29. Yap A, Hope TA, Graves CE, Kluijfhout W, Shen WT, Gosnell JE, et al. A cost-utility analysis of 18F-fluorocholine-positron emission tomography imaging for localizing primary hyperparathyroidism in the United States. *Surgery* 2022; **171:** 55-62. doi: 10.1016/j.surg.2021.03.075

30. van Mossel S, Saing S, Appelman-Dijkstra N, Quak E, Schepers A, Smit F, et al. Cost-effectiveness of one-stop-shop [(18)F]fluorocholine PET/CT to localise parathyroid adenomas in patients suffering from primary hyperparathyroidism. *Eur J Nucl Med Mol Imaging* 2024. **51:** 3585-95. doi: 10.1007/s00259-024-06771-1.

research article

Whole-body PET/MRI to detect bone metastases: comparison of the diagnostic performance of the sequences

Onur Levent Ulusoy[1,2], Sadık Server, [1,2] Murat Yesilova[1], Nagihan İnan[1,2]

[1] Demiroglu Bilim University, İstanbul, Turkey
[2] Derpartment of Radiology, Florence Nigtingale Hospitals, İstanbul, Turkey

Radiol Oncol 2024; 58(4): 494-500.

Received 2 June 2024
Accepted 24 October 2024

Correspondence to: Dr. Nagihan İnan, M.D., Demiroğlu Bilim Üniv., İstanbul, Turkey; Department of Radiology, Florence Nigtingale Hospitals, İstanbul, Turkey. E-mail: nagihan.inangurcan@florence.com.tr

Disclosure: No potential conflicts of interest were disclosed.

Background. Whole-body positron emission tomography/magnetic resonance imaging (WB-PET/MRI) is increasingly used in the initial evaluation of oncology patients. The purpose of this study was to compare the diagnostic performance of WB MRI sequences, attenuation-corrected raw data positron-emission tomography (AC PET), and PET/MRI fused images to detect bone metastases.

Patients and methods. We included 765 consecutive oncologic patients who received WB-PET/MRI from between January 2017 and September 2023. The presence of bone metastases was assessed using the individual sequences by two radiologists. Interobserver agreement was calculated. A receiver operating characteristic (ROC) analysis was performed to assess the performance of each individual sequence and fused images.

Results. Interobserver agreement for the detection of bone metastases on all sequences ranged from good to very good. The reading of the combination of MRI sequences with PET images showed statistically significantly better performance than the reading of individual MRI sequences and PET component only. Contrast enhanced T1 W Volume-interpolated breath-hold examination (CE T1W VIBE) sequence superior to PET for the detection of bone metastasis, but the statistical significance was not as high as with T1W-PET and CE T1W-PET fused images. The highest performance was achieved by the fused CE T1W- PET images with sensitivity of 100%, specificity of 92%, PPV of 96%, and NPV of 100%.

Conclusions. The combination of these CE T1W VIBE sequences with PET images have the highest diagnostic performance in detecting bone metastases in oncologic patients. This sequence should be integrated in WB-PET/MRI acquisitions for initial staging of cancer.

Key words: bone metastases; hybrid imaging; positron-emission tomography; magnetic resonance imaging

Introduction

In oncology patients, bone metastases are common, often arising from primary cancers like breast, prostate, lung, and others. Early detection of bone metastasis is critical for accurate staging and optimal treatment. Treatment strategies may involve a combination of systemic therapies, radiation, and supportive care to manage symptoms and improve the quality of life for patients with bone metastases.[1-3]

Imaging techniques such as X-rays, bone scans, computed tomography (CT), magnetic resonance imaging (MRI), and positron emission tomography (PET) scans help in detecting and evaluating the extent of bone metastases. X-rays are often used as a first step, while bone scans can reveal areas with increased bone activity. CT and MRI

provide detailed images, and PET scans can help detect metastases at an early stage by highlighting abnormal metabolic activity.[4-8]

Whole-body positron emission tomography/magnetic resonance imaging (WB-PET/MRI) is a state of art hybrid imaging technique used in oncology to provide detailed information about both the anatomy and metabolic activity of tissues. It combines the functional information from PET with the detailed structural images from MRI, offering a comprehensive view for oncology patients. The combined data can enhance the accuracy of lesion detection. This integrated approach aids in more accurate diagnosis, staging, and treatment planning for cancer. It may provide better sensitivity and specificity compared to stand-alone modalities. However, the diagnostic performance of PET-MRI sequences for detecting bone metastases can vary depending on factors such as the specific imaging protocol, the type and location of metastases, and the underlying conditions of the patients.[9]

To our knowledge, there is currently no published article comparing the accuracy of WB-PET/MRI sequences in diagnosing bone metastases and work in this area is warranted. The purpose of this study was to compare the diagnostic performance of an individual sequences [pre-contrast T1 weighted (W) Turbo Flash, contrast enhanced T1W Volume-interpolated breath-hold examination (CE T1W VIBE), attenuation-corrected raw data positron-emission tomography (AC PET), and PET/MRI fused images (T1W-PET, CE T1W-PET)] to detect bone metastases in oncology patients.

Patients and methods

Patients

Seven hundred sixty-five consecutive patients with histopathologicaly proven primary malignancy who received WB-PET/MRI between January 2017 and September 2023 were evaluated, retrospectively. Two hundred forty-five patients with missing MRI sequences, insufficient image quality, and insufficient data for diagnosis were excluded from the study. As a result, 520 patients with histopathologically proven of their primary malignant tumors by surgery and/or biopsy were included in this research (317 males and 203 females; mean age of 59.27 ± 13.53 years, range 21-83 years). Among these patients, 76 (14.62%) of them had bone metastases (53 males and 23 females; mean age of 56.57±14.60 years, range 24-72); 444 of them had no bone metastases. A total of 152 bone metastases in 76 patients were included in the final evaluation.

The study was approved by the ethics committee (The ethical approval number: 2024/177) and because it was a retrospective study, written permission was not required.

Imaging protocol

After fasting for at least 6 hours, the blood glucose level was assessed with a blood glucose meter (One Touch Vita; Life Scan, Milpitas, CA, USA) before imaging to ensure that it was <140 mg/dl. WB-PET/MRI was performed 45 ± 10 minutes after ^{18}F-Fluorodeoxyglucose (FDG) injection (average dosages, 4.541 MBq/kg weight; spectrum, 370-400 MBq). The WB-PET/MRI images were acquired in supine position on a 3 tesla Biograph mMR scanner (Siemens Healthcare, Erlangen, Germany) using a 16-channel head and neck surface coil, three 12-channel body coils, and 56 lutetium oxy orthosilicate avalanche photodiode PET detector blocks. These body coils were combined to form a multichannel WB coil by using the total imaging matrix technology. The WB images were obtained in 5 to 6 bed positions according to the size of the patient and each bedtime position was maintained between 2 and 2.5 min. In all patients, the WB PET/MRI covered the entire body from head to knee. For the attenuation correction, 4-point Dixon images were obtained in the coronal plane. The comprehensive MRI protocol consisted of T2-W single-shot echo train (HASTE; TR/TE, 1,500 ms/87 ms) and T1-W slice-selective Turbo Flash (TR/TE, 1,600 ms/2.5 ms) in the axial planes. PET acquisition occurred simultaneously during the WB MRI acquisition. Following the precontrast images, a gadolinium-based contrast agent [Dotarem®(Gadoterate Meglumine)] was used to obtain breath-hold 3D VIBE dynamic postcontrast images (TR/TE, 4.56 ms/2.03 ms) covering the upper abdomen in the arterial, portal venous, and late venous phases. Following the acquisition of the dynamic upper abdominal images, continuous breath-hold 3D VIBE images were acquired in the axial plane from head to knee. All the sections were combined, resulting in uninterrupted WB coverage. The total scan duration of the WB-PET/MRI examination was 50–60 min.

Imaging evaluation

In our research, two radiologists (S.S., and N.I.), one had 15 years of experience, and the other had

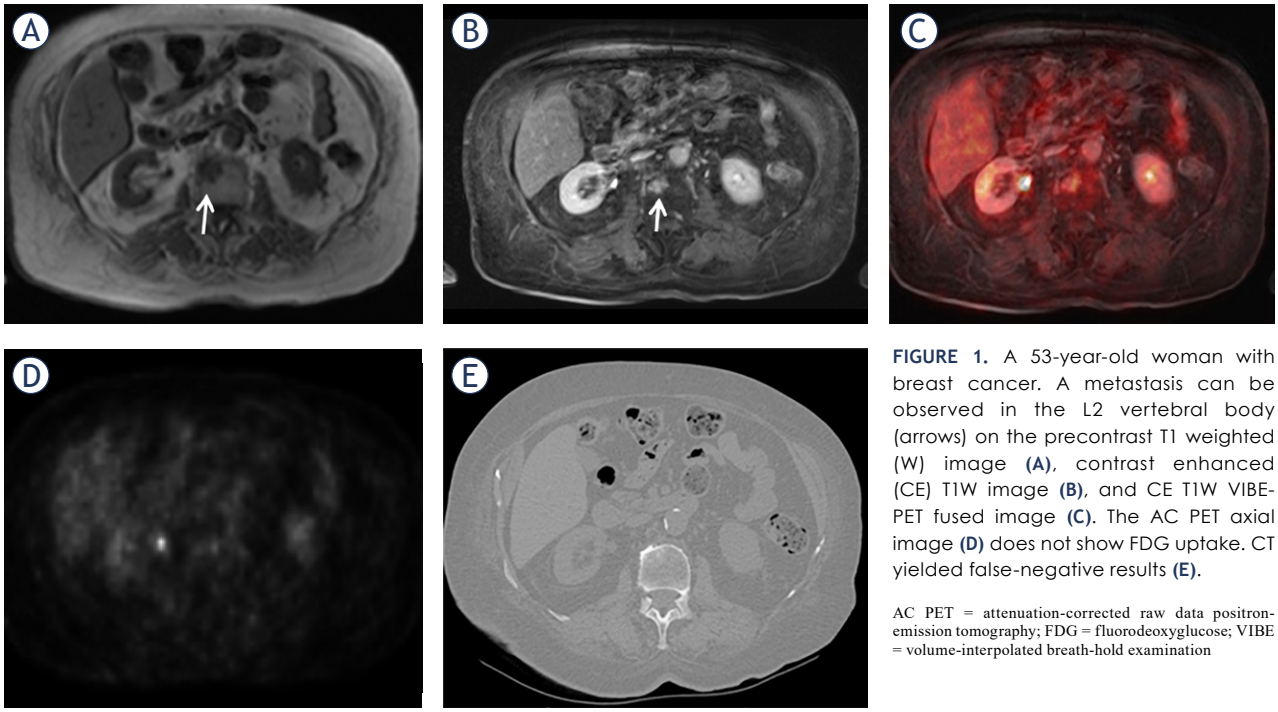

FIGURE 1. A 53-year-old woman with breast cancer. A metastasis can be observed in the L2 vertebral body (arrows) on the precontrast T1 weighted (W) image **(A)**, contrast enhanced (CE) T1W image **(B)**, and CE T1W VIBE-PET fused image **(C)**. The AC PET axial image **(D)** does not show FDG uptake. CT yielded false-negative results **(E)**.

AC PET = attenuation-corrected raw data positron-emission tomography; FDG = fluorodeoxyglucose; VIBE = volume-interpolated breath-hold examination

20 years of experience in reading MRI and both had 8 years of experience in reading hybrid imaging, performed all readings, in consensus. The presence of bone involvement on the individual sequences [pre-contrast T1W, CE T1W VIBE, AC PET, and PET/MRI fused images (T1W-PET, CE T1W-PET)] were reviewed separately, in a random order and at 1-month intervals to avoid any recall bias. The following widely accepted findings were applied to determine the presence of bone metastasis. Normal marrow was defined on T1W images as the homogeneous signal intensity that was higher than that of discs and muscles. A focal bone metastasis was defined by low signal intensity on T1W (lower than or equal to the signal intensity of discs or muscles), showing contrast enhancement, and pathologic FDG activation on PET images.[10] Discrepant findings were resolved by consensus decision making in a separate session between the readers. The readers were blinded to patient identity, status, and clinical and biological data.

The reference standard for bone metastases was constructed in consensus by the readers along with a third reader who had 22 years' experience in reading musculoskeletal MRI (O.L.U.). The third reader reviewed all baseline and follow-up CT or MRI examinations (6.2±1.6 month, and histopathological data). Increase or decrease in size of lesions after therapy or newly occurred cortical destruction were regarded as signs of malignancy.

False-positive and false-negative findings of any reading were assessed during the consensus reading by two readers. False-positive findings were degenerative disease, vertebral hemangioma, fracture, focal bone marrow hyperplasia, and diffuse heterogeneous or hyperplastic bone marrow; false-negative findings were sclerotic lesions, poor contrast between lesions and surrounding hypercellular bone marrow.[11]

Statistical analysis

Statistical analyses were performed using Statistical Package for Social Sciences for Windows software version 25 (IBM Corp.; Armonk, NY, USA). Interobserver agreement for each MR sequence between the two readers was assessed. The degree of agreement was determined by using the kappa value, and categorized as follows: 0–0.20, slight agreement; 0.21–0.40, fair agreement; 0.41–0.60, moderate agreement; 0.61–0.80, good agreement; and 0.81–1.00, excellent agreement.

The variables were investigated using the Kolmogorov-Smirnov test to determine whether the distribution was normal. Because most variables except for age were not normally distributed, Fried man's test was conducted to evaluate whether there was a significant change in the total number of detected bone metastasis among the different sequences.

A receiver operating characteristic (ROC) analysis was performed to assess the performance of each individual sequence and fused images according to the reference standard. The area under the curve (AUC) was reported along with a 95% confidence interval (CI). The sensitivity, specificity, positive predictive value (PPV), and negative predictive value (NPV) were calculated. Finally, pairwise comparisons of the AUC values were performed to rank the individual sequences and fused images according to diagnostic accuracy, using a chi-squared test of equality of ROC curves' areas. A p value < 0.05 indicates statistical significance for all tests.

Results

Patient characteristics

Table 1 shows tumor histopathologic features. Primary malignancies included lung cancer (*n* =26), hepatobiliary carcinoma (*n* =12), genitourinary carcinoma (*n* = 8), gastrointestinal cancer (*n* = 7), and breast cancer (*n* = 23). Metastases were in the ribs (*n* = 18), sternum (*n* =7), pelvic bones (*n* = 23), femur (*n* =13), cervical (*n* = 19), thoracic (*n* =22), lumbar (*n* = 32), and sacral vertebrae (*n* = 18).

Inter-observer agreement

Interobserver agreement for the detection of bone metastases on all sequences was ranged from good to very good (Table 2).

Diagnostic performance of sequences

The results on diagnostic performance of sequences, PET images, and fused images are summarized in Table 3. The reading of the combination of MRI sequences with PET images showed statistically significantly better performance than the reading of individual MRI sequences and PET component only. CE T1W MRI superior to PET for the detection of bone metastasis, but the statistical significance was not as high as with T1W-PET and CE T1W-PET. The highest performance was achieved by the fused CE T1W MRI/PET images with sensitivity of 100%, specificity of 92%, PPV of 96%, and NPV of 100%.

TABLE 1. Tumor histopathologic features

Primary malignant tumors	n
Hepatobiliary	12
Gastrointestinal	7
Genitourinary	8
Breast	23
Lung	26

TABLE 2. Inter-observer variability for the detection of bone metastases on all sequences

Sequences	kappa	95 %CI
Precontrast T1W	0.86	0.69–0.92
CE T1W VIBE	0.87	0.77–0.94
AC PET	0.83	0.76–0.90
T1W-PET	0.86	0.78–0.91
CE T1W-PET	0.88	0.82–0.94

AC PET = attenuation-corrected raw data positron-emission tomography; CE = contrast enhanced; VIBE = volume-interpolated breath-hold examination

Discussion

Among the various imaging modalities currently available to detect bone metastasis, hybrid techniques with ^{18}F-FDG PET/CT or PET/MRI which fuse morphological and functional data are the most sensitive and specific. In these hybrid techniques, PET/CT is used much more widely due to its short imaging time advantage and easy accessibility. For this reason, there are many studies comparing the diagnostic sensitivity of PET/CT with other methods. As a result, the superiority of PET/CT for the detection of metastases was reported in most of these studies.[12-16] A meta-analysis including 145 studies compared ^{18}F-FDG PET/CT, CT, MRI, and bone scintigraphy for the detection of bone metastases.[17] The results indicated sensitivity and specificity of PET and MRI higher than for CT and bone scintigraphy alone. While ^{18}F-FDG PET/CT was reported higher sensitivity for osteolytic metastases, the same is not true for osteoblastic metastases. The reason for this might be the different uptake mechanism in osteolytic and osteoblastic bone metastases. Osteoblast activity resulting increase of bone matrix and decrease in cell density resulting lower FDG activation.[18,19] Hence, the diagnostic value of PET/CT will decrease and that of MRI will increase, especially in these osteoblastic metastases.

There are some studies comparing the performance of MRI sequences with PET/CT images.[20-23]

TABLE 3. Diagnostic performance of sequences

Sequences	Sensitivity (%)	Specificity (%)	95%CI	AUC	P	PPV (%)	NPV (%)
Precontrast T1W	78	50	63.2-78.3	0.587 ± 0.064	0.191	75	54
CE T1W VIBE	82	58	67.3-88.9	0.751 ± 0.065	0.024	79	63
AC PET	80	54	67.9-79.4	0.667 ± 0.065	0.013	78	58
T1W-PET	84	61.5	72.2-91.9	0.796 ± 0.063	0.003	81	67
CE T1W-PET	100	92	74.0-99.8	0.952 ± 0.067	0.001	96	100

AC PET = attenuation-corrected raw data positron-emission tomography; AUC = area under the curve; CE = contrast enhanced; CI = confidence interval; NPV = negative predictive value; PPV = positive predictive value; VIBE = volume-interpolated breath-hold examination

For examples, Jambor *et al*. compared the diagnostic accuracy of 99mTc-hydroxymethane diphosphonate (99mTc-HDP) planar bone scintigraphy, 99mTc-HDP SPECT, 99mTc-HDP SPECT/CT, 18F-NaF PET/CT and whole-body MRI, including diffusion weighted imaging, DWI for the detection of bone metastases in high risk breast and prostate cancer patients.[21] As a result, the authors shown that WB MRI DWI and 18F-NaF PET/CT being superior to conventional nuclear imaging techniques for discovering bone metastases. They were also found that, WB MRI DWI was as accurate as 18F-NaF PET/CT for the detection of bone metastases. Considering the cost, availability and radiation dose, WB MRI DWI may be a preferred choice in comparison with 18F-NaF PET/CT. In this study, it was also reported that the sensitivity of PET CT was lower, especially in hypometabolic osteoblastic metastases. Therefore, WB-PET/MRI may be more sensitive in detecting metastases with hypometabolic activity, due to the superior soft tissue resolution of MRI.

There are few studies investigating the diagnostic value of WB-PET/MRI in detecting bone metastases.[24-32] A study has shown that the overall performance of PET/MRI and PET/CT was equivalent for detection and characterization of bone lesions. However, lesion delineation of PET-positive findings was superior in PET/MR imaging with diagnostic T1W TSE or T1W Dixon in-phase sequences compared with PET/CT. This finding might be clinically important for bone metastases with low uptake on PET.[24] Beiderwellen and colleagues examined total of 75 bone lesions, of which 48 lesions were metastases, and 27 lesions were benign.[25] The results indicated that PET/MRI allowed identification of all bone metastases, while PET/CT identified 45 of 48 bone metastases correctly (94%). In benign lesions, PET/CT outperformed PET/MRI by correctly identifying 96% bone lesions compared with 67% in PET/MRI. The benign lesions were missed by PET/MRI consisted of PET negative osteosclerotic lesions. A retrospective study comparing 68 Ga-PSMA PET/MRI and PET/CT in prostate cancer showed higher conspicuity of bone lesions on MRI compared with CT ($p < 0.006$). In conclusion, it was reported PET/MRI has excellent diagnostic performance in evaluating osseous metastases.[32]

As a result of these few studies, the diagnostic superiority of PET/MRI has been reported. However, there is no study comparing the performance of PET/MRI sequences for bone metastases. Our data showed that the CE T1W-PET fused images showed superior lesion detection rate than only PET component. This may reflect the superiority of PET/MRI over PET/CT with its ability to assess early infiltration of bone marrow with malignant tissue with the excellent soft tissue contrast of MRI. Tumor proliferation in the bone marrow results in hypointense T1 and hyperintense T2 signal, as well as relatively strong contrast media uptake, regularly seen in osteolytic disease. In contrast to these findings, the described signal changes might be less pronounced or even absent in osteoblastic metastases because of the lower tumor cellularity.[10,33] The use of morphologic and functional MR imaging techniques enables the assessment of complementary data in bone metastases and increases the accurate assignment of PET-positive findings to anatomic structures.

Our study has limitations, including the limited number of patients and lack of histopathologic

confirmation for every lesion. The results should be considered as preliminary and larger studies are needed to show the potential of FDG-PET/MR. As we know, DWI has high diagnostic accuracy for detecting bone metastases. However, we routinely obtain WB T1W, T2W, CE T1W images, dynamic liver and postcontrast 3D T1W brain images for evaluating of oncologic patients. DWI sequences are not routinely taken in order not to prolong the imaging time further. Therefore, we could not analyze the diagnostic accuracy of DWI images. This is one of the limitations of our study.

For detecting bone metastases, the differences between MRI-based attenuation correction (AC) in PET/MRI and CT-derived AC in PET/CT are especially pronounced. Bone metastases detection relies on accurate AC, and the artifacts in MRI-based AC can significantly impact accuracy and reliability. MRI primarily captures soft tissues based on proton density, and bone, especially cortical bone, produces very low MRI signal. This results in misclassification of bone as soft tissue or air, leading to underestimation of attenuation in bone-dense regions. CT directly measures tissue densities, including bone, providing accurate attenuation values for both cortical and trabecular bone. This makes CT-derived AC highly reliable for bone metastases detection, as bone attenuation is appropriately accounted for. Lesions in bone-rich areas are more likely to be detected and quantified accurately because the higher attenuation of bone is correctly incorporated into the PET images. PET/MRI is more prone to missing metastases near bone-air interfaces (e.g., skull), whereas PET/CT provides better accuracy in these regions. MRI-based AC is more affected by metal artifacts, reducing lesion detectability near metal implants, while CT-based AC is more robust.[34,35]

Replacing PET/MRI with a combination of sequential MRI and PET/CT for lesion detection is a topic of interest in clinical imaging, as each modality offers unique advantages. PET/MRI has the advantage of providing both metabolic and anatomical data in a single session, which can streamline the patient experience and reduce total scan time. This simultaneous acquisition can be especially useful in detecting lesions in soft tissues, such as in neuroimaging (e.g., brain tumors), liver, or prostate, where soft-tissue contrast is critical. Conducting two separate imaging sessions (MRI and PET/CT) requires more logistical coordination and may be time-consuming for the patient. In clinical practice, many institutions already perform PET/CT followed by targeted MRI for specific regions (e.g., brain, liver, prostate), so this workflow is already well established. While MRI provides the same soft-tissue contrast as in PET/MRI, the lack of simultaneous acquisition can sometimes lead to misalignment between PET and MRI data, particularly in organs prone to motion (e.g., lungs, abdomen). But CT-based AC offers better accuracy for bone and air interfaces, leading to more accurate PET quantification, especially in whole-body oncological imaging and detection of bone metastases. PET/MRI offers a lower radiation dose compared to sequential MRI and PET/CT, making it more attractive for cases where minimizing radiation exposure is crucial.[34,35]

In addition to commonly used radionuclides like 99mTc and ^{18}F-FDG, Fluorine-18 Sodium Fluoride (18F-NaF) is highly sensitive for detecting bone metastases because it is rapidly incorporated into the bone matrix at sites of osteoblastic activity, which is typically elevated in metastatic bone lesions. ^{18}F-NaF PET/CT provides higher resolution and more precise localization of bone metastases compared to traditional bone scintigraphy using ^{99}mTc. It is particularly advantageous in patients where early detection is crucial, such as those with breast, prostate, and lung cancers that commonly metastasize to the bone.[36]

Conclusions

In conclusion, our results showed that FDG-PET/MRI may be beneficial in patients with primary malignancy to detect early bone metastasis without radiation exposure. The metabolic information from PET data together with the diagnostic accuracy of CE T1W-PET fused images may increase the sensitivity of detection.

References

1. Yu H, Tsai YY, Hoffe SE. Overview of diagnosis and management of metastatic disease to bone. *Cancer Control* 2012; **19:** 84-91. doi: 10.1177/107327481201900202
2. Baüerle T, Semmler W. Imaging response to systemic therapy for bone metastases. *Eur Radiol* 2009; **19:** 2495-507. doi: 10.1007/s00330-009-1443-1
3. Vassiliou V, Andreopoulos D, Frangos S, Tselis N, Giannopoulou E, Lutz S. Bone metastases: assessment of therapeutic response through radiological and nuclear medicine imaging modalities. *Clin Oncol* 2011; **23:** 632-45. doi: 10.1016/j.clon.2011.03.010
4. O'Sullivan GJ, Carty FL, Cronin CG. Imaging of bone metastasis: an update. *World J Radiol* 2015; **7:** 202. doi: 10.4329/wjr.v7.i8.202
5. Even-Sapir E, Metser U, Mishani E. The detection of bone metastases in patients with high-risk prostate cancer: 99mTc-MDP planar bone scintigraphy, single-and multi-field-of-view SPECT, 18F-fluoride PET, and 18F-fluoride PET/CT. *J Nucl Med* 2006; **47:** 287-97. PMID: 16455635

6. Römer W, Nömayr A, Uder M, Werner Bautz, Torsten Kuwert. SPECT-guided CT for evaluating foci of increased bone metabolism classified as indeterminate on SPECT in cancer patients. *J Nucl Med* 2006; **47:** 1102-6. PMID: 16818944

7. Utsunomiya D, Shiraishi S, Imuta M, Tomiguchi S, Kawanaka K, Morishita S, et al. Added value of SPECT/CT fusion in assessing suspected bone metastasis: comparison with scintigraphy alone and nonfused scintigraphy and CT. *Radiology* 2006; **238:** 264-71. doi: 10.1148/radiol.2373041358

8. Schmidt GP, Schoenberg SO, Schmid R, Stahl R, Tiling R, Becker CR, et al. Screening for bone metastases: whole-body MRI using a 32-channel system versus dual-modality PET-CT. *Eur Radiol* 2007; **17:** 939-49. doi: 10.1007/s00330-006-0361-8

9. Kogan F, Broski SM, Yoon D, Gold GE. Applications of PET-MRI in musculoskeletal disease. *J Magn Reson Imaging* 2018; **48:** 27-47. doi:10.1002/jmri.26183

10. Vanel D, Dromain C, Tardivon A. MRI of bone marrow disorders. *Eur Radiol* 2000; **10:** 224-229. doi: 10.1007/s003300050038

11. Padhani AR, Koh DM, Collins DJ. Whole-body diffusion weighted MR imaging in cancer: current status and research directions. *Radiology* 2011; **261:** 700-18. doi: 10.1148/radiol.11110474

12. Hildebrandt MG, Gerke O, Baun C, Falch K, Hansen JA, Farahani ZA, et al. [181F] fluorodeoxyglucose (FDG)-positron emission tomography (PET)/ computed tomography (CT) in suspected recurrent breast cancer: a prospective comparative study of dual-time-point FDG-PET/CT, contrast-enhanced CT, and bone scintigraphy. *J Clin Oncol* 2016; **34:** 1889-97. doi: 10.1200/JCO.2015.63.5185

13. Park S, Yoon J-K, Lee SJ, Kang SY, Yim H, An Y-S. Prognostic utility of FDG PET/CT and bone scintigraphy in breast cancer patients with bone-only metastasis. *Medicine* 2017; **96:** e8985. doi: 10.1097/MD.0000000000008985

14. Du Y, Cullum I, Illidge TM, Ell PJ. Fusion of metabolic function and morphology: sequential [18F] fluorodeoxyglucose positron-emission tomography/computed tomography studies yield new insights into the natural history of bone metastases in breast cancer. *J Clin Oncol* 2007; **25:** 3440-7. doi: 10.1200/JCO.2007.11.2854

15. Krüger S, Buck AK, Mottaghy FM, Hasenkamp E, Pauls S, Schumann C, et al. Detection of bone metastases in patients with lung cancer: 99mTc-MDP planar bone scintigraphy, 18F-fluoride PET or 18F-FDG PET/CT. *Eur J Nucl Med Mol Imaging* 2009; **36:** 1807. doi: 10.1007/s00259-009-1181-2

16. Hahn S, Heusner T, Kümmel S, Köninger A, Nagarajah J, Müller S, et al. Comparison of FDG-PET/CT and bone scintigraphy for detection of bone metastases in breast cancer. *Acta Radiol* 2011; **52:** 1009-14. doi: 10.1258/ar.2011.100507

17. Yang HL, Liu T, Wang XM, Xu Y, Deng SM. Diagnosis of bone metastases: a meta-analysis comparing 18FDG PET, CT, MRI and bone scintigraphy. *Eur Radiol* 2011; **21:** 2604-17. doi: 10.1007/s00330-011-2221-4

18. Huyge V, Garcia C, Vanderstappen A, Alexiou J, Gil T, Flamen P. Progressive osteoblastic bone metastases in breast cancer negative on FDG-PET. *Clin Nucl Med* 2009; **34:** 417-20. doi: 10.1097/RLU.0b013e3181a7d03c

19. Nakai T, Okuyama C, Kubota T, Yamada K, Ushijima Y, Taniike K, et al. Pitfalls of FDG-PET for the diagnosis of osteoblastic bone metastases in patients with breast cancer. *Eur J Nucl Med Mol Imaging* 2005; **32:** 1253-8. doi: 10.1007/s00259-005-1842-8

20. Liu T, Cheng T, Xu W, Yan WL, Liu J, Yang HL. A metanalysis of 18FDG-PET, MRI and bone scintigraphy for diagnosis of bone metastases in patients with breast cancer. *Skeletal Radiol* 2011; **40:** 523-31. doi: 10.1007/s00256-010-0963-8

21. Jambor I, Kuisma A, Ramadan S, Huovinen R, Sandell M, Kajander S, et al. Prospective evaluation of planar bone scintigraphy, SPECT, SPECT/CT, 18F-NaF PET/CT and whole body 1.5T MRI, including DWI, for the detection of bone metastases in high risk breast and prostate cancer patients: SKELETA clinical trial. *Acta Oncol* 2016; **55:** 59-67. doi: 10.3109/0284186X.2015.1027411

22. Ghanem N, Uhl M, Brink I, Schäfer O, Kelly T, Moser E, et al. Diagnostic value of MRI in comparison to scintigraphy, PET, MS-CT and PET/CT for the detection of metastases of bone. *Eur J Radiol* 2005; **55:** 41-55. doi: 10.1016/j.ejrad.2005.01.016

23. Qu X, Huang X, Yan W, Wu L, Dai K. A meta-analysis of 18 FDG-PET–CT, 18 FDG-PET, MRI and bone scintigraphy for diagnosis of bone metastases in patients with lung cancer. *Eur J Radiol* 2012; **81:** 1007-15. doi: 10.1016/j.ejrad.2011.01.126

24. Eiber M, Takei T, Souvatzoglou M, Fürst S, Gaertner FC, Loeffelbein DJ, et al. Performance of whole-body integrated 18F-FDG PET/ MR in comparison to PET/CT for evaluation of malignant bone lesions. *J Nucl Med* 2014; **55:** 191-7. doi: 10.2967/jnumed.113.123646

25. Beiderwellen K, Huebner M, Heusch P, Grueneisen J, Ruhlmann V, Nensa F, et al. Whole-body [(1)(8)F]FDG PET/MRI vs. PET/CT in the assessment of bone lesions in oncological patients: initial results. *Eur Radiol* 2014; **24:** 2023- 30. doi: 10.1007/s00330-014-3229-3

26. Löfgren J, Mortensen J, Rasmussen SH, Madsen C, Loft A, Hansen AE, et al. A prospective study comparing 99mTc-hydroxyethylene-diphosphonate planar bone scintigraphy and whole-body SPECT/CT with 18F-fluoride PET/CT and 18F-fluoride PET/MRI for diagnosing bone metastases. *J Nucl Med* 2017; **58:** 1778-85. doi: 10.2967/jnumed.116.189183

27. Bruckmann NM, Kirchner IJ, Umutlu L, Fendler WF, Seifert R, Hermann K, et al. Prospective comparison of the diagnostic accuracy of 18F-FDG PET/MRI, MRI, CT, and bone scintigraphy for the detection of bone metastases in the initial staging of primary breast cancer patients. *Eur Radiol* 2021; **31:** 8714-24. doi: 10.1007/s00330-021-07956-0

28. Catalano OA, Nicolai E, Rosen BR, Luongo A, Catalano M, Iannace C, et al. Comparison of CE FDG-PET/CT with CE-FDG-PET/MR in the evaluation of osseous metastases in breast cancer patients. *Br J Cancer* 2015; **112:** 1452-60. doi: 10.1038/bjc.2015.112

29. Sonni I, Minamimoto R, Baratto L, Gambhir SS, Loening AM, Vasanawala SS, et al. Simultaneous PET/MRI in the evaluation of breast and prostate cancer using combined Na[18F] F and [18F]FDG: a focus on skeletal lesions. *Mol Imaging Biol* 2020; **22:** 397-406. doi: 10.1007/s11307-020-01471-2

30. Sawicki LM, Grueneisen J, Schaarschmidt BM, Buchbender C, Nagarajah J, Umutlu L, et al. Evaluation of 18F-FDG PET/MRI, 18F-FDG PET/CT, MRI, and CT in whole-body staging of recurrent breast cancer. *Eur J Radiol* 2016; **85:** 459-65. doi: 10.1016/j.ejrad.2015.12.010

31. Samarin A, Hullner M, Queiroz MA, Stolzmann P, Burger IA, Schulthess G, et al. 18F-FDG-PET/MR increases diagnostic confidence in detection of bone metastases compared with 18F-FDG-PET/CT. *Nucl Med Commun* 2015; **36:** 1165-1173. doi: 10.1097/MNM.0000000000000387

32. Freitag MT, Radtke JP, Hadaschik BA, Kopp-Schneider A, Eder M, Kopka K, et al. Comparison of hybrid 68Ga-PSMA PET/MRI and 68Ga-PSMA PET/CT in the evaluation of lymph node and bone metastases of prostate cancer. *Eur J Nucl Med Mol Imaging* 2016; **43:** 70-83. doi: 10.1007/s00259-015-3206-3

33. Steinborn MM, Heuck AF, Tiling R, Bruegel M, Gauger L, Reiser M. Whole-body bone marrow MRI in patients with metastatic disease to the skeletal system. *J Comput Assist Tomogr* 1999; **23:** 123-9. doi: 10.1097/00004728-199901000-00026

34. Zhan Y, Zhang G, Li M, Zhou X. Whole-body MRI vs. PET/CT for the detection of bone metastases in patients with prostate cancer: a systematic review and meta-analysis. *Front Oncol* 2021; **11:** 633833. doi: 10.3389/fonc.2021.633833

35. Bashir U, Mallia A,Stirling J, Joemon J, MacKewn J, Charles-Edwards G, et al. PET/MRI in oncological imaging: state of the art. *Diagnostics* 2015; **5:** 333-57. doi: 10.3390/diagnostics5030333

36. Araz M, Aras G, Kucuk ON. The role of 18F-NaF PET/CT in metastatic bone disease. *J Bone Oncol* 2015; **16:** 92-7. doi: 10.1016/j.jbo.2015.08.002

research article

The initial results of MRI-TRUS fusion prostate biopsy in high volume tertiary center

Tomaz Smrkolj[1,2], Milena Taskovska[1,2], Iztok Ditz[1,2], Klemen Cernelc[1], Simon Hawlina[1,2]

[1] Department of Urology, Ljubljana University Medical Centre, Ljubljana, Slovenia
[2] Chair of Surgery, Faculty of Medicine, University of Ljubljana, Ljubljana, Slovenia

Radiol Oncol 2024; 58(4): 501-508.

Received 9 June 2024
Accepted 9 October 2024

Correspondence to: Assist. Prof. Simon Hawlina, M.D., Ph.D., Chair of Surgery, Faculty of Medicine, University of Ljubljana, Ljubljana, Slovenia. E-mail: simon.hawlina@kclj.si

Disclosure: No potential conflicts of interest were disclosed.

Background. Multiparametric magnetic resonance imaging (mpMRI) is a prerequisite for targeted prostate biopsy. The aim of our study was to evaluate the performance and learning curve of the mpMRI- transrectal ultrasound (TRUS) software image fusion (MRI-TRUS fusion) biopsy (BX) process in the first year after its introduction in our urology department.

Patients and methods. MRI-TRUS fusion BX was performed in 293 patients with at least one Prostate Imaging-Reporting and Data System (PIRADS) ≥3 lesion. The proportion of patients and lesions with positive histopathologic result for prostate cancer (PCa) was analyzed. The learning curve for MRI-TRUS fusion BX was assessed at institutional and individual level. Positive BX lesions were further analyzed by PIRADS and Gleason scores.

Results. The proportion of patients with positive histopathologic results for targeted BX, systematic BX, and combined BX was 53.9%, 47.9%, and 63.5%, respectively. The chi-square test for the proportion of PCa positive patients showed no significant difference between the time-based patient groups at the institutional level and no significant difference between individual urologists. PIRADS score ($p < 0.001$), total PSA concentration ($p = 0.05$), prostate volume ($p < 0.001$) and number of cores per lesion ($p = 0.034$) were significant predictors of a positive histopathologic result in a lesion-based analysis. Clinically significant PCa (csPCa) was confirmed in 34.7% of the 412 BX lesions and 76.4% of the 187 positive PCa lesions.

Conclusions. MRI-TRUS fusion targeted BX significantly improves the overall rate of PCa detection compared with systematic BX alone. No steep learning curve was observed in our urologists. The proportion of lesions with clinically insignificant PCa was low, limiting overdiagnosis of PCa.

Key words: prostate cancer; targeted prostate biopsy; learning curve; complications

Introduction

Prostate cancer (PCa) is the second most common cancer in men worldwide. The estimated age-standardized incidence rate is highest in Western and Northern Europe, North America, Australia and New Zealand.[1] In Slovenia, PCa is the most common solid neoplasm in men (excluding skin cancer) with a share of 18.6% and an estimated incidence rate of 162 per 100,000 in 2022.[2] The incidence rate of PC in Western countries and Slovenia has increased dramatically from the early 1990s to the last decade, mainly due to the use of prostate specific antigen (PSA) as a tumor marker for PCa.[2-4]

PSA is a serine protease that is produced almost exclusively by epithelial cells in the prostate. Therefore, serum PSA is an organ specific marker that can be elevated in benign prostate diseases such as inflammation and prostate enlargement in addition to PCa.[5,6] The majority of men with elevated PSA levels and/or suspicious digitorectal examination (DRE) of prostate underwent tran-

srectal (systematic) template biopsy (BX) in the first decades after the introduction of the PSA to confirm the PCa diagnosis and initiate treatment. Systematic BX templates have evolved over the years in terms of the number and location of cores[7,8], however, these templates have focused primarily on the posterior and lateral peripheral zones and much less on the transitonal zone and anterior portion of the prostate.

The natural history of PCa in many older men is protracted and does not cause significant health problems during their expected lifespan. The concept of incidentally found and clinically insignificant PCa (cisPCa) was introduced to reduce the risk of overtreatment.[3,9]

To limit the number of unnecessary BXs in men with elevated PSA due to benign disease or cisPCa, novel tumor markers have been developed that may aid in the decision to perform BX, e.g., pro-PSA, Prostate Health Index, prostate cancer antigen 3 (PCA3), Select MDX[10-13], however, tumor markers do not provide information about the location of PCa within the prostate.

In the last ten years, multiparametric magnetic resonance imaging (mpMRI) has become the imaging modality of choice for the diagnosis of PCa.[14] mpMRI has an excellent sensitivity of 91% to 95% for clinically significant PCa (csPCa) and a low yield (21% to 29%) for small cisPCa, while having a high negative predictive value (NPV) of 63% to 98%.[15-17] mpMRI reporting has been standardized in the Prostate Imaging-Reporting and Data System (PIRADS) and each lesion is classified into one of 5 groups of increasing risk for csPCa according to radiological criteria.[18]

Another major advantage of mpMRI is that it provides information about the exact location of the suspicious lesion in the prostate. In the pre-mpMRI era, suspicious hipoehoic lesions in the prostate were identified with transrectal ultrasound (TRUS) in about half of patients with PCa.[19,20] With mpMRI, it is possible to identify suspicious lesions on the BX under cognitive guidance, TRUS – mpMRI software image fusion (MRI-TRUS fusion) or in-bore MRI BX. Although some studies found no significant difference between the performance of the three BX targeting methods mentioned above[21,22], other studies report advantages of MRI-TRUS fusion and in-bore MRI BX compared to cognitive guidance.[23,24]

The aim of our study was to evaluate the performance and learning curve of the MRI-TRUS fusion BX process in the first year after its introduction in a high-volume clinical setting.

Patients and methods

Patients

The study was approved by the National Medical Ethics Committee of the Republic of Slovenia (0120-69/2023/3) and was conducted in full compliance with the principles of the Declaration of Helsinki.

Patients with at least one clearly defined PIRADS ≥ 3 lesion who underwent MRI-TRUS fusion targeted BX in an outpatient clinic of the Urology Department of UMC Ljubljana were included in the study. The exclusion criteria were: no clearly defined suspicious lesion on mpMRI of the prostate, patients in whom only systematic BX was performed, patients with a contraindication for transrectal ultrasound (TRUS) BX, in whom biopsy was cancelled.

A total of 293 patients who underwent MRI-TRUS fusion targeted BX between June 2021 and June 2022 were retrospectively included in our study.

Detection methods

Multiparametric MRI

In patients scheduled for MRI-TRUS fusion targeted BX, mpMRI was performed by different radiologists on different MRI machines in several public hospitals and several private centers in the Republic of Slovenia. The choice of center for mpMRI was at the discretion of the patients.

Contouring of MRI lesions

Contouring of prostate boundaries and each suspicious lesion was performed using MIM software (version 7.1.2, MIM software inc., Cleveland, OH, USA) by 3 certified urologists (with 19, 7 and 6.5 years of experience on systematic BX) who had previously participated in several certified mpMRI reading courses. Each radiologist-reported lesion with PIRADS ≥ 3 was identified and contoured on the T2 axial, T2 sagital, DWI and ADC mpMRI maps. In a minority of cases, T1 contrast-enhanced axial mpMRI maps had to be reviewed to clearly identify the lesion. PIRADS score of a lesion and its largest diameter were recorded for further analysis.

Transrectal MRI fusion targeted BX

All patients received peroral antibiotic prophylaxis with phosphomycin (3g) the evening before BX. No bowel preparation or swab sampling was

performed before the procedure. MRI-TRUS fusion targeted BX was performed on a bk3000 ultrasound machine (BK Medical Holding Company, Inc., Peabody, Massachusetts, USA) equipped with freehand 3D electromagnetic tracking device (Ascension Technology Corporation, Shelburne, VT, USA) with MIM software (version 6.9.7, MIM software inc., Cleveland, OH, USA) installed. A Triplane 12 MHz transrectal transducer was used in all patients. Prior to BX, a periprostatic anesthetic block with 6 ml of 2% lidocaine was administered bilaterally at the base of the prostate through the BX needle sheath. During the BX session, DRE of the prostate was performed and the volume of the prostate was measured by TRUS examination. During targeted BX, up to three contoured lesions were sampled from each patient. Systematic BX was then performed on the remaining, non-sampled lateral peripheral zone of the prostate. The number of systematic BX cores depended on the number and position of the targeted BX cores and prostate volume. Post-BX complications were determined via the hospital information system by reviewing patient records within the 1-month post-biopsy period.

The number of certified urologists and residents performing MRI-TRUS fusion targeted BX gradually increased over the 1-year period. Each new member of the BX team was instructed in image fusion and the proper technique of targeted BX and was supervised by one of the three certified urologists of the contouring team for at least 5 to 10 patients.

Histopathology report

The BX cores of the patients were analyzed in the histopathology laboratory of the Institute of Pathology at the Faculty of Medicine in Ljubljana, Slovenia. The histopathologic results were divided into two categories: *the negative group* (BPH, prostatitis and high-grade prostatic intraepithelial neoplasia (HGPIN)) and *the positive - malignant group* (PCa, atypical small acinar proliferation (ASAP) and suspected PCa). Gleason grade and score of each targeted lesion and systemic biopsy cores were noted separately for analysis. We defined csPCa as a Gleason score ≥ 7 and a Gleason grade group ≥ 2.

Statistical analysis

Data were analyzed using SPSS software (Statistical Package for the Social Sciences, version 29.0, IBM Corp., Armonk, NY, USA). Mean, median, minimum value, maximum value and standard deviation were used to indicate numerical variables. The proportion of positive histopathologic results was calculated for both patient-based and lesion-based analysis. Pearson's chi-square test was used to analyze the effects of categorical variables on the proportion of patients with positive histopathological findings. Univariate binary logistic regression was performed to analyze the impact of numeric variables on the proportion of patients with positive histopathology. In the lesion-based analysis, a multiple binary logistic regression analysis was performed for numeric and categorical covariates affecting a positive histopathologic result. The proportion of post-procedural complications was calculated. A p-value of less than 0.05 was considered statistically significant.

TABLE 1. Patient and lesion characteristics

	min	max	mean ± SD	median
Age (years)	35	91	69.0 ± 7.9	70.0
*Total PSA concentration (ng/mL)	0.45	115.4	9.7 ± 11.7	7.0
Prostate volume (ml)	15	313	52.8 ± 32.3	45
No. lesions biopsied in a patient	1	3	1.4 ± 0.6	1.0
Largest diameter of lesion (mm)	3.0	41.0	12.8 ± 6.6	11.5
No. of cores per lesion targeted BX	1	8	4.26 ± 1.2	4.0
No. of cores systematic BX	0	14	6.9 ± 1.8	6.0
No. of MRI-TRUS fusion targeted BX performed by urologist before	1	65	22.5 ± 19.7	20.0

*PSA = in patients with 5-alpha reductase inhibitors (5ARI) therapy total PSA concentration was doubled. Number of patients is 293, number of lesions is 412.

BX = biopsy; MRI-TRUS = magnetic resonance imaging - transrectal ultrasound; SD = standard deviation

Results

In the first year, we performed MRI-TRUS fusion targeted BX in 293 patients, while systematic BX was performed in 288 of these patients. In 25 patients 3 targeted lesions were sampled, in 69 patients 2 lesions were sampled and in the remaining 199 patients 1 lesion was sampled (Table 1).

Patient based analysis

The proportion of patients with a positive histopathologic result for targeted BX, where at least one of the targeted BX was positive, was 53.9% (158/293). The proportion of patients with a posi-

TABLE 2. Comparison of time-based patient groups for learning curve estimation on institution level

	Targeted BX			Systematic BX			Overall BX		
	Pearson χ^2	df	sig	Pearson χ^2	df	sig	Pearson χ^2	df	sig
2 patient groups	0.458	1	0.498	0.658	1	0.417	0.291	1	0.590
3 patient groups	2.145	2	0.342	2.265	2	0.322	1.373	2	0.503
6 patient groups	4.807	5	0.440	2.872	5	0.720	2.322	5	0.803

BX = biopsy; df = degrees of freedom; sig = significance

tive histopathology result for systematic BX was 47.9% (138/288). The overall proportion of patients with positive histopathology for at least one targeted or systematic BX was 63.5% (186/288). 28 patients with negative targeted BX had positive systematic BX, and in this group histopathology reports had identified 3 patients with ASAP, 10 patients with G6 (3+3), 9 patients with G7 (3+4), 3 patients with G7 (4+3), 2 patients with G8 (4+4) and one patient with G9 (4+5). Therefore, the targeted BX alone would have missed 5.2% (15/288) csPCa in all patients who had targeted BX and added 4.5% (13/288) cisPCa.

To assess the impact of the learning curve on the proportion of patients with a positive histopathologic result for targeted BX, systematic BX, and overall BX (targeted and systematic BX combined) at the institutional level, a chi-square test for independence was performed. Based on the date of BX, patients were divided into two, three and six time-based groups (Table 2). No significant differences were found.

A chi-square test of independence was performed to assess the effect of the learning curve on the proportion of patients with a positive histopathologic result for targeted BX, systematic BX, and overall BX at the individual urologist level. For targeted BX, Pearson χ2, df and sig were 9.124, 12 and 0.692, respectively. For systematic BX Pearson χ2, df and sig were 10.431, 12 and 0.578, respectively. For overall BX Pearson χ2, df and sig were 9.465, 12 and 0.613, respectively. In addition, univariate binary logistic regression analysis of the effect of the number of previous MRI-TRUS fusion targeted BX sessions performed by a urologist on the probability of a positive histopathologic result at subsequent BX yielded odds ratios of 1.011 (p = 0.169), 1.007 (0.372), and 1.014 (p = 0.107) for targeted BX, systematic BX, and overall BX (targeted and systematic combined), respectively. No significant differences were found.

TABLE 3. Proportion of positive targeted biopsy (BX) lesions categorised by Prostate Imaging-Reporting and Data System (PIRADS) score

	Negative BX	Positive BX	Total
PIRADS 3 (%)	104 (81.9%)	**23 (18.1%)**	127
PIRADS 4 (%)	108 (52.9%)	**96 (47.1%)**	204
PIRADS 5 (%)	13 (16.0%)	**68 (84.0%)**	81

Lesion based analysis

Of 412 targeted BX lesions, 187 were positive for PCa (45.4%). 127 lesions were classified as PIRADS 3 (30.8%), 204 lesions as PIRADS 4 (49.5%) and 81 lesions as PIRADS 5 (19.7%). The proportion of positive targeted BX lesions increased with increasing PIRADS score (Table 3).

Multiple binary logistic regression analysis on the covariates influencing a positive histopathologic result in targeted BX of a lesion revealed significant odds ratios for prostate volume, total PSA concentration, PIRADS score, and number of cores per sampled lesion (Table 4).

Our results show that 20.9% of all positive lesions had a Gleason score of 6 (International Society of Urological Pathology (ISUP) grade group 1), representing a cisPCa, while 76.4% had a Gleason score of 7 or more (ISUP grade group ≥2), representing a csPCa (Figure 1).

Stratifying Gleason score of lesions across PIRADS 3 category shows that 56.5% of the positive lesions had a Gleason score of 7 (Figure 2).

Complication rate analysis

Of the 293 patients, 13 (4.4%) were found to have complications. The infectious complications that required hospitalization were: epididymitis in 1 patient (0.3%), prostatitis in 5 patients (1.7%) and urosepsis in 2 patients (0.7%). Hematuria treated on an outpatient basis was observed in 2 patients

TABLE 4. Results of multiple logistic regression of positive histopathologic result

	Sig	Odds ratio	95% C.I. for odds ratio	
			Lower	Upper
Max lesion diameter	0.945	0.998	0.955	1.044
Prostate volume	**< 0.001**	**0.978**	**0.968**	**0.988**
***Total PSA concentration**	**0.050**	**1.050**	**1.000**	**1.103**
PIRADS 3	**< 0.001**			
PIRADS 4	**< 0.001**	**3.208**	**1.848**	**5.567**
PIRADS 5	**< 0.001**	**16.222**	**6.475**	**40.645**
Number of cores per lesion	**0.034**	**1.238**	**1.016**	**1.508**
Number of previous patients with targeted BX performed by urologist	0.113	1.013	0.997	1.028

*PSA = in patients with 5-alpha reductase inhibitors (5ARI) therapy PSA concentration was doubled.

BX = biopsy; C.I. = confidence interval; PIRADS = Prostate Imaging-Reporting and Data System score; Sig = significance

(0.7%). Minor complications immediately after BX (nausea, syncope and dizziness) occurred in 3 patients (0.9%).

Discussion

Patient based analysis discussion

In our study, we evaluated the performance and learning curve of the MRI-TRUS fusion BX process in the first year after its introduction in our department. Compared with our previous series from before the mpMRI era, which was based on data from 5272 patients with systematic BX (2009 to 2013) and in which 39.8% patients had a positive histopathologic result[25], the present study showed a significantly higher proportion of patients with a positive histopathologic result in both targeted and systematic BX (53.9% and 47.9%, respectively) and overall BX (targeted plus systematic BX) (63.9%). In addition, the number of patients undergoing prostate BX has significantly decreased from an average of 1054 patients per year in 2009–2013 to 391 patients per year (293 patients with targeted and systematic BX in the study and 98 patients with systematic BX only who were not included in the study) due to mpMRI, which is now a main diagnostic method for the indication of BX in patients with elevated PSA concentration. Our present data are similar to the results of a recent study that reported a positive histopathologic result for systematic BX in 57% of patients and for general BX in 68% of patients.[26] Although the advantage of targeted BX over systematic BX seems obvious, systematic BX adds up to 11% over targeted PCa detection rates alone, so the combination of targeted and systematic BX is still recommended.[27] In addition, Malewski *et al*. investigated the added value of systematic BX in patients with PIRADS 5 lesions and argued that the identification of other PCa foci besides the index lesion with systemic BX could influence the treatment decision.[28]

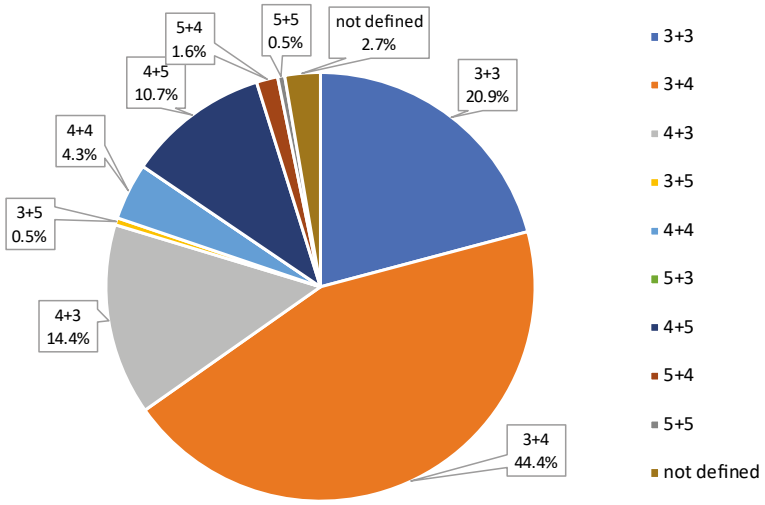

FIGURE 1. Gleason score of all positive biopsy (BX) lesions. Category »not defined« includes lesions with suspect cores for carcinoma, undefined Gleason score in invasive carcinoma and atypical small acinar proliferation (ASAP).

Contrary to expectations, we did not observe significant differences in the proportions of patients with positive histopathologic result in targeted, systematic and overall BX when patients were stratified into time-based groups (2, 3, or 6 groups), which should reflect the learning curve for the overall MRI-TRUS fusion process of targeted BX in our department at the institutional

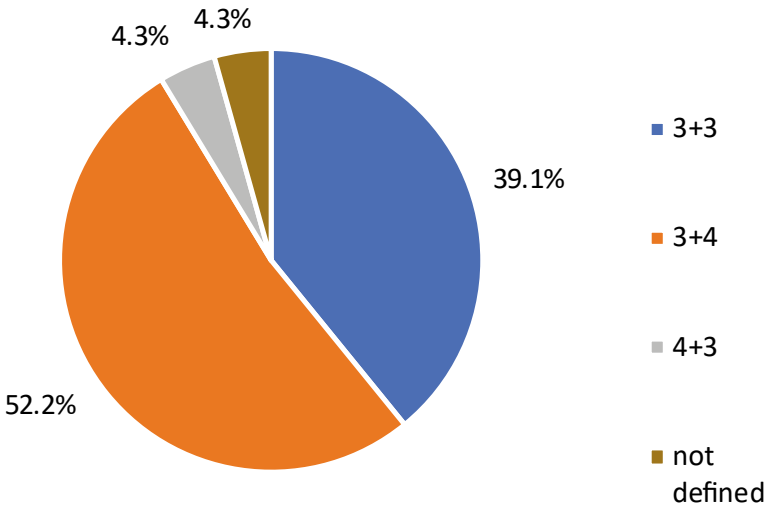

FIGURE 2. Gleason score of Prostate Imaging-Reporting and Data System (PIRADS) 3 positive biopsy (BX) lesions.

level, including the process of identifying lesions described in the radiologic report and contouring them. Comparison of PCa detection rates between urologists also showed no significant differences, although the number of BX sessions varied significantly between urologists. According to studies, the learning curve of MRI-TRUS fusion in targeted BX flattens out at the individual level between 50 and 100 patients[29,30], however, another study that followed the progress of a single novice urologist found only an increased rate of positive cores in targeted BX, but not a significantly higher proportion of patients with positive histopathologic result in the second group of 42 patients compared to the first group of 42 patients.[31] In addition, a recent study comparing the results of MRI-TRUS fusion targeted BX between consultants and trained residents found no significant difference in PCa detection rates, duration of the procedure, pain, or complication rates of the BX procedure.[32] One of the reasons for variable results in terms of learning curve may suggest that the technological advancement of MRI-TRUS fusion-targeted BX devices has reached a level where individual differences between operators are mitigated.

Lesion based analysis discussion

In the second part of our study, we focused on the targeted lesion analysis. The most important variable influencing the probability of a lesion being PCa positive is the PIRADS classification, followed by prostate volume, the number of cores taken from a lesion and the total PSA concentration. The odds ratio for a positive PIRADS 4 and 5 lesion is more than 3 and 16 times higher, respectively, than for a PIRADS 3 lesion. Surprisingly, the maximum lesion diameter had no significant influence on the probability of a lesion being PCa positive. The rates of positive lesions stratified by PIRADS category in our study, with the exception of PIRADS 4, are similar to the results of a recent study in which 17%, 63%, and 88% of all lesions were positive in PIRADS 3, 4, and 5, respectively.[33] The low rate of positive targeted BX in PIRADS 3 lesions raises the question of whether PIRADS 3 lesions should undergo BX at all. Figure 2 suggests that if PIRADS 3 lesions were excluded from BX, 56.5% PIRADS 3 lesions with csPCa would have been missed, but the absolute number of missed lesions in our study would be only 13. Schenker *et al*. have reported that although PIRADS 3 lesions have an equivocal probability of csPCa, their study found an overall PCa detection rate of only 26.8% and 14.6% for csPCa in these lesions, respectively[34], while Nicola *et al*. have suggested that PSA density, age, and tumor volume should be considered when deciding on BX of PIRADS 3 lesions.[35]

In the present study, the proportion of csPCa-positive lesions among all targeted BX lesions was 34.7% (76.4% of 45.4% lesions), which is comparable to data from the literature.[36] Of all positive lesions, 76.4% were csPCa, suggesting a relatively low rate of PCa overdiagnosis in our series.

Discussion on complication rates

One of the main reasons why the EAU guidelines recommend the transperineal approach for prostate biopsy is the lower rate of postprocedural infectious complications, even though the transperineal approach is often associated with significant logistical problems[3], which are particularly problematic for high-volume centers (e.g., the need for general anesthesia in the operating room and the longer duration of the procedure). Our data show that the cumulative hospitalization rate due to infectious complications with the transrectal approach was 2.7%, but most of the patients received only one dose of antibiotic prophylaxis with phosphomycin the evening before BX during the study period, which was adjusted the following year with an additional dose of phosphomycin 24 hours after the procedure. The sepsis rate was 0.7% in the first

year, which is significantly lower than in a recent meta-analysis of transrectal procedures, in which the subgroup of patients with antibiotic prophylaxis had a sepsis rate of 1.7%, and comparable to the subgroup of patients who received rectal disinfection with povidone-iodine before BX in addition to antibiotic prophylaxis (0.6%). Furthermore, our sepsis rate was significantly lower compared to a UK national study of 73630 patients comparing the transperineal (1.03% sepsis rate) to the transrectal (1.35% sepsis rate) approach[37], and comparable to the sepsis rates (0.7%) cited by Cheng *et al*. who also estimate the cumulative rate of infectious conditions to be 2%.[37] In addition, the ProBE-PC clinical trial compared infectious and noninfectious complications in 351 and 367 patients undergoing transrectal and transperineal prostate BX, respectively. Cumulative infectious events occurred in 2.6% and 2.7% of participants for transrectal and transperineal prostate BX, respectively, while none of the participants in either group developed sepsis.[38]

Besides retrospecitve nature, the main limitation of the present study is the relatively large number of participating urologists and radiologists from different radiology centers with different MRI equipment in Slovenia, which resulted in considerable heterogeneity in the reporting of mpMRI and performing MRI-TRUS fusion BX and might also affect our results and conclusions on learning curve. On the other hand, this shortcoming is mitigated to some extent by the large number of patients in the study and the fact that prostate contouring and supervision of BX process was performed by a small number of experienced urologists. In addition, the results reflect the real-life circumstances in high-volume centers where it is rarely possible to ensure strictly regulated research conditions. Patel *et al*. analyzed reports from 10 radiologists performing mpMRI and 5 urologists performing MRI-TRUS fusion BX PCa in 865 patients to estimate individual variability in overall and csPCa detection rates and found significant variability among radiologists but not among urologists, although both rates improved over time. They concluded that improving the quality of mpMRI PIRADS reporting is a key area to focus on.[36]

Conclusions

The introduction of MRI-TRUS fusion to targeted BX significantly improves the overall rate of PCa detection compared to systematic BX alone, however systematic BX should still be performed during targeted BX session in the contemporary clinical practice. Due to the simplified technical aspects of the BX procedure, no steep learning curve was observed among our urologists. The proportion of lesions with cisPCa was low, limiting the overdiagnosis of PCa. The rate of infectious complications was acceptable and not inferior to published data on transrectal and transperineal BX.

AI disclosure

Statement: During the preparation of this paper, the authors used InstaText for Word tool to improve English language in the manuscript. After using this tool, the authors have reviewed and edited the content as required and take full responsibility for the content of the publication.

References

1. Culp MB, Soerjomataram I, Efstathiou JA, Bray F and Jemal A. Recent global patterns in prostate cancer incidence and mortality rates. *Eur Urol* 2020; **77:** 38-52. doi: 10.1016/j.eururo.2019.08.005
2. Zadnik V, Gašljević G, Hočevar M, Jarm K, Pompe-Kirn V, Strojan P, et al. *Cancer in Slovenia 2019*. [Internet]. Oncology Institute Ljubljana. Cancer Epidemiology and Registry. Cancer Registry of the Republic of Slovenia; 2022. p. 1-65. [cited 2024 May 27]. Available at: https://www.onko-i.si/rrs
3. Cornford P, Tilki D, van den Bergh RCN, Briers E, Eberli D, De Meerleer M, et al. Prostate cancer. *EAU guidelines 2024*. [Internet]. European Association of Urology; 2024. [cited 2024 May 27]. Available at: https://uroweb.org/guidelines/prostate-cancer
4. Stamey TA, Yang N, Hay AR, McNeal JE, Freiha FS and Redwine E. Prostate-specific antigen as a serum marker for adenocarcinoma of the prostate. *N Engl J Med* 1987; **317:** 909-16. doi: 10.1056/NEJM198710083171501
5. Sokoll LJ, Chan DW, Mikolajczyk SD, Rittenhouse HG, Evans CL, Linton HJ, et al. Proenzyme psa for the early detection of prostate cancer in the 2.5-4.0 ng/ml total psa range: preliminary analysis. *Urology* 2003; **61**: 274-6. doi: 10.1016/s0090-4295(02)02398-1
6. Hedelin H, Johansson N and Stroberg P. Relationship between benign prostatic hyperplasia and lower urinary tract symptoms and correlation between prostate volume and serum prostate-specific antigen in clinical routine. *Scand J Urol Nephrol* 2005; **39:** 154-9. doi: 10.1080/00365590510007685
7. Chambo RC, Tsuji FH, de Oliveira Lima F, Yamamoto HA and de Jesus CM. What is the ideal core number for ultrasound-guided prostate biopsy? *Korean J Urol* 2014; **55:** 725-31. doi: 10.4111/kju.2014.55.11.725
8. Walz J, Graefen M, Chun FK, Erbersdobler A, Haese A, Steuber T, et al. High incidence of prostate cancer detected by saturation biopsy after previous negative biopsy series. *Eur Urol* 2006; **50**: 498-505. doi: 10.1016/j.eururo.2006.03.026
9. Bell KJ, Del Mar C, Wright G, Dickinson J and Glasziou P. Prevalence of incidental prostate cancer: a systematic review of autopsy studies. *Int J Cancer* 2015; **137:** 1749-57. doi: 10.1002/ijc.29538
10. Jansen FH, van Schaik RH, Kurstjens J, Horninger W, Klocker H, Bektic J, et al. Prostate-specific antigen (PSA) isoform p2PSA in combination with total PSA and free PSA improves diagnostic accuracy in prostate cancer detection. *Eur Urol* 2010; **57:** 921-7. doi: 10.1016/j.eururo.2010.02.003
11. Loeb S and Catalona WJ. The Prostate Health Index: a new test for the detection of prostate cancer. *Ther Adv Urol* 2014; **6:** 74-7. doi: 10.1177/1756287213513488

12. Deras IL, Aubin SM, Blase A, Day JR, Koo S, Partin AW, et al. PCA3: a molecular urine assay for predicting prostate biopsy outcome. *J Urol* 2008; **179:** 1587-92. doi: 10.1016/j.juro.2007.11.038

13. Van Neste L, Hendriks RJ, Dijkstra S, Trooskens G, Cornel EB, Jannink SA, et al. Detection of high-grade prostate cancer using a urinary molecular biomarker-based risk score. *Eur Urol* 2016; **70:** 740-8. doi: 10.1016/j.eururo.2016.04.012

14. Futterer JJ. Multiparametric MRI in the detection of clinically significant prostate cancer. *Korean J Radiol* 2017; **18:** 597-606. doi: 10.3348/kjr.2017.18.4.597

15. Drost FH, Osses DF, Nieboer D, Steyerberg EW, Bangma CH, Roobol MJ, et al. Prostate MRI, with or without MRI-targeted biopsy, and systematic biopsy for detecting prostate cancer. *Cochrane Database Syst Rev* 2019; **4:** CD012663. doi: 10.1002/14651858.CD012663.pub2

16. Bratan F, Niaf E, Melodelima C, Chesnais AL, Souchon R, Mege-Lechevallier F, et al. Influence of imaging and histological factors on prostate cancer detection and localisation on multiparametric MRI: a prospective study. *Eur Radiol* 2013; **23:** 2019-29. doi: 10.1007/s00330-013-2795-0

17. Futterer JJ, Briganti A, De Visschere P, Emberton M, Giannarini G, Kirkham A, et al. Can clinically significant prostate cancer be detected with multiparametric magnetic resonance imaging? A systematic review of the literature. *Eur Urol* 2015; **68:** 1045-53. doi: 10.1016/j.eururo.2015.01.013

18. Weinreb JC, Barentsz JO, Choyke PL, Cornud F, Haider MA, Macura KJ, et al. PI-RADS Prostate Imaging - Reporting and Data System: 2015, Version 2. *Eur Urol* 2016; **69:** 16-40. doi: 10.1016/j.eururo.2015.08.052

19. Xu G, Li JH, Xiang LH, Yang B, Chen YC, Sun YK, et al. Transrectal ultrasound examination of prostate cancer guided by fusion imaging of multiparametric MRI and TRUS: avoiding unnecessary mpMRI-guided targeted biopsy. *Asian J Androl* 2023; **25:** 410-5. doi: 10.4103/aja202276

20. Littrup PJ and Bailey SE. Prostate cancer: the role of transrectal ultrasound and its impact on cancer detection and management. *Radiol Clin North Am* 2000; **38:** 87-113. doi: 10.1016/s0033-8389(05)70151-2

21. Wegelin O, Exterkate L, van der Leest M, Kummer JA, Vreuls W, de Bruin PC, et al. The FUTURE Trial: a multicenter randomised controlled trial on target biopsy techniques based on magnetic resonance imaging in the diagnosis of prostate cancer in patients with prior negative biopsies. *Eur Urol* 2019; **75:** 582-90. doi**:** 10.1016/j.eururo.2018.11.040

22. Simmons LAM, Kanthabalan A, Arya M, Briggs T, Barratt D, Charman SC, et al. Accuracy of transperineal targeted prostate biopsies, visual estimation and image fusion in men needing repeat biopsy in the PICTURE Trial. *J Urol* 2018; **200:** 1227-34. doi: 10.1016/j.juro.2018.07.001

23. Wegelin O, van Melick HHE, Hooft L, Bosch J, Reitsma HB, Barentsz JO, et al. Comparing three different techniques for magnetic resonance imaging-targeted prostate biopsies: a systematic review of in-bore versus magnetic resonance imaging-transrectal ultrasound fusion versus cognitive registration. Is there a preferred technique? *Eur Urol* 2017; **71:** 517-31. doi: 10.1016/j.eururo.2016.07.041

24. Watts KL, Frechette L, Muller B, Ilinksy D, Kovac E, Sankin A, et al. Systematic review and meta-analysis comparing cognitive vs. image-guided fusion prostate biopsy for the detection of prostate cancer. *Urol Oncol* 2020; **38:** 734 e19- e25. doi: 10.1016/j.urolonc.2020.03.020

25. Smrkolj T. [Transrectal ultrasound and needle biopsy of the prostate]. [Slovenian]. *Zdrav Vestn* 2015; **84:** 834-42. doi: 10.6016/ZdravVestn.1299

26. Ortner G, Mavridis C, Fritz V, Schachtner J, Mamoulakis C, Nagele U, et al. The added value of MRI-based targeted biopsy in biopsy-naive patients: a propensity-score matched comparison. *J Clin Med* 2024; **13:** 1. doi: 10.3390/jcm13051355

27. Connor MJ, Miah S, Jayadevan R, Khoo CC, Eldred-Evans D, Shah T, et al. Value of systematic sampling in an mp-MRI targeted prostate biopsy strategy. *Transl Androl Urol* 2020; **9:** 1501-9. doi: 10.21037/tau.2019.07.16

28. Malewski W, Milecki T, Szemplinski S, Tayara O, Kuncman L, Kryst P, et al. Prostate biopsy in the case of PIRADS 5 - is systematic biopsy mandatory? *J Clin Med* 2023; **12:** 5612. doi: 10.3390/jcm12175612

29. Kasabwala K, Patel N, Cricco-Lizza E, Shimpi AA, Weng S, Buchmann RM, et al. The learning curve for magnetic resonance imaging/ultrasound fusion-guided prostate biopsy. *Eur Urol Oncol* 2019; **2:** 135-40. doi: 10.1016/j.euo.2018.07.005

30. Xu L, Ye NY, Lee A, Chopra J, Naslund M, Wong-You-Cheong J, et al. Learning curve for magnetic resonance imaging/ultrasound fusion prostate biopsy in detecting prostate cancer using cumulative sum analysis. *Curr Urol* 2023; **17:** 159-64. doi: 10.1097/CU9.0000000000000116

31. Mager R, Brandt MP, Borgmann H, Gust KM, Haferkamp A and Kurosch M. From novice to expert: analyzing the learning curve for MRI-transrectal ultrasonography fusion-guided transrectal prostate biopsy. *Int Urol Nephrol* 2017; **49:** 1537-44. doi: 10.1007/s11255-017-1642-7

32. Turchi B, Lombardo R, Franco A, Tema G, Nacchia A, Cicione A, et al. Residents and consultants have equal outcomes when performing transrectal fusion biopsies: a randomized clinical trial. *Curr Oncol* 2024; **31:** 747-58. doi: 10.3390/curroncol31020055

33. Rodriguez-Cabello MA, Mendez-Rubio S, Sanz-Miguelanez JL, Moraga-Sanz A, Aullo-Gonzalez C and Platas-Sancho A. Prevalence and grade of malignancy differences with respect to the area of involvement in multiparametric resonance imaging of the prostate in the diagnosis of prostate cancer using the PI-RADS version 2 classification. *World J Urol* 2023; **41:** 2155-63. doi: 10.1007/s00345-023-04466-0

34. Schlenker B, Apfelbeck M, Armbruster M, Chaloupka M, Stief CG and Clevert DA. Comparison of PIRADS 3 lesions with histopathological findings after MRI-fusion targeted biopsy of the prostate in a real world-setting. *Clin Hemorheol Microcirc* 2019; **71:** 165-70. doi: 10.3233/CH-189407

35. Nicola R and Bittencourt LK. PI-RADS 3 lesions: a critical review and discussion of how to improve management. *Abdom Radiol (NY)* 2023; **48:** 2401-5. doi: 10.1007/s00261-023-03929-7

36. Patel HD, Halgrimson WR, Sweigert SE, Shea SM, Turk TMT, Quek ML, et al. Variability in prostate cancer detection among radiologists and urologists using MRI fusion biopsy. *BJUI Compass* 2024; **5:** 304-12. doi: 10.1002/bco2.294

37. Berry B, Parry MG, Sujenthiran A, Nossiter J, Cowling TE, Aggarwal A, et al. Comparison of complications after transrectal and transperineal prostate biopsy: a national population-based study. *BJU Int* 2020; **126:** 97-103. doi: 10.1111/bju.15039

38. Mian BM, Feustel PJ, Aziz A, Kaufman RP, Jr., Bernstein A, Avulova S, et al. Complications following transrectal and transperineal prostate biopsy: results of the ProBE-PC Randomized Clinical Trial. *J Urol* 2024; **211:** 205-13. doi: 10.1097/JU.0000000000003788

research article

Liver volumetry improves evaluation of treatment response to hepatic artery infusion chemotherapy in uveal melanoma patients with liver metastases

Sebastian Zensen[1], Hannah L Steinberg-Vorhoff[1], Aleksandar Milosevic[1], Heike Richly[2], Jens T Siveke[3,4], Marcel Opitz[1], Johannes Haubold[1], Yan Li[1], Michael Forsting[1], Benedikt Michael Schaarschmidt[1]

[1] Institute of Diagnostic and Interventional Radiology and Neuroradiology, University Hospital Essen, Germany
[2] Department of Medical Oncology, West German Cancer Center, University of Duisburg-Essen, Essen, Germany
[3] Bridge Institute of Experimental Tumor Therapy, West German Cancer Center, University Medicine Essen, Essen, Germany
[4] Division of Solid Tumor Translational Oncology, German Cancer Research Center (DKFZ) and German Cancer Consortium (DKTK), partner site Essen, Heidelberg, Germany

Radiol Oncol 2024; 58(4): 509-516.

Received 2 August 2024
Accepted 9 October 2024

Correspondence to: Sebastian Zensen, Ph.D., M.D., Institute of Diagnostic and Interventional Radiology and Neuroradiology, University Hospital Essen, Hufelandstraße 55, 45147 Essen, Germany. E-mail: sebastian.zensen@uk-essen.de

Disclosure: No potential conflicts of interest were disclosed.

Background. In uveal melanoma patients, short-term evaluation of treatment response to hepatic artery infusion chemotherapy (HAIC) using the Response Evaluation Criteria in Solid Tumors (RECIST) 1.1 criteria is challenging due to the diffuse metastatic spread. As liver enlargement can frequently be observed, this study aims to compare RECIST 1.1 and liver volumetry (LV) for the evaluation of HAIC treatment response.

Patients and methods. Treatment response was evaluated in 143 patients (mean age 65.1 ± 10.9 years, 54% female) treated by HAIC by RECIST 1.1 and LV on CT imaging performed before and after HAIC. In LV, different increases in liver volume were evaluated to set an effective threshold to distinguish between stable disease (SD) and progressive disease (PD). Overall survival (OS) was calculated as the time from first HAIC to patient death using Kaplan-Meier test and multivariate analysis was performed for RECIST 1.1 and LV.

Results. In the overall population, median OS (mOS) was 13.5 months (95% CI 11.2–15.8 months). In LV, a threshold of 10% increase in liver volume was suited to identify patients with significantly reduced OS (SD: 103/143 patients, mOS 15.9 months; PD: 40/143 patients, 6.6 months; $p < 0.001$). Compared to RECIST 1.1, LV was the only significant prognostic factor that was able to identify a decreased OS.

Conclusions. In uveal melanoma patients with liver metastases, LV with a threshold for liver volume increase of 10% was suitable to evaluate treatment response and would be able to be used as a valuable add-on or even alternative to RECIST 1.1.

Key words: uveal melanoma; computed tomography; liver volumetry; staging

Introduction

Uveal melanoma (UM) is the most frequent primary malignancy of the eye and accounts for around 5% of all melanomas.[1,2] Over the course of the disease, 50% of all patients develop metastases, with the liver being the most common site in 70–90% of cases.[3-5] If liver metastases occur, the prognosis

worsens considerately with a 1-year survival rate of about 13% and a median overall survival (mOS) of 2–5 months.[6,7] Due to their diffuse and infiltrative growth pattern, liver metastases rapidly lead to fatal liver failure. Hence, even in the presence of extrahepatic metastases, aggressive local tumor treatment is key to improve survival.[8] Due to diffuse metastatic spread, therapies targeting the whole organ such as transarterial chemoembolization (TACE), radioembolization (RE) or hepatic arterial infusion chemotherapy (HAIC) are possible treatment options.[9,10] Here, especially HAIC plays an important treatment option due to its low rate of side effects that has been shown to prolong progression-free survival with less severe hematologic side effects.[11]

As liver metastases in UM patients often show rapid progression demanding immediate changes in the therapeutic regimen, short-term staging is necessary to evaluate treatment response. However, established tumor response assessment of UM liver metastases using the Response Evaluation Criteria in Solid Tumors (RECIST) 1.1 and its derivatives is challenging. As it is difficult to define a single lesion due to the diffuse liver involvement, a high interobserver measurement variability and thus an inconsistent assessment of response to treatment can be observed.[12-14] However, we observed that considerate liver enlargement occurs in the later stages of the disease. Furthermore, liver volume would be a parameter that could be easily and (potentially automatically) monitored by liver volumetry (LV) over the course of the disease.[15]

To validate if changes in liver volume can also be observed in the earlier stages of the disease, the aim of this study is to compare RECIST 1.1 and LV for the evaluation of treatment response to HAIC in UM patients with liver metastases.

Patients and methods

Patient cohort

In this retrospective observational study design, all UM patients who underwent first HAIC for treatment of unresectable UM liver metastases in our department between October 2013 and December 2020 were identified using the Radiology Information System (RIS). Inclusion criteria were: 1) HAIC as only liver directed therapy of liver metastases; 2) no prior surgical therapy of liver metastases; 3) no additional interventions in addition to or during the first HAIC, such as coil embolization of hepatic arteries or use of degradable starch microspheres (DSM); 4) abdominal CT imaging performed no more than 5 days before and at least 5 weeks after first HAIC but before second HAIC. Patients without CT imaging before or after first HAIC were excluded. Ethical approval for this retrospective single-center study was granted by the local ethics committee and the requirement to obtain informed consent was waived (19-8703-BO).

Hepatic artery infusion chemotherapy

HAIC was performed as described by our research group before via a transfemoral access.[10,16] Then, a microcatheter was placed either into the proper hepatic artery or selectively into the left and the right hepatic artery and a starting dose of 40 mg melphalan was infused via an automated injector. In our department, HAIC was repeated every 6 to 8 weeks for local tumor control, as this time interval is considered safe and feasible based on pharmacokinetic data from intravenous administration of the chemotherapeutic agent.[17,18] Before each HAIC, a contrast-enhanced CT scan was performed to assess tumor response and intensify local tumor treatment in case of disease progression.

Evaluation of treatment response by RECIST 1.1 and liver volumetry

A CT scan was performed one to three days before the first HAIC. The next CT scan was performed 6–8 weeks after the first HAIC without intermediate further local therapy of liver metastases, usually on the day before the second HAIC. All CT scans were acquired in arterial phase of the liver and in venous phase of the whole abdomen. Then, CT images acquired before and after first HAIC were evaluated by LV and RECIST 1.1. using syngo.via (Siemens Healthineers, Erlangen, Germany). LV was performed software-based manually in consensus by two radiologists blinded to outcomes using CT images of the venous phase. RECIST 1.1 evaluation was restricted to the liver. In accordance with RECIST 1.1, the maximum diameter of up to two lesions were analyzed. To correct for perfusion differences, we aimed to assess one lesion in each liver lobe.[19] To assess the impact of treatment induced changes detectable by RECIST 1.1 and liver volumetry, OS was calculated as the time from first HAIC to patient death. No separate analysis was performed for patients with extrahepatic metastases, as their presence is known not to affect survival.[8]

Statistics and data analysis

Statistical analysis was performed using GraphPad Prism 5.01 (GraphPad Software, San Diego, USA) and SPSS Statistics 28 (IBM, New York, USA). To determine normal distribution, D'Agostino-Pearson test was applied. Normally distributed data are reported as mean ± standard deviation (SD), non-normally distributed data as median and interquartile range (IQR). Wilcoxon matched pairs test was used to analyze target lesion parameters and liver volumes. Interrater concordance of LV and RECIST 1.1 was assessed by Cohen's κ-coefficient. Concordance was classified as published by Landis and Koch as no agreement (κ < 0), slight (κ:0.00–0.20), fair (κ:0.21–0.40), moderate (κ:0.41–0.60), substantial (κ:0.61–0.80) or almost perfect (κ:0.81–1.00) agreement.[20] Overall survival between different groups of liver volume changes, RECIST 1.1 evaluation and combined assessment were compared using Kaplan-Meier curves and log-rank (Mantel-Cox) test. Cox proportional hazards regression model was used to determine hazard ratios (HRs) and the corresponding 95% confidence intervals (CI) of RECIST 1.1 and LV evaluation. A p-value lower than 0.05 was considered statistically significant.

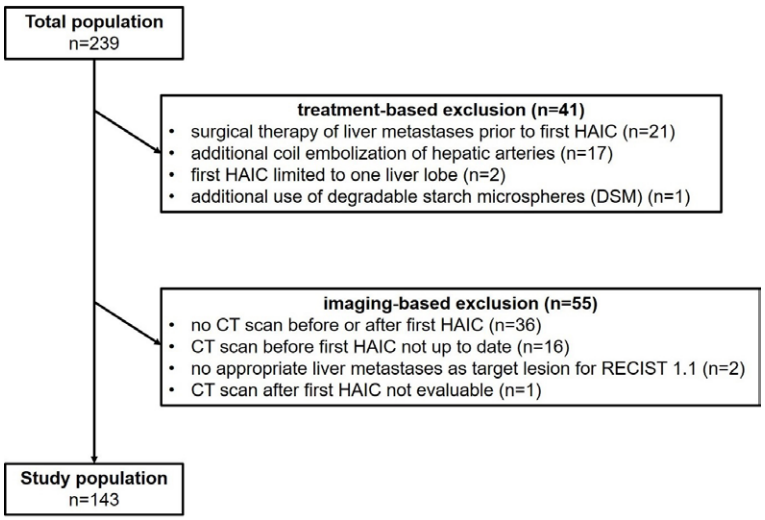

FIGURE 1. Flowchart of analyzed study population with exclusion criteria.

HAIC = hepatic arterial infusion chemotherapy

Results

Patient cohort characteristics

Between October 2013 and December 2020, 239 patients underwent their first HAIC for the treatment of UM liver metastases, of which 96 patients did not meet the inclusion criteria and were therefore excluded. A total of 143 patients could be included in the analysis (Figure 1).

Treatment-based exclusion criteria were: prior surgical therapy for liver metastases (22%, 21/96), additional coil embolization of hepatic arteries (18%, 17/96), first HAIC limited to one liver lobe (2%, 2/96) and additional use of degradable starch microspheres (DSM) (1%, 1/96). Imaging-based exclusion criteria were: no CT scan before or after first HAIC (38%, 36/96), no current CT scan prior to the intervention (17%, 16/96), no appropriate target lesion for RECIST 1.1 evaluation (2%, 2/96) and CT scan not evaluable due to accompanying liver hematoma (1%, 1/96).

Mean patient age at first HAIC was 65.1 years (SD 10.9, range 28–85) and 54% (77/143) of patients were female. A median number of five HAICs were performed (IQR 3–9, range 1–26). At the time point of data collection (December 2021), a total of 86% (123/143) were deceased, 9% (12/143) were alive and 6% (8/143) were lost to follow-up with a median follow-up time of 1.8 months (IQR 1.6–2.0). Median time period between CT scans before and after first HAIC was 48 days (IQR 44–53). mOS of all patients was 13.5 months (95% CI 11.2–15.8).

Feasibility of liver volumetry for evaluation of treatment response

In the entire study population, liver volume before the first HAIC was 1735 ml (IQR 1431–2189 ml, range 889–7116 ml) and after the first HAIC was 1780 ml (IQR 1461–2329 ml, 827–7078 ml, p < 0.0001). The change in liver volume was a median increase of 4% (IQR -2.6% - +11.1%) ranging from a decrease of 20.4% to an increase of 37.6%. First, we performed an explorative data analysis to assess the impact of different changes in liver volume on overall survival using Kaplan-Meier curves (Figure 2).

mOS was comparable for decreasing liver volume (53/143 patients, mOS 15.9 months) and a small increase in liver volume up to 10% (50/143 patients, mOS 15.4 months, p = 0.7852, Figure 2). In contrast, both an increase in liver volume of 10–20% (25/143 patients, mOS 7.9 months, 95% CI 3.6–12.2 months) and more than 20% (15/143 patients, mOS 5.7 months, 95% CI 4.8–6.6 months) were associated with significantly decreased mOS compared to both decreasing or up to 10% increasing liver volume (p < 0.001, Figure 2, Table 1). Accordingly,

TABLE 1. Comparison of median overall survival (mOS) differentiated by different changes in liver volume before and after first hepatic artery infusion chemotherapy

Liver volume change			Log-rank (Mantel-Cox) test					
			Increase 0–10%		Increase 10–20%		Increase > 20%	
	N	mOS [months]	Chi-square	p	Chi-square	p	Chi-square	p
Decrease	53	15.9	0.1	0.7852	14.2	0.0002	32.3	< 0.0001
Increase 0–10%	50	15.4			15.8	< 0.0001	33.4	< 0.0001
Increase 10–20%	25	7.9					1.9	0.162
Increase > 20%	15	5.7						

an increase in liver volume of more than 10% was chosen as the threshold to classify patients as PD by LV, as this was associated with significantly decreased mOS. In contrast, a decrease of liver volume or an increase up to 10% was considered SD. For LV, no patient was evaluated as partial response if a RECIST 1.1 analogue threshold of a 30% decrease in volume was chosen. A complete response for LV is not applicable.

Treatment response evaluation by RECIST 1.1

Measurements of liver target lesions used to evaluate treatment response to HAIC according to RECIST 1.1 are shown in Table 2. In RECIST 1.1, mOS was significantly shorter in patients with PD (8.5 months, 95% CI 5.5–11.5 months, 22/143 patients) than with SD (14.6 months, 95% CI 11.9–17.3 months, 121/143 patients, Chi-square = 9.302, p = 0.0023, Figure 3A). No patient was classified as complete response or partial response according to RECIST 1.1 criteria.

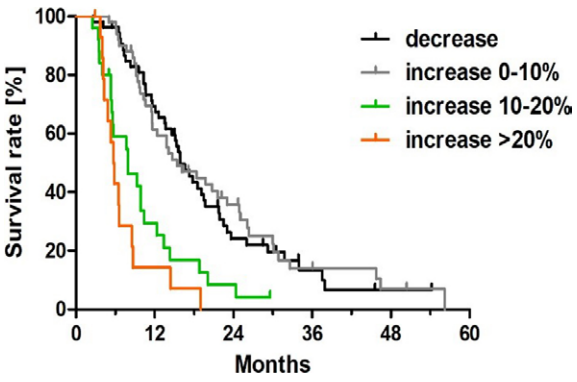

FIGURE 2. Kaplan-Meier curves of overall survival differentiated by change in liver volume of patients with uveal melanoma with liver metastases after first hepatic artery infusion chemotherapy.

Treatment response evaluation by liver volumetry with a threshold of 10% increase in liver volume

Liver volume measurements used to evaluate treatment response to HAIC according to LV with a threshold of 10% increase in liver volume are shown in Table 2. In LV, mOS was significantly shorter in patients with PD (6.6 months, 95% CI 4.4–8.8 months, 40/143 patients) than with SD (15.9 months, 95% CI 12.7–19.1 months, 103/143 patients, Chi-square = 39.28, p < 0.001) (Figure 3B). Initial liver volumes prior to the initial HAIC between patients with PD (1903 ml, IQR 1481–2529 ml) and SD (1678 ml, IQR 1426–2176 ml) were not significantly different (p = 0.2007, Table 2).

Combined treatment response evaluation by RECIST 1.1 and liver volumetry

Two image examples of concordant evaluations by RECIST 1.1 and LV are shown in Figure 4.

The agreement of LV with RECIST 1.1 was only considered as fair according to the inter-rater reliability analysis with about a quarter (35/143) of discordant evaluations (κ=0.289, 95% CI: 0.118-0.461, Table 3).

Therefore, we further compared the discordant evaluations with both RECIST 1.1 and LV applied in combination. Here, in patients with SD according to RECIST 1.1, mOS was still significantly shorter if changes in LV were > 10% and therefore considered as PD according to LV (RECIST 1.1 SD / LV PD: mOS 6.6 months, 27/143 patients) compared to LV SD (RECIST 1.1 SD / LV SD: mOS 16.6 months, 95/143 patients, Chi-square=28.45, p< 0.001) (Table 3, Figure 5).

In contrast, for all cases with changes < 10% in LV, mOS was not significantly different regardless the results of the RECIST 1.1 assessment: (RECIST 1.1 PD / LV SD: mOS 12.8 months, 8/143 patients, RECIST 1.1 SD / LV SD: mOS 16.6 months, 95/143 patients, Chi-square=1.84, p = 0.175, Table 3,

TABLE 2. Results of evaluation of treatment response to hepatic artery infusion chemotherapy (HAIC) by RECIST 1.1 and liver volumetry

	Before first HAIC	After first HAIC	p-value
RECIST 1.1[a]			
(Sum of) longest diameter(s) of target lesion(s) [mm]			
Total study cohort (n = 143)	48.6 (IQR 36.3–69.2)	50.8 (IQR 35.3–76.5)	0.0008
SD (n = 122)	47.7 (IQR 36.2–70.5)	48.0 (IQR 34.5–71.1)	0.3485
PD (n = 21)	55.2 (IQR 34.3–68.9)	73.0 (IQR 46.5–85.3)	< 0.0001
Liver volumetry			
Total liver volume [ml]			
Total study cohort (n = 143)	1735 (IQR 1431–2189)	1780 (IQR 1461–2329)	< 0.0001
SD (liver volume decreases or increases up to max. 10%) (n=103)	1678 (IQR 1426–2176)	1714 (IQR 1430–2151)	0.6691
PD (liver volume increases more than 10%) (n=40)	1903 (IQR 1481–2529)	2203 (IQR 1692–2946)	<0.0001

[a] RECIST 1.1 criteria as published.[19] Values are given as median and interquartile range (IQR).

SD = stable disease; PD = progressive disease

Figure 5). Univariate Cox hazard regression analysis indicated that both RECIST 1.1 and LV showed high prognostic value, whereas in the subsequent multivariate analysis only LV remained an independent prognostic factor (Table 4).

Discussion

HAIC is an important and valuable palliative treatment option for liver metastases in patients with UM.[1,18,21] Short-term assessment of treatment response can be difficult using the commonly used RECIST 1.1 criteria because lesion delineation is challenging due to diffuse organ involvement, leading to increased, reader-dependent measurement variability and inconsistent treatment response evaluation.[12-14] The results of our study can be subsumed in three key points. First, when selecting 10% increase in liver volume as the threshold for PD in LV, more patients with significantly lower OS are identified than by RECIST 1.1. Second, LV and RECIST 1.1 show only fair agreement in the evaluation of treatment response to HAIC. Third, even patients with RECIST 1.1 SD have significantly lower OS when an increase in liver volume of 10% or more is observed in LV.

Tumors that involve the liver often show an asymmetrical and heterogeneous necrosis pattern, which complicates a precise evaluation of treatment response in follow-up imaging.[12] Therefore, in patients with disseminated liver metastasis, as in UM, measurements of target lesions are often not reliable, making accurate assessment of treatment response difficult.[22] However, growing liver metastases lead in parallel to an enlargement of

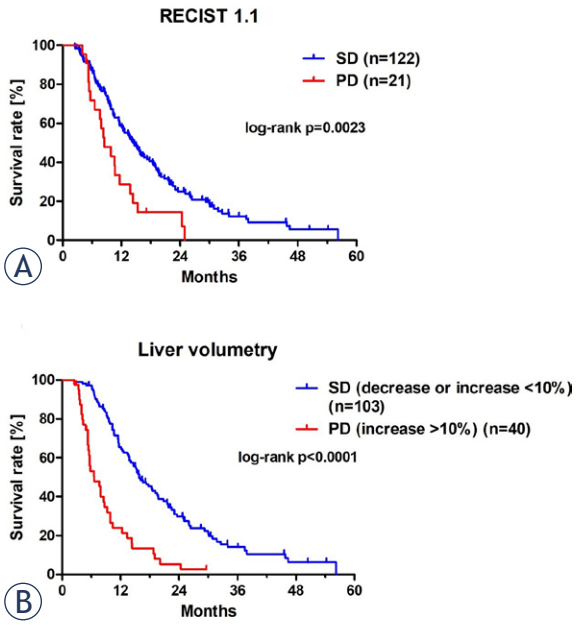

FIGURE 3. Overall survival of evaluation of treatment response by RECIST 1.1 **(A)** and liver volumetry with a threshold of 10% **(B)** of liver volume increase of uveal melanoma patients with liver metastases treated by hepatic artery infusion chemotherapy. Kaplan-Meier curves show overall survival separately for patients evaluated as stable disease (SD) and progressive disease (PD). In liver volumetry, patients with an increase in liver volume more than 10% were classified as PD and with decrease or increase below 10% as SD. RECIST 1.1 criteria as published.[19]

TABLE 3. Median overall survival and accordance of treatment response evaluation by RECIST 1.1 and liver volumetry with a threshold of 10% increase in liver volume

	Liver volumetry		
	SD (Liver volume decreases or increases up to max. 10%)	PD (Liver volume increases more than 10%)	Total
RECIST 1.1 criteria			
SD	16.6 months (n = 95)	6.6 months (n = 27)	14.6 months (n = 122)
PD	12.8 months (n = 8)	7.7 months (n = 13)	8.5 months (n = 21)
Total	15.9 months (n = 103)	6.6 months (n = 40)	12.6 months (n = 143)

Cohen's κ = 0.289, 95% CI = 0.118–0.461

SD = stable disease; PD = progressive disease

the liver volume, which can be easily assessed by LV.[22,23]

Our results show that increases in liver volume of up to 10% are not associated with significantly reduced OS compared to decreasing liver volume. However, a threshold of 10% liver volume increase in LV is well suited to identify patients with significantly reduced OS. Therefore, for the clinical application of LV to evaluate treatment response, we propose a volume increase of 10% as the threshold to distinguish between PD and SD in UM patients with liver metastases. For liver metastases in CRC, LV was also shown to be useful for evaluating treatment response, and the threshold for differentiating between SD and PD was 9.5% liver volume gain, which was very similar to our finding.[22] Our results show that LV as well as RECIST 1.1 are suitable for evaluation of treatment response but show only moderate inter-rater reliability with about a quarter of discordant cases. Here, LV can identify more patients than RECIST 1.1 whose life expectancy is significantly decreased. Our data show that even if patients are evaluated as PD by RECIST 1.1, they do not have a significantly decreased OS if their liver volume does not increase by more than 10%. However, if patients are considered SD by RECIST 1.1, but their liver volume increases by more than 10%, their OS is still significantly decreased. These findings are underlined by Cox regression analysis. Here, both LV and RECIST 1.1 have a high prognostic value in assessing treatment response after HAIC. However, after subsequential multivariate analysis, only LV remained an independent prognostic factor. Hence, LV might be a helpful tool to identify non-responders to HAIC that might profit from treatment escalation or potentially other treatment approaches such as RE, radiotherapy or surgery, which are established concepts in other hepatic malignancies apart from hepatocellular carcinomas.[9,24-26] Additionally, when local treatment options are no longer feasible, systemic therapies such as immunotherapy or targeted therapies may offer further treatment possibilities.

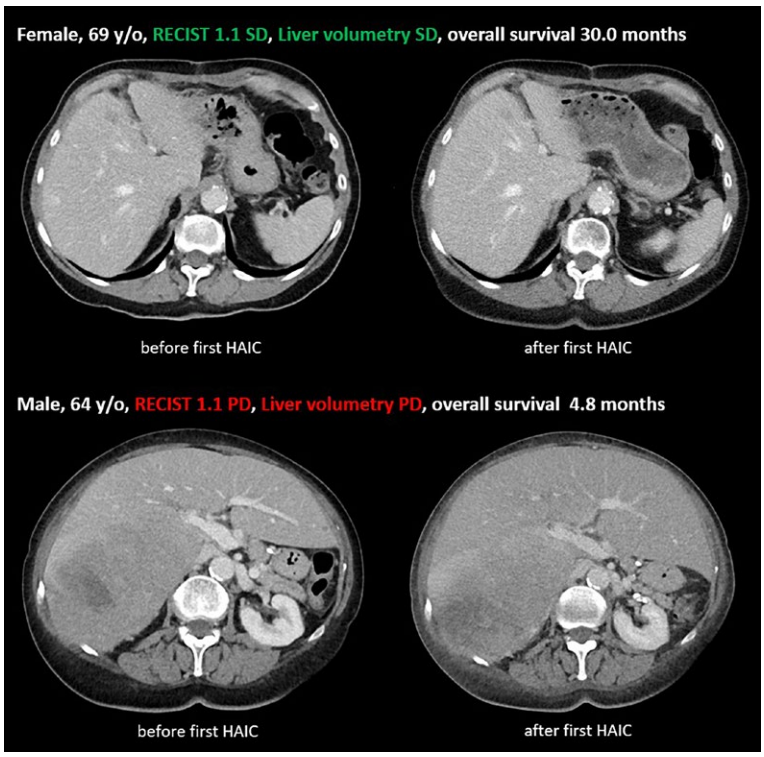

FIGURE 4. Image examples of CT examinations in portal venous phase before and after first hepatic artery infusion chemotherapy (HAIC) for two patients with evaluations according to RECIST 1.1 and liver volumetry (LV) as stable disease (SD) and progressive disease (PD). Liver metastases are marked with arrows.

Furthermore, liver volumes between SD and PD evaluated patients were not significantly different before the first HAIC, so initial liver volume was

TABLE 4. Univariate and multivariate Cox proportional hazards regression model of evaluation of treatment response to hepatic artery infusion chemotherapy by RECIST 1.1 and liver volumetry

Analysis				Univariate			Multivariate		
Covariate	Category	n	Median OS (95% CI)	HR (95% CI)		p	HR (95% CI)		p
RECIST 1.1[a]	SD	122	14.6 (11.9–17.3)	Reference			Reference		
	PD	21	8.5 (5.5–11.5)	2.11	1.29–3.45	0.003	1.19	0.92–1.55	0.184
Liver volumetry	SD (liver volume decreases or increases up to max. 10%)	103	15.9 (12.7–19.1)	Reference			Reference		
	PD (liver volume increases more than 10%)	40	6.6 (4.4–8.8)	1.84	1.51–2.26	<0.001	1.77	1.43–2.19	< 0.001

[a] RECIST 1.1 criteria as published.[19]

HR = hazard ratio; OS = overall survival; PD = progressive disease; SD = stable disease

not a predictor of significant liver volume change in this study.

Although RECIST 1.1 is the widely used and standardized method for assessing response to treatment in oncologic, LV not only offers additional information but also has methodological advantages compared to RECIST 1.1: LV is a robust method that can be performed as part of the usual CT imaging performed for staging. As the whole organ is assessed, common problems in RECIST 1.1 evaluations leading to inaccurate therapy response evaluation such as varying contrast or poorly delineated lesions due to diffuse organ involvement as well as inter- and intrareader variability can be circumvented by LV.[27-29] In addition, intrareader variability, which is a frequent problem in RECIST 1.1 measurements, might be reduced and thus improve patient response assessment.[30] Here, especially advancing developments in software and artificial intelligence might transform LV into an automatically acquired datapoint.[31-33] This would allow LV to be easily included as an additional parameter in staging and clinical practice. Despite these promising initial results, these approaches are nevertheless so far experimental and are therefore neither established in clinical routine nor ready for clinical use.

The limitations of our study are its retrospective and single-center study design. Evaluation by LV and RECIST 1.1 was performed by the same radiologist for each of the examinations to avoid interobserver variability. Therefore, these data should be confirmed in prospective studies once automated software solutions for liver volumetry are commercially available. Furthermore, evaluation of treatment response was assessed only after the first HAIC, so follow-up studies should confirm applicability to later time periods in treatment and course of the disease.

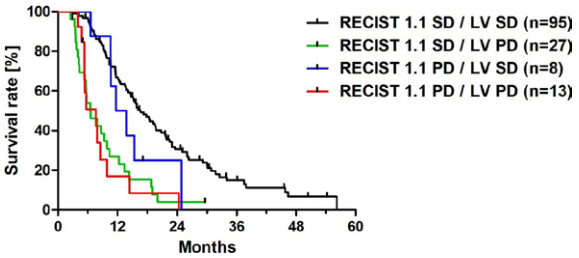

FIGURE 5. Kaplan-Meier curves for the combined RECIST 1.1 and liver volumetry (LV) evaluation of treatment response with a threshold of 10% increase in liver volume in uveal melanoma patients with liver metastases treated by hepatic artery infusion chemotherapy.

PD = progressive disease; SD = stable disease .

In conclusion, in UM patients with liver metastases, LV might be a suitable and in the future robust method to evaluate treatment response by a reliable identification of non-responders to HAIC and a consecutively shortened life expectancy. Hence, it can be used as a valuable add-on or even alternative to RECIST 1.1 to evaluate treatment response in this patient cohort. A threshold for liver volume increase of 10% was effective in distinguishing PD from SD in UM patients with liver metastases.

Acknowledgments

We acknowledge support by the Open Access Publication Fund of the University of Duisburg-Essen.

References

1 Rowcroft A, Loveday BPT, Thomson BNJ, Banting S, Knowles B. Systematic review of liver directed therapy for uveal melanoma hepatic metastases. *HPB (Oxford)* 2020; **22:** 497-505. doi: 10.1016/j.hpb.2019.11.002

2 Singh AD, Turell ME, Topham AK. Uveal melanoma: trends in incidence, treatment, and survival. *Ophthalmology* 2011; **118:** 1881-5. doi: 10.1016/j.ophtha.2011.01.040

3 Rietschel P, Panageas KS, Hanlon C, Patel A, Abramson DH, Chapman PB. Variates of survival in metastatic uveal melanoma. *J Clin Oncol* 2005; **23:** 8076-80. doi: 10.1200/JCO.2005.02.6534

4 Damato BE, Coupland SE. Differences in uveal melanomas between men and women from the British Isles. *Eye* 2012; **26:** 292-9. doi: 10.1038/eye.2011.272

5 Diener-West M, Reynolds SM, Agugliaro DJ, Caldwell R, Cumming K, Earle JD, et al. Development of metastatic disease after enrolment in the COMS trials for treatment of choroidal melanoma: Collaborative Ocular Melanoma Study Group Report No. 26. *Arch Ophthalmol* 2005; **123:** 1639-43. doi: 10.1001/archopht.123.12.1639

6 Gragoudas ES, Egan KM, Seddon JM, Glynn RJ, Walsh SM, Finn SM, et al. Survival of patents with metastases from uveal melanoma. *Ophthalmology* 1991; **98:** 383-90. doi: 10.1016/s0161-6420(91)32285-1

7 Chew AL, Spilsbury K, Isaacs TW. Survival from uveal melanoma in Western Australia 1981-2005. *Clin Exp Ophthalmol* 2015; **43:** 422-8. doi: 10.1111/ceo.12490

8 Bedikian AY, Legha SS, Mavligit G, Carrasco CH, Khorana S, Plager C, et al. Treatment of uveal melanoma metastatic to the liver. A review of the M. D. Anderson cancer center experience and prognostic factors. *Cancer* 1995; **76:** 1665-70. doi: 10.1002/1097-0142(19951101)76:9<1665::aid-cncr2820760925>3.0.co;2-j

9 Schelhorn J, Richly H, Ruhlmann M, Lauenstein TC, Theysohn JM. A single-center experience in radioembolization as salvage therapy of hepatic metastases of uveal melanoma. *Acta Radiol Open* 2015; **4:** 2047981615570417. doi: 10.1177/2047981615570417

10 Heusner TA, Antoch G, Wittkowski-Sterczewski A, Ladd SC, Forsting M, Verhagen R, et al. Transarterial hepatic chemoperfusion of uveal melanoma metastases: survival and response to treatment. *RoFo* 2011; **183:** 1151-60. doi: 10.1055/s-0031-1281743

11 Leyvraz S, Piperno-Neumann S, Suciu S, Baurain JF, Zdzienicki M, Testori A, et al. Hepatic intra-arterial versus intravenous fotemustine in patients with liver metastases from uveal melanoma (EORTC 18021): a multicentric randomized trial. *Ann Oncol* 2014; **25:** 742-6. doi: 10.1093/annonc/mdt585

12 Duran R, Chapiro J, Frangakis C, Lin M, Schlachter TR, Schernthaner RE, et al. Uveal melanoma metastatic to the liver: the role of quantitative volumetric contrast-enhanced MR imaging in the assessment of early tumor response after transarterial chemoembolization. *Transl Oncol* 2014; **7:** 447-55. doi: 10.1016/j.tranon.2014.05.004

13 Erasmus JJ, Gladish GW, Broemeling L, Sabloff BS, Truong MT, Herbst RS, et al. Interobserver and intraobserver variability in measurement of non-small-cell carcinoma lung lesions: implications for assessment of tumor response. *J Clin Oncol* 2003; **21:** 2574-82. doi: 10.1200/JCO.2003.01.144

14 Thiesse P, Ollivier L, Di Stefano-Louineau D, Négrier S, Savary J, Pignard K, et al. Response rate accuracy in oncology trials: reasons for interobserver variability. Groupe Français d'Immunothérapie of the Fédération Nationale des Centres de Lutte Contre le Cancer. *J Clin Oncol* 1997; **15:** 3507-14. doi: 10.1200/JCO.1997.15.12.3507

15 Koitka S, Gudlin P, Theysohn JM, Oezcelik A, Hoyer DP, Dayangac M, et al. Fully automated preoperative liver volumetry incorporating the anatomical location of the central hepatic vein. *Sci Rep* 2022; **12:** 16479. doi: 10.1038/s41598-022-20778-4

16 Zensen S, Opitz MK, Ludwig JM, Haubold J, Richly H, Siveke JT, et al. Radiation dose aspects of hepatic artery infusion chemotherapy in uveal melanoma patients with liver metastases. *Cardiovasc Intervent Radiol* 2022; **45:** 841-5. doi: 10.1007/s00270-022-03130-1

17 Pinguet F, Culine S, Bressolle F, Astre C, Serre MP, Chevillard C, et al. A phase I and pharmacokinetic study of melphalan using a 24-hour continuous infusion in patients with advanced malignancies. *Clin Cancer Res* 2000; **6:** 57-63. PMID: 10656432

18 Boone BA, Perkins S, Bandi R, Santos E, McCluskey K, Bartlett DL, et al. Hepatic artery infusion of melphalan in patients with liver metastases from ocular melanoma. *J Surg Oncol* 2018; **117:** 940-6. doi: 10.1002/jso.24984

19 Eisenhauer EA, Therasse P, Bogaerts J, Schwartz LH, Sargent D, Ford R, et al. New response evaluation criteria in solid tumours: revised RECIST guideline (version 1.1). *Eur J Cancer* 2009; **45:** 228-47. doi: 10.1016/j.ejca.2008.10.026

20 Landis JR, Koch GG. The measurement of observer agreement for categorical data. *Biometrics* 1977; **33:** 159-74. PMID: 843571

21 Karydis I, Gangi A, Wheater MJ, Choi J, Wilson I, Thomas K, et al. Percutaneous hepatic perfusion with melphalan in uveal melanoma: a safe and effective treatment modality in an orphan disease. *J Surg Oncol* 2018; **117:** 1170-8. doi: 10.1002/jso.24956

22 Kalkmann J, Forsting M, Stattaus J. Liver volume variations as a parameter to assess therapy response in advanced metastatic liver disease. *Onkologie* 2011; **34:** 30-4. doi: 10.1159/000323373

23 Purkiss SF, Williams NS. Growth rate and percentage hepatic replacement of colorectal liver metastases. *Br J Surg* 1993; **80:** 1036-8. doi: 10.1002/bjs.1800800838

24 Opitz M, Zensen S, Ludwig JM, Weber M, Alatzides G, Seifert R, et al. Radiation dose aspects and establishment of diagnostic reference levels for90Y radioembolisation during angiographic procedure. *J Radiol Prot* 2022; **42(3).** doi: 10.1088/1361-6498/ac8f9e

25 Schaarschmidt BM, Wildgruber M, Kloeckner R, Nie J, Steinle V, Braat AJAT, et al. 90Y Radioembolization in the treatment of neuroendocrine neoplasms: results of an international multicenter retrospective study. *J Nucl Med* 2022; **63:** 679-85. doi: 10.2967/jnumed.121.262561

26 Schaarschmidt BM, Kloeckner R, Dertnig T, Demircioglu A, Müller L, Auer TA, et al. Real-life experience in the treatment of intrahepatic cholangiocarcinoma by 90Y radioembolization: a multicenter retrospective study. *J Nucl Med* 2023; **64:** 529-35. doi: 10.2967/jnumed.122.264598

27 Krasovitsky M, Lee YC, Sim H-W, Chawla T, Moore H, Moses D, et al. Interobserver and intraobserver variability of RECIST assessment in ovarian cancer. *Int J Gynecol Cancer* 2022; **32:** 656-61. doi: 10.1136/ijgc-2021-003319

28 Suzuki C, Torkzad MR, Jacobsson H, Aström G, Sundin A, Hatschek T, et al. Interobserver and intraobserver variability in the response evaluation of cancer therapy according to RECIST and WHO-criteria. *Acta Oncol* 2010; **49:** 509-14. doi: 10.3109/02841861003705794

29 Kuhl CK, Alparslan Y, Schmoee J, Sequeira B, Keulers A, Brümmendorf TH, et al. Validity of RECIST Version 1.1 for response assessment in metastatic cancer: a prospective, multireader study. *Radiology* 2019; **290:** 349-56. doi: 10.1148/radiol.2018180648

30 Gafita A, Rauscher I, Fendler WP, Murthy V, Hui W, Armstrong WR, et al. Measuring response in metastatic castration-resistant prostate cancer using PSMA PET/CT: comparison of RECIST 1.1, aPCWG3, aPERCIST, PPP, and RECIP 1.0 criteria. *Eur J Nucl Med Mol Imaging* 2022; **49:** 4271-81. doi: 10.1007/s00259-022-05882-x

31 Hagen F, Mair A, Bitzer M, Bösmüller H, Horger M. Fully automated whole-liver volume quantification on CT-image data: comparison with manual volumetry using enhanced and unenhanced images as well as two different radiation dose levels and two reconstruction kernels. *PloS one* 2021; **16:** e0255374. doi: 10.1371/journal.pone.0255374

32 Cai W, He B, Fan Y, Fang C, Jia F. Comparison of liver volumetry on contrast-enhanced CT images: one semiautomatic and two automatic approaches. *J Appl Clin Med Phys* 2016; **17:** 118-27. doi: 10.1120/jacmp.v17i6.6485

33 Suzuki K, Epstein ML, Kohlbrenner R, Garg S, Hori M, Oto A, et al. Quantitative radiology: automated CT liver volumetry compared with interactive volumetry and manual volumetry. *AJR Am J Roentgenol* 2011; **197:** W706-12. doi: 10.2214/AJR.10.5958

research article

Idarubicin-loaded drug-eluting microspheres transarterial chemoembolization for intermediate stage hepatocellular carcinoma: safety, efficacy, and pharmacokinetics

Spela Korsic[1,2], Josko Osredkar[3,4], Alojz Smid[2,5], Klemen Steblovnik[2,6], Mark Popovic[7], Igor Locatelli[4], Jurij Trontelj[4], Peter Popovic[1,2]

[1] Clinical Institute of Radiology, University Medical Centre Ljubljana, Ljubljana, Slovenia
[2] Faculty of Medicine, University of Ljubljana, Ljubljana, Slovenia
[3] Institute of Clinical Chemistry and Biochemistry, University Medical Centre Ljubljana, Ljubljana, Slovenia
[4] Faculty of Pharmacy, University of Ljubljana, Ljubljana, Slovenia
[5] Department of Gastroenterology and Hepatology, University Medical Centre Ljubljana, Ljubljana, Slovenia
[6] Department of Cardiology, University Medical Centre Ljubljana, Ljubljana, Slovenia
[7] Biotechnical Faculty, University of Ljubljana, Ljubljana, Slovenia

Radiol Oncol 2024; 58(4): 517-526.

Received 5 August 2024
Accepted 28 August 2024

Correspondence to: Špela Koršič, M.D., Clinical Institute of Radiology, University Medical Centre Ljubljana, Zaloška 7, 1000 Ljubljana, Slovenia. E-mail: spela.korsic@kclj-si.

Disclosure: No potential conflicts of interest were disclosed.

Background. Transarterial chemoembolization (TACE) is the treatment of choice for the intermediate stage hepatocellular carcinoma (HCC). Doxorubicin remains the most used chemotherapeutic agent in TACE, although *in vitro* screening has demonstrated that idarubicin exhibits greater cytotoxicity against HCC. This study aimed to evaluate safety, efficacy, and pharmacokinetics of idarubicin-loaded drug-eluting microspheres TACE (DEMIDA-TACE) in intermediate stage HCC patients.

Patients and methods. Between September 2019 and December 2021, 31 consecutive intermediate stage HCC patients (96.8% cirrhotic) were included to this study. 2 mL of LifePearl™ microspheres (100 µm) loaded with 10 mg of 1 mg/mL idarubicin were used for treatment. The adverse events, objective response rate (ORR), progression free survival (PFS), time to TACE untreatable progression (TTUP), median overall survival (mOS), and pharmacokinetics were evaluated.

Results. There were 68 TACE procedures performed. Adverse events grade ≥ 3 were noted after 29.4% procedures. The ORR was 83.9%, median PFS and TTUP were 10.5 months (95% CI: 6.8–14.3 months) and 24.6 months (95% CI: 11.6–37.6 months), respectively. Median OS was 36.0 months (95% CI: 21.1–50.9 months). Significant differences between patients achieving objective response (OR) and those with progressive disease were observed regarding idarubicinol and combined idarubicin-idarubicinol plasma concentrations at 72 hours post-procedure, higher plasma concentrations were observed in patients achieving OR ($p = 0.014$ and 0.014; cut-off values 1.2 and 1.29 ng/mL, respectively).

Conclusions. DEMIDA-TACE emerges as a safe and effective method of treatment for the intermediate stage HCC with low rates of adverse events alongside high tumor response, favourable disease control and overall survival. Idarubicinol and combined idarubicin-idarubicinol plasma concentrations at 72 hours post-procedure may serve as prognostic factors for achieving OR.

Key words: hepatocellular carcinoma; drug-eluting microspheres transarterial chemoembolization; idarubicin; safety; efficacy; pharmacokinetics

Introduction

Hepatocellular carcinoma (HCC) is the most frequent primary liver cancer and therefore crucial global medical concern.[1,2]

According to the guidelines of the European Association for the Study of the Liver (EASL), transarterial chemoembolization (TACE) is the treatment of choice for the BCLC-B (Barcelona Clinic Liver Cancer) group, *i.e.* intermediate stage of HCC patients.[3,4]

Despite the wide use of TACE, treatment strategies and procedures are not standardized across different institutions. TACE can be performed as conventional TACE (cTACE) using lipiodol, or with drug-eluting microspheres (DEM-TACE).[3,5] DEM-TACE allows slow release of chemotherapeutic agents, enhancing the duration and intensity of local ischemia.[6-8] To date, the most used chemotherapeutic agent in TACE is doxorubicin, even though the evidence supporting its use is limited.[9]

In 2011, *in vitro* cytotoxicity screening aimed at selecting the most efficient drug against HCC evaluated 11 most used anticancer drugs. These included anthracyclines (doxorubicin, epirubicin, idarubicin and related mitoxantrone), platinum derivates (cisplatin, carboplatin, and oxaliplatin), antimetabolites (5-flourouracil and gemcitabine), the alkylating antibiotic mitomycin C, and the taxane paclitaxel. Idarubicin proved to be the most toxic drug against HCC *in vitro*, moreover, it also demonstrated efficacy against the resistant SNU-449 cell line where doxorubicin failed to achieve 50% cell death.[9]

Idarubicin is an anthracycline, to date mostly used for the treatment of acute leukaemia, when administrated intravenously. The superior cytotoxicity of idarubicin towards HCC is presumed to result from its high hepatic penetration and highly lipophilic nature compared to other anthracyclines, resulting in high hepatic concentrations. High intracellular concentrations of idarubicin are necessary to achieve its cytotoxicity against multidrug resistance (MDR) mechanisms.[9] In the liver, idarubicin undergoes reduction to its metabolite idarubicinol, which retains pharmacological activity and is considered equipotent as the parent drug.[10]

Another important feature of idarubicin is its ability to be loaded in drug-eluting microspheres by positively charged protonated amine group of idarubicin hydrochloride interacting with negatively charged sulphonate group of microspheres.[11-13]

Moreover, the first results of *in vivo* phase I and II safety and efficacy trials of idarubicin use in cTACE and DEM-TACE have shown promising outcomes in terms of safety profiles and objective response.[12-16] Therefore, we designed present prospective study to evaluate safety, efficacy, and pharmacokinetics of idarubicin-loaded DEM-TACE (DEMIDA-TACE) for the intermediate stage HCC patients.

Patients and methods

The study strictly followed the ethical guidelines of the Helsinki Declaration for biomedical research involving human subjects. Approval for the study was obtained from the Republic of Slovenia National Medical Ethics Committee on the 19th of March 2019, with the assigned approval number 0120-64/2019/5.

Patient selection

Between September 2019 and December 2021, 31 consecutive intermediate stage HCC patients who did not meet exclusion criteria and signed the informed consent were enrolled to this prospective single-institution study. Exclusion criteria included Child-Pugh liver cirrhosis > 8 points, portal vein thrombosis, iodine contrast agent allergy, left ventricular ejection fraction (LVEF) < 50%, acute liver, kidney and/or cardiovascular failure, and women of childbearing age.

The decisions for DEM-TACE and inclusion in the study were reached through weekly multidisciplinary tumour board (MTB) meetings at our institution. The MTB comprises experts in abdominal and interventional radiology, gastroenterology, hepatobiliary surgery, nuclear medicine, and oncology.

The final day of the follow-up for the purpose of present study was December 31, 2023.

Procedures

All patients received prophylactic antibiotic treatment (*i.e.* 1000 mg of amoxicillin/clavulanic acid) and were scheduled for tumour biopsy in the same session as the first DEMIDA-TACE procedure. Patients were treated using a mixture of 2 mL LifePearl™ (Terumo Europe, Leuven, Belgium) drug-eluting microspheres of 100 μm in diameter loaded with 10 mg of 1 mg/mL idarubicin (Zavedos®, Pfizer, France). Superselective ap-

proach to treatment with Progreat™ microcatheter (Terumo Europe, Leuven, Belgium) was used in all patients. Before initiating microspheres delivery, a cone-beam computed tomography (CBCT) using Artis Zee floor with DynaCT (Siemens, Forchheim, Germany) was performed to verify the microcatheter's accurate positioning within the feeding artery to ensure a complete coverage of the targeted lesions. For the visualization, a nonionic contrast agent (Ultravist 370®, Bayer HealthCare, Germany or Visipaque 320, GE Healthcare, Norway) was administered using a power injector (Avanta®, Medrad, Bayer HealthCare, Germany). In patients with multisegmental or bilobar disease, the position of the microcatheter was changed within the same session to ensure superselective delivery to each lesion. The idarubicin-microspheres mixture delivery was slow (1 mL/min) and discontinued after complete dosage administration or at early stasis.

Adverse events

Safety was evaluated by clinical and laboratory monitoring. Adverse events were assessed according to the Common Terminology Criteria for Adverse Effects v. 5.0 (CTCAE), AEs grade ≥ 3 were noted.[17] Potential toxicity was assessed in the inpatient setting until the patient's discharge, in the outpatient setting at 72 hours post-procedure, and again after 14 days, as well as with follow-up imaging. Baseline and follow-up peripheral venous blood samples were obtained to assess liver enzymes (alanine aminotransferase [ALT], aspartate aminotransferase [AST], gamma-glutamyl transferase [GGT]), complete blood count (CBC), differential blood count (DBC), coagulation tests, bilirubin, albumin, kidney function (urea, creatinine, estimated glomerular filtration rate [eGFR]) and alpha fetoprotein (AFP).

Before inclusion in the study, all patients underwent a cardiac ultrasound performed by an experienced cardiologist to exclude individuals with a LVEF lower than 50%. For cardiotoxicity evaluation, LVEF was measured at baseline, 1 month after the first treatment, and 2 months after the completion of the first cycle of treatment.

Response to treatment

All patients underwent a baseline four-phase contrast enhanced CT 1 day before the treatment. Treatment response was evaluated based on follow-up contrast enhanced CT according to modified Response evaluation criteria in solid tumours (mRECIST) by a randomly assigned experienced abdominal and/or interventional radiologists.[18] The first follow-up CT for the evaluation of treatment response was scheduled 2 months after completing the first cycle of treatment. Depending on the disease burden, the first treatment cycle consisted of 1, 2 or 3 procedures to ensure complete coverage of tumours before the first treatment response evaluation. An objective response (OR) to treatment was reported in patients achieving a complete response (CR) or a partial response (PR). In cases of OR, follow-up CT was scheduled every 3 months the first year, after that, follow-up imaging was scheduled every 6 months or until progression of disease (PD). Every patient achieving stable disease (SD) or PD was re-evaluated by the MTB for further treatment strategies.

Pharmacokinetic study

For the pharmacokinetic study, plasma levels of idarubicin and its major metabolite idarubicinol were measured at baseline (*i.e.* before the first procedure) and at 5, 15, 30 minutes, 2, 6, 10, 24, and 72 hours after the first procedure. All samples were obtained from peripheral venous blood and were immediately centrifuged upon collection. After centrifugation, the plasma samples were extracted by tert-buthylmethyl ether with 10% isopropanol and then subjected to analysis by a high-performance liquid chromatograph Agilent 1290 Infinity II (Waldbronn, Germany), coupled to a hybrid triple quadrupole/ion trap mass spectrometer Sciex 5500 Qtrap (Framingham, MA, USA). The method was validated in terms of selectivity, accuracy, precision, recovery, relative matrix effect, stability, and sensitivity with the lower limit of quantitation at 0.025 ng/mL for both idarubicin and idarubicinol. The mean peak plasma concentration (C_{max}) and mean time to peak plasma concentration (T_{max}) of idarubicin and idarubicinol were determined, moreover the mean area under the concentration curves from 0 to 72 hours (AUC_{0-72}) was calculated using the trapezoidal method.

Statistical analysis

Categorical variables were expressed using frequencies and percentages. Continuous variables were expressed as the mean and standard deviation (SD), in case of skewed distributions, median and range were used.

Progression free survival (PFS) was defined as the time from the first TACE procedure until

TABLE 1. Baseline patient's demographic, clinical, laboratory and imaging characteristics

Sex, number of patients (%)	
Male/female	28 (90.3)/3 (9.7)
Age, years	
Mean ± SD	70.6 ± 6.7
Cirrhosis, n. (%)	
Yes/No	30 (96.8)/1 (3.2)
Cirrhosis aetiology, n. (%)	
Ethylic	21 (67.7)
NASH	4 (12.9)
Hemochromatosis	2 (6.5)
HBV	1 (3,2)
HCV	1 (3,2)
Cryptogenic	1 (3,2)
Portal hypertension, n. (%)	
Yes/No	21 (67.7)/10 (32.3)
Ascites, n. (%)	
Yes/No	10 (32.3)/21(67.7)
Laboratory characteristics	
GGT, median (range) [μkat/L]	1.72 (0.24–14.83)
AST, mean ± SD [μkat/L]	0.80 ± 0.26
ALT, mean ± SD [μkat/L]	0.71 ± 0.39
Total bilirubin, mean ± SD [μmol/L]	25.03 ± 15.9
Albumin, mean ± SD [g/L]	40.90 ± 5.00
AFP, median (range) [kU/L]	5.3 (1–4062.5)
Child-Pugh score (n = 30)	
Mean points ± SD	5.8 ± 1.0
Child-Pugh class (n = 30)	
A/B, n (%)	23 (76.7)/7 (23.3)
Imaging characteristics	
Number of lesions, mean ± SD [mm]	3.1 ± 2.1
Diameter of largest lesion, mean ± SD [mm]	44.8 ± 23.0
Cumulative diameter of lesions, mean ± SD [mm]	75.7 ± 39.8
Unilobar disease, n (%)	16 (51.6)
Bilobar disease, n (%)	15 (48.4)
LVEF (%)	
Mean ± SD	64.1 ± 8.7

AFP = alpha fetoprotein; ALT = alanine aminotransferase; AST = aspartate aminotransferase; GGT = gamma-glutamyl transferase; HBV = hepatitis B virus; HCV = hepatitis C virus; LVEF = left ventricular ejection fraction; NASH = non-alcoholic steatohepatitis

initial progression, either after which patient remained a candidate for retreatment with TACE or underwent discontinuation of TACE from all causes (including death). Time to TACE untreatable progression (TTUP) was defined as the time from the first TACE procedure until discontinuation of TACE after radiological and/or clinical progression that prevented retreatment with TACE. Median PFS and TTUP were calculated using the Kaplan-Meier method.

Median follow-up was calculated from the day of the first TACE until either death or the end of the study using the reverse Kaplan-Meier method. Survival was calculated from the day of the first TACE until death, surviving patients were censored at the end of the study. Survival curves were determined using the Kaplan-Meier method. To assess potential associations between pharmacokinetic parameters and response to treatment or other clinical outcomes, non-parametric Mann-Whitney U tests and logistic regression models were conducted, respectively. p-values < 0.05 were considered statistically significant. Additionally, receiver operating characteristic (ROC) curves were plotted to evaluate the prognostic value of idarubicin/idarubicinol plasma concentrations and to identify optimal cut-off values.

The statistical analyses were performed using IBM® SPSS® Statistics Version 29.0.2.0. (International Business Machines Corporation, Armonk, New York, USA) for macOS.

Results

Patients

The baseline demographic, clinical, laboratory and imaging characteristic of 31 intermediate stage HCC patients who were enrolled to present study are summarized in Table 1. Most patients were male (90.3%). The mean patient age was 70.6 ± 6.7 years. Most patients (96.8%), except one, presented with cirrhotic liver, of them 67.7% of ethylic aetiology. The second most common cause of cirrhosis was non-alcoholic steatohepatitis (NASH). Cirrhosis was classified as Child-Pugh A and B in 23 (76.7%) and 7 (23.3%) patients, respectively. Clinical signs of portal hypertension and ascites were observed in 21(67.7%) and 10 (32.3%) patients, respectively. Baseline median serum AFP was 5,3 kU/L (range: 1-4062.5). Sixteen (51.6%) patients presented with unilobar disease. The mean number of lesions per patient was 3.1 ± 2.1 and the mean diameter of largest lesion was 44.8 ± 22.9 mm. The mean baseline LVEF was 64.1 ± 8.7 %.

Procedures

Overall, 68 DEMIDA-TACE procedures were performed. Depending on the disease burden, patients

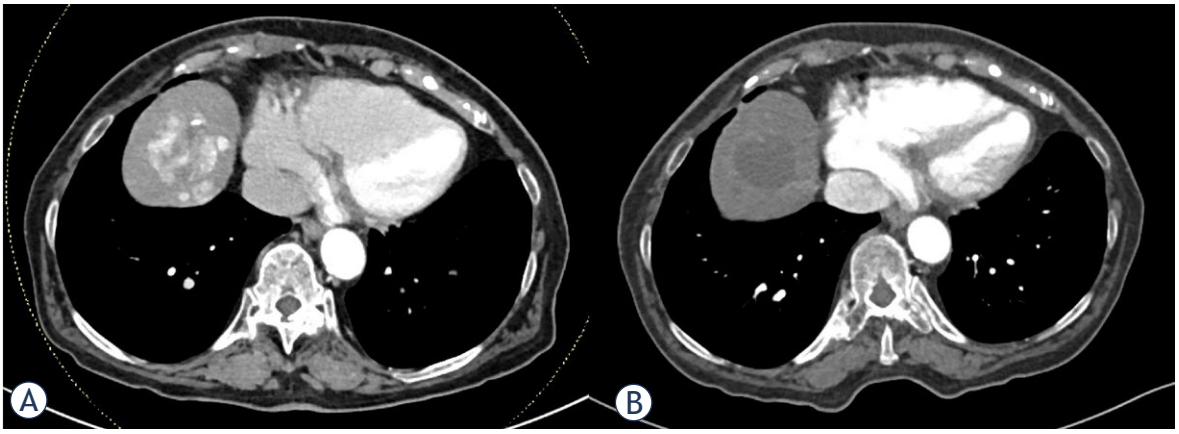

FIGURE 1. CT slices showing a mRECIST partial response to idarubicin-loaded drug-eluting microspheres (DEMIDA) - transarterial chemoembolization (TACE) in the VIII. segment of cirrhotic liver. **(A)** Baseline CT showing multifocal hepatocellular carcinoma (HCC). The diameter of the largest tumour was 38 mm; **(B)** Only minimally enhancing largest target lesion at the first treatment response evaluation, the diameter of viable lesion was 4 mm.

underwent 1 (3.2%), 2 (74.2%) or 3 (22.6%) procedures before the first efficacy evaluation.

Adverse events

Overall, AEs grade ≥ 3 were noted after 20 (29.4%) procedures in 13 (41.9%) patients. AE grade 3 elevation of AST, GGT, ALT and bilirubin was observed in 7 (10.3%), 4 (5.9%), 4 (5.9%), and 3 (4.4%) procedures, respectively. While the laboratory changes observed were transient, they persisted up to 72 hours after the procedure. Notably, all but 1 patient, who presented with grade 3 elevation of GGT, returned to their pre-treatment laboratory status at 14 days follow-up after the first procedure.

Grade 3 abdominal pain was noted in 7 (10.3%) of procedures. No grade ≥ 3 haematologic and cardiotoxicity was observed. Three (in 4.4% of all procedures) major complications were noted: a pseudoaneurysm formation at the puncture site, which was treated by endovascular embolization with coils; and an infection of necrotic target lesion with abscess formation, necessitating percutaneous drainage and antibiotic treatment in two patients. Postembolization syndrome (*i.e.* abdominal pain, fever, nausea, elevation (doubling of baseline value) of liver enzymes, leucocytosis) was observed after 10 (14.7%) procedures.

Response to treatment

At the first follow-up imaging, an OR in target lesions was achieved in 29 patients (93.5%). An overall OR was achieved in 26 (83.9%) patients (Figure 1). Overall CR and PR were achieved in 9 (29% of all 31 patients) and 17 (54.8%) patients, respectively. Three patients achieved PR in target lesions, however overall TACE treatable PD due to development of new lesions. Two patients presented with clinical and radiological (PD in target lesions as well as development of new lesions) TACE untreatable progression: first patient died 5.4 months after the first procedure due to progression to macrovascular invasion of the middle hepatic vein and inferior vena cava; second patient with intrahepatic progression and decompensation of liver cirrhosis died 6.5 months after the first procedure.

During the follow-up, progression (or death) was observed in 30 (96.8%) patients. The median PFS was 10.5 months (95% CI: 6.8–14.3 months). Thirteen patients (43.3% of patients with progression) underwent additional on-demand TACE treatment. Five (16.7%) patients received systemic therapy, while 8 (27%) received best supportive care. One (3.3%) patient underwent surgical resection. During the follow-up, TACE untreatable progression was observed in 18 (58,1%) patients. The median TTUP was 24.6 months (95% CI: 11.6–37.6 months).

Survival

During the median follow-up of 30 months (95% CI 29.0–31.0 months), 16 patients died. The 1- and 2-year survival rates were 87% and 71%, respectively. Median OS was 36.0 months (95% CI 21.1–50.9 months) (Figure 2).

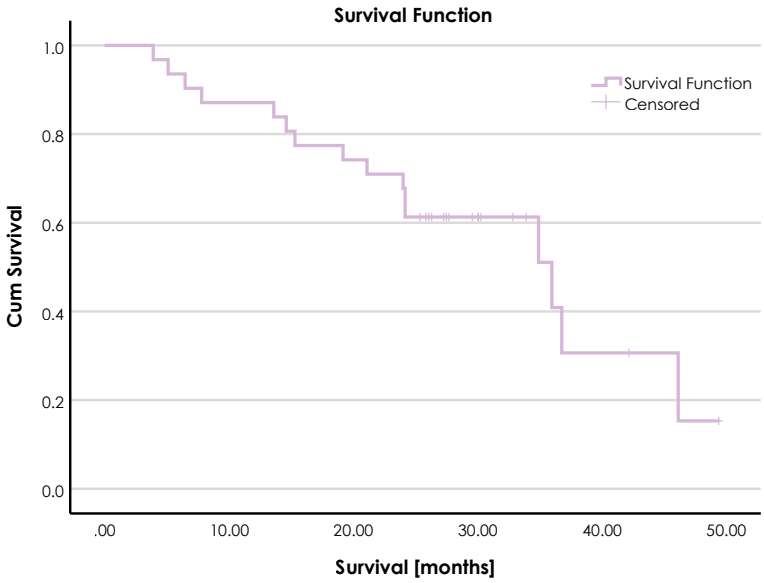

FIGURE 2. Kaplan-Meier curve for overall survival.

Idarubicin pharmacokinetics

The idarubicin and idarubicinol plasma concentrations within the initial 72-hour period following DEMIDA-TACE remained low, with the mean C_{max} of 9.1 ± 5.0 ng/mL and 3.7 ± 1.6 ng/mL, respectively (Figure 3). The median T_{max} for idarubicin was 5 min (range, 5–15 min), indicating rapid systemic absorption following hepatic intra-arterial administration. In contrast, idarubicinol plasma concentrations exhibited a slower increase, with a median T_{max} of 10 hours (range, 2–24 hours). However, the mean AUC_{0-72} for idarubicinol was higher at 179.7 ± 81.4 ng/mL*h compared to idarubicin (mean AUC_{0-72} 54.0 ± 25.8 ng/mL*h) over the same 72-hour period, indicating a greater overall exposure to the metabolite rather than the parent drug.

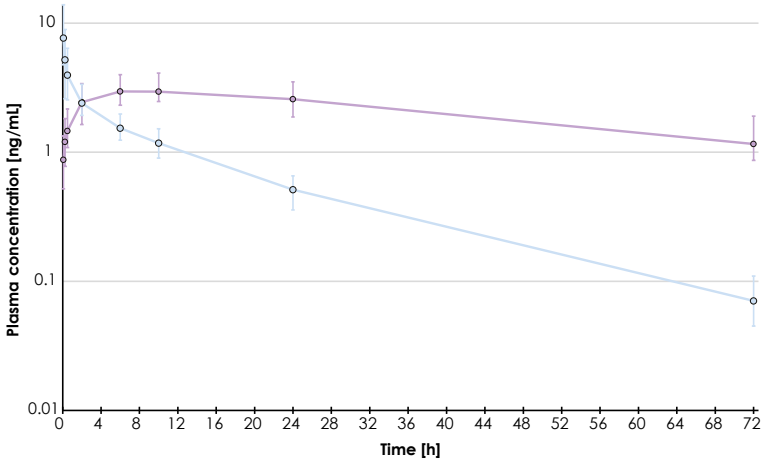

FIGURE 3. Geometric mean plasma concentration profiles for idarubicin (blue) and idarubicinol (purple) (n = 31). Error bars indicate first and third quartiles of plasma concentrations.

Patients achieving OR had significantly higher concentrations at 72 hours for both idarubicin and idarubicinol (p = 0.024 and 0.014, respectively), as well as their combined concentration (p = 0.014), compared to those with PD. The cut-off values for OR were identified at 1.2 ng/mL and 1.29 ng/mL for idarubicinol and combined idarubicin-idarubicinol plasma concentration, respectively (Figure 4). The sensitivity and specificity of both cut-off values were 0.72 and 1, respectively. Median idarubicinol and combined idarubicin-idarubicinol plasma concentration at 72 hours were 1.62 ng/mL (range, BLOQ–2.93 ng/mL) and 1.72 ng/mL (range, BLOQ–3.07 ng/mL), respectively. However, in terms of AUC_{0-72} for idarubicin, idarubicinol and their combined plasma concentration, no significant differences were observed between OR and PD groups.

Furthermore, no significant differences were observed in pharmacokinetic parameters between patients experiencing AEs grade ≥ 3 and those without such events.

Discussion

The present prospective study aimed to evaluate safety, efficacy, and pharmacokinetics of DEMIDA-TACE for the intermediate stage HCC patients. The promising outcomes of present study suggest that this approach to treatment holds significant potential in the management of HCC.

To our knowledge, our study is the largest in terms of the study population treated with DEMIDA-TACE using LiferPearl™ microspheres. The mechanical and pharmacological properties of LiferPearl™ microspheres have been studied *in vitro* and compared with four commonly used microspheres (LifePearl, DC Bead, HepaSphere, and Tandem).[19] The PARIS registry study enrolled 97 patients including 22 patients treated with idarubicin loaded DEM and 75 patients treated with doxorubicin loaded DEM.[20]

In our study population, AEs grade ≥ 3 were noted in 41.9% patients after 29.4% procedures, including postembolization syndrome observed after 10 (14.7%) procedures. The PARIS registry using LiferPearl™ microspheres loaded with either idarubicin or doxorubicin reported AEs grade ≥ 3 in 13.4% patients, mainly related to postembolization syndrome. Moreover, the PARIS registry

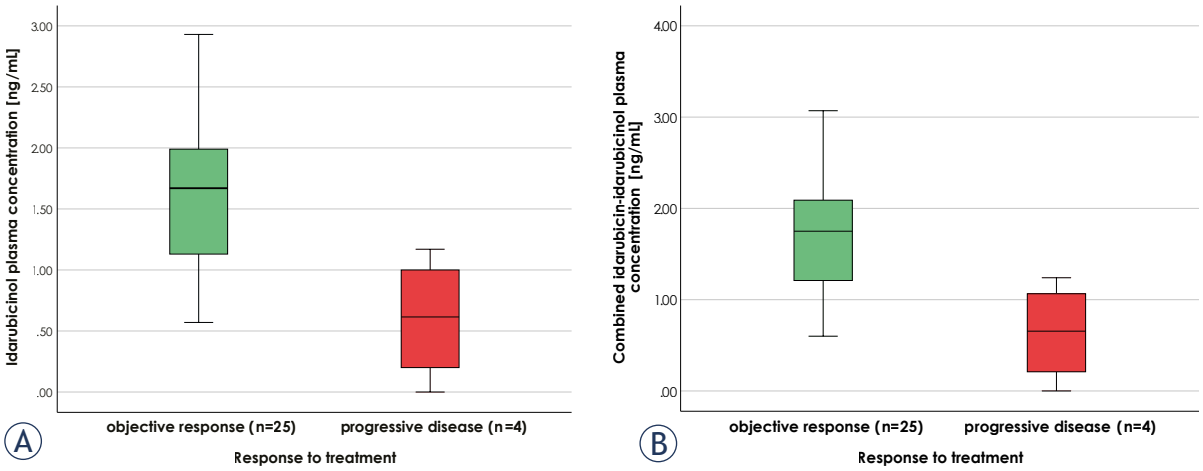

FIGURE 4. Idarubicinol **(A)** and combined idarubicin-idarubicinol **(B)** plasma concentrations at 72 hours post-procedure in patients with objective response to treatment or progressive disease (n = 29).

reported no AEs grade ≥ 3 laboratory changes except one transient hyperbilirubinemia. However, one patient with a history of heart insufficiency died from heart failure two days after DEMIDA-TACE performed with 4 mL of LifePearl™ loaded with 5 mg/mL of idarubicin, without postembolization syndrome.[20] When administrated intravenously, the main safety concern for idarubicin is dose-limiting cardio- and haematological toxicity. No cardiotoxicity was noted in our study population, consistent with other research on DEMIDA-TACE.[14,15,20,21] This can be explained by the cumulative cardiotoxic dose of idarubicin set at 93 mg/m^2.[22] Theoretically, a patient with an average body surface area of 1.8 m^2 and normal LVEF can undergo 17 sessions of TACE using 10 mg of idarubicin before reaching this threshold. Furthermore, studies have shown that idarubicin-induced cardiomyopathy is uncommon with cumulative doses up to 290 mg/m^2.[14,22] No haematological toxicity was observed in our study population. In a phase I dose-escalation trial study of 21 patients treated with TANDEM (Boston Scientific, Marlborough, Massachusetts) microspheres, half of haematological grade 3 AEs observed were thrombocytopenia, which occurred in patients with a baseline platelet count < 75 000 per mmc.[14] In a study of 72 patients by the same institution, grade 3–4 AEs after 52% of sessions, being primarily biological (such as elevation of AST, ALT, bilirubin, GGT, glucose, AP and lipase, in order of frequency), while clinical manifestations (such as abdominal pain, fatigue, fever and ascites) were observed to a lesser extent. Additionally, hepatobiliary complications were reported in 2 sessions, including gallbladder necrosis in one patient and multi-organ failure leading to death in another.[22] It is noteworthy that in PARIS registry there were no significant differences in the rate of hepatobiliary toxicities between idarubicin (10/31, 9.7%) and doxorubicin (26/156, 16.7%; p = 0.58) groups. However, there was a trend towards less hepatobiliary toxicities in the idarubicin group, despite significantly lower number of patients with cirrhosis, which has a protective role against hepatobiliary complications.[20,23,24] Of 3 major complications (4,4% of all procedures) in the present study, pseudoaneurysm at puncture site cannot be reliably attributed to the use of idarubicin. Four major complications have been reported out of 452 TACE (0.9%) in 144 patients, that were treated with DEMDOX-TACE at our institution between February 2010 and December 2018. An ischemic cerebrovascular insult to the cerebellum following a non-target embolization (the tumour feeding artery being the right internal mammary artery); a radial artery thrombosis following a trans radial approach; a variceal bleeding resulting from emesis after the procedure; and an infection of the necrotic tumour, which resolved after antibiotic treatment.[25] Those complications, as well as major complications in the present study, were not related to the specific chemotherapeutic agent. The hepatic intraarterial administration of idarubicin-loaded drug-eluting microspheres allows maximizing drug exposure in the targeted tumour while minimizing systemic exposure and potential systemic toxicity, suggesting that DEMIDA-

TACE holds significant potential for optimizing therapeutic outcomes while minimizing AE.

The ORR of 83.9% within 2 months after first cycle of DEMIDA-TACE (including 29.5% CR) in our study is in line with the best previously reported OR rate for LifePearl™ microspheres ranging between 76% and 90.9%.[26-30] The reported OR at the first follow-up imaging in our group of patients treated with DEMDOX-TACE was 91.0%. Additionally, CR rate achieved in those patients was higher than in our idarubicin group, 55.0% *vs.* 29.5%, respectively.[25] PARIS registry reported an 81% ORR in target lesions and 72.9% overall ORR.[20] The best reported ORR by Guiu *et al.* was 65% (61% after the first session, 64% after the second, 61% after the third, 50% after the forth session).[22] High ORR observed in patients treated at our institution, using doxorubicin or idarubicin, are likely attributable to the regular superselective approach using microcatheter and repeated CBCT for depicting lesions and feeding arteries within the same session. While this approach prolongs procedures, it also ensures superselective delivery to each target lesion, likely resulting in higher OR.[25,31]

Our reported median OS of 36.0 months (95% CI 21.1–50.9 months) is in line with the reported median OS in patients treated with TACE, which ranges from less than 20 months in real life cohorts, up to 45 months in well-selected patients.[32] According to the BCLC 2022 update, the expected survival of patients treated with TACE is more than 30 months.[4] The reported median OS in our DEMDOX-TACE group was 25.8 months. The 1- and 2-year survival rates in those patients were 85% and 53%, respectively, whereas in our idarubicin group, 1- and 2-year survival rates were 87% and 71%, respectively.[25]

Today, the reported OS results not only from DEM-TACE, but also from additional and subsequent treatment strategies, including systemic therapies that have highly improved during the past years namely due to the combined immune- and VEGF inhibitors therapy. PFS and TTUP were introduced as secondary endpoints, as they serve as a surrogate marker of OS to minimize the impact of other treatment strategies.[3,33,34] The median PFS and median TTUP of 10.5 months and 24.6 months, respectively, are the longest reported in patients treated with DEMIDA-TACE. The PARIS registry reported median PFS of 10.4 and 15.7 months in their idarubicin and doxorubicin group, respectively, with a shorter median PFS in the idarubicin group being explained by the larger size of treated tumours in this group.[20] In our DEMDOX-TACE experience, the reported median PFS was 10.2 months, comparable with the present idarubicin group.[25] Guiu *et al.* reported median PFS of 6.6 months in their IDASPHERE II trial and time to treatment failure (time until TACE discontinuation due to any reason, including death) of 14.4 months in patients treated with idarubicin-loaded TANDEM beads (Boston Scientific, Marlborough, Massachusetts).[15,21]

The plasma concentrations of both idarubicin and idarubicinol within the 72-hour post DEM-TACE remained low, demonstrating the ability of DEM to release idarubicin in a sustained manner. The median T_{max} of 5 minutes suggests that idarubicin reaches its maximum systemic concentration relatively quickly after hepatic intraarterial administration, consistent with the results of IDASPHERE phase 1 trial, thus demonstrating an initial moderate burst release. In contrast, plasma concentrations of idarubicinol increased slowly; with a median T_{max} of 10 hours even slower than with DC Bead™ (Biocompatibles, Surrey, UK) microspheres, for which Boulin *et al.* reported a median T_{max} of 6 hours (range 2–6 hours). However, the mean AUC_{0-72} results of 54.0 ± 25.8 ng/mL*h and 179.7 ± 81.4 ng/mL*h, for idarubicin and idarubicinol, respectively) are closer to those of the 15 mg dose study group from IDASPHERE I, for which values of mean AUC_{0-72} were reported as 146.8 ± 134.9 ng/mL*h and 256.0 ± 79.9 ng/mL*h, respectively. This may be attributable to various factors: a higher lower limit of quantification in IDASPHERE study (1 ng/mL *vs.* 0.025 ng/mL) as well as use of different brand and sizes of microspheres (DC Bead™ of 300–500 μm vs. LifePearl 100 μm), as indeed for the same volume of microspheres, smaller microspheres size have a larger number of microspheres resulting in more contact surface likely resulting in faster and higher elution.[14]

The higher mean AUC_{0-72} for idarubicinol compared to idarubicin indicates a greater overall exposure to the metabolite rather than the parent drug. The significant difference observed in idarubicin, idarubicinol, and their combined plasma concentrations at 72 hours between patients achieving OR and those with PD suggests that pharmacokinetics may serve as predictive factor for treatment outcomes. In patients with idarubicinol and combined idarubicin-idarubicinol plasma concentrations at 72 hours post-procedure above the defined cut-off values (1.2 and 1.29 ng/mL, respectively), achieving OR to treatment is associated with a 0.72 sensitivity and 1.0 specificity. Further investigations

with larger sample sizes are warranted to confirm these findings.

Limitations of present study include a single institution setting with a small study population and no control group treated with DEMDOX-TACE. However, the results of present study were compared to those of our previously published retrospective study involving 144 consecutive patients treated with DEMDOX-TACE at our institution.[25]

In conclusion, our study demonstrates promising results regarding the safety, efficacy, and pharmacokinetics of DEMIDA-TACE in intermediate stage HCC patients. Lifepearl™ microspheres efficient delivery of idarubicin to the targeted lesions resulting in minimal systemic toxicity, a high ORR, prolonged PFS and TTUP, and favourable OS, support the use of idarubicin as a viable alternative to doxorubicin in DEM-TACE. Further multicentric randomized trials are warranted to objectively assess the potential superiority of idarubicin over doxorubicin and other commonly used anticancer drugs in this setting.

Idarubicinol and combined idarubicin-idarubicinol plasma concentrations at 72 hours post-procedure may serve as prognostic factors for achieving OR.

Refrences

1. Ferlay J, Ervik M, Lam F, Laversanne M, Colombet M, Mery L, Piñeros M, et al. *Global Cancer Observatory: cancer today*. Lyon, France: International Agency for Research on Cancer; 2024. [cited 2024 Feb 1]. Available at: https://gco.iarc.who.int/today
2. Vogel A, Meyer T, Sapisochin G, Salem R, Saborowski A. Hepatocellular carcinoma. *Lancet* 2022; **400:** 1345-62. doi: 10.1016/S0140-6736(22)01200-4
3. European Association for the Study of the Liver. EASL Clinical Practice Guidelines: management of hepatocellular carcinoma. *J Hepatol* 2018; **69:** 182-236. doi: 10.1016/j.jhep.2018.03.019
4. Reig M, Forner A, Rimola J, Ferrer-Fàbrega J, Burrel M, Garcia-Criado Á, et al. BCLC strategy for prognosis prediction and treatment recommendation: The 2022 update. *J Hepatol* 2022; **76:** 681-93. doi: 10.1016/j.jhep.2021.11.018
5. Ducreux M, Abou-Alfa GK, Bekaii-Saab T, Berlin J, Cervantes A, de Baere T, et al. The management of hepatocellular carcinoma. Current expert opinion and recommendations derived from the 24th ESMO/World Congress on Gastrointestinal Cancer, Barcelona, 2022. *ESMO Open* 2023; **8:** 101567. doi: 10.1016/j.esmoop.2023.101567
6. Raoul JL, Forner A, Bolondi L, Cheung TT, Kloeckner R, de Baere T. Updated use of TACE for hepatocellular carcinoma treatment: How and when to use it based on clinical evidence. *Cancer Treat Rev* 2019; **72:** 28-36. doi: 10.1016/j.ctrv.2018.11.002
7. Varela M, Real MI, Burrel M, Forner A, Sala M, Brunet M, et al. Chemoembolization of hepatocellular carcinoma with drug eluting beads: efficacy and doxorubicin pharmacokinetics. *J Hepatol* 2007; **46:** 474-81. doi: 10.1016/j.jhep.2006.10.020
8. Lammer J, Malagari K, Vogl T, Pilleul F, Denys A, Watkinon A, et al. Prospective randomized study of doxorubicin-eluting-bead embolization in the treatment of hepatocellular carcinoma: results of the PRECISION V study. *Cardiovasc Interv Radiol* 2010; **33:** 41-52. doi: 10.1007/s00270-009-9711-7
9. Boulin M, Guiu S, Chauffert B, Delhom E, Schmitt A, Hillon P, et al. Screening of anticancer drugs for chemoembolization of hepatocellular carcinoma. *Anticancer Drugs* 2011; **22:** 741-8. doi: 10.1111/apt.12746
10. Robert J. Clinical pharmacokinetics of idarubicin. *Clin Pharmacokinet* 1993; **24:** 275-88. doi: 10.2165/00003088-199324040-00002
11. Guiu B, Hincapie G, Thompson L, Wu Y, Boulin M, Cassinotto C, et al. An in vitro evaluation of four types of drug-eluting embolics joaded with idarubicin. *J Vasc Interv Radiol* 2019: **30:** 1303-9. doi: 10.1016/j.jvir.2018.12.022
12. Favelier S, Boulin M, Hamza S, Cercueil JP, Cherblanc V, Lepage C, et al. Lipiodol trans-arterial chemoembolization of hepatocellular carcinoma with idarubicin: First experience. *Cardiovasc Intervent Radiol* 2013; **36:** 1039-46. doi: 10.1007/s00270-012-0532-8
13. Guiu B, Schmitt A, Reinhardt S, Deltenre P, Denys A, Lepida A, et al. Idarubicin-loaded ONCOZENE drug-eluting embolic agents for chemoembolization of hepatocellular carcinoma: in vitro loading and release and in vivo pharmacokinetics. *J Vasc Interv Radiol* 2015; **26:** 262-70. doi: 10.1016/j.jvir.2014.08.021
14. Boulin M, Hillon P, Cercueil JP, Raoul JL, Lepage C, Barbare JC, et al. Idarubicin-loaded beads for chemoembolisation of hepatocellular carcinoma: results of the IDASPHERE phase I trial. *Aliment Pharmacol Ther* 2014; **39:** 1301-13. doi: 10.1111/apt.12776
15. Guiu B, Chevallier P, Assenat E, Barbier E, Merle P, Bouvier A, et al. Idarubicin-loaded beads for chemoembolization of hepatocellular carcinoma: the IDASPHERE II single-arm phase II trial 2019; **291:** 801-8. doi: 0.1148/radiol.2019182399
16. Guiu B, Jouve JL, Schmitt A, Minello A, Bonnetain F, Cassinotto C, et al. Intra-arterial idarubicin_lipiodol without embolisation in hepatocellular carcinoma: the LIDA-B phase I trial. *J Hepatol* 2018; **68:** 1163-71. doi: 10.1016/j.jhep.2018.01.022.
17. Common Terminology Criteria for Adverse Events v. 5.0 [internet]. [cited 2024 Jan 3]. Available at: https://ctep.cancer.gov/protocoldevelopment/electronic_applications/docs/ctcae_v5_quick_reference_5x7.pdf
18. Lencioni R, Llovet J. Modified RECIST (mRECIST) assessment for hepatocellular carcinoma. *Semin Liver Dis* 2010; **30:** 52-60. doi: 10.1055/s-0030-1247132
19. Guiu B, Hincapie G, Thompson L, Wu Y, Boulin M, Cassinotto C, et al. An in vitro evaluation of four types of drug-eluting embolics loaded with idarubicin. *J Vasc Interv Radiol* 2019; **30:** 1303-9. doi: 10.1016/j.jvir.2018.12.022.
20. de Baere T, Guiu B, Ronot M, Chevallier P, Sergent G, Tancredi I, et al. Real life prospective evaluation of new drug-eluting platform for chemoembolization of patients with hepatocellular carcinoma: PARIS registry. *Cancers* 2020; **12:** 3405. doi: 10.3390/cancers12113405
21. Guiu B, Colombat S, Piron L, Hermida M, Allimant C, Pierredon-Foulongne MA, et al. Transarterial chemoembolization of hepatocellular carcinoma with idarubicin-loaded tandem drug-eluting embolics. *Cancers* 2019; **11:** 987. doi: 10.3390/cancers11070987
22. Anderlini P, Benjamin RS, Wong FC, Kantarjian HM, Andreeff M, Kornblau SM, et al. Idarubicin cardiotoxicity: a retrospective study in acute myeloid leukemia and myelodysplasia. *J Clin Oncol* 1995; **13:** 2827-34. doi: 10.1200/JCO.1995.13.11.2827
23. Guiu B, Deschamps F, Aho S, Munck F, Dromain C, Boige V, et al. Liver/biliary injuries following chemoembolisation of endocrine tumours and hepatocellular carcinoma: Lipiodol vs. drug-eluting beads. *J Hepatol* 2012; **56:** 609-17. doi: 10.1016/j.jhep.2011.09.012
24. Shi Z, Wang D, Jiang H, Kang T, Yi R, Cui L. Comparison of CalliSpheres® microspheres drug-eluting beads and conventional transarterial chemoembolization in hepatocellular carcinoma patients: a randomized controlled trial. *Radiol Oncol* 2023; **57:** 70-9. doi: 10.2478/raon-2023-0001
25. Korsic S, Levasic N, Dezman R, Zupan LAL, Trotovsek B, Jansa R, et al. Safety and efficacy of drug-eluting microspheres chemoembolization under cone beam computed tomography control in patients with early and intermediate stage hepatocellular carcinoma. *Radiol Oncol* 2022; **56:** 311-8. doi: 10.2478/raon-2022-0019
26. Gomes FV, Oliveira JA, Correia MT, Costa NV, Abrantes J, Torres D, et al. Chemoembolization of hepatocellular carcinoma with drug-eluting polyethylene glycol embolic agents: single-center retrospective analysis in 302 patients. *J Vasc Interv Radiol* 2018; **29:** 841-9. doi: 10.1016/j.jvir.2018.02.004

27. Lucatelli P, Ginnani Corradini L, De Rubeis G, Corona M, Saba L, Catalano C, et al. Balloon-occluded transcatheter arterial chemoembolization (b-TACE) for hepatocellular carcinoma performed with polyethylene-glycol epirubicin-loaded drug-eluting embolics: safety and preliminary results. *Cardiovasc Intervent Radiol* 2019; **42:** 853-62. doi: 10.1007/s00270-019-02192-y

28. Aliberti C, Carandina R, Sarti D, Mulazzani L, Pizzirani E, Guadagni S, et al. Chemoembolization adopting polyethylene glycol drug-eluting embolics loaded with doxorubicin for the treatment of hepatocellular carcinoma. *AJR Am J Roentgenol* 2017; **209:** 430-4. doi: 10.2214/AJR.16.17477

29. Fiorentini G, Sarti D, Carandina R, Mincarelli C, Candelari R, Argirò R, et al. A review discussing the use of polyethylene glycol microspheres in the treatment of hepatocellular carcinoma. *Future Oncol* 2019; **15:** 695-703. doi: 10.2217/fon-2018-0425

30. Veloso Gomes F, de Baère T, Verset G, Coimbra É, Tovar-Felice G, Malagari K, et al. Transarterial chemoembolization with anthracyclines-loaded polyethylene glycol drug eluting microspheres for the treatment of hepatocellular carcinoma: a pooled multicentric analysis of survival in 580 patients. *Cardiovasc Intervent Radiol* 2023; **46:** 436-46. doi: 10.1007/s00270-023-03362-9

31. Popovic P, Stabuc B, Jansa R, Garbajs M. Survival of patients with intermediate stage hepatocellular carcinoma treated with superselective transarterial chemoembolization using doxorubicin-loaded DC Bead under cone-beam computed tomography control. *Radiol Oncol* 2016; **50:** 418-26. doi: 10.1515/raon-2015-0045

32. Vogel A, Cervantes A, Chau I, Daniele B, Llovet JM, Meyer T, et al. Hepatocellular carcinoma: ESMO Clinical Practice Guidelines for diagnosis, treatment and follow-up. *Ann Oncol* 2018; **29:** iv238-55. doi: 10.1093/annonc/mdy308

33. Bruix J, Reig M, Rimola J, Vilana R, Burrel M, Llovet JM, et al. Clinical decision making and research in hepatocellular carcinoma: pivotal role of imaging techniques. *Hepatology* 2011; **54:** 2238-44. doi: 10.1002/hep.24670

34. Wang H, Li B, Wang Y, Zhang J, Wu Y, Fan W, Li J. Time to untreatable progression is an appropriate surrogate endpoint for overall survival in patients with hepatocellular carcinoma after transarterial chemoembolization. *J Cancer Res Ther* 2020; **16:** 301-8. doi: 10.4103/jcrt.JCRT_898_19

research article

Assessment of chemical-shift and diffusion-weighted magnetic resonance imaging in differentiating malignant and benign vertebral lesions in oncologic patients. A single institution experience

Marija B Mijaljevic[1], Zorica C Milosevic[2], Slobodan Đ Lavrnic[1], Zorica M Jokovic[3], Danica I Ninkovic[1], Radoje M Tubic[1], Rajna R Jankovic[1]

[1] Department of Radiology, Institute of Oncology and Radiology of Serbia, Belgrade, Serbia
[2] Faculty of Medicine, University of Belgrade, Belgrade, Serbia
[3] Department of Radiology, University Children's Hospital, Belgrade, Serbia

Radiol Oncol 2024; 58(4): 527-534.

Received 11 April 2024
Accepted 25 July 2024

Corresponding author: Marija Mijaljevic, Department of Radiology, Institute of Oncology and Radiology of Serbia, Pasterova 14, 11000 Belgrade, Serbia. E-mail: marija.mijaljevic@ncrc.ac.rs

Disclosure: No potential conflicts of interest were disclosed.

Background. To analyze the contribution of two non-standard magnetic resonance imaging (MRI) techniques the chemical-shift image (CSI), and diffusion-weighted imaging (DWI) in distinguishing malignant and benign vertebral bone marrow lesions (VBMLs).

Patients and methods. Conventional spine MRI protocol, followed by CSI and DWI was performed with a 1.5 T system on 102 oncologic patients between January 2020 and December 2023. From the identified 325 VBMLs, 102 representative lesions (one per patient) were selected. VBMLs were divided into malignant (n = 74) and benign (n = 28) based on histopathology, or imaging follow-up. The quantitative parameters for VBMLs assessment were signal intensity ratio (SIR) derived from CSI and apparent diffusion coefficient (ADC) derived from DWI.

Results. The malignant VBMLs had significantly higher SIR values ($p < 0.05$) and lower ADC values compared to benign VBMLs ($p < 0.05$). The area under the curve (AUC) was 0.953 ($p < 0.001$) for SIR, and 0.894 for ADC ($p < 0.001$) (cut-off at > 0.82, and ≤ 1.57×10^{-3} mm^2/s, respectively). The sensitivity and specificity for SIR were 93.6%, and 88.5%, while for ADC were 88.2% and 92.3% (respectively). The combined use of SIR and ADC improved the diagnostic accuracy to AUC of 0.988 ($p < 0.001$, cut-off at > 0.19), sensitivity, and specificity of 100.0% and 90.9% (respectively).

Conclusions. Quantitative parameters, SIR and ADC, derived from two non-standard MRI techniques, CSI, and DWI, showed diagnostic strength in differentiating malignant and benign VBMLs. Combining both methods can further enhance the diagnostic performance and accuracy of spine MRI in clinical practice.

Key words: magnetic resonance; chemical-shift imaging; diffusion-weighted imaging; bone marrow lesions

Introduction

Differentiating benign from malignant lesions in the spinal column is one of the key goals of neuro-oncological imaging. Skeletal metastases are the most common malignant tumors of the bone system in adults, with a high incidence, especially in the case of breast and prostate cancer, where they

account for up to 70% of cases.[1] The spinal column is a frequent site of metastases, involving various structures such as bone, epidural space, leptomeninges, and spinal cord. Metastases of the spinal column tend to be multiple. For instance, in breast cancer, they are commonly found in the thoracic and lumbar regions, followed by the cervical region (63.6%, 53.8%, and 21.7%, respectively).[2] MRI of the spinal column has a high sensitivity and specificity in detecting metastases in bone structures (91%, and 95%, respectively).[1,3] However, on a conventional MRI examination of the spinal column, malignant and some benign lesions appear identical, representing a radiological diagnostic challenge. The conventional MRI examination sometimes can not differentiate benign from malignant fractures.[4] Furthermore, a personal history of cancer does not necessarily imply malignant vertebral body infiltration and benign spine lesions in oncologic patients can cause diagnostic dilemmas, such as incidental findings of preformed benign lesions, or osteoporotic vertebral fractures due to endocrine therapy for breast cancer.[5]

Clinical work-up pathways of malignant and benign vertebral bone marrow lesions (VBMLs) are divergent, and differentiation of etiology is crucial. The development and application of non-standard MRI techniques for spine examination are aimed at increasing the diagnostic accuracy of MRI examination. One such technique is a gradient-echo MRI technique of chemical-shift imaging (CSI) in-phase (IP) and out-of-phase (OOP). The physicochemical principle of the CSI IP-OOP MRI technique is based on the different oscillation frequencies of water and fat protons.[6] Due to the presence of water and fat in normal fatty or hematopoietic red bone marrow, on the CSI-OOP sequence signal intensity (SI) of the bone marrow fat is suppressed. On the contrary, the complete replacement of normal bone marrow by malignant cells should result in lack of fat suppression on the oposite phase images.[7]

Diffusion-weighted magnetic resonance imaging (DWI) is another non-standard MRI technique for differentiating VBMLs. Quantifying the diffusion of water molecules in tissue through a numerical parameter – the apparent diffusion coefficient (ADC)- shows that the ADC value of normal bone marrow is 0.2–0.6 x 10^{-3} mm^2/s.[8] This represents a physiological restriction of water diffusion due to the anatomical trabeculated structure of the vertebral spongiosa and fat in the bone marrow. The disrupted bone structure in pathologically altered bone marrow leads to different ADC values, depending on the type of pathology. However, the degree of increase of ADC value in benign lesions is higher compared to malignant lesions.[9]

In the era of a transition to artificial intelligence and machine learning in neuroimaging, the spine MRI examination with different imaging sequences and optimization of protocols still represent an important part of the clinical routine in oncologic institutions. Our study aimed to analyze and combine two non-standard MRI techniques, CSI IP-OOP, and DWI, as additional methods to conventional spine MRI in distinguishing malignant and benign VBMLs.

Patients and methods

The retrospective study was conducted at the Institute of Oncology and Radiology of Serbia. The study was in accordance with the ethical standards of the institutional and national research committee and was approved by the Ethics committee of our institution (No. 284-01/2022/3). Each patient completed and signed an informed consent for the MRI examination.

Patients characteristics

The spine MRI examinations performed between January 2020 and December 2023 were reviewed. The inclusion criteria were as follows: (1) pathohistologically verified primary malignancy; (2) initial conventional spine MRI examination to determine the clinical stage of the disease; (3) follow-up conventional MRI examination after completed oncological treatment, including the patients with and without clinical suspicion of metastases in the spinal column; (4) CSI IP-OOP and DWI techniques; (5) applied one or more of the following procedures: biopsy with pathohistological (PH) verification of VBML; scintigraphy (Sci); positron emission tomography/computed tomography (PET/CT); adequate clinical and neuroradiological follow-up for 6 months or longer after the detection of lesion(s), which will ensure the final etiology. Apart from general contraindications to MRI, the exclusion criteria were as follows: (1) a focal lesion < 1 cm in diameter; (2) systemic anticancer therapy and/or radiotherapy in the region of interest completed 6 months before MRI examination; (3) inability of the patient to adequately withstand the examination; (4) inappropriate MRI views of the spinal column for technical reasons; (5) patients under 18 years of age.

According to the mentioned criteria, 102 successive patients with 325 VBMLs were enrolled in the study, 85 women (83%) and 17 men (17%). The mean age of patients was 61.8 years (range 30–85 years). The malignancies were: breast cancer in 62 patients (60.8%), lung cancer in 10 (9.8%), prostate cancer in 7 (6.9%), melanoma in 4 (3.9%), and others – a total of 19 patients (18.6%), i.e ≤ 2 patients with one of the following histological types: colorectal cancer, cervical cancer, endometrial cancer, renal cell carcinoma, oesophageal cancer, nasopharyngeal cancer, laryngeal cancer, hepatocellular carcinoma, salivary gland cancer, multiple myeloma, lymphoma, medulloblastoma, and malignant hemangioendothelioma.

The distribution of VBMLs in 102 patients was: thoracic spine in 51 (50.0%), lumbar spine in 38 (37.2%), sacrum in 12 (11.8%), and cervical spine in one patient (1.0%). Solitary VBML was found in 30 patients (29.4%) and multiple lesions in 72 patients (70.6%).

The VBMLs were classified as either benign or malignant. The diagnosis was made based on the biopsy and PH confirmation in 10 patients (9.8%). In the absence of HP confirmation, the diagnosis was made based on the additional imaging studies – Sci in 28 patients (27.5%) and PET/CT in 8 patients (7.8%), or the follow-up MRI examination. VMBLs that had MRI characteristics typical of benign lesions and had stable appearances during follow-up MRI examinations of at least 6 months were classified as benign.[10]

MRI protocol

Data were acquired with a 1.5 T MRI system (Magnetom Avanto Fit, Siemens, Germany) using phased-array spine coils. The routine clinical MRI protocol used at our institution included T1-weighted (T1W), T2W, short tau inversion recovery (STIR) MRI sequences precontrast, T1W fat-suppressed (FS) with an intravenous bolus of a gadobutrol (Gd-DO3A-butrol; Gadovist, 0.1 mmol/kg, 1 mmol/ml; Bayer Healthcare, Germany) contrast agent, at a rate of 3–5 ml/s. The parameters of routine clinical MRI protocol were: T1W TSE (TR/TE 613/9.8), T2W TSE (TR/TE 3380/89), STIR TSE (TR/TE 2370/78; inversion time, 160 ms), T1WFS TSE after contrast medium application (TR/TE 881/9.8), slice thickness 3 mm (cervical), 4 mm (thoracic and lumbar spine), matrix size 384 x 384 mm.

The non-standard examination protocols were the CSI IP-OOP technique and DWI with ADC maps, performed in the sagittal plane. The image acquisition parameters of the CSI IP-OOP technique included FOV 262x350 mm, matrix size 426x320 mm, (TR/TE in phase 118/5.27, out of phase 118/2.35), thickness section 3 mm (cervical), 4 mm (thoracic and lumbar spine). DWI sequence was acquired before contrast agent administration with fat saturation single-shot TSE sequence (TR/TE 3000/99; 128 x 92 matrix, flip angle 180 degrees, using b values of 100 s/mm^2 and 400 s/mm^2).

Image analysis

Images were analyzed using a Syngo via program (Siemens Medical Solutions, USA). The region of interest (ROI) was drawn manually and placed at a single slice with the largest possible lesion diameter, where the lesion was best seen on T1W, STIR, DWI, CSI-IP, and CSI-OOP sequences. Then it was copied to another image using the software paste option to the same image position. Areas close to the rim, lesions with intralesional hemorrhage, or necrotic areas were excluded from measurement. In the cases of numerous similar focal VBMLs in the same patient, ROI was chosen for only one of the most prominent lesions, to reduce the potential statistical influence of multiple similar lesions in single patients: 51 ROIs (50.0%) were located in the thoracal spine, 38 ROIs (37.3%) in the lumbar spine, 12 ROIs (11.7%) in the sacral and one ROI (1.0%) in the cervical spine.

On the CSI-IP and CSI-OOP sequences, SI of bone marrow was measured by manually placing the ROI. Signal intensity ratio (SIR) was calculated with the obtained SI values at ROI, according to the formula: "SIR = out-of-phase signal intensity value / in-phase signal intensity value" which was used in previous studies to distinguish benign from malignant bone marrow involvement. [11]

The software calculation of the ADC value was performed after manually placing the ROI on a representative part of the image. A methodology for defining the cut-off values of ADC between benign and malignant lesions was according to previous studies.[12]

Both quantitative image analyses, SIR, and ADC were performed in consensus by two radiologists with 10 years (M.M.) and 5 years (D.N.) of clinical experience in the field of MRI neuro-oncology and a physicist (S.G.) with more than 15 years of experience in CSI IP-OOP technique and DWI.[13]

All researchers were blinded to patient-related information, including histological types of lesions.

FIGURE 1. A 50-year-old woman with breast cancer and focal benign vertebral bone marrow lesion (VBML) (arrows). A round-shaped, abnormal signal intensity change in the bone marrow is evident in the L1 body on sagittal T1-weighted **(A)**, short tau inversion recovery (STIR), **(B)**, contrast-enhanced fat- satureted T1-weighted **(C)** in-phase T1-weighted **(D)**, out-of-phase T1-weighted **(E)** images. Apparent diffusion coefficient (ADC) **(F)** value is 1.74 x 10^{-3} mm^2/s. The signal intensity ratio (SIR) value is calculated as 0.8 and is consistent with benignity. Standardized Uptake Value (SUV) on PET scan excluded malignancy. After one year of follow-up, the lesion STIR/postcontrast hyperintensity almost disappeared.

Statistical analysis

The mean value, standard deviation, ranges and percentages were determined for parameters describing the study group. Receiver operating characteristic (ROC) and area under the curve (AUC) analyses, as well as the cut-off values, sensitivity, and specificity, were used to compare the diagnostic performance of the SIR, ADC, and combination (SIR, ADC) in terms of distinguishing focal benign VBMLs from metastases. Between-group differences in the SIR, and ADC values, were compared using the Mann-Whitney U-test. The multivariate regression analysis formula with SIR and ADC values was: y = -2,461–14,426*ADC + 28,085*SIR. Statistical analyses were performed using the software package R (version 4.2.3). For all assessments, a p-value < 0.05 was taken to indicate statistical significance.

Results

Analysis of spinal MRI was performed in a total of 28 (27.5%) benign and 74 (72.5%) malignant VBMLs. The benign VBMLs were: vertebral fractures in 12 patients, atypical hemangiomas in 10 patients, Schmorl's nodes in three patients, focal hematopoietic islands in two patients, and aggressive vertebral body hemangioma in one patient. The malignant VBMLs were: metastases in 70 patients, spinal lymphomas in two patients, malignant hemangioendothelioma in one patient, and multiple myeloma in one patient. Representative images for benign and malignant VBMLs are given in Figure 1 and 2.

The median SIR value and range for the malignant lesions were 0.99 (0.78–1.37), while for the benign lesions, they were 0.65 (0.24–1.04). The median ADC value and range for the malignant lesions were 1.22 x 10^{-3} mm^2/s (0.89–1.75 x 10^{-3} mm^2/s), while for the benign lesions, they were 1.74 x 10^{-3} mm^2/s (0.73–2.24 x 10^{-3} mm^2/s). The SIR values of malignant lesions were significantly higher compared to benign lesions ($p < 0.05$), while the ADC values of malignant lesions were statistically significantly lower compared to benign lesions ($p < 0.05$).

The diagnostic performance of SIR, ADC, and their combination (SIR, ADC) in the differentiation of VBMLs is shown in Table 1 and Figure 3. The AUC, cut-off values, sensitivity, and specificity showed a high agreement of SIR and ADC in the differentiation of benign and malignant VBMLs. The combination of SIR and ADC demonstrated the best diagnostic performance (AUC = 0.988, 95% confidence interval [CI] = 0.872–1.000), with a sensitivity of 100.0% and specificity of 90.9%.

Discussion

The number of patients with malignant tumors is increasing, and the medical research in the field of neuro-oncology represents a step closer to optimal therapy and potential cure for the patient.[14] The development of bone metastases is a classical unfavorable prognostic factor, implying a palliative

FIGURE 2. A 75-year-old woman with breast cancer and five focal malignant vertebral bone marrow lesions (VBMLs), the most prominent in the L1 body (arrows) which we chose to analyze. Abnormal signal intensity change is evident on sagittal T1-weighted **(A)**, short tau inversion recovery (STIR), **(B)**, contrast-enhanced fat-satureted T1-weighted **(C)** in-phase T1- weighted **(D)**, and out-of-phase T1-weighted **(E)**. Apparent diffusion coefficient (ADC) **(F)** value is 0.99 x 10^{-3} mm^2/s. The signal intensity ratio (SIR) value is calculated as 1.07. which indicates the malignant lesion. Sci suggested malignant lesions.

TABLE 1. Diagnostic performance of the signal intensity ratio (SIR), apparent diffusion coefficient (ADC), and combination (SIR, ADC) for differentiating benign from malignant vertebral bone marrow lesions (VBMLs)

Parameters	AUC (95% CI)	Standard error	p	Cut-off	Sensitivity (%)	Specificity (%)
SIR	0.953 (0.886–0.987)	0.029	< 0.001	> 0.82	93.6	88.5
ADC	0.894 (0.769–0.965)	0.077	< 0.001	≤ 1.57	88.2	92.3
Combination (SIR, ADC)	0.988 (0.872–1.000)	0.014	< 0.001	> 0.19	100.0	90.9

AUC = area under the curve; CI = confidence interval; p = significance level

Cut-off values are given in units of x10^{-3} mm^2/s for ADC.

approach to the therapy and poor overall survival. However, technological advancements introduced various surgical procedures with curative intent for selected patients, particularly those with solitary bone metastases. Understanding different mechanisms related to the pathogenesis of bone metastases developed some promising systemic therapies targeting specific malignant cell types, advancing the concept of precision therapy in oncology.[15] All these facts highlight the importance of imaging methods in guiding treatment decisions and improving patient outcomes.

In our study, out of a total of 102 VBMLs, 28 (27.5%) were classified as benign and 74 (72.5%) as malignant. Among the malignant lesions, metastases were the most common, accounting for 70 out of the 74 malignant lesions, while among the benign lesions, vertebral fractures (12 cases) and atypical hemangiomas (10 cases) were the most frequently observed lesions. It is worth mentioning that in the group of malignant VBMLs, extremely rare skeletal metastases of medulloblastoma, and malignant hemangioendothelioma were present.

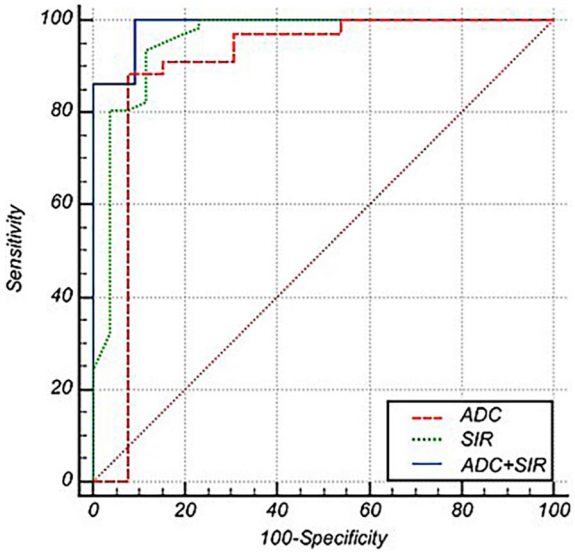

FIGURE 3. The receiver operating characteristic (ROC) curves of the apparent diffusion coefficient (ADC) (red line), signal intensity ratio (SIR) (green line), and combined SIR and ADC (blue line). The ROC curves show that the combined SIR and ADC have the highest AUC for differentiating benign from malignant vertebral bone marrow lesions (VBMLs), followed by the SIR and ADC.

TABLE 2. The studies of diffusion-weighted imaging in the differentiation of bone marrow lesions

Authors	No. of lesions	Clinical features	Technical parameters No. of image planes	Technical parameters b values (s/mm²)	ADC cut-off values (× 10^{-3} mm²/s)
Park *et al.*[9]	86	Traumatic CFs vs. tumor infiltration with/without malignant CFs	Single shot SE EPI	0, 400, 1000	1.14
Kwack *et al.*[10]	126	Focal benign lesion vs. metastases	Single-shot echo-planar	0, 800	0.995
Geith *et al.*[12]	46	Osteoporotic vs. malignant CFs	Single shot TSE	100, 250, 400	1.7
Park *et al.*[23]	58	Hyperplastic hematopoietic BM vs. malignant BM lesions	Single shot SE EPI	0, 800	0.695
Schmeel *et al.*[27]	89	Benign (traumatic, inflammatory, and primary) vs. malignant (metastatic and hematologic)	Single-shot spin-echo echo-planar with multislice short TI inversion recovery fat suppression	0, 800	1.08
Pozzi *et al.*[29]	116	Benign primary tumors vs. bone metastases vs. malignant primary tumors	Spin-echo echo-planar technique	0, 1000	0.952 (benign vs. malignant tumors)
Hajalioghli *et al.*[30]	23	Atypical hemangiomas and metastases	Spin-echo single-shot echo-planar with fat suppression	50, 400	0.958
Lee *et al.*[31]	51	Schmorl nodes vs. bone metastases	Single-shot (FOCUS, GE Healthcare)	0, 400, 1000	1.028

ADC = apparent diffusion coefficient; BM = bone marrow; CF = compression fracture; DWI = diffusion-weighted imaging, EPI = echo planar imaging; SE = spin echo; TSE = turbo spin echo

The SIR values derived from the CSI IP-OOP technique in our study demonstrated high sensitivity (93.6%) and specificity (88.5%) in distinguishing between benign and malignant VBMLs. The AUC was 0.953 (95% CI, 0.886–0.987). Malignant VBMLs exhibited significantly higher SIR values than benign VBMLs, with a cut-off value of > 0.82. A comparison of our results with previous investigations supports the diagnostic performance of CSI. A study by Disler *et al*. in the late 1990s provided initial insights into the predictive capability of the SIR between in-phase and out-of-phase images for distinguishing neoplastic or non-neoplastic lesions, achieving a sensitivity of 100% and specificity of 94–100%.[16] Similarly, studies by van Vucht *et al*. and Zajick *et al*. confirmed the accuracy of CSI in distinguishing between neoplastic and non-neoplastic lesions. However, Zajick *et al*. noted limitations in differentiating malignant bone tumors from non-fat-containing benign bone tumors.[17,18] A meta-analysis by Suh *et al*. supported the efficacy of CSI in distinguishing between benign and malignant VBMLs, with high sensitivity, specificity, and an AUC of 0.95 (95% CI, 0.93–0.97), with sensitivity and specificity rates of 92% and 89%, respectively.[19] Despite comparable results among the mentioned studies, variations existed in the histology characteristics of the lesions and the applied techniques (such as minimum TR and TE, flip angle, slice thickness, gradient-echo CSI, or the Dixon method). These differences may influence the overall diagnostic performance and should be considered when interpreting each study findings.

The ADC values derived from DWI in our study revealed notable sensitivity and specificity in distinguishing between benign and malignant VBMLs (88.2% and 92.3%, respectively). The AUC was 0.894 (95% CI, 0.769–0.965), indicating the strong discriminative ability of DWI. Malignant lesions were characterized by significantly lower ADC values (cut-off value of ≤ 1.57 × 10^{-3} mm²/s). Diffusion was measured at values of b = 0 s/mm² and b = 400 s/mm², according to the meta-analysis that suggested low-b-value as more valuable parameters than standard-b-value DWI for discriminating malignant from benign vertebral compression fractures.[20]

Considerable technical variability of the DWI exists among different institutions (such as Echo Planar Imaging or Fast Spin Echo methods, fat suppression methods, and selected b-values).[20,21] Owing to the lack of standardization in DWI protocols and technical factors, quantitative measurements derived from DWI may have limited reproducibility with frequent substantial overlap between the cut-off values, reducing their applicability in clinical practice.[22]

An interpretation of ADC values is complex and varies significantly depending on the histology characteristics of the lesions. Although the ADC values of benign VBMLs are higher than malignant ones[8,9], certain benign lesions, such as

hyperplastic bone marrow have low ADC values due to the preserved bone and bone marrow structures.[23] Additionally, the usefulness of ADC values in differentiating malignancy from infection was not consistently demonstrated across the studies.[22,24] Furthermore, according to a study by Maeda *et al*., the false negative results of a malignant vertebral compression fracture may appear due to the necrotic tumor tissue, a large amount of associated interstitial edema, and an increased perfusion fraction in the hypervascular portion of the lesion.[25] Summarized data of DWI characteristics in different studies are given in Table 2.

The cut-off ADC values obtained in our study were comparable to the results of Park HJ *et al*. and Geith *et al*.[9,12] The similarity of technical conditions and prevalence of benign fractures among benign lesions across all studies could be a reason for concordant results. On the contrary, Kwack *et al*. reported significantly different ADC cut-off values compared to our results ($\leq 995 \times 10^{-6}$ mm^2/s versus $\leq 1.57 \times 10^{-3}$ mm^2/s).[10] The authors compared benign VBMLs and metastases, but the benign compression fractures and Schmorl's nodes were excluded from the analysis. Suh *et al*. reported a sensitivity of 89% and specificity of 87% of ADC for differentiating benign and malignant VBMLs and compression fractures, similar to our results.[26]

In our study, the diagnostic accuracy was additionally improved with the combination of CSI IP-OOP and DWI techniques, with a sensitivity of 100% and specificity of 90.9% compared to either single quantitative assessment, with a cut-off value of > 0.19. Combined CSI IP-OOP and DWI techniques had an AUC of 0.988 (95% CI, 0.872–1.000). Similar improvement in the diagnostic accuracy with a combination of CSI and DWI was reported by Schmeel *et al*. in the analysis of benign VBMLa (traumatic, inflammatory, and primary spine tumors) versus malignant (metastatic and hematologic).[27]

Diagnosis of multiple vertebral lesions with similar MRI morphologic appearances is typically not in question and is usually attributed to metastases. Conversely, identifying the etiology of solitary lesions presents a greater challenge. Our findings demonstrate that chemical-shift and diffusion-weighted MRI can detect subtle differences between malignant lesions and their surrounding microenvironments compared to benign lesions. Therefore, these two non-standard MRI techniques might be effectively applied to clarify the diagnosis of solitary vertebral lesions using quantitative parameters, such as SIR and DWI.

Our study had several limitations. First, the study group demonstrated histological diversity among VBMLs. Although metastases were the most prevalent malignant type, variations within both benign and malignant histological types were present. Additionally, the sample size for the benign group was small. Future studies with larger sample sizes are warranted to overcome this limitation and ensure a more accurate differentiation of VBMLs. Second, not all VBMLs were histopathologically proven. Third, the subjectivity of readers during ROI selection could alter the values of SIR and ADC. Fourth, age and hematopoietic status can influence vertebral marrow composition, and are in correlation with both methods, CSI and DWI.[28] Although the majority of our patients were female patients after natural or artificial menopause, we did not include hormonal and hematological data in our study.

In conclusion, the non-standard MRI techniques, CSI IP-OOP, and DWI, can significantly enhance the diagnostic accuracy of MRI in distinguishing between benign and malignant VBMLs. Moreover, the synthesis of CSI IP-OOP and DWI can further augment the diagnostic precision of MRI spine examinations. The capacity of non-standard MRI techniques to detect subtle, histologically diverse pathological processes within vertebral body marrow emphasizes the imperative need for standardization of MRI techniques, and the analysis of larger and more homogeneous histological lesion types. This will undoubtedly contribute to the broader application of non-standard MRI techniques in routine clinical assessments of VBMLs.

References

1. Heindel W, Gübitz R, Vieth V, Weckesser M, Schober O, Schäfers M. The diagnostic imaging of bone metastases. *Dtsch Arztebl Int* 2014; **111:** 741-47. doi: 10.3238/arztebl.2014.0741
2. Chen WZ, Shen JF, Zhou Y, Chen XY, Liu JM, Liu ZL. Clinical characteristics and risk factors for developing bone metastases in patients with breast cancer. *Sci Rep* 2017; **7:** 1325. doi: 10.1038/s41598-017-11700-4
3. Soliman M, Taunk NK, Simons RE, Osborne JR, Kim MM, Szerlip NJ, et al. Anatomic and functional imaging in the diagnosis of spine metastases and response assessment after spine radiosurgery. *Neurosurg Focus* 2017; **42:** E5. doi: 10.3171/2016.9. FOCUS16350
4. Oztekin O, Ozan E, Hilal Adibelli Z, Unal G, Abali Y. SSH-EPI diffusion-weighted MR imaging of the spine with low b values: is it useful in differentiating malignant metastatic tumor infiltration from benign fracture edema? *Skeletal Radiology* 2009; **38:** 651-8. doi: 10.1007/s00256-009-0668-z
5. Shapiro CL. Osteoporosis: a long-term and late-effect of breast cancer treatments. *Cancers* 2020; **12:** 3094. doi: 10.3390/cancers121130945
6. Xiao Z, Li J, Li C, Zhang Y, She D, Cao D. Chemical shift MR imaging in the lumbar vertebra: the effect of field strength, scanner vendors and flip angles in repeatability of signal intensity index measurement. *BMC Med Imaging* 2016; **16:** 64. doi: 10.1186/s12880-016-0167-3

7. Ragab Y, Emad Y, Gheita T, Mansour M, Abou-Zeid A, Ferrari S, et al. Differentiation of osteoporotic and neoplastic vertebral fractures by chemical shift {in-phase and out-of phase} MR imaging. *Eur J Radiol* 2009; **72:** 125-33. doi: 10.1016/j.ejrad.2008.06.019

8. Dietrich O, Geith T, Reiser MF, Baur-Melnyk A. Diffusion imaging of the vertebral bone marrow. *NMR Biomed* 2017; **30:** e333. doi: 10.1002/nbm.3333

9. Park HJ, Lee SY, Rho MH, Chung EC, Kim MS, Kwon HJ, et al. Single-shot echo-planar diffusion-weighted MR imaging at 3T and 1.5T for differentiation of benign vertebral fracture edema and tumor infiltration. *Korean J Radiol* 2016; **17:** 590-7. doi: 10.3348/kjr.2016.17.5.590

10. Kwack KS, Lee HD, Jeon SW, Lee HY, Park S. Comparison of proton density fat fraction, simultaneous R2*, and apparent diffusion coefficient for assessment of focal vertebral bone marrow lesions. *Clin Radiol* 2020; **75:** 123-30. doi: 10.1016/j.crad.2019.09.141

11. Akman B, Ata Korkmaz HA, Sarı A. Efficacy of chemical shift MRI for differentiating diffuse red bone marrow reconversion and hematological malignancies. *Turk J Med Sci* 2019; **49:** 644-52. doi: 10.3906/sag-1812-125

12. Geith T, Schmidt G, Biffar A, Dietrich O, Duerr HR, Reiser M, et al. Quantitative evaluation of benign and malignant vertebral fractures with diffusion-weighted MRI: what is the optimum combination of b values for ADC-based lesion differentiation with the single-shot turbo spin-echo sequence? *AJR Am J Roentgenol* 2014; **203:** 582-8. doi: 10.2214/AJR.13.11632

13. Schmeel FC, Lakghomi A, Lehnen NC, Haase R, Banat M, Wach J, et al. Proton density fat fraction spine MRI for differentiation of erosive vertebral endplate degeneration and infectious spondylitis. *Diagnostics* 2021;**12:** 78. doi: 10.3390/diagnostics12010078

14. Soerjomataram I, Bray F. Planning for tomorrow: global cancer incidence and the role of prevention 2020-2070. *Nat Rev Clin Oncol* 2021; **18:** 663-72. doi: 10.1038/s41571-021-00514-z

15. Yang W, Pan Q, Huang F, Hu H, Shao Z. Research progress of bone metastases: from disease recognition to clinical practice. *Front Oncol* 2023; **12:** 1105745. doi: 10.3389/fonc

16. Disler DG, McCauley TR, Ratner LM, Kesack CD, Cooper JA. In-phase and out-of-phase MR imaging of bone marrow: prediction of neoplasia based on the detection of coexistent fat and water. *AJR Am J Roentgenol* 1997; **169:** 1439-47. doi: 10.2214/ajr.169.5.9353477

17. van Vucht N, Santiago R, Pressney I, Saifuddin A. Role of in-phase and out-of-phase chemical shift MRI in differentiation of non-neoplastic versus neoplastic benign and malignant marrow lesions. *Br J Radiol* 2021; **94:** 20200710. doi: 10.1259/bjr.20200710

18. Zajick DC Jr, Morrison WB, Schweitzer ME, Parellada JA, Carrino JA. Benign and malignant processes: normal values and differentiation with chemical shift MR imaging in vertebral marrow. *Radiology* 2005; **237:** 590-6. doi: 10.1148/radiol.2372040990

19. Suh CH, Yun SJ, Jin W, Park SY, Ryu CW, Lee SH. Diagnostic performance of in-phase and opposed-phase chemical-shift imaging for differentiating benign and malignant vertebral marrow lesions: a meta-analysis. *AJR Am J Roentgenol* 2018; **211:** W188-W197. doi: 10.2214/AJR.17.19306

20. Luo Z, Litao L, Gu S, Luo X, Li D, Yu L, et al. Standard-b-value vs low-b-value DWI for differentiation of benign and malignant vertebral fractures: a meta-analysis. *Br J Radiol* 2016; **89:** 20150384. doi: 10.1259/bjr.20150384

21. Biffar A, Dietrich O, Sourbron S, Duerr HR, Reiser MF, Baur-Melnyk A. Diffusion and perfusion imaging of bone marrow. *Eur J Radiol* 2010;**76:** 323-8. doi: 10.1016/j.ejrad.2010.03.011

22. Mourad C, Cosentino A, Nicod Lalonde M, Omoumi P. Advances in bone marrow imaging: strengths and limitations from a clinical perspective. *Semin Musculoskelet Radiol* 2023; **27:** 3-21. doi: 10.1055/s-0043-1761612

23. Park S, Kwack KS, Chung NS, Hwang J, Lee HY, Kim JH. Intravoxel incoherent motion diffusion-weighted magnetic resonance imaging of focal vertebral bone marrow lesions: initial experience of the differentiation of nodular hyperplastic hematopoietic bone marrow from malignant lesions. *Skeletal Radiol* 2017; **46:** 675-83. doi: 10.1007/s00256-017-2603-z

24. Dumont RA, Keen NN, Bloomer CW, Schwartz BS, Talbott J, Clark AJ, et al. Clinical utility of diffusion-weighted imaging in spinal infections. *Clin Neuroradiol* 2019; **29:** 515-22. doi: 10.1007/s00062-018-0681-5

25. Maeda M, Sakuma H, Maier SE, Takeda K. Quantitative assessment of diffusion abnormalities in benign and malignant vertebral compression fractures by line scan diffusion-weighted imaging. *AJR Am J Roentgenol* 2003; **181:** 1203-9. doi: 10.2214/ajr

26. Suh CH, Yun SJ, Jin W, Lee SH, Park SY, Ryu CW. ADC as a useful diagnostic tool for differentiating benign and malignant vertebral bone marrow lesions and compression fractures: a systematic review and meta-analysis. *Eur Radiol* 2018; **28:** 2890-902. doi: 10.1007/s00330-018-5330-5

27. Schmeel FC, Enkirch SJ, Luetkens JA, Faron A, Lehnen N, Sprinkart AM, et al. Diagnostic accuracy of quantitative imaging biomarkers in the differentiation of benign and malignant vertebral lesions: combination of diffusion-weighted and proton density fat fraction spine MRI. *Clin Neuroradiol* 2021; **31:** 1059-70. doi: 10.1007/s00062-021-01009-1

28. Tsujikawa T, Oikawa H, Tasaki T, Hosono N, Tsuyoshi H, Yoshida Y, et al. Whole-body bone marrow DWI correlates with age, anemia, and hematopoietic activity. *Eur J Radiol* 2019; **118:** 223-30. doi: 10.1016/j.ejrad.2019.07.022

29. Pozzi G, Albano D, Messina C, Angileri SA, Al-Mnayyis A, Galbusera F, et al. Solid bone tumors of the spine: diagnostic performance of apparent diffusion coefficient measured using diffusion-weighted MRI using histology as a reference standard. *J Magn Reson Imaging* 2018; **47:** 1034-42. doi: 10.1002/jmri.25826

30. Hajalioghli P, Daghighi MH, Ghaffari J, Mirza-Aghazadeh-Attari M, Khamanian J, Ghaderi P, et al. Accuracy of diffusion-weighted imaging in discriminating atypical vertebral haemangiomas from malignant masses in patients with vertebral lesions: a cross-sectional study. *Pol J Radiol* 2020 6; **85:** e340-e347. doi: 10.5114/pjr.2020.97602

31. Lee JH, Park S. Differentiation of schmorl nodes from bone metastases of the spine: Use of apparent diffusion coefficient derived from DWI and fat fraction derived from a dixon sequence. *AJR Am J Roentgenol* 2019; **213:** W228-W235. doi: 10.2214/AJR.18.21003

research article

Impact of right-sided breast cancer adjuvant radiotherapy on the liver

Gonca Hanedan Uslu[1], Filiz Taşçı[2]

[1] Department of Radiation Oncology, İstinye University, Faculty of Medicine, İstanbul, Turkey
[2] Department of Radiology, Recep Tayyip Erdogan University Faculty of Medicine, Rize, Turkey

Radiol Oncol 2024; 58(4): 535-543.

Received 6 August 2024
Accepted 17 September 2024

Correspondence to: Assoc. Prof. Gonca Hanedan Uslu, M.D., Department of Radiation Oncology, İstinye University, Faculty of Medicine, İstanbul, Turkey. E-mail: goncadilek.hanedanuslu@isu.edu.tr

Disclosure: No potential conflicts of interest were disclosed.

Background. In patients with right-sided breast cancer the liver can be partially irradiated during adjuvant radiotherapy (RT). We aimed to determine breast cancer RT effects on liver using with magnetic resonance elastography (MRE) and biological results.

Patients and methods. This retrospective study enrolled 34 patients diagnosed with right-sided breast cancer who underwent adjuvant RT. Liver segment assessments were conducted using MRE for all participants. Additionally, a complete blood count and liver enzyme analysis were performed for each patient. All measurements were taken both prior to the initiation and upon completion of RT.

Results. A statistically significant difference was found in ALT ($p = 0.015$), ALP ($p = 0.026$), total protein ($p = 0.037$), and albumin ($p = 0.004$) levels before and after RT. The highest mean liver stiffness (kPa) value was recorded in segment 8, while the lowest was observed in segment 6. A weak but statistically significant positive correlation was found between segment 5 stiffness and liver volume ($p = 0.039$). Additionally, a statistically significant positive correlation was detected between ALP levels and the stiffness values in segment 4A ($p = 0.020$) and segment 6 ($p = 0.003$). Conversely, a weak negative correlation was observed between the stiffness values in segment 8 and post-RT total protein levels ($p = 0.031$).

Conclusions. MRE can help us identify the level of fibrotic stiffness in the liver segments within the RT area without establishing clinical symptoms. MRE can support the clinician in evaluating the liver functions of right breast cancer patients who underwent RT. We assume these results will facilitate new studies with a large number of patients on MRE imaging at certain intervals in the follow-up of patients with right breast cancer who received RT before the development of radiation-induced liver disease (RILD).

Key words: radiotherapy; right -sided breast cancer; magnetic resonance elastography; radiation-induced liver disease; liver fibrosis

Introduction

Radiotherapy (RT) is a crucial component of breast cancer treatment due to its ability to achieve local-regional cancer control and improve survival outcomes. However, certain side effects of RT may sometimes surpass the disease-related issues themselves, becoming primary determinant of patient survival.[1]

In conventional radiotherapy techniques, it is often impossible to completely protect nearby healthy organs adjacent to the irradiated volume. The more space occupied by organs with relatively low resistance to radiotherapy − referred to as "critical organs" − within the treatment area, the more severe the side effects tend to become.[2] Critical organs include the liver and kidneys during abdominal irradiation, the intestines during

pelvic irradiation, and the lenses during brain irradiation.[3,4]

In recent years, efforts have been made to mitigate the adverse patient outcomes associated with radiotherapy, especially to minimize the late side effects in left-sided breast cancer. Techniques such as intensity-modulated radiotherapy (IMRT) and deep inspiration breath hold (DIBH) are some of them. The use of these techniques has become widespread in the treatment of left-sided breast cancer, and their use for right-sided breast cancer is also recommended.[5,6]

Due to its anatomical location, the liver may be partially irradiated during adjuvant radiotherapy for patients with right-sided breast cancer.[7] The tolerable dose for a healthy liver is generally considered to be 30 Gy. Radiation-induced liver disease (RILD) is defined in tissue exposed to doses exceeding 30–35 Gy.[8] Therefore, liver dose restrictions are in place and are essential during abdominal radiotherapy, yet the liver is not typically regarded as an organ at risk (OAR) in breast cancer.[9]

The extent of liver damage due to irradiation can only be detected through radiological imaging techniques such as abdominal CT, ultrasound, or MRI unless clinical symptoms are present. In recent years, magnetic resonance elastography (MRE) has been increasingly used to diagnose liver diseases early. The liver MRE technique has been well described.[10] MRE is a noninvasive technique for staging liver fibrosis with excellent reproducibility.[11] The European and American Liver Research Associations recommend using transient elastography performed with Fibroscan® to detect liver fibrosis in patients with suspected nonalcoholic fatty liver disease (NAFLD).[7] A reliable, reproducible, non-invasive method was an unmet need to evaluate liver fibrosis. Beginning to elucidate the pathophysiology of liver fibrosis at the molecular level has made it possible to use serum markers for diagnosis. However, there is a need for another tool that will support the relationship between serum markers and histology and/or reflect histology more. Today, the best method to meet this need is transient elastography. Fibroscan® is a high-tech device that numerically measures the elasticity of soft tissues with this principle. MRE could be leveraged as a diagnostic tool for evaluating chronic liver diseases to assess hepatic fibrosis. It can detect a larger portion of the liver with very good resolution in contrast with liver biopsy assessment. Additionally, MRE could be utilized as an imaging method for identifying liver fibrosis that correlates well with liver biopsy in several chronic liver diseases and NAFLD. MRE has also been shown to be superior to other noninvasive methods in assessing liver fibrosis.[12] The risk of developing classic RILD is 5% to 35% when the entire liver is irradiated with 30 to 35 Gy.[13] MRE is a noninvasive technique for staging liver fibrosis with excellent reproducibility. According to data obtained from previous study, liver stiffness (LS) ≤ 3 kPa is considered normal, and LS > 3 kPa is considered compatible with fibrosis.[14] MRE is a better method for diagnosing and staging liver fibrosis as it is not influenced by factors such as obesity, ascites, inflammation, or etiology.[15] The accuracy and reliability of MRE in diagnosing all stages of liver fibrosis, especially late-stage fibrosis and cirrhosis, have been confirmed by meta-analyses.[16]

Currently, there is limited information available regarding the late-stage effects of RT on liver function in breast cancer patients. The primary aim of this study was to assess the effects of adjuvant radiotherapy on the liver in patients with right-sided breast cancer. The secondary objective was to examine the relationship between MRE findings and biological markers in determining the extent of liver involvement due to radiotherapy.

Patients and methods

Study population

This retrospective and descriptive study carried out in the radiation oncology clinic of a university hospital. To work; patients with primary right -sided breast cancer who had abdominal MRE examinations within at least three months after completion of RT were selected. Patients with liver disease, patients using drugs that could damage the liver other than standard drugs used in breast cancer treatment, and patients with liver function tests (LFT) values outside the reference range before RT were not included in the study. The files of 167 patients, whose adjuvant RT was completed within one year and who were admitted to the hospital for their final follow-up, were examined retrospectively, and the study was completed with 34 patients who met the sample acceptance criteria.

Ethical consideration

All procedures followed were in accordance with the ethical standards of the responsible committee on human experimentation (institutional and national) and with the Helsinki Declaration of 1975, as revised in 2008. Ethics committee approval has

been granted from our institution with protocol number (2023/111, date 27.04.2023).

Radiotherapy

The RT plans of all patients with breast cancer were made with the same technique and dose in our clinic. Varian R brand 13.6 version Eclipse contouring system using simulation tomographies were taken on a ToshibaR Aqullion LB model, 80 cm wide CT simulator device. Radiotherapy for all patients was planned according to standard ESTRO guidelines. After the official publication, the breast/chest wall and lymph node clinical target volumes (CTV) were delineated according to ESTRO guidelines. The planning target volüme (PTV) was cropped 2–3 mm under the skin. The prescribed dose was 50 Gy in 25 fractions (2 Gy/fraction) to the breast/chest wall and/or lymph nodes. When a breast with boost was indicated, it was delivered sequentially at 10–16 Gy doses in 5-8 fractions.

The objective was the homogenous cover of 95% of the PTV by >95% isodoses. Fifty consecutive treatment plans to the breast or chest wall with lymph node irradiation were used to calculate dose-volume histogram (DVH) values for each OAR (medullaspinalis, heart, ipsilateral-contralateral lung, contralateral breast, and liver). These dose values were classified in increasing order and divided into four quartiles. For all new treatment plans, the lower than Q2 dose constraint is now applied to each organ-at-risk to obtain optimal and sufficient beam intensity modulation to comply with clinical constraints. These dose constraints aimed to decrease the doses of OAR in patients with complex anatomy and/or irradiation volumes. Radiotherapy dose information (PTV volume, PTV mean, PTV max, liver volume, liver V30 Gy, liver mean) was recorded.

Data collection

Liver function tests and radiological imaging results of the patients were collected from hospital records, and radiotherapy treatment dose information and liver dose information were collected from the radiation oncology clinic data archive.

Biological hepatic function assessment

These tests are performed periodically in the hospital according to patient monitoring protocols. To evaluate liver functions, ALT, AST, GGT, LDH,

TABLE 1. Patients characteristics (N = 34)

Characteristics	
Age, years	**Mean ± SD (min-max)** 52.53± 9.38 (32-68)
	N(%)
Smoking	
No	10 (29.4)
Yes	24 (70.6)
Alcohol	
No	34 (100)
NAC	
Yes	15(44.1)
No	19(55.9)
Surgery	
BCS	21(61.8)
MRM	13(38.2)
Stage	
1A	10(29.4)
2A	14(41.2)
2B	3(8.8)
3A	7(20.6)
Histopathological	
IDC	31(91.2)
ILC	1(2.9)
IMC	1(2.9)
ITC	1(2.9)

BCS = breast-conserving surgery; IDC = invasive ductal carcinoma; ILC = invasive lobular carcinoma; IMC = invasive medullar carcinoma; ITC = invasive tubuler carcinoma; MRM = modified radical mastectomy; NAC = neoadjuvant chemotherapy; RT = radiotherapy

TABLE 2. Dosimetric date

Characteristics	Value (range)
RT dose (Gy)	60.0 (50-67)
PTV volume (cc)	1063.35 (372.6-2389.6)
PTV max (cGy)	6282.4 (5323.8-7050.9)
Liver volüme (cc)	1436.1 (843.8-2298.1)
Liver V30Gy (%)	1.7 (0-12.03)
Liver mean (cGy)	759.6 (133.8-1699.8)

RT = radiotherapy; PTV = planing target volume

TABLE 3. Comparison of before and after radiotherapy (RT) blood parameters

	Before RT		After RT		Test statistics	p-value
	Mean ± SD	Median (min - max)	Mean ± SD	Median (min - max)		
ALP	79.44 ± 34.28	71,5 (33-202)	90.5 ± 53.19	82.0 (39-357)	Z = -2.232	**0.026**
ALT	24.84 ± 12.95	21.0 (8-62)	20.26 ± 1.,89	17.0 (8-63)	Z = -2.423	**0.015**
AST	23.21 ± 7.88	21.0 (13-48)	24.32 ± 12.51	21.0 (13-74)	Z = -0.089	0.929
GGT	35.42 ± 34.08	23.0 (7-160)	33.56 ± 30.68	24.0 (12-170)	Z = -0.241	0.809
LDH	228.14 ± 64.71	224.5 (108-401)	216.85 ± 45.95	210.5 (140-310)	t = 0.968	0.340
Total protein	71.15 ± 4.88	71.0 (51-80)	72.94 ± 3.25	72.65 (64.8-79)	Z = -2.082	**0.037**
Albumin	41.91 ± 2.21	42.0 (38-45)	43.36 ± 2.87	43.05 (35.6-48.7)	t = -3.12	**0.004**
Total bilirubin	0.52 ± 0.26	0.48 (0.11-1.3)	0.51 ± 0.29	0.46 (0.19-1.9)	Z= -0.128	0.898

ALP = alkaline phosphatase; ALT = alanine transaminase; AST = aspartate transaminase; GGT = gamma gulutamil transpeptida; LDH = lactat dehidrogenes; Z = Wilcoxon Tes; t = Paired Two Sample t Test

TABLE 4. Distribution of kPa values in liver segments and stages (distribution of each response)

Segment (Grade)	n(%)
Segment-2	
1	13 (38.2)
2	14 (41.1)
3	1 (2.9)
N	6 (17.6)
N~ or Chronic Inflammation	14 (41.1)
Segment 4a	
1	13 (38.2)
2	20 (58.8)
3	11 (32.3)
4	2 (5.8)
N	6 (17.6)
N~ or Chronic Inflammation	3 (8.8)
Segment 8	
1	9 (26.4)
2	14 (41.1)
3	12 (35.2)
4	7 (20.5)
N	4 (11.7)
N~ or Chronic Inflammation	4 (11.7)
Segment 7	
1	2 (5.8)
2	2 (5.8)
N	19 (55.8)
N~ or Chronic Inflammation	13 (38.2)
Segment 3	
1	4 (11.7)
2	4 (11.7)
N	16 (47.0)
N~ or Chronic Inflammation	14 (41.1)
Segment 4b	
1	8 (23.5)
2	9 (26.4)
3	1 (2.9)
N	17 (50.0)
N~ or Chronic Inflammation	8 (23.5)
Segment 5	
1	7 (20.5)
2	7 (20.5)
N	15 (44.1)
N~ or Chronic Inflammation	12 (35.2)
Segment 6	
1	1 (2.9)
2	1 (2.9)
N	19 (55.8)
N~ or Chronic Inflammation	14 (41.1)

N = normal

ALP, Total Protein, Albumin and T. Bilirubin results were evaluated. The data of the patients before the treatment and at least 3 months after the end of the treatment were evaluated.

Radiologic imaging

The effect of RT on the liver was evaluated with MRE.The majority of liver MREs were performed with Discovery 750-Watt MR imaging device (GE Healthcare, Chicago, IL) as a treatment position MR imaging for radiation planning. The liver MRE technique has been well described. Four axial slices were obtained through the largest cross-section of the liver. Mean liver parenchyma stiffness was calculated by averaging across manually drawn regions of interest, including only liver parenchyma, and measured by the reading radiologist. MRE results were evaluated by the second author, a radiologist. Based on previous study, LS ≤ 3 kPa was considered normal, and LS > 3 kPa was consistent with fibrosis.[6] Patients' liver stiffness measurement (LSM) was obtained using the W General Review program on the AW Server system. This method measured all liver segments in kilopascals (kPa) by drawing 1 cm or more from the liver edge using the free region of interest (ROI) tool to obtain measurements. Both qualitative and quantitative measurements were made. All segment measurements were made in size images that provide the best anatomical detail of the liver, avoiding the liver edge (≥1 cm from the liver edge), extra-hepatic tissues, fissures, gallbladder fossa, and large blood vessels. Values <2.5 kPa Normal, 2.5–2.9 kPa Normal or inflammation, 2.9–3.5 kPa grade 1–2 fibrosis, 3.5–4 kPa grade 2–3 fibrosis, 4–5 kPa Grade 4–5 fibrosis was considered compatible with > 5 kPa 5 fibrosis or cirrhosis. Steatosis was measured by the CAP method, expressed in decibels per meter (dB/m), and fibrosis was determined by the TE, expressed in kilopascals (kPa). All fibrosis and steatosis measurements were conducted with the Fibroscan® 530 Echosens device. Measurements were taken by placing the elastography probe on the right lobe of the liver from the intercostal space (mid-axillary line, between the 9th and 11th intercostal spaces) while the patient was lying in the dorsal decubitus position with his right arm in maximum abduction. The probe used (M or XL) was selected by the automatic recommendation software on the FibroScan® machine. Elastography CAP values were classified between S0–S3 based on Petroff's scale, and elasticity (fibrosis) values were classified between F0–F4 based on Eddowes' scale.[17,18] Elastography was performed during abdominal MRI examinations at the patients' last clinical follow-up.

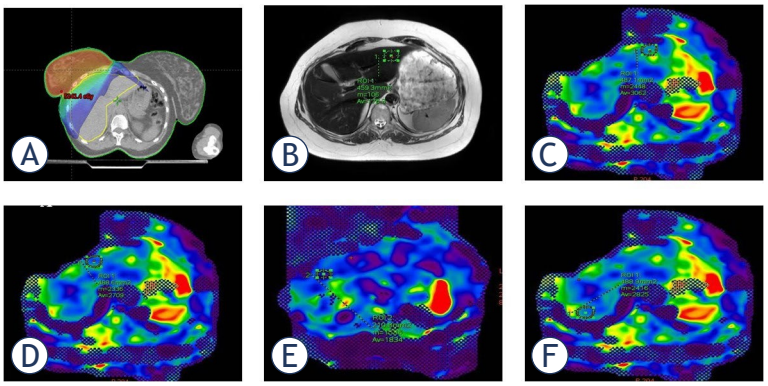

FİGURE 1. A 46-year-old female patient with a history of breast cancer and undergoing with breast-conserving surgery (BCS). **(A)** Liver distribution of radiotherapy (RT) dose (1000cGy) applied to breast; **(B)** T2 Weighted image; **(C)** Segment-2; **(D)** Segment-4A; **(E)** Segment-8; **(F)** Liver MR elastography examination from Segment-7 Elastogram measurements obtained during. When drawing the OAR, non-parenchymal structures (i.e., large vessels, bile ducts, gallbladder) that would affect the measurement were avoided. The color elastogram with a scale of 0–8 kPa shows the stiffness distribution in organs for qualitative evaluation. Orange or red regions have higher hardness values, and blue and purple regions have lower hardness values. Measured as segment-2 (3.06 Kpa), segment-4A (2.709 kPA), segment-8 (1.834 kPA), segment-7 (2.825 kPA). In the measurement made from liver segment-2, Stage 1–2 fibrosis was found. Segment-7 was normal or compatible with chronic inflammation, and the other segments were normal.

Statistical analysis

Data were analyzed with IBM SPSS V23. Compliance with normal distribution was examined with the Shapiro-Wilk Test. Independent Samples t-test, A paired Two-Sample t-test and Pearson Correlation Coefficient compared data with normal distribution according to binary groups. Mann Whitney U Test, Wilcoxon Test and Spearman's rho Correlation Coefficient was used for data that did not comply with normal distribution. Analysis results were presented as mean ± standard deviation (SD) and median (minimum–maximum). The significance level was taken as $p < 0.050$.

Results

The female population consisted of included 34 patients, with a median age 52.5 years (range, 32 to 68 years). Table 1 summarizes patients clinical characteristics and table 2 dosimetric data.

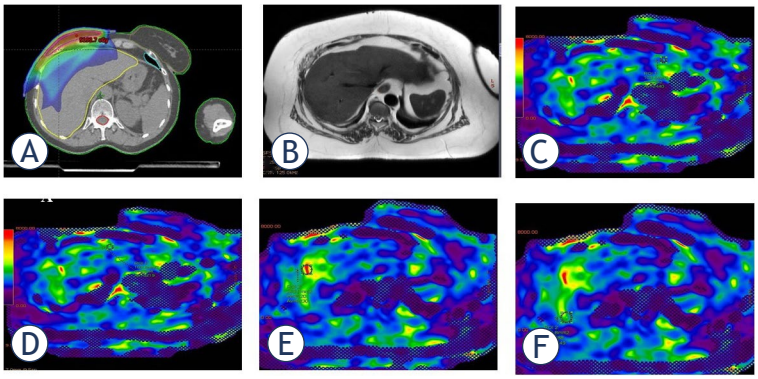

FİGURE 2. A 46-year-old female patient with a history of breast cancer who underwent modified radical mastectomy(MRM). **(A)** Liver distribution of RT dose (1000cGy) applied to chest wall location; **(B)** T2 Weighted image; **(C)** Segment-2; **(D)** Segment-4A; **(E)** Segment-8; **(F)** Liver MRE examination from segment-7 Elastogram measurements obtained during. When drawing the OAR, nonparenchymal structures (i.e., large vessels, bile ducts, gallbladder) that would affect the measurement were avoided. The color elastogram with a scale of 0-8 kPa shows the stiffness distribution in organs for qualitative evaluation. Orange or red regions have higher hardness values, and blue and purple regions have lower hardness values. Measured as segment-2 (3.44 Kpa), segment-4A (3.219 kPA), segment-8 (5.930 kPA), segment-7 (3.449 kPA). The measurement made from liver segment-2,-4A,-7 was found to be compatible with Stage 1–2 fibrosis, and the measurement from segment-8 was found to be compatible withs Stage 4 fibrosis.

We found a statistically significant difference in the before and after RT measurements of ALT (p = 0.015), ALP (p = 0.026), total protein (p = 0.037) and albumin (p = 0.004) (Table 3). While the ALP, total protein and albumin values of the patients increased after radiotherapy; we determined that the ALT value decreased.

The mean kPa value for liver highest value segment-8 was 3.5 (range 2–5.79); the lowest value in segment-6 was 2.3 (range 1.42–3.01) (Figure 3). kPa stage rates and distributions in liver segments are shown in Table 4. The most frequent stage observed in segment-4A was 1 (38.2%) and 2 (58.8%), while in segment-8, the most common stage was 1 (26.4%) and 2 (41.1%). Also in Figures 1 and 2, examples of RT dose distributions and liver MRE images of two patients are shown.

Table 5 shows the relationship between kPa values, liver volumes, liver V30Gy and liver mean in liver segments. A weak positive correlation was found between the measurements in segment-5 and liver volume (r = 0.355; p = 0.039). Moreover, a weak but statistically significant positive correlation was observed between Segment-4A (r = 0.398; p = 0.020) and Segment-6 (r = 0.500; p = 0.003) values with ALP levels. Conversely, a weak negative correlation (r = -0.370; p = 0.031) was identified between T.PRO levels and Segment-8 values post-RT (Table 6.)

The liver volume median was 1566.6cc (range 1014–2123,5) in those with breast-conserving surgery (BCS) and 1290.6 cc (range 843,8–2298,1) in those with modified radical mastectomy (MRM). No statistically significant difference in the median V30Gy liver volume according to surgery (p > 0.05) has been achieved. The median V30Gy value was 1.9 cc in patients with BCS and 1.4 cc in patients with MRM. There was no statistically significant difference (p > 0.025) between the mean liver volume according to surgery (Table 7).

Discussion

This study aimed to examine the right breast RT effect to the liver with non-invasive advanced MRE measurements and biochemical values. One of the most important aspects could be elaborated as the limited number of MRE devices in our country and the importance of data.

TABLE 5. Relationship between kPa values and liver volume in liver segments

Liver segments (kPA values)	Liver volüme (cc)	Liver V 30Gy	Liver mean (Gy)
Segment 2	r = 0.109; p = 0.539	r = 0.089; p = 0.616	r = 0.171; p = 0.332
Segment 4A	r = 0.239; p = 0.173*	r = 0.088; p = 0.619	r = -0.014; p = 0.938*
Segment 8	r = 0.107; p = 0.548*	r = -0.043; p = 0.809	r = -0.144; p = 0.417*
Segment 7	r = 0.266; p = 0.129	r = -0.139; p = 0.432	r = -0.115; p = 0.517
Segment 3	r = -0.068; p = 0.701*	r = -0.057; p = 0.749	r = -0.188; p = 0.286*
Segment 4B	r = 0.284; p = 0.103*	r = 0.224; p = 0.203	r = 0.186; p = 0.293*
Segment 5	**r = 0.355; p = 0.039**	r = -0.074; p = 0.679	r = -0.074; p = 0.677
Segment 6	r = 0.062; p = 0.729*	r = 0.073; p = 0.683	r = 0.017; p = 0.926*

R = Spearman's rho Correlation Coefficient; r* = Pearson Correlation Coefficient

TABLE 6. Relationship between after-RT segment values and liver RT dose and biochemical variables

	Segment 2	Segment 4A	Segment 8	Segment 7	Segment 3	Segment 4B	Segment 5	Segment 6
Liver Volüm	r=0,109; p=0.539	r=0.239; p=0.173*	r=0.107; p=0.548*	r=0.266; p=0.129	r=-0.068; p=0.701*	r=0.284; p=0.103*	**r=0.355; p=0.039**	r=0,062; p=0,729*
Liver V 30Gy	r=0,089;p=0.616	r=0,088; p=0,619	r=-0,043; p=0,809	r=-0,139; p=0,432	r=-0,057; p=0,749	r=0,224; p=0,203	r=-0,074; p=0,679	r=0,073; p=0,683
ALP	r=0,102;p=0.565	**r=0,398; p=0,020**	r=0,175; p=0,323	r=0,298; p=0,087	r=0,149; p=0,401	r=0,227; p=0,198	r=0,002; p=0,993	**r=0,500; p=0,003**
ALT	r=0,145;p=0.413	r=0,165; p=0,351	r=0,246; p=0,16	r=0,259; p=0,139	r=0,172; p=0,331	r=0,163; p=0,357	r=0,107; p=0,546	r=0,294; p=0,092
T.PRO	r=-0,129; p=0,469	r=0,1; p=0,575*	**r=-0,37; p=0,031***	r=-0,148; p=0,404	r=0,145; p=0,412*	r=0,016; p=0,929*	r=0,041; p=0,818	r=0,17; p=0,337*
ALB	r=0,026; p=0,882	r=0,235; p=0,18*	r=-0,113; p=0,526*	r=0,11; p=0,535	r=0,036; p=0,839*	r=0,227; p=0,196*	r=0,013; p=0,943	r=0,074; p=0,679*

ALB = albumin; ALP = alkaline phosphatase; ALT = alanine transaminase; T.PRO = total proteine; r = Spearman's rho Korelasyon Katsayısı; r* = Pearson Korelasyon Katsayısı

The liver is a sensitive organ to radiation. During ionizing radiation therapy, radiotoxicity usually accumulates in the normal tissues around the tumor, resulting in 24.7% of patients developing varying degrees of RILD.[19] RILD is a form of subacute liver injury caused by RT. Radiation doses of 50–70 Gy are considered to be effective for controlling most solid malignant tumors; however, approximately 5–10% of patients develop classic RILD when their whole liver is exposed to the cumulative dose of 30–35 Gy.[20] A dose of 2 Gy/day infractionated irradiation as cancer radiotherapy is sufficient to cause RILD. Patients ALP, total protein, and albumin levels increased after RT. An elevation of ALP is associated with the classical RILD.[21] On the contrary, AST, GGT, LDH, and total bilirubin levels were not affected by radiotherapy in our study.

Liver segments 8 and 4 are the anatomical regions closest to the right breast RT region. In this study, we determined the segment with the highest kPa value. It may pose a risk for the development of RLID. During right breast radiotherapy, some specific segments of the liver had been affected more than others. Stage 2 was highest in segments-4A (58.82%) and 8 (41.18%), and the most common stage was 1–2 in segments-4A (38.2%) and segment-8 as 26.5%. Only there was a relationship between segment five measurements and liver volume values. RILD is a multi-stage, multi-step dynamic process. It links a range of responses through a complex cascade response network in which various RNAs, oxidative stress, inflammation, aging, fibrosis, and immune responses interact under the regulation of multiple signaling pathways. Alleviating tissue

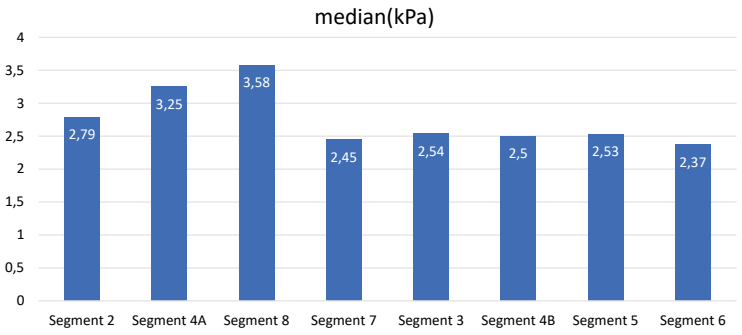

FIGURE 3. Patients kPa values in liver segments.

TABLE 7. Comparison of liver values according to surgery

	Surgery					
	BCS		MRM			
	Mean ± SD	Median (min-max)	Mean ± SD	Median (min-max)	Test Statistics	p-value
Liver Volume (cc)	1552.46 ± 320.52	1566.6 (1014–2123.5)	1408.3 ± 361.23	1290. (843.8–2298.1)	t = 1.214	0.233
Liver V 30Gy (%)	3.1 ± 3.03	1.9 (0–9.1)	2.8 ± 3.93	1.4 (0–12.03)	U = 111.5	0.381
Liver mean (Gy)	765.46 ± 339.81	756.7 (257.2–1564.2)	729.81 ± 451.29	762.5 (133.8–1699.8)	t = 0.262	0.795

BCS = breast conserving surgery; MRM = modified radical mastectomy; T = Independent Samples t Test; U = Mann-Whitney U-test

damage, restoring cell homeostasis, eliminating inflammation, and reducing cytotoxicity are essential for treating RILD.[22]

In this study, we determined that there was liver stiffness with MRE without deteriorating serum markers. Serum biomarkers have also been explored for liver fibrosis evaluation, but their lack of specificity poses a challenge as they may also be released during inflammation in other tissues.[23] MRE has also been shown to be superior to other noninvasive methods in assessing liver fibrosis.[24] MRE can also be used in the follow-up of NAFLD patients non-invasively. A recent study showed a 15% increase in MRE-LSM (liver stiffness measurement) is the strongest predictor of progression to advanced fibrosis in patients with NAFLD.[25] Tamaki *et al*. also proposed that a combination of MRE with FIB-4 score (MEFIB index) be used for detecting patients with NAFLD and significant fibrosis for enrollment in NASH clinical trials.[26] Beyond that, MRE-LSM is shown to be a significant predictor of the development of cirrhosis, as baseline LSM is predictive of the development of liver-related events such as decompensation or death.[27] A recent study that evaluated the MEFIB index showed excellent negative predictive value for hepatic decompensation in patients with NAFLD-related cirrhosis. In this study, the investigators also observed that MRE-LSM is associated with hepatic decompensation, hepatocellular carcinoma, and death in patients with NAFLD-related cirrhosis.[28]

Regarding the outcomes of this research, no significant difference was observed between BCS and MRM surgery according to the liver radiotherapy doses applied to patients with right breast cancer. Although one could expect that individuals who had undergone MRM could be affected more than BCS patients as the ratio of radiation exposed volume was higher, no significant difference has been observed. However, this might be attributed to the low level of liver V30Gy in the MRM group. Also, no statistically significant difference existed in mean liver volume according to surgery; additionally, no statistically significant difference in the median 30Gy liver volume according to surgery has been achieved.

Limitations

This study is not without its limitations. One significant limitation is the relatively small sample size, which may restrict the generalizability of the findings. Future studies with larger samples would provide more robust and reliable conclusions. Another limitation arises from the heterogeneity of the patient population, as the study included individuals at varying stages of their condition. While this may offer a broader perspective, it also introduces variability that could potentially affect the consistency of the results. Addressing these limitations in future research would strengthen the validity of the findings and provide a more comprehensive understanding of the issue. This study has some limitations. One of them is sample size. The other one is retrospective data collection and analysis, as well as a heterogeneous group.

Conclusions

Despite the limited sample size, this study is among the few that examine the effects of breast radiotherapy on the liver using both (MRE) and biochemical markers. Regarding the outcomes of this research, MRE can help us identify the level of fibrotic stiffness in the liver segments within the RT area without establishing clinical symptoms. MRE can support the clinician in evaluating the liver functions of right breast cancer patients who underwent RT. We assume these results will facilitate new studies with a large number of patients on MRE imaging at certain intervals in the follow-up of patients with right breast cancer who received RT before the development of RILD.

References

1. Darby SC, McGale P, Taylor CW, Peto R. Long-term mortality from heart disease and lung cancer after radiotherapy for early breast cancer: prospective cohort study of about 300,000 women in US SEER cancer registries. *Lancet Oncol* 2005; **6:** 557-65. doi: 10.1016/s1470-2045(05)70251-5
2. Darby SC, Ewertz M, McGale P, Bennet AM, Blom-Goldman U, Brønnum D, et al. Risk of ischemic heart disease in women after radiotherapy for breast cancer. *N Engl J Med* 2013; **368:** 987-98. doi: 10.1056/NEJMoa1209825
3. Zhang J, Jiang S, Zhang R, Zhang L. Increased 18F-FAPI uptake in radiation-induced liver injury. *Clin Nucl Med* 2023; **48:** e474-e6. doi:10.1097/RLU.0000000000004801
4. Adediran OA, Lawal IO, Muzahir S, Bhave MA, Friend S, Fielder B, et al. A discordant pattern of uptake on 68 Ga-PSMA PET/CT versus 18 F-Fluciclovine PET/CT in radiation-induced hepatitis: implications for early postradiotherapy imaging-based response assessment. *Clin Nucl Med* 2023; **48:** e202-e3. doi: 10.1097/RLU.0000000000004565
5. Haji G, Nabizade U, Kazimov K, Guliyeva N, Isayev I. Liver dose reduction by deep inspiration breath hold technique in right-sided breast irradiation. *Radiat Oncol J* 2019; **37:** 254-8. doi: 10.3857/roj.2019.00206
6. Nissen HD, Appelt AL. Improved heart, lung and target dose with deep inspiration breath hold in a large clinical series of breast cancer patients. *Radiother Oncol* 2013; **106:** 28-32. 10.1016/j.radonc.2012.10.016
7. Malnick SDH, Alin P, Somin M, Neuman MG. Fatty liver disease-alcoholic and non-alcoholic: similar but different. *Int J Mol Sci* 2022; **23:** 16226. doi: 10.3390/ijms232416226

8. Navin PJ, Olson MC, Mendiratta-Lala M, Hallemeier CL, Torbenson MS, Venkatesh SK. Imaging features in the liver after stereotactic body radiation therapy. *Radiographics* 2022; **42:** 2131-48. doi: 10.1148/rg.220084

9. Hama Y, Tate E. MRI-guided stereotactic ablative radiation therapy for liver metastasis from pancreatic cancer. *J Cancer Res Ther* 2022; **18(Supp):** S489-92. doi: 10.4103/jcrt.JCRT_1091_20

10. Venkatesh SK, Ehman RL. Magnetic resonance elastography of liver. *Magn Reson Imaging Clin N Am* 2014; **22:** 433-46. doi: 10.1016/j.mric.2014.05.001

11. Venkatesh SK, Yin M, Ehman RL. Magnetic resonance elastography of liver: technique, analysis, and clinical applications. *J Magn Reson Imaging* 2013; **37:** 544-55. doi: 10.1002/jmri.23731

12. Idilman IS, Karcaaltincaba M. The role of magnetic resonance elastography in the evaluation of nonalcoholic fatty liver disease. *Hepatol Forum* 2023; **4:** 1-2. doi: 10.14744/hf.2023.2023.0004

13. Chiang CL, Chiu KWH, Chan KSK, Lee FAS, Li JCB, Wan CWS, et al. Sequential transarterial chemoembolisation and stereotactic body radiotherapy followed by immunotherapy as conversion therapy for patients with locally advanced, unresectable hepatocellular carcinoma (START-FIT): a single-arm, phase 2 trial. *Lancet Gastroenterol Hepatol* 2023; **8:** 169-78. doi: 10.1016/S2468-1253(22)00339-9

14. Nielsen J, Kjær MS, Rasmussen A, Chiranth D, Willemoe GL, Henriksen BM, et al. Noninvasive prediction of advanced fibrosis in pediatric liver disease-discriminatory performance of 2D shear wave elastography, transient elastography and magnetic resonance elastography in comparison to histopathology. *Diagnostics* 2022; **12:** 2785. doi: 10.3390/diagnostics12112785

15. Gheorghe G, Bungău S, Ceobanu G, Ilie M, Bacalbaşa N, Bratu OG, et al. The non-invasive assessment of hepatic fibrosis. *J Formos Med Assoc* 2021; **120:** 794-803. doi: 10.1016/j.jfma.2020.08.019

16. Hsu C, Caussy C, Imajo K, Chen J, Singh S, Kaulback K, et al. Magnetic resonance vs transient elastography analysis of patients with nonalcoholic fatty liver disease: a systematic review and pooled analysis of individual participants. *Clin Gastroenterol Hepatol* 2019; **17:** 630-7.e8. doi: 10.1016/j.cgh.2018.05.059

17. Petroff D, Blank V, Newsome PN, Shalimar, Voican CS, Thiele M, et.al. Assessment of hepatic steatosis by controlled attenuation parameter using the M and XL probes: an individual patient data meta-analysis. *Lancet Gastroenterol Hepato*l 2021; **6:** 185-98. doi: 10.1016/S2468-1253(20)30357-5

18. Eddowes PJ, Sasso M, Allison M, Tsochatzis E, Anstee QM, Sheridan D, et al. Accuracy of FibroScan Controlled Attenuation parameter and liver stiffness measurement in assessing steatosis and fibrosis in patients with nonalcoholic fatty liver disease. *Gastroenterology* 2019; **156:** 1717-30. doi: 10.1053/j.gastro.2019.01.042

19. Jun BG, Kim YD, Cheon GJ, Kim ES, Jwa E, Kim SG, et al. Clinical significance of radiation-induced liver disease after stereotactic body radiation therapy for hepatocellular carcinoma. *Korean J Intern Med* 2018; **33:** 1093-2. doi: 10.3904/kjim.2016.412

20. Treiber T, Treiber N, Meister G. Regulation of microRNA biogenesis and its crosstalk with other cellular pathways. *Nat Rev Mol Cell Biol* 2019; **20:** 5-20. doi: 10.1038/s41580-018-0059-1

21. Lauffer DC, Miglierini P, Kuhn PA, Thalmann SU, Gutierres-Demierre N, Khomsi F, et al. Impact of adjuvant radiotherapy on biological and clinical parameters in right-sided breast cancer. *Cancer Radiother* 2021; **25:** 469-75. doi: 10.1016/j.canrad.2021.04.007

22. Zhou YJ, Tang Y, Liu SJ, Zeng PH, Qu L, Jing QC, et al. Radiation-induced liver disease: beyond DNA damage. *Cell Cycle* 2023; **22:** 506-26. doi: 10.1080/15384101.2022.2131163

23. Agbim U, Asrani SK. Non-invasive assessment of liver fibrosis and prognosis: an update on serum and elastography markers. *Expert Rev Gastroenterol Hepatol* 2019; **13:** 361-74. doi: 10.1080/17474124.2019.1579641

24. Bi J, Liu L, Qin T. Comparison of magnetic resonance elastography and transient elastography in the diagnosis of hepatic fibrosis: a systematic review and meta-analysis. *Ann Palliat Med* 2021; **10:** 8692-700. doi: 10.21037/apm-21-1176

25. Ajmera VH, Liu A, Singh S, Yachoa G, Ramey M, Bhargava M, et al. Clinical utility of an increase in magnetic resonance elastography in predicting fibrosis progression in nonalcoholic fatty liver disease. *Hepatology* 2020; **71:** 849-60. doi: 10.1002/hep.30974

26. Tamaki N, Imajo K, Sharpton S, Jung J, Kawamura N, Yoneda M, et al. Magnetic resonance elastography plus fibrosis-4 versus fibroscan-aspartate aminotransferase in detection of candidates for pharmacological treatment of NASH-related fibrosis. *Hepatology* 2022; **75:** 661-72. doi: 10.1002/hep.32145

27. Gidener T, Ahmed OT, Larson JJ, Mara KC, Therneau TM, Venkatesh SK, et al. Liver stiffness by magnetic resonance elastography predicts future cirrhosis, decompensation, and death in NAFLD. *Clin Gastroenterol Hepatol* 2021; **19:** 1915-24.e6. doi: 10.1016/j.cgh.2020.09.044

28. Ajmera V, Kim BK, Yang K, Majzoub AM, Nayfeh T, Tamaki N, et al. Liver stiffness on magnetic resonance elastography and the MEFIB index and liver-related Outcomes in Nonalcoholic Fatty Liver Disease: a systematic review and meta-analysis of individual participants. *Gastroenterology* 2022; **163:** 1079-89.e5. doi: 10.1053/j.gastro.2022.06.073

research article

Analysis of early diagnostic pathway for prostate cancer in Slovenia

Mateja Kokalj Kokot[1,2], Spela Mirosevic[1], Nika Bric[3], Davorina Petek[1,4]

[1] Department of Family Medicine, Faculty of Medicine, University of Ljubljana, Ljubljana, Slovenia
[2] Primary Healthcare Centre Grosuplje, Grosuplje, Slovenia
[3] Sector for Oncology Epidemiology and Cancer Registry, Institute of Oncology Ljubljana, Ljubljana, Slovenia
[4] Medical Centre Zdravje, Ljubljana, Slovenia

Radiol Oncol 2024; 58(4): 544-555.

Received 28 March 2024
Accepted 25 July 2024

Correspondence to: Assist. Mateja Kokalj Kokot, M.D., Department of Family Medicine, Faculty of Medicine, University of Ljubljana, Poljanski nasip 58, SI-1000 Ljubljana, Slovenia. E-mail: mateja.kokaljkokot@mf.uni-lj.si

Disclosure: No potential conflicts of interest were disclosed.

Background. Prostate cancer (PCa) is a prevalent male malignancy globally. Prolonged diagnostic intervals are associated with poorer outcomes, emphasizing the need to optimize this process. This study aimed to evaluate the doctor and primary care interval, research their impact on patient survival and explore opportunities to improve PCa diagnostic pathway in primary care.

Patients and methods. A retrospective cohort study using cancer patients' anonymised primary care data and data of the Slovenian Cancer Registry.

Results. The study found that the doctor interval had a median duration of 0 days (interquartile range ([IQR] 0–6) and primary care interval a median duration of 5 days (IQR 0–58). Longer intervals were observed in patients with more than two comorbidities, where general practitioners didn't have access to laboratory diagnostic tests within their primary health care centre and when patients first presented with symptoms (reported symptoms at first presentation: dysuria, lower urinary tract symptoms [LUTS], abdominal pain). The analysis also revealed a statistically significant association between lower 5-year survival rate and the accessibility of laboratory and ultrasound diagnostics in primary healthcare centres and a shorter 5-year survival of symptomatic patients in comparison to patients who were identified by elevated levels of prostate specific antigen (PSA).

Conclusions. This study shows that treating suspected PCa in primary care has a significant impact on 5-year survival. Several factors contribute to better survival, including easy access to laboratory and abdominal ultrasound in primary care centres. The study highlights the complex array of factors shaping PCa diagnosis, beyond individual clinicians' skills, encompassing test and service availability.

Key words: prostate cancer; doctor interval; primary care interval

Introduction

Prostate cancer is a common malignant tumour and has the highest incidence of all non-cutaneous cancers worldwide in males. It is also the fifth leading cause of cancer death among men in 2020.[1] In Slovenia the 2020 age-standardized (World standard population) incidence rate was 62.7.[2] In Central and Eastern Europe it was 46.4 and 59.1 in Southern Europe.[1] The ageing population undoubtedly influences the increasing incidence of prostate cancer. However, the proportional growth of elderly individuals (aged 65 years and older) in Slovenia has not escalated sufficiently to solely account for this rise in prostate cancer incidence. For example, in 1991, the proportion of elderly people in Slovenia was 11.2% and the crude incidence rate for prostate cancer was 26.3 per 100,000 individu-

als. In 2001, the proportion of elderly increased to 14.3% and the crude incidence rate for prostate cancer was 74.5.[3,4] The dramatic increase in the incidence of prostate cancer over the past two decades is not due to any newly identified risk factor, but rather to the increasing use of the prostate-specific antigen (PSA) test in healthy men and therefore detection of a large number of cancers that would have otherwise remained undetected for life. Data for recent years indicate that we have already reached the peak incidence of prostate cancer.[2] The histological incidence far surpasses the proportion of individuals in whom the disease is manifested, and while there has always been a tendency not to misdiagnose those with prostate cancer, there is increasing focus on identifying patients who are treated by watchful waiting. Prostate cancer is characterised by a slow natural course of the disease, with the majority of patients dying from other, non-cancer related causes.[5,6] Both the incidence and mortality rates of prostate cancer in Slovenia are above the European average. In 2020, Slovenia reported an age-standardized (World standard population) mortality rate of 14.9, while Central and Eastern Europe recorded a rate of 13.7, the highest among all European regions.[1,2]

Much effort has already been applied to optimize early detection in prostate cancer and some medical professional societies and organizations recommend prostate cancer screening or discussing screenings with men of suitable age and life expectancy.[7] Many countries in Europe have joined PRAISE-U project to establish screening programme for prostate cancer.[8] In primary care-based health care systems, in which the general practitioner (GP) is the patient's first contact and triages the patient's further access to the system, most prostate cancer patients either present to a GP with symptoms (dysuria, lower urinary tract symptoms (LUTS), abdominal pain) or an elevated level of PSA is found in asymptomatic patients. Therefore, timely recognition of cancer-related complaints and adequate referral by the GP are and will remain essential to reduce time to diagnosis until successful screening programmes are introduced. Even though the association between time intervals in the diagnostic pathway and clinical outcomes is complex and remains debated, evidence suggests an association between shorter times to diagnosis and more favourable outcomes in breast cancer, colorectal, head and neck, testicular cancer and melanoma.[9,10] Optimising the diagnostic pathway from first presentation to diagnosis and start of treatment, usually interpreted as shortening the diagnostic phase, has therefore been a main objective of health care organisations involved in cancer care worldwide. For some countries in Europe, the duration of several of these intervals has been charted.[11-17] For other countries, such as Slovenia, the duration of these intervals is unknown. International comparison of the duration of diagnostic intervals in different health care systems and cultural environments is important to identify system-, disease- and patient- related factors that contribute to an unnecessarily prolonged patient journey. Exploring the duration of the diagnostic pathway in Slovenia and how primary care contributes to it generates relevant information on international differences in the duration of the diagnostic pathway. This provides the opportunity to distinguish underlying mechanisms of delay, including system-, disease- and patient-related delay.

The aims of the study were (i) to evaluate the duration and specifics of management during the doctor and primary care intervals in Slovenia, (ii) to investigate the potential association between the durations of the intervals, sociodemographic and organizational variables and (iii) to assess the association between these variables, intervals and the 5-year survival rates of prostate cancer patients in Slovenia.

Patients and methods

Study design, data source and patient selection

A retrospective cohort study was performed using data from the Slovenian Cancer Registry and primary care data collected from selected GPs and family doctors with whom these patients were registered at the time of the study. Cancer Registry of Republic of Slovenia provides reliable and detailed information on Slovene cancer patients since 1950. This study was part of the research project of the Institute of Oncology Ljubljana, in collaboration with the Department of Family Medicine, Faculty of Medicine, University of Ljubljana, and the Clinical Department of Urology, University Medical Centre Ljubljana, entitled Integrated analysis of the early management of patients with urological cancers, assessing delays in referral, diagnosis and first treatment. The study was reviewed and approved by the Commission of the Republic of Slovenia for Medical Ethics (0120-233/2019/4).

We included all newly diagnosed prostate cancer patients during the year 2014 in the Slovenian

Cancer Registry database. Consecutively, 1431 patients with all stages of prostate cancer were included. We then linked the Cancer Registry data to the National Insurance Company Registry in order to identify each patient's GP and send them a questionnaire. The exclusion criterion was if the diagnosis of prostate cancer was made at the autopsy (29 patients). A flowchart of patients' data inclusion in our study is presented in Figure 1. We asked the GPs to collect information from the patient's records and complete the attached questionnaire on management of the initial symptoms of the disease, the diagnostics performed and referral decisions, using the dates and information given in the patients' medical record and discharge letters from hospitals. We also asked them about the accessibility to diagnostics (laboratory, abdominal ultrasound) in their primary healthcare centre. Non-responders received a reminder after eight months.

Data collection

Doctor interval and primary care interval

The intervals were defined according to the Aarhus statement.[18,19] Doctor interval was defined as the period of time from first consultation in primary care to beginning of the first investigation in primary care. Date of first presentation was defined as the first contact with the GP (in person or telemedicine) with possible prostate cancer related signs and/or symptoms. The questionnaire allowed the GP to choose from six different reasons why the patient chose to see a doctor, with multiple choices also possible. Possible symptoms and signs reported by the patient at first presentation were dysuria, LUTS and lower abdominal pain. Additional reasons for visiting the doctor included a family history of cancer, an elevated PSA level detected during routine check-ups (preventive examination, opportunistic screening, regular annual follow-up for chronic diseases, occupational health and safety check-up), and doctors could also choose other. Those were the cases where prostate cancer was not first suspected in the GP's practice but elsewhere, e.g. during hospitalisation for another illness, as reported by the GPs in the questionnaire notes. GPs themselves set the most accurate date estimate for the first presentation after reviewing the patient's records.

They also noted if and when they performed a digital rectal exam, referred the patient to the abdomen ultrasound and/or checked the patient blood (complete blood count [CBC] and/or C-reactive protein [CRP] and/or PSA) and/or urine. All of the stated actions counted as first investigation in primary care. We calculated the length of the doctor interval based on the date of the first presentation and the date of the earliest diagnostic procedure.

Primary care interval was defined as the period of time from first presentation in primary care to referral to urologist. Date of referral was defined as the day the referral letter to the urologist was written, which was also stated by the GP.

If the date of first presentation was the same or later than the date of the earliest diagnostic procedure, the duration of doctor interval was coded as 0 days. Similarly, if the date of first presentation was the same as the date of the referral to urologist, the duration of primary care interval was coded as 0 days. If the length of any interval was equal to or more than one year, it was coded as 365 days.

Characteristics

The decision to collect data for certain characteristics and to include them in our analyses was based on previously reported diagnostic procedures and predictors in the literature[20–25], on clinical relevance of patients and disease characteristics, and on availability of data in the Cancer registry and primary care data. The questionnaire was approved by the entire research team. We collected data on age, level of education, stage of cancer, comorbidities, symptoms and signs at first presentation, vital status 5 years after diagnosis and location of their GP's primary health care centre.

The Slovenian Cancer Registry Database uses a simplified definition of stages at diagnosis for solid tumours, classifying them into localized, spread (regional) and metastatic stage of disease. The simplified stage definition generally follows the TNM classification. Localized stage includes all cancers where the tumour has been classified as T1 and T2. In these cases, neither regional lymph node involvement nor distant metastases are found (N0, M0). The spread stage includes tumours classified as T3 and T4 and/or with regional lymph node metastases (N1), without presence of metastases in distant lymph nodes or organs (M0). A disease with metastases in distant lymph nodes or organs is classified as a metastatic stage (M1).[2]

Statistical analysis

The data on the patients' demographics, cancer stage, symptoms at first presentation, comorbidi-

ties, diagnostics executed at the primary health care centre, region of GP's practice and accessibility to diagnostic tests reported in questionnaires were collected and managed in Microsoft Access Database 2007-2016 Version. Additional data processing was performed in Excel (Microsoft Office Professional Plus 2019). Descriptive statistics, including means, median, standard deviations and frequencies, were calculated to provide an overview of the data distribution. To examine the relationships between variables, we used Independent Sample T-test and chi-square tests for categorical variables. In case of the presence of variables with non-normal distributions, we also used the Mann-Whitney U-test. To identify potential predictors for the outcome variable, we performed a multiple logistic regression analysis that included the relevant sociodemographic, clinical and organizational variables.

To account for missing data that occurred randomly and without a recognizable pattern, we conducted multiple imputation and analysis using Version 29.0 of the IBM SPSS Statistics. This technique allows the estimation of missing values by creating multiple plausible imputation datasets, thereby maintaining statistical power, and minimizing bias.

All statistical analyses were performed using IBM SPSS Statistics with the significance level set at $p < 0.05$.

Results

Patients' characteristics

Among the cohort of 1431 patients registered with a diagnosis of prostate cancer in the Cancer Registry in 2014, we successfully obtained primary care data for a total of 814 patients, as illustrated in Figure 1.

The included patients' average age was 69 years, with a standard deviation of 8.5 years. Detailed sociodemographic and clinical characteristics of the prostate cancer patients included in this study are presented in Table 1.

Doctor and primary care intervals' characteristics

The median duration of the doctor interval, in terms of days, was found to be 0, with an interquartile range spanning from 0 to 6 days. The median duration of the primary care interval was 5 days, with an interquartile range extending from 0 to 58 days. The average number of visits to the doctor during the primary care interval was 1.68 (SD 0.9), range 1–5. Table 2 provides also the mean of the intervals.

For the analysis of the doctor and primary care intervals, we excluded the Zasavska region due to a limited sample size, with only three patients included in the study, which did not provide sufficient statistical power for meaningful analysis. Consequently, our analysis was based on a dataset consisting of 811 patients. Table 3 shows the diagnostic procedures performed by the GP and their access to laboratory and abdominal ultrasound within the primary health care centre, overall and by region.

Table 4 presents the median and interquartile range data for the duration of the doctor and primary care intervals, computed based on patient and presentation characteristics.

Statistically significant longer doctor intervals were observed in patients who had localized vs. metastatic cancer stage, presence of more than two comorbidities, where GPs' didn't have access to laboratory diagnostic tests (CBC, CRP, urine, PSA) within their primary health care centre and when patients first presented with symptoms (reported symptoms at first presentation: dysuria, LUTS, abdominal pain).

The primary care interval was also statistically significantly longer in patients who had more than two comorbidities, where GPs' didn't have access to laboratory tests within their primary health care centre and when patients first presented with symptoms. In addition, there was a marked difference between the Osrednjeslovenska and Savinjska regions, with the former having the longest and the latter the shortest primary care interval.

To further elucidate the relationship between the predictor variables and the primary care interval, we employed a logistic regression model (Table 5). We set the limit at a primary level interval duration of 14 days. Omnibus tests of the model coefficients yielded a chi-square statistic of 53.642 at 11 degrees of freedom, resulting in a p-value of less than 0.001. This indicates robust overall significance of the prediction model, confirming that the independent variables significantly contribute to the variability in the primary care interval. Nevertheless, the Nagelkerke R^2 coefficient indicates that only 9.4% of the variance of the dependent variable is explained by the model, reflecting the complexity of health service utilization behaviour. The model's -2 log-likelihood of 1018.153 indicates a satisfactory fit to the empirical data.

TABLE 1. Sociodemographic and clinical characteristics of prostate cancer patients (N = 814)

Characteristics	Sample of prostate cancer patients, n (%)
Age (mean ± SD), range: 44–97	69.0 ± 8.5
Age, groups	
< 65	265 (32.5)
65–75	357 (43.9)
> 75	192 (23.6)
Cancer stage	
Localized	572 (70.3)
Spread	191 (23.4)
Metastatic	51 (6.3)
Education	
Primary/Elementary education	280 (34.4)
Secondary/High school education	386 (47.4)
Higher education	148 (18.2)
Comorbidities	
No. of comorbidities (mean ± SD), range: 0–6	1.2 ± 1.2
None	290 (35.6)
1–2	410 (50.4)
> 2	114 (14)
Number of patients by region of the primary health care centre's location	
Pomurska	106 (13)
Podravska	114 (14)
Koroška	31 (3.8)
Savinjska	85 (10.4)
Zasavska	3 (0.4)
Spodnjeposavska	25 (3.1)
JV Slovenija	53 (6.5)
Osrednjeslovenska	204 (25.1)
Gorenjska	69 (8.5)
Notranjsko-kraška	27 (3.3)
Goriška	56 (6.9)
Obalno-kraška	41 (5.0)
Symptoms and signs at first presentation (multiple options possible)	
Dysuria	111 (13.6)
LUTS	307 (37.7)
Pain in the abdomen	63 (7.7)
Family history of cancer	17 (2.1)
Elevated PSA	246 (30.2)
Other	130 (16)
Alive 5-years after diagnosis	610 (74.9)

JV Slovenija = South-East Slovenia; Koroška = Carinthia; LUTS = lower urinary tract symptoms; Obalno-kraška = Coastal-Karst; Osrednjeslovenska = Central Slovenia; PSA = prostate specific antigen

TABLE 2. Duration of doctor and primary care interval

	mean (± SD)	range
Doctor interval, days	37.5 (92.8)	0–365
Primary care interval, days	67.4 (123.8)	0–365

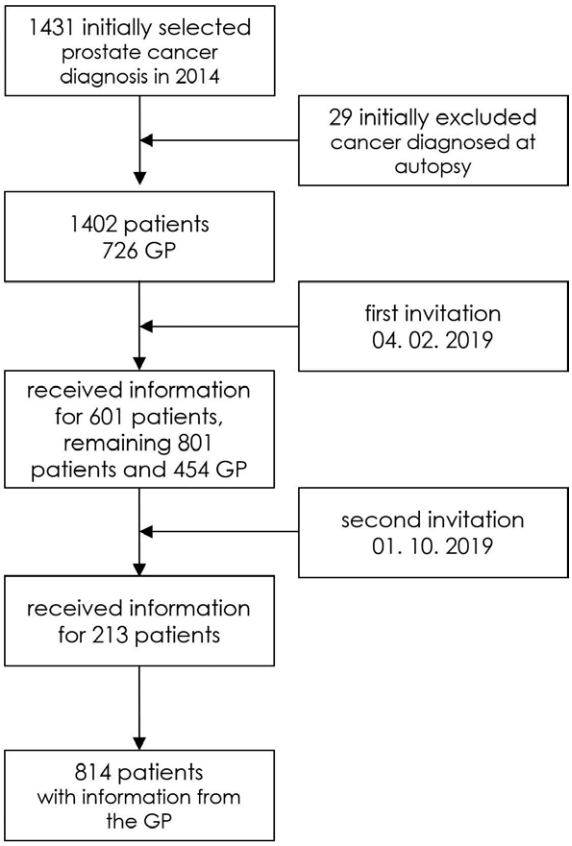

FIGURE 1. Flowchart of patient selection.

GP = general practitioner

5-year survival analysis

In the group of 814 prostate cancer patients, 610 (74.9%) were alive five years after diagnosis.

Our analysis showed statistically significant differences in 5-year survival depending on the accessibility of laboratory and ultrasound diagnostics in primary health care centres (Table 6). In addition, we observed lower 5-year survival in symptomatic patients.

There were statistically significant differences between the duration of primary care interval and 5-year survival (204 dead patients, mean primary care interval 90.18 and 610 alive patients with mean interval 59.79, p-value = 0.007).

Discussion

This study provides an overview of early management of patients with prostate cancer in family medicine in Slovenia. Our aim was to evaluate the treatment timelines and specificities within

TABLE 3. Diagnostic procedures performed by the general practitioner (GP) and their access to laboratory and abdominal ultrasound within the primary health care centre, overall and by region (N = 811)

Diagnostic procedures performed by GPs	**Sample of prostate cancer patients, n (%)**				
CBC, CRP	497 (61.1)				
PSA	664 (81.6)				
Urine	471 (57.9)				
US	434 (53.3)				
DRE	255 (31.3)				
Diagnostic procedures performed by GPs by region	**CBC, CRP**	**PSA**	**urine**	**US**	**DRE**
Pomurska (N = 106)	48 (45.3)	77 (72.6)	52 (49.1)	39 (36.8)	34 (32.1)
Podravska (N = 114)	77 (67.5)	95 (83.3)	60 (52.6)	68 (59.6)	23 (20.2)
Koroška (N = 31)	15 (48.4)	24 (77.4)	13 (41.9)	4 (12.9)	11 (35.5)
Savinjska (N = 85)	55 (64.7)	64 (75.3)	61 (71.8)	50 (58.8)	26 (30.6)
Spodnjeposavska (N = 25)	14 (56)	20 (80)	16 (64)	11 (44)	13 (52)
JV Slovenija (N = 53)	35 (66)	39 (73.6)	25 (47.2)	19 (35.8)	11 (20.8)
Osrednjeslovenska (N = 204)	135 (66.2)	180 (88.2)	131 (64.2)	140 (68.6)	46 (22.5)
Gorenjska (N = 69)	48 (69.6)	63 (91.3)	44 (63.8)	39 (56.5)	22 (31.9)
Notranjsko-kraška (N = 27)	21 (77.8)	23 (85.2)	19 (70.4)	20 (74.1)	15 (55.6)
Goriška (N = 56)	28 (50)	45 (80.4)	29 (51.8)	22 (39.3)	33 (58.9)
Obalno-kraška (N = 41)	19 (46.3)	32 (78)	19 (46.3)	20 (48.8)	19 (46.3)
Accessibility to diagnostic tests in the primary health care centre	**Sample of prostate cancer patients, n (%)**				
Laboratory (CBC, CRP, urine)	734 (90.2)				
Laboratory (PSA)	653 (80.2)				
US	306 (37.6)				
Accessibility to diagnostic tests in the primary health care centre by region	CBC, CRP, urine		PSA		US
Pomurska (N = 106)	96 (90.6)		79 (74.5)		34 (32.1)
Podravska (N = 114)	98 (86)		89 (78.1)		42 (36.8)
Koroška (N = 31)	28 (90.3)		26 (83.9)		22 (71)
Savinjska (N = 85)	78 (91.8)		63 (74.1)		36 (42.4)
Spodnjeposavska (N = 25)	23 (92)		16 (64)		10 (40)
JV Slovenija (N = 53)	46 (86.8)		42 (79.2)		15 (28.3)
Osrednjeslovenska (N = 204)	187 (91.7)		173 (84.8)		74 (36.3)
Gorenjska (N = 69)	63 (91.3)		60 (87)		31 (44.9)
Notranjsko-kraška (N = 27)	24 (88.9)		20 (74.1)		7 (25.9)
Goriška (N = 56)	53 (94.6)		52 (92.9)		23 (41.1)
Obalno-kraška (N = 41)	36 (87.8)		31 (75.6)		12 (29.3)

CBC = complete blood count; CRP = C-reactive protein; DRE = digital rectal exam; GP = general practitioner; JV Slovenija = South-East Slovenia; Koroška = Carinthia; Obalno-kraška = Coastal-Karst; Osrednjeslovenska = Central Slovenia PSA = prostate specific antigen; US = abdominal ultrasound

the doctor and primary care interval. The median length of the doctor interval was very short at 0 days, the primary care interval exhibited a median duration of 5 days. Our study demonstrated statistically significant correlation of cancer stage, comorbidities, and the accessibility of laboratory tests within primary health care centres and survival of prostate cancer patients. The presence of laboratory tests within primary health care centres emerged as a significant determinant of the primary care interval's duration and 5-year survival.

The exclusion of 617 patients' of 1431 patients total from our analysis was necessitated by various reasons outlined in Figure 1. It is worth not-

TABLE 4. The distribution and association of selected characteristics with doctor and primary care interval. (N = 811)

	N	%	Doctor Interval			Primary care interval		
			Median	Interquartile range	P	Median	Interquartile range	P
Age groups					0.131			0.382
< 65	264	32.55	0	0–4		5	0–65	
65–75	355	43.77	0	0–5		4	0–51	
> 75	192	23.67	0	0–20		7	0–73	
Education					0.437			0.204
Primary/Elementary education	278	34.28	0	0–6		7	0–38	
Secondary/High school education	385	47.47	0	0–5		3	0–53	
Higher education	148	18.25	0	0–18		7	0–127	
Region of the location of primary health care centre					0.863			0.021
Pomurska	106	13.07	0	0–18		3	0–62	
Podravska	114	14.06	0	0–20		8	0–50	
Koroška	31	3.82	0	0–20		0	0–42	
Savinjska	85	10.48	0	0–3		0	0–28	
Spodnjeposavska	25	3.08	0	0–10		3	0–91	
JV Slovenija	53	6.54	0	0–7		1	0–62	
Osrednjeslovenska	204	25.15	0	0–5		10	0–88	
Gorenjska	69	8.51	0	0–2		4	0–54	
Notranjo-kraška	27	3.33	0	0–7		6	0–127	
Goriška	56	6.90	0	0–5		4	0–34	
Obalno–kraška	41	5.06	0	0–20		4	0–48	
Cancer stage					0.037			0.058
Localized	569	70.16	0	0–8		6	0–65	
Spread	191	23.55	0	0–1		1	0–28	
Metastatic	51	6.29	0	0–38		3	0–336	
Comorbidities					0.001			0.026
None	288	35.51	0	0–31		7	0–101	
1–2	409	50.43	0	0–4		5	5–44	
> 2	114	14.06	0	0–1		0	0–33	
GP access to laboratory (CBC,CRP,urine)					< 0.001			< 0.001
Yes	732	90.26	0	0–4		3	0–37	
No	79	9.74	40	0–330		365	0–365	
GP access to laboratory (PSA)					< 0.001			< 0.001
Yes	651	80.27	0	0–2		3	0–37	
No	160	19.73	0	0–177		21	0–365	
GP access to US					0.781			0.124
Yes	306	37.73	0	0–5		4	0–31	
No	505	62.27	0	0–7		5	0–78	
Symptomatic patient					< 0.001			0.001
Yes	399	49.20	0	0–12		5	0–42	
No	219	27.00	0	0–0		0	0–18	

CBC = complete blood count; CRP = C-reactive protein; DRE = digital rectal exam; GP = general practitioner; JV Slovenija = South-East Slovenia; Koroška = Carinthia; Obalno-kraška = Coastal-Karst; Osrednjeslovenska = Central Slovenia; PSA = prostate specific antigen; US = abdominal ultrasound

ing that the proportion of cases excluded due to missing interval data was similar in our study to previous studies.[11]

Evidence about the length of the doctor interval in patients with different cancers is sparse. We found a study of Denmark's cancer patients[26], where median duration of doctor interval for prostate cancer patients was 0 days and interquartile range (IQR) 0–6 days, which is the same as in our study. One of the reasons for a short doctor interval is that in primary-level diagnostic procedures, doctors sometimes use laboratory and ultrasound tests already performed prior to this first visit (e.g. blood and urine taken from the patient a month earlier, or an abdominal ultrasound performed three months earlier - doctor's interval is negative, marked as 0 days in the analysis). In this way they omit unnecessary duplication of tests and expedite further management of suspected prostate cancer.

There were no statistical differences in the duration of doctor interval between different age groups, levels of education, region of primary health care centre and accessibility to abdominal ultrasound in the primary health care centre. The duration was statistically significant longer when patients had no comorbidities, when they first presented with symptoms in comparison to elevated PSA value and where there was not access to laboratory diagnostics (CBC, CRP, urine, PSA) in primary health care centre. We interpret these results by assuming that multimorbid patients see their doctor more often, for different reasons, and thus are more likely to report or be asked about different symptoms and signs, as opposed to patients without comorbidities. In patients with elevated PSA levels in the blood, the guidelines recommend that prostate cancer should be excluded, so the decision to refer to a urologist was easy and quick. Dysuria, LUTS and abdominal pain are typical symptoms of a number of different diseases and are not in themselves of great predictive value for a cancer diagnosis.[27–29] Men experiencing urinary problems were more inclined to seek medical attention compared to asymptomatic men, leading to more frequent PSA testing and consequently earlier detection of prostate cancer. Our study focused on diagnosing prostate cancer cases in 2014 rather than estimating the overall prevalence that year. Therefore, it's probable that symptomatic cases outnumber asymptomatic ones. In Slovenian primary health care centers, PSA testing is more commonly conducted for symptomatic men or as part of annual check-ups for those undergoing therapy for benign prostatic hyperplasia, rather than for routine screening of asymptomatic individuals. Interestingly, we found that patients with stage spread cancer had the shortest doctor interval, while patients with metastatic cancer had the longest. This may be due to non-specific or absent symptoms and signs in localised prostate cancer. Symptoms and signs become more frequent and pronounced in spread stage of cancer and those caused by metastatic cancer could also be wrongly attributed to other patient's comorbidities. Considering health system factors, international comparisons suggests that the problem of early cancer diagnosis is ubiquitous across contemporary health systems, including high-income countries, though the same underlying problem is manifested differently depending on health service organisation, healthcare professional cultures, and the public understanding of cancer.[10] This is the first study using Slovenian data to show a correlation between not having easy access to laboratory diagnostics (CBC, CRP, urine, PSA)

TABLE 5. Logistic regression model on predicting primary care interval

Variables in the Equation	B	Wald	Exp(B) (95% CI)
Age	-0.004	0.144	0.996 (0.979, 1.015)
Education primary vs secondary	-0.359	4.223	0.698 (0.496, 0.984)*
Education primary vs higher	0.145	0.452	1.156 (0.757, 1.765)
Cancer stage localized vs spread	-0.336	3.315	0.714 (0.497, 1.026)
Cancer stage localized vs metastatic	-0.316	0.955	0.729 (0.387, 1.374)
No comorbidities	-0.070	1.051	0.932 (0.815, 1.066)
First symptom - dysuria	-0.175	0.592	0.840 (0.538, 1.310)
First symptom – LUTS	-0.084	0.228	0.919 (0.650, 1.300)
First symptom – abdominal pain	0.132	0.222	1.141 (0.659, 1.977)
First symptom – family history of cancer	0.257	0.249	1.293 (0.471, 0.913)
First symptom – elevated PSA	-0.486	5.804	0.615 (0.414, 0.913)*
Accessible US diagnostics	-0.160	0.940	0.852 (0.616, 1.178)
Accessible laboratory diagnostics (PSA)	-0.196	0.660	0.822 (0.512, 1.319)
Accessible laboratory diagnostics (CBC,CRP,urine)	-1.139	11.375	0.320 (0.165, 0.620)***
Constant	1.483	4.119	4.405 *

CBC = complete blood count; CRP = C-reactive protein; LUTS = lower urinary tract symptoms; PSA = prostate specific antigen; US = abdominal ultrasound

*p < 0.05, **p < 0.01, ***p < 0.001

TABLE 6. 5-year survival in relation to sociodemographic and organizational variables

Variables	Dead n (%)	Alive n (%)	P value
Age groups			< 0.001
< 65	32 (12)	233 (88)	
65–75	72 (20.2)	285 (79.8)	
> 75	100 (52)	92 (48)	
Education			< 0.001
Primary/Elementary education	91 (32.5)	189 (67.5)	
Secondary/High school education	84 (21.8)	302 (78.2)	
Higher education	29 (19.6)	119 (80.4)	
Region of the location of primary health care centre			NS
Pomurska	32 (30.2)	74 (69.8)	
Podravska	34 (29.8)	80 (70.2)	
Koroška	9 (29)	22 (71)	
Savinjska	18 (21.2)	67 (78.8)	
Spodnjeposavska	5 (20)	20 (80)	
JV Slovenija	15 (28.3)	38 (71.7)	
Osrednjeslovenska	44 (21.6)	160 (78.4)	
Gorenjska	17 (24.6)	52 (75.4)	
Notranjo-kraška	6 (22.2)	21 (77.8)	
Goriška	14 (25)	42 (75)	
Obalno-kraška	10 (24.4)	31 (75.6)	
Cancer stage			< 0.001
Localized	124 (21.7)	448 (78.3)	
Spread	36 (18.8)	155 (81.2)	
Metastatic	44 (86.3)	7 (13.7)	
Comorbidities			< 0.001
None	72 (24.8)	218 (75.2)	
1–2	86 (21)	324 (79)	
>2	46 (40.4)	68 (59.6)	
GP access to laboratory (CBC,CRP,urine)			< 0.001
Yes	159 (21.7)	575 (78.3)	
No	45 (56.2)	35 (43.8)	
GP access to laboratory (PSA)			< 0.001
Yes	136 (20.8)	517 (79.2)	
No	68 (42.2)	93 (57.8)	
GP access to US			< 0.05
Yes	62 (20.3)	244 (79.7)	
No	142 (28)	366 (72)	
Symptomatic patient			< 0.001
Yes	103 (25.8)	296 (74.2)	
No	29 (13.2)	190 (86.8)	

CBC = complete blood count; CRP = C-reactive protein; DRE = digital rectal exam; GP = general practitioner; JV Slovenija = South-East Slovenia; Koroška = Carinthia; NS = not statistically significant; Obalno-kraška = Coastal-Karst; Osrednjeslovenska = Central Slovenia; PSA = prostate specific antigen; US = abdominal ultrasound

in primary health care centres, longer duration of doctor and primary care interval and worse 5-year survival. Considering the impact of the length of the intervals on 5-year survival, we assume that the longer intervals are indicative of the broader health care situation (the influence of the patient, the doctor and the local health care system characteristics), which as a whole influenced the survival of this patient.

The duration of the primary care interval has been investigated in several studies.[11,13,14,17,30,31] The median duration of the primary care interval in our study was 5 days, with an interquartile range (IQR) extending from 5 to 58 days which is shorter than in Helsper et al study, where the median was 14 days (IQR 3-153).[15] Lyratzopoulos et al[11] reported the mean length of primary care interval in prostate cancer patients 31 days (25th Centile 2 days, 90th Centile 74 days) whereas in our study the mean was 67.4 days with SD 123.8. The duration was, similar to doctor interval, statistically significant longer when patients had no comorbidities, when they first presented with symptoms in comparison to elevated PSA value and where there was no direct access to laboratory diagnostics (CBC, CRP, urine, PSA) in primary health care centres. Surprisingly, we observed a significant difference between the Osrednjeslovenska and Savinjska regions, with the latter showing a shorter primary care interval. This was the only parameter that showed difference in the Slovenian regions. Osrednjeslovenska region is the most densely populated, the largest in terms of number of inhabitants and the second largest in terms of area. In 2014 the Savinjska region had less than half as many inhabitants as the Osrednjeslovenska region and had the lowest proportion of the population aged over 80 years in the country (4.3%). Osrednjeslovenska region had the highest gross domestic product (GDP) per capita in the country (25.329 €/resident), 11.7% registered unemployment rate and 11.4% of people at risk of poverty. Savinjska region had a regional GDP of 16.455 €/resident, 13.9% registered unemployment rate and 15% of people at risk of poverty.[32] Lower socio-economic factors are usually associated with longer intervals.[12,33,34] In 2014 Savinjska and Osrednjeslovenska region had the same age-standardized prostate cancer incidence rate (99.2 vs. 100.1). Savinjska region had a higher standardized death rate (574.8 vs. 463.0) and age-standardized death rate due to neoplasms (231.4 vs. 189.4) than Osrednjeslovenska region.[35] Taking all these data into account, it is difficult to explain the shorter primary care interval in the Savinjska region.

In this study we also aimed to explore potential associations between the duration of primary care interval and the 5-year survival rates among prostate cancer patients in Slovenia. As expected we found worse 5-year survival in older patients, with higher cancer stages, lower education and more comorbidities.[25] Survival was not influenced by the region where the GP worked. We found a statistically significant difference in 5-year survival in patients with lower access to laboratory tests and abdominal ultrasound by their GP, and in symptomatic patients compared to those with a first contact due to a detected elevated PSA level. Other research has also confirmed that the quality and speed of the diagnostic process is influenced by a number of factors beyond the diagnostic skills of individual clinicians, such as the tests and services available to them, time constraints to consultation duration and the quality of doctor-patient communication.[10]

The use of the Slovenian Cancer Registry database enabled a comprehensive analysis as a substantial number of patients diagnosed with prostate cancer in 2014 were included. This large cohort provides robust statistical power and improves the generalizability of the study results. By using registry information, all patients diagnosed with prostate cancer in 2014 were identified and included in the study, minimizing potential selection bias and ensuring a representative sample. The limitation was the 58% response rate. As part of the study, GPs were encouraged to review both paper and electronic patient records, including discharge letters, to ensure comprehensive and accurate reporting. This approach aimed to reduce recall bias and increase the validity of the results.

The retrospective nature of the study, relying on established diagnoses and historical data, brings inherent limitations. In particular, the study focused on the doctor and primary care interval rather than the patient interval, which could affect the accuracy of reported symptoms and timing. Despite efforts to minimize recall errors, incomplete information in some questionnaires may have led to information bias, particularly with regard to the duration of doctor and primary care intervals. This bias could underestimate the actual intervals as it is based on fragment-ed or incomplete patient records. The change of GP chosen by patients between diagnosis and data collection, coupled with the variability of medical record systems, posed a challenge in accessing complete and consistent data. Paper records were frequently relied upon, which were often incomplete and difficult to decipher, while electronic records experienced compatibility issues, further complicating data retrieval and potentially leading to missing or inaccurate information. The presence of missing data leads to uncertainty about the actual performance or recording of diagnostic procedures, such as digital rectal examinations, which could affect the completeness and reliability of results. The same applies to shared decision-making. Clinical practice guidelines on prostate cancer screening using the PSA test have clearly recommended that clinicians practice shared decision making - a process involving clinician-patient discussion of the pros, cons, and uncertainties of screening. However, studies have shown that most men have never engaged in shared decision-making conversations with a healthcare provider about PSA testing.[36,37] In our study, shared decision-making was not recorded in the GP's medical records, but we cannot say with certainty that it was not carried out either.

This study provides a comprehensive examination of early management of prostate cancer patients within the primary healthcare system in Slovenia and offers valuable insights into diagnostic timelines and their impact on patient outcomes. The significant correlations found between the duration of intervals, 5-year survival rates and accessibility of laboratory diagnostics emphasize the crucial role of timely and comprehensive diagnostic testing in improving prognosis. From a clinical perspective, these findings underscore the importance of ensuring adequate resources and infrastructure for diagnostic testing in primary health care centres to minimize delays in diagnosis and optimize patient care. In addition, the observed regional differences in diagnostic intervals highlight the need for targeted interventions to address inequalities in access to healthcare and improve diagnostic efficiency in different regions. From a research perspective, these findings provide a basis for further investigation of the underlying factors influencing diagnostic processes and the effectiveness of interventions aimed at reducing diagnostic delays. Future research efforts should prioritize the validation of these findings through longitudinal studies and comparative analyses, while exploring new strategies to increase diagnostic efficiency and improve patient outcomes in prostate cancer. This study also emphasizes the need for further investigation of the factors that influence an individual's decision to seek primary health care services, particularly those beyond the scope of the variables included in the current model.

Acknowledgments

We are grateful to all our colleagues who participated in the study and all members of the V3-1713 research group.

This research was funded by the Ministry of Education, Science and Sport of the Republic of Slovenia. Grant V3-1713. Principal investigator: Vesna Zadnik.

References

1. Sung H, Ferlay J, Siegel RL, Laversanne M, Soerjomataram I, Jemal A, et al. Global cancer statistics 2020: GLOBOCAN estimates of incidence and mortality worldwide for 36 cancers in 185 countries. *CA Cancer J Clin* 2021; **71:** 209-49. doi: 10.3322/caac.21660
2. Zadnik V, Gašljević G, Hočevar M, Jarm K, Pompe-Kirn V, Strojan P, et al, editors. *Cancer in Slovenia* 2020 [Internet]. Ljubljana: Institute of Oncology Ljubljana, Epidemiology and Cancer Registry, Slovenian Cancer Registry; 2023. Available from: http://www.onko-i.si/rrs/
3. Zaletel M, Vardič D, Hladnik M, editors. *[Health statistical yearbook of Slovenia 2017].* [Slovenian]. [internet]. Ljubljana: NIJZ; 2019. Available from: https://nijz.si/publikacije/zdravstveni-statisticni-letopis-slovenije-2017/
4. Zadnik V, Primic Zakelj M, Lokar K, Jarm K, Ivanus U, Zagar T. Cancer burden in Slovenia with the time trends analysis. *Radiol Oncol* 2017; **51:** 47-55. doi: 10.1515/raon-2017-0008
5. Hamdy FC, Donovan JL, Lane JA, Mason M, Metcalfe C, Holding P, et al. 10-year outcomes after monitoring, surgery, or radiotherapy for localized prostate cancer. *N Engl J Med* 2016; **375:** 1415-24. doi: 10.1056/NEJMoa1606220
6. Wilt TJ, Brawer MK, Jones KM, Barry MJ, Aronson WJ, Fox S, et al. Radical prostatectomy versus observation for localized prostate cancer. *N Engl J Med* 2012; **367:** 203-13. doi: 10.1056/NEJMoa1113162
7. Jain MA, Leslie SW, Sapra A. *Prostate cancer screening*. Treasure Island (FL): StatPearls Publishing; 2023.
8. PRAISE-U – Uroweb. Smart early dectection of prostate cancer. [Internet]. European Association of Urology [cited 2024 Jan 7]. Available at: https://uroweb.org/praise-u
9. Neal RD, Tharmanathan P, France B, Din NU, Cotton S, Fallon-Ferguson J, et al. Is increased time to diagnosis and treatment in symptomatic cancer associated with poorer outcomes? Systematic review. *Br J Cancer* 2015; **112(Suppl 1):** S92-107. doi: 10.1038/bjc.2015.48
10. Nicholson BD, Lyratzopoulos G. Progress and priorities in reducing the time to cancer diagnosis. *Br J Cancer* 2023; **128:** 468. doi: 10.1038/s41416-022-02045-5
11. Lyratzopoulos G, Saunders CL, Abel GA, McPhail S, Neal RD, Wardle J, et al. The relative length of the patient and the primary care interval in patients with 28 common and rarer cancers. *Br J Cancer* 2015; **112(Suppl 1):** S35-40. doi: 10.1038/bjc.2015.40
12. Petrova D, Špacírová Z, Fernández-Martínez NF, Ching-López A, Garrido D, Rodríguez-Barranco M, et al. The patient, diagnostic, and treatment intervals in adult patients with cancer from high- and lower-income countries: A systematic review and meta-analysis. *PLoS Med* 2022; **19:** e1004110. doi: 10.1371/journal.pmed.1004110
13. Bosch X, Montori-Palacin E, Martínez-Ferrer R, Aldea A, Moreno P, López-Soto A. Time intervals in the care pathway to cancer diagnosis during the COVID-19 pandemic: a large retrospective study from a high-volume center. *Int J Cancer* 2023; **152:** 384-95. doi: 10.1002/ijc.34260
14. Jessen NH, Jensen H, Helsper CW, Falborg AZ, Glerup H, Gronbaek H, et al. Cancer suspicion, referral to cancer patient pathway and primary care interval: a survey and register study exploring 10 different types of abdominal cancer. *Fam Pract* 2021; **38:** 589-97. doi: https://pubmed.ncbi.nlm.nih.gov/33904928/
15. Helsper C, van Erp N, Peeters P, de Wit N. Time to diagnosis and treatment for cancer patients in the Netherlands: room for improvement? *Eur J Cancer* 2017; **87:** 113-21. doi: 10.1016/j.ejca.2017.10.003
16. Nguyen DD, Haeuser L, Paciotti M, Reitblat C, Cellini J, Lipsitz SR, et al. Systematic review of time to definitive treatment for intermediate risk and high risk prostate cancer: are delays associated with worse outcomes? *J Urol* 2021; **205:** 1263-74. doi: 10.1097/JU.0000000000001601
17. van Erp NF, Helsper CW, Olyhoek SM, Janssen RRT, Winsveen A, Peeters PHM, et al. Potential for reducing time to referral for colorectal cancer patients in primary care. *Ann Fam Med* 2019; **17:** 419-27. doi: 10.1370/afm.2446
18. Weller D, Vedsted P, Rubin G, Walter FM, Emery J, Scott S, et al. The Aarhus statement: improving design and reporting of studies on early cancer diagnosis. *Br J Cancer* 2012; **106:** 1262-7. doi: 10.1038/bjc.2012.68
19. Coxon D, Campbell C, Walter FM, Scott SE, Neal RD, Vedsted P, et al. The Aarhus statement on cancer diagnostic research: turning recommendations into new survey instruments. *BMC Health Serv Res* 2018; **18:** 677. doi: 10.1186/s12913-018-3476-0
20. Cranfield BM, Koo MM, Abel GA, Swann R, McPhail S, Rubin GP, et al. Primary care blood tests before cancer diagnosis: National Cancer Diagnosis Audit data. *Br J Gen Pract* 2023; **73:** E95-103. doi: 10.3399/BJGP.2022.0265
21. Cranfield BM, Abel GA, Swann R, Moore SF, McPhail S, Rubin GP, et al. Pre-referral primary care blood tests and symptom presentation before cancer diagnosis: National Cancer Diagnosis Audit Data. *Cancers* 2023; **15:** 3587. doi: 10.3390/cancers15143587
22. Harris M, Brekke M, Dinant GJ, Esteva M, Hoffman R, Marzo-Castillejo M, et al. Primary care practitioners' diagnostic action when the patient may have cancer: an exploratory vignette study in 20 European countries. *BMJ Open* 2020; **10:** e035678. doi: 10.1136/bmjopen-2019-035678
23. Sekhoacha M, Riet K, Motloung P, Gumenku L, Adegoke A, Mashele S. Prostate cancer review: genetics, diagnosis, treatment options, and alternative approaches. *Molecules* 2022; **27:** 5730. doi: 10.3390/molecules27175730
24. Wilkinson AN. Cancer diagnosis in primary care: Six steps to reducing the diagnostic interval. *Can Fam Physician* 2021; **67:** 265-8. doi: 10.46747/cfp.6704265
25. Koo MM, Swann R, McPhail S, Abel GA, Renzi C, Rubin GP, et al. Morbidity and measures of the diagnostic process in primary care for patients subsequently diagnosed with cancer. *Fam Pract* 2022; **39:** 623-32. doi: 10.1093/fampra/cmab139
26. Hansen RP, Vedsted P, Sokolowski I, Søndergaard J, Olesen F. Time intervals from first symptom to treatment of cancer: a cohort study of 2,212 newly diagnosed cancer patients. *BMC Health Serv Res* 2011; **11:** 284. doi: 10.1186/1472-6963-11-284
27. Gnanapragasam VJ, Greenberg D, Burnet N. Urinary symptoms and prostate cancer-the misconception that may be preventing earlier presentation and better survival outcomes. *BMC Med* 2022; **20:** 264. doi: 10.1186/s12916-022-02453-7
28. Holtedahl K, Borgquist L, Donker GA, Buntinx F, Weller D, Campbell C, et al. Symptoms and signs of urogenital cancer in primary care. *BMC Primary Care* 2023; **24:** 1-15. doi: 10.1186/s12875-023-02063-z
29. Scheel BI, Holtedahl K. Symptoms, signs, and tests: the general practitioner's comprehensive approach towards a cancer diagnosis. *Scand J Prim Health Care* 2015; **33:** 170-7. doi: 10.3109/02813432.2015.1067512
30. Swann R, Lyratzopoulos G, Rubin G, Pickworth E, McPhail S. The frequency, nature and impact of GP-assessed avoidable delays in a population-based cohort of cancer patients. *Cancer Epidemiol* 2020; **64:** 101617. doi: 10.1016/j.canep.2019.101617
31. Lim AWW, Mesher D, Gentry-Maharaj A, Balogun N, Widschwendter M, Jacobs I, et al. Time to diagnosis of Type I or II invasive epithelial ovarian cancers: a multicentre observational study using patient questionnaire and primary care records. *BJOG* 2016; **123:** 1012-20. doi: 10.1111/1471-0528.13447
32. Bajželj M. [Statistical portrait of Slovenian regions 2026]. [Slovenian]. [internet]. Ljubljana: Statistical Office of the Republic of Slovenia; 2016. [cited 2024 Feb 6]. Available at: https://www.stat.si/dokument/8941/regije-v-stevilkah.pdf

33. Petrova D, Garrido D, Špacírová Z, Fernández-Martínez NF, Ivanova G, Rodríguez-Barranco M, et al. Duration of the patient interval in breast cancer and factors associated with longer delays in low-and middle-income countries: a systematic review with meta-analysis. *Psychooncology* 2023; **32:** 13-24. doi: 10.1002/pon.6064

34. Huepenbecker SP, Sun CC, Fu S, Zhao H, Primm K, Giordano SH, et al. Factors impacting the time to ovarian cancer diagnosis based on classic symptom presentation in the United States. *Cancer* 2021; **127:** 4151-60. doi: 10.1002/cncr.33829

35. Zaletel M, Vardič D, Hladnik M, editors. *[Health statistical yearbook of Slovenija 2014].* [Slovenian]. [internet]. Ljubljana: National Institute of Public Health; 2016. Available at: https://nijz.si/publikacije/zdravstveni-statisticni-letopis-2014/

36. Han PKJ, Kobrin S, Breen N, Joseph DA, Li J, Frosch DL, et al. National evidence on the use of shared decision making in prostate-specific antigen screening. *Ann Fam Med* 2013; **11:** 306-14. doi: 10.1370/afm.1539

37. Bhojani N, Miller LE, Zorn KC, Chughtai B, Elterman DS, Bhattacharyya S, et al. Prevalence and determinants of shared decision-making for PSA testing in the United States. *Prostate Cancer Prostatic Dis* 2024. doi: 10.1038/s41391-024-00843-x

research article

Tracheostomy before and during COVID-19 pandemic

Sara Jensterle[1], Janez Benedik[2,3], Robert Sifrer[1,3]

[1] Department of Otorhinolaryngology and Cervicofacial Surgery, University Medical Centre Ljubljana, Ljubljana, Slovenia
[2] Department of Anaesthesiology and Surgical Intensive Therapy, University Medical Centre Ljubljana, Ljubljana, Slovenia
[3] Faculty of Medicine, University of Ljubljana, Ljubljana, Slovenia

Radiol Oncol 2024; 58(4): 556-564.

Received 4 April 2024
Accepted 16 May 2024

Correspondence to: Assist. Prof. Robert Šifrer, M.D., Ph.D., Department of Otorhinolaryngology and Cervicofacial Surgery, University Medical Centre Ljubljana, Slovenia. E-mail: robert.sifrer@kclj.si and Assist. Prof. Janez Benedik, M.D., Ph.D., Department of Anaesthesiology and Surgical Intensive Therapy, University Medical Centre Ljubljana, Slovenia. E-mail: janez.benedik@kclj.si

Disclosure: No potential conflicts of interest were disclosed.

Background. The aim of the study was to provide insight into the influence of the COVID-19 on the frequency and characteristics of urgent and emergent tracheostomies (TS), comparing data collected both before and during the pandemic. Our two hypotheses were that *during COVID-19, more TS were performed in the emergent setting* and that *during COVID-19 more TS were performed under general anaesthesia.*

Patients and methods. The research was retrospective. The study period included the two years before and after the COVID-19 outbreak in Slovenia. Forty-one patients in each period met the inclusion criteria. Their medical charts were reviewed. The anamnestic, clinical, surgical and anaesthesiological data were collected. The two groups of patients from corresponding time periods were statistically compared.

Results. Predominantly men required the surgical resolution of acute upper airway obstruction (76% of patients). The causes for acute respiratory distress included head and neck cancer (62%), infections (20%), vocal cord paralysis (16%), and stenosis (2%). There were no statistically significant differences either in the (emergent/urgent) setting of TS or in the type of anaesthesia used. Both hypotheses were rejected. A statistically significant rise in use of the C-MAC laryngoscope during COVID-19 (from 3% to 15%) was reported.

Conclusions. The outbreak of COVID-19 did not have a statistically significant effect on the frequency of performing emergent and urgent tracheostomies nor on the use of general or local anaesthesia. It did, however, require a change of intubation technique. Consequently, a significant rise in the use of the C-MAC laryngoscope was noted.

Key words: upper airway obstruction; emergent tracheostomy; urgent tracheostomy; anaesthesia; SARS-CoV-19; orotracheal intubation

Introduction

Acute respiratory distress (ARD) due to upper airway obstruction (UAO) is a life-threatening medical situation leading to, both, the imminent irreparable ischemic damage of the brain and/or cardiac arrest if not treated properly and promptly. These catastrophic events can occur in a matter of minutes. Thus, quick, determinate action is required in order to provide an alternative air conduit and ensure a clear, patent airway.[1-3]

After the identification of the site and degree of the UAO, which is the first step, further measures are taken to circumvent the obstructed airway. The first option is orotracheal intubation (OTI) most commonly performed by an anaesthesiologist under general anaesthesia. It is followed by an open tracheostomy (TS), which is usually performed by an otorhinolaryngologist or other appropriately, adequately trained surgical specialist.

Clinical conditions of ARD, where the patient can neither be intubated nor ventilated, are known

as "cannot intubate-cannot ventilate" situations (CICV) and represent truly emergent clinical scenarios requiring a quick and effective surgical approach to the airway.[4] The literature describes two surgical options for resolving ARD in the circumstances of CICV: the cricothyrotomy (CTT) and the tracheostomy (TS).

In December 2019, a new strand of Coronavirus, now named SARS-CoV-2 was discovered. Its outbreak negatively affected healthcare accessibility all over the world and, among other things, demanded the adaptation of surgical procedures to avoid viral transmission to healthcare providers. In regards to TS, the opening of the trachea and excision of tracheal window as the essential steps of the TS, might cause cough generating a large quantity of aerosol containing mucus, blood, and the virus. This would be directed towards the surgical and anaesthesiological teams, so the contamination of healthcare personnel with SARS-CoV-2 is highly probable during ordinary, i.e. not adapted, TS.[5]

There is a plethora of articles in the pertinent literature discussing the various surgical and anaesthesiological adaptations of the TS to the pandemic of COVID-19. Some of them were also proposed by our department.[4,6]

In this study, we chose to analyse the changing paradigm of ARD treated by TS as a result of the outbreak of COVID-19. The aim was to provide an in-depth comparison between the two eras (before the outbreak *vs*. during the COVID-19 pandemic) including the causes of ARD, the indications for emergent and urgent TS, the risk factors in the case of a difficult intubation, the surgical and anaesthesiological aspects of TS as well as the timing of the surgery. Our hypotheses firstly focused on the proposition that *"during the pandemic there were more TS performed in the emergent setting"*, and, secondly that *"during COVID-19 more TS were performed under general anaesthesia"*.

Patients and methods

This retrospective study was conducted at the Department of Otorhinolaryngology and Cervicofacial Surgery at the University Medical Centre of Ljubljana, Slovenia. Medical charts, surgical and anaesthesiological reports from consecutive patients treated with TS for UAO associated with ARD during a four-year-long period, i.e., between 4th of March 2018 and the 3rd of March 2022 were reviewed. The data associated with the patient, ARD, the risk factors for difficult OTI, surgical establishment of alternative airway and anaesthesiological parameters were all systematically collected.

The patients were categorised into two groups, i.e., those managed during the COVID-19 pandemic (study group) and those treated before the outbreak of COVID-19 (control group). The dividing date was the 4th of March 2020 as this was the day when the first case of COVID-19 was reported in Slovenia. Thus, the length of each period was exactly two years. The groups were statistically compared according to the above-mentioned parameters under evaluation.

From the point of a time-dependent aspect of TS, the TS were divided into emergent and urgent ones.[7] For the purpose of our study, one of the following criteria had to be fulfilled for the definition of the emergent TS:

- The TS was performed on working days during regular hours immediately following the establishment of the UAO diagnosis. The on-going elective surgical program of the department was interrupted to carry out the TS.
- The TS was performed during "on duty" service.
- The TS was performed following the diagnostic direct laryngoscopy during which the imminent deterioration of the upper airway obstruction was recognised or suspected.
- The TS was performed in a CICV scenario.

On the other hand, if the dyspnoea was not severe enough to demand an emergent procedure, the TS was defined as urgent:

- The TS was not performed immediately after the establishment of UAO but scheduled for (at least) the following day.
- The TS did not fulfil the criteria for emergent TS

The elective TS performed, for example, in patients with curative or palliative treatment of head-and-neck cancer (HNC), with long-term OTI or with chronic aspiration were excluded from the study.

The statistical analyses were performed using the IBMI SPSS Statistics Version 25 (Chicago, IL). For comparative analyses, the Chi-Square test, Fisher's exact test, t-test, and Mann-Whitney U test were used. All statistical tests were two-sided and *p*-values below 0.05 were considered statistically significant.

This study has been approved by the National Medical Ethics Committee of the Republic of Slovenia on 26th of May 2022 under the number 0120-176/2022/3.

TABLE 1. The main causes of upper airway obstruction

Causes of upper airway obstruction	No. of patients	Ratio (%)
All patients	82	100
Laryngeal cancer	24	29
Pharyngeal cancer	20	24
Cancer of other primary sites	7	9
Infections	16	20
Bilateral vocal cord paralysis	13	16
Laryngo-tracheal stenosis	2	2

Results

All patients, both periods

A total of 82 patients were included into the study. The mean age of the patients was 69 years (range 28–97) and 62 (76%) of these were male.

From the surgical aspect, in the majority of the patients (72, 88%) the UAO was solved by means of a TS. The CTT as the first step in resolving upper airway obstruction was used in 6 cases (7%) and was transformed into TS immediately. Re-TS was performed in 4 cases (5%), meaning a patient already had a TS beforehand, and was successfully decannulated afterwards. From the aspect of emergency, the TS was considered emergent in 59 (72%) and urgent in 23 (28%) patients. In most of the cases, the surgery was performed by experienced otorhinolaryngologists, namely, in 68 patients (83%). In the remaining 14 cases (17%), the TS was performed by residents under the supervision of the experienced surgeon.

The UAO was most commonly caused by HNC (62%, 51 patients). The primary tumour sites included the larynx in 24 patients (47%), pharynx in 20 patients (39%), and other primary sites in 7 patients (14%). Other causes for the obstruction were infections including both mucosal upper airway infections and deep neck infections, as well as bilateral vocal cord paralysis and laryngotracheal stenosis. These results are detailed in Table 1. The UAO was caused by a single disease in 60 patients (73%), whereas in the remaining 22 patients (27%) multiple causes were registered. In these cases, the cause playing the most significant role was considered to be the main one.

Among the symptoms accompanying the dyspnoea, dysphagia was reported by 26 patients (32%), pain in 19 patients (23%), inspiratory stridor in 31 patients (38%), and biphasic stridor in a single patient (1%). The trismus was present in 6 cases (7%).

Thirty-six patients were previously treated for various diseases of the head and neck: 14 patients (17%) by surgery, 11 patients (13%) received radiotherapy (RT) and 11 patients (13%) chemo-radiotherapy (CRT).

Taking into account the 51 patients with HNC as a cause of UAO requiring TS at the time of our study, 33 had de novo cancer while 18 had a recurrence or a new primary cancer. Specifically, 20% (10/51) had previously received RT and 16% (8/51) CRT.

Thirty-one patients had other causes of the UAO, namely infections, bilateral vocal cord paralysis and laryngotracheal stenosis. Thirteen percent (4/31) had a history of previous HNC and were treated by RT (one patient) and CRT (three patients).

Sixty-six (80%) patients had an available ASA score and were classified as ASA II (7%, 6/82), ASA III (53%, 44/82), and ASA IV (20%, 16/82).

Mallampati score was noted in 44 patients (54%, 44/82). Most of them (17%, 14/82) were ranked with the highest score 4, whilst score 3, 2 and 1 were attributed to 16% (13/82), 12% (10/82), and 9% (7/82) of patients, respectively.

Mouth opening was noted in 41 examinees. An adequate mouth opening was defined as an interincisor distance of more than 3 cm, as opposed to inadequate of less than 3 cm. Forty-one percent (34/82) of those were evaluated to have adequate mouth opening, whereas in 9% (7/82) it was inadequate.

Hyo-mental and thyro-mental distances were noted in 28 and 12 patients, respectively. Hyothyromental distance was the parameter coined by us for the purpose of the study and comprises the measurement of either of the two distances. It was obtained in 40 examinees. The distance was sufficient in 43% of the patients (35/82) and insufficient in 6% (5/82).

In 77 patients (94%), general anaesthesia was used, while in the remaining 5 patients (6%), the TS was performed under local anaesthesia.

The data, considering the type of the orotracheal tube, was able to be retrieved in 43 patients. Predominantly, a wire tube was used (39%, 32/82). A curved tube was used more seldomly (8 %, 7/82), while the straight tube was the least frequently used (5%, 4/82). The data concerning the manner of OTI in terms of the glottic exposure was reported in 67 cases. In 9% of the OTI (7/82), C-MAC video laryngoscope was used.

TABLE 2. A comparison of the risk factors in all patients before and during the COVID-19 outbreak in Slovenia

Risk factor	Overall	Before the outbreak of COVID-19	During the pandemic of COVID-19	p value
All patients	82	41	41	
Patients				
Age (years) mean, range	66.8 (28–97)	64.8 (28–91)	68.8 (42–97)	0.172[a]
Male sex	62 (76%)	31 (76%)	31 (76%)	1.00[c]
Body weight (kg) mean, range	73.5 (35–143)	71.9 (35–143)	75.2 (43–110)	0.512 [a]
Body height (cm) mean, range	172 (150–185)	172 (150–185)	173 (152–183)	0.933 [a]
Body mass index (kg/m^2), mean, range	25.4 (12.7–37.6)	24.2 (12.7–37.6)	27.6 (19,4–35,5)	0.178 [a]
The upper airway obstruction				
Respiratory distress duration (days), median, range	6 (1–180)	10.5 (1–90)	3 (1–180)	0.373 [b]
Causes of acute airway obstruction				0.826 [c]
Laryngeal cancer	24 (29%)	12 (29%)	12 (29%)	
Pharyngeal cancer	20 (24%)	8 (20%)	12 (29%)	
Other cancers	7 (9%)	5 (12%)	2 (5%)	
Inflammation	16 (20%)	8 (20%)	8 (20%)	
Vocal cord paralysis	13 (16%)	7 (17%)	6 (15%)	
Laryngotracheal stenosis	2 (2%)	1 (2%)	1 (2%)	
Multiple causes	22 (27%)	11 (27%)	11 (27%)	1.000 [c]
Respiration space (mm) mean, range	2.3 (1–5)	2.5 (1–4)	2.2 (1–5)	0.635[a]
Symptoms				
Dysphagia	26 (32%)	12 (29%)	14 (34%)	0.635 [c]
Trismus	6 (7%)	5 (12%)	1 (2%)	0.101[d]
Pain	19 (23%)	8 (20%)	11 (27%)	0.432 [c]
Stridor				0.504 [c]
Inspiratory	31 (38%)	17 (42%)	14 (34%)	
Biphasic	1 (1%)	0	1 (2%)	
Previous treatment				
Surgery	14 (17%)	5 (12%)	9 (22%)	0.379[d]
RT	11 (13%)	5 (12%)	6 (15%)	1.000[d]
CRT	11 (13%)	5 (12%)	6 (15%)	1.000[d]
Surgery				
Re-TS	4 (5%)	0	4 (10%)	0.116 [d]
Cricothyrotomy	6 (7%)	3 (7%)	3 (7%)	1.000 [d]
Surgeon specialist	68 (83%)	34 (83%)	34 (83%)	1.000 [c]
Time-dependent aspect of TS				0.806 [c]
Emergent	59 (72%)	29 (71%)	30 (73%)	
Urgent	23 (28%)	12 (29%)	11 (27%)	
Duration (hour) median, range	0.75 (0.25–2.50)	0.75 (0.25–2.5)	0.88 (0.25–2)	0.546 [b]
Anaesthesia				1.000[d]
Local	5 (6%)	2 (5%)	3 (7%)	
General	77 (94%)	39 (95%)	38 (93%)	

Risk factor	Overall	Before the outbreak of COVID-19	During the pandemic of COVID-19	p value
Duration (hour) median, range	1.50 (0.75–3.25)	1.5 (0.75–3.25)	1.75 (1–3,25)	0.198 [b]
ASA classification				0.952[c]
II	6 (7%)	3 (7%)	3 (7%)	
III	44 (53%)	23 (56%)	21 (51%)	
IV	16 (20%)	9 (22%)	7 (17%)	
Unknown	10 (20%)	6 (15%)	10 (25%)	
Mallampati classification				0.810 [c]
I	7 (9%)	5 (12%)	2 (5%)	
II	10 (12%)	6 (15%)	4 (10%)	
III	13 (16%)	7 (17%)	6 (14%)	
IV	14 (17%)	7 (17%)	7 (17%)	
Unknown	38 (46%)	16 (39%)	22 (54%)	
Mouth opening				0.207[d]
Inadequate	7 (9%)	6 (15%)	1 (2%)	
Adequate	34 (41%)	18 (44%)	16 (39%)	
Unknown	41 (50%)	17 (41%)	24 (59%)	
Hyo/thyromental distance				1.000 [c]
Insufficient	5 (6%)	3 (7%)	2 (5%)	
Sufficient	35 (43%)	21 (51%)	14 (34%)	
Unknown	42 (51%)	17 (42%)	25 (61%)	
Endotracheal tube type				0.072 [c]
Wire	32 (39%)	18 (44%)	14 (34%)	
Straight	4 (5%)	4 (10%)	0	
Curved	7 (8%)	2 (5%)	5 (12%)	
Unknown	39 (48%)	17 (41%)	22 (54%)	
Orotracheal intubation				0.043 [d] *
C-MAC laringoscope	7 (9%)	1 (3%)	6 (15%)	
Laryngoscope	60 (73%)	35 (85%)	25 (61%)	
Unknown	15 (18%)	5 (12%)	10 (24%)	

ASA = American Society of Anaesthesiologists; COVID-19 = Coronavirus infectious disease 19; CRT = chemo-radiotherapy; RT = radiotherapy; TS = tracheostomy

[a] = T test, [b]= Mann-Whitney U-test, [c]= hi-square test, [d]= Fisher exact test

A comparison of all patients regarding the period before and during COVID-19

Out of a total of 82 patients that were included in the study, 41 of them comprised the study group with the same number of patients included in the control group.

The parameters concerning the characteristics of the patients and prior treatments as well as the data associated with the actual disease causing UAO and its management from both a surgical and anaesthesiological perspective were statistically compared. The results of the statistical comparison between the study and control group are presented in Table 2.

Regarding the main questions of the study, there were no differences between the study and control group in our research. Namely, before the outbreak of COVID-19, TS was performed in the emergent setting in 71% (29/41) of patients, whereas during the COVID-19 pandemic, that number was 73% (30/41). Thus, there is no statistically

significant difference demonstrated (p = 0.806). Furthermore, there was no statistically significant difference in relevance to the general anaesthesia (p = 1.000), either, as before the era of COVID-19, TS was performed under general anaesthesia in 95% (39/41) and during the pandemic in 93% (38/41) of patients.

Nevertheless, Table 2 gives us insight into some differences between the two groups, with the most prominent ones implicated through endotracheal intubation. A trend of less frequent use of the straight orotracheal tube during the pandemic (0%, 0/41) in comparison to the time prior to the COVID-19 (10%, 4/41) outbreak has been noted. There is an increase in the use of the curved tube from 5% (2/41) to 12% (5/41), the difference is, however, not statistically significant (p = 0.072). The change in implementation of the C-MAC videolaryngoscope proved to be statistically significant (p = 0.043). Before COVID-19, it was used in 3% (1/41) of cases and in 15% (6/41) of cases during COVID-19.

A comparison of patients with HNC regarding the period before and during COVID-19

Since some of the risk factors are specific for patients with HNC (such as prior RT and CRT) and not for patients with other diseases, another comparison was made. This included 51 patients with HNC, 26 of whom were in the study group and 25 in the control group. The results are depicted below in Table 3.

There were no differences in the primary tumour sites between the two periods. Nevertheless, we observed a trend of higher incidence in the invasion of hypopharynx in the study group as opposed to the control group (39% *vs*. 12%, p = 0.052).

There was also a significant rise in the use of C-MAC during COVID-19, from 4% to 23% (p = 0.047).

Discussion

The first hypothesis

Throughout the study period, the TS due to ARD caused by UAO was performed in 72% as an emergency surgical procedure. The rates of emergent TS before and during the COVID-19 pandemic were 71% and 73%, respectively. This difference did not attain statistical significance. Therefore, our first hypothesis stating that *"during the pandemic there were more TS performed in the emergent setting"* was rejected.

During the epidemic, access to sport and outdoor activities was severely limited. As physical activity diminished, the average body mass index rose from 24,2 to 27,6 kg/m^2, so not significantly. Similarly, patients' access to their general practitioners was also limited so patients received no regular medical attention. The cancers, inflammations and other medical conditions progressed unimpededly leading to higher stages of diseases and more clinical problems when patients finally found their way to their doctors. In this way, the suboptimal accessibility of general practitioners could explain the (not significantly) decreased width of the airway – from 2.5 to 2.2 mm at the narrowest point of the airway. An elevated BMI and decreased width of airways led us to expect a higher rate of difficult intubations and emergent TS in COVID-19 on account of the urgent ones. However, this was not the case, as the difference did not emerge as significant.

For the same reasons, more patients with CICV situations were expected. The literature offers two options to treat ARD in a CICV scenario: CTT and TS.[8] In emergent situations, otorhinolaryngologists, as a general rule, prefer TS, which is supported by our results – 93% of patients received TS, whereas only 7% received CTT, which was then immediately converted into TS. The decision for (a more complicated, longer and riskier) TS as opposed to a (technically less demanding and speedier) CTT in the emergent setting is surprising. Moreover, The Advanced Trauma Life Support (ATLS) guidelines recommend CTT in an emergency CICV situation.[9] Nevertheless, the otorhinolaryngologists are trained in emergent surgical airway management very early on in their careers, so the educational goals in the residency programmes prepare them to perform TS within a few minutes.[4,10] This actually means that the otorhinolaryngologists are more experienced in performing TS than CTT explaining the low rate of CTT on account of TS in an emergency setting. However, for all other specialists who may not have TS in their residency programme, the CTT is suggested followed by the referral of the patient to the closest otorhinolaryngological unit.

There was an equal rate of CTT during both periods – 7%. A higher rate was expected during COVID-19 as the Slovenian national guidelines for emergent TS during the era of COVID-19 advised CTT as the first step in emergent TS.[4] However, the guidelines target a CICV situation in COVID-19

TABLE 3. A comparison of the risk factors in patients with HNC before and during the COVID-19 outbreak in Slovenia

Risk Factor	Overall	Before the Outbreak of COVID-19	During the Pandemic of COVID-19	p value
All Patients	51	25	26	
Patients				
Age (years) mean, range	66.2 (28–88)	64.6 (28–88)	67.8 (42–87)	0.374 [a]
Male sex	44 (86%)	22 (88%)	22 (85%)	1.000 [d]
Primary site				0.365 [c]
Laryngeal cancer	24 (47%)	12 (48%)	12 (46%)	
Pharyngeal cancer	20 (39%)	8 (32%)	12 (46%)	
Other cancers	7 (14%)	5 (20%)	2 (8%)	
Invasion of subsites				
Glottis	21 (42%)	13 (52%)	8 (31%)	0.124 [c]
Supraglottis	32 (63%)	16 (64%)	16 (62%)	0.856 [c]
Subglottis	11 (22%)	6 (24%)	5 (19%)	0.743 [d]
Trachea	2 (4%)	1 (4%)	1 (4%)	1.000 [d]
Hypopharynx	13 (26%)	3 (12%)	10 (39%)	0.052 [d]
Oropharynx	16 (31%)	10 (40%)	6 (23%)	0.193 [c]
Oral cavity	8 (16%)	4 (16%)	4 (15%)	1.000 [d]
Respiration Space (mm), mean, range	2.4 ± 1.5 (1–5)	3 ± 1.7 (1–4)	2.2 ± 1.5 (1–5)	0.714 [b]
Previous treatment				
Surgery	8 (16%)	3 (12%)	5 (19%)	0.703 [d]
RT	10 (20%)	4 (16%)	6 (23%)	0.726 [d]
CRT	8 (16%)	4 (16%)	4 (15%)	1.000 [d]
Surgery				
Time-dependent aspect of TS				0.806 [c]
Emergent	34 (67%)	16 (64%)	18 (69%)	
Urgent	17 (33%)	9 (36%)	8 (31%)	
Orotracheal intubation				0.047 [d] *
C-MAC	7 (14%)	1 (4%)	6 (23%)	
Laryngoscope	38 (74%)	22 (88%)	16 (62%)	
Unknown	6 (12%)	2 (8%)	4 (15%)	

COVID-19 = coronavirus infectious disease 19; CRT = chemo-radiotherapy); RT = radiotherapy, TS = tracheostomy

[a] = T test, [b] = Mann-Whitney U-test, [c] = hi-square test, [d] = Fisher exact test

patients or those with an unknown COVID-19 status. Since the incidence of true CICV situations is only 0.4%[11] the amount of CTT performed before and during COVID-19, remained the same.

The second hypothesis

The TS were performed over the entire four-year-long period, mainly under general anaesthesia – in 94% of cases. Again, there are no statistically significant differences demonstrated in the periods before or during the pandemic, where general anaesthesia was used in 93% and 95% of cases, respectively. Therefore, our second hypothesis claiming that *"during COVID-19 more TS were performed in the general anaesthesia"* was also rejected.

Irrespective to the studied periods, we noticed a significantly higher percentage of TS under general anaesthesia as compared to reports from the literature.[12,13] At first, TS under local anaesthesia is

much more unpleasant and uncomfortable for the patient as well as for the surgeon. Furthermore, the dyspnoeic, restless and hypoxic patients frequently do not cooperate with the surgical team and impede the course of the surgery. In addition, the opening of the trachea results in the generation of aerosol potentially transmitting the SARS-CoV-2 and/or other diseases to the health personnel.[4,5] To conclude, TS under local anaesthesia is associated with a great many issues and is, therefore, avoided. This applies to all patients and does not depend on the presence of the COVID-19.

Secondly, with the advent of sophisticated equipment such as C-MAC, the bonfils endoscope and procedures such as transnasal awake fiberoptic intubation[11,14], the endotracheal intubation almost always succeeds. This would explain the high rate of implementation of general anaesthesia in TS. Therefore, TS under local anaesthesia is reserved only for occasional occurrences of CICV.

Thirdly, as TS under general anaesthesia generates less aerosol due to the surgical technique adjustment, we expected fewer TS under local anaesthesia during COVID-19. We attribute the lack of the expected difference to the fact that there were not many CICV occurrences in the studied period, as they are rare, per se.[11] According to the Slovenian guidelines in the case of an occurrence of CICV in COVID-19, CTT under general anaesthesia is proposed as one of the essential steps of the emergent TS in patients with COVID-19.[4,15] CICV incidence was not determined in our study, however, with an incidence of 0.4% from the literature[11], we expected only occasional CICV cases.[11,16,17]

Other comparisons

In the majority of OTI, a wire tube was used (32 patients, 39%), which is also recommended in surgical procedures and difficult intubations.[18] There was a trend demonstrating the less frequent use of the straight tube (10% *vs.* 0) and more frequent use of the curved endotracheal tubes (5% *vs.* 12%) during the pandemic. The preference for curved tubes during COVID-19 could be explained by its convenient use in combination with C-MAC, especially in the case of a difficult intubation. Curved tubes reduce the risk of obstruction due to folding, in comparison to a straight tube. The diversity of tube types in the study could also be attributed to various anaesthesiologists being involved in emergent TS and therefore a deviation from regular intubation protocol.

The increased use of C-MAC during COVID-19 proved to be statistically significant, as it rose from 3% to 15%. What is more, it was also considered statistically significant during a separate analysis of patients with HNC (4% *vs.* 23%). This can be attributed to international guidelines, which recommend C-MAC video-laryngoscopes in patients with confirmed or suspected COVID-19 since it enables a further and, consequently, safer distance between the anaesthesiologist's face and patient's mouth, therefore minimising the anesthesiologist's exposure to the contaminated aerosol.[19] Video laryngoscopes enable the anaesthesiologist to execute the intubation and observe the insertion of the tip of the tube on a monitor rather than looking directly into the patient's airway. An additional benefit to this method is the shorter intubation time required.[18]

An interesting trend was also noted from the perspective of tumour subsites invasion. After the separate analysis of patients with HNC, we noted an increase in HNCs invading the hypopharynx. This rose from 12% in the control group to 39% in the study group. This trend could be attributed to the fact that patients, due to COVID-19, sought medical help later, with more widely spread cancer.

The appearance of the SARS-CoV-2 had a significant impact on the management of UAO, both in Slovenia and around the world. Although COVID-19 changed the surgical and anaesthesiological perspectives of the management of ARD in patients with UAO, emergent TS remains one of the most important and time-honoured solutions. The study compared the time period before the onset of COVID-19 to that during the epidemics. Eighty-two patients were included in the study with 41 in each observed period.

The elderly male patients were (not significantly) more often affected by ARD caused by UAO and required intervention more often than younger, female counterparts. The UAO was most often caused by HNC (62%), followed by patients with inflammatory diseases (20%) and recurrent laryngeal nerve palsy (16%). Among HNC, the laryngeal (47%) and pharyngeal cancer (39%) predominated.

Conclusions

In terms of TS, the comparison between the two eras (before the outbreak *vs.* during the COVID-19 pandemic) revealed no significant differences nei-

ther in the proportions of emergent and urgent TS nor in use of general or local anaesthesia. However, the C-MAC video laryngoscope was (statistically significantly) more often used during COVID-19 (from 3% to 15%) which goes hand in hand with the international anaesthesiological guidelines.

References

1. Berlac P, Hyldmo PK, Kongstad P, Kurola J, Nakstad AR, Sandberg M. Pre-hospital airway management: guidelines from a task force from the Scandinavian Society for Anaesthesiology and Intensive Care Medicine. *Acta Anaesthesiol Scand* 2008; **52:** 897-907. doi: 10.1111/j.1399-6576.2008.01673.x
2. Henderson JJ, Popat MT, Latto IP, Pearce AC. Difficult Airway Society guidelines for management of the unanticipated difficult intubation. *Anaesthesia* 2004; **59:** 675-94. doi: 10.1111/j.1365-2044.2004.03831.x
3. Apfelbaum JL, Hagberg CA, Caplan RA, Blitt CD, Connis RT, Nickinovich DG, et al. Practice guidelines for management of the difficult airway: an updated report by the American Society of Anesthesiologists Task Force on Management of the Difficult Airway. *Anesthesiology* 2013; **118:** 251-70. doi: 10.1097/ALN.0b013e31827773b2
4. Šifrer R, Urbančič J, Piazza C, van Weert S, García-Purriños F, Benedik J, et al. Emergent tracheostomy during the pandemic of COVID-19: Slovenian National Recommendations. *Eur Arch Otorhinolaryngol* 2021; **278:** 2209-17. doi: 10.1007/s00405-020-06318-8
5. Philpott C, Burrows S. Aerosol-generating procedures in ENT. London: Head and Neck (ENT UK) at The Royal College of Surgeons of Englan; Legeforeningen. [internet]. 2020. [cited 2020 Apr 5]. Available at: https://www.legeforeningen.no/contentassets/8d2b776522c34deb8f57fa618cb07c32/aerosol-generating-procedures-in-ent_compressed.pdf
6. Šifrer R, Benedik J, Aničin A. Elective open "shield tracheostomy" in patients with COVID-19. *Eur Arch Otorhinolaryngol* 2022; **279:** 891-7. doi: 10.1016/j.bja.2022.07.032
7. World Health Organization. Emergency and trauma care. Emergency care systems for universal health coverage: ensuring timely care for the acutely ill and injured. Report by the Director-General. [internet]. 2019. [cited 2023 May 7]. Available at: http://apps.who.int/gb/ebwha/pdf_files/WHA71/A71_4-en.pdf?ua=1or.
8. Dillon JK, Christensen B, Fairbanks T, Jurkovich G, Moe KS. The emergent surgical airway: cricothyrotomy vs. tracheotomy. *Int J Oral Maxillofac Surg* 2013; **42:** 204-8. doi: 10.1016/j.ijom.2012.10.021
9. American College of Surgeons. *Advanced trauma life support*. Chicago: American College of Surgeons, Committee on Trauma; 2018.
10. European Union of Medical Specialists (Uems). *Logbook Oto-Rhino-Laryngology-Head and Neck Surgery* (Revision 2018) *Training Programme*. [internet]. 2018. [cited 2023 May 8]. Available at: http://orluems.com/gestor/upload/LOGBOOK%20REVISED%20FINAL%202019.pdf
11. Cabrini L, Baiardo Redaelli M, Ball L, Filippini M, Fominskiy E, Pintaudi M, et al. Awake fiberoptic intubation protocols in the operating room for anticipated difficult airway: A systematic review and meta-analysis of randomized controlled trials. *Anesth Analg 2019*; **128:** 971-80. doi: 10.1213/ANE.0000000000004087
12. Altman KW, Waltonen JD, Kern RC. Urgent surgical airway intervention: a 3 year county hospital experience. *Laryngoscope* 2005; **115:** 2101-4. doi: 10.1097/01.mlg.0000180176.66968.0f
13. Waldron J, Padgham ND, Hurley SE. Complications of emergency and elective tracheostomy: a retrospective study of 150 consecutive cases. *Ann R Coll Surg Engl* 1990; **72:** 218-20. PMID: 2382943
14. Kim H, So E, Karm MH, Kim HJ, Seo KS. Learning fiberoptic intubation for awake nasotracheal intubation. *J Dent Anesth Pain Med* 2017; **17:** 297-305. doi: 10.17245/jdapm.2017.17.4.297
15. Šifrer R, Iglič Č. [Elective open tracheostomy in a patient with COVID-19]. [Slovenian]. *Zdrav Vestn* 2020; **89:** 680-91. doi: 10.6016/ZdravVestn.3111
16. Piazza C, Filauro M, Dikkers FG, Nouraei SAR, Sandu K, Sittel C, et al. Long-term intubation and high rate of tracheostomy in COVID-19 patients might determine an unprecedented increase of airway stenoses: a call to action from the European Laryngological Society. *Eur Arch Otorhinolaryngol* 2021; **278:** 1-7. doi: 10.1007/s00405-020-06112-6
17. Schnittker R, Marshall SD, Berecki-Gisolf J. Patient and surgery factors associated with the incidence of failed and difficult intubation. *Anaesthesia* 2020; **75:** 756-66. doi: 10.1111/anae.14997
18. Apfelbaum JL, Hagberg CA, Connis RT, Abdelmalak BB, Agarkar M, Dutton RP, et al. American Society of Anesthesiologists Practice guidelines for management of the difficult airway. *Anesthesiology* 2022; **136:** 31-81. doi: 10.1097/ALN.0000000000004002
19. Saito T, Taguchi A, Asai T. Videolaryngoscopy for tracheal intubation in patients with COVID-19. *Br J Anaesth* 2020; **125:** e284-6. doi: 10.1016/j.bja.2020.06.002

research article

Relation of *JAK2* V617F allele burden and coronary calcium score in patients with essential thrombocythemia

Ajda Drofenik[1], Ales Blinc[2,3], Mojca Bozic Mijovski[2,4], Tadej Pajic[5,6], Matjaz Vrtovec[2,7], Matjaz Sever[3,8*]

[1] Department of Cardiology, Division of Internal Medicine, University Medical Centre Ljubljana, Ljubljana, Slovenia
[2] Department of Vascular Diseases, Division of Internal Medicine, University Medical Centre Ljubljana, Ljubljana, Slovenia
[3] Faculty of Medicine, University of Ljubljana, Ljubljana, Slovenia
[4] Facultyof Pharmacy, University of Ljubljana, Ljubljana, Slovenia
[5] Clinical Institute for Genomic Medicine, University Medical Centre Ljubljana, Ljubljana, Slovenia
[6] Faculty of Medicine, University of Maribor, Maribor, Slovenia
[7] Department of Dermatovenerology, University Medical Centre Ljubljana, Ljubljana, Slovenia
[8] Department of Haematology, Division of Internal Medicine, University Medical Centre Ljubljana, Ljubljana, Slovenia

Radiol Oncol 2024; 58(4): 565-572.

Received 24 March 2024
Accepted 1 June 2024

Correspondence to: Prof. Matjaž Sever, M.D., Ph.D., University Medical Center Ljubljana, Zaloška 7, SI-1000 Ljubljana, Slovenia.
E-mail: matjaz.sever@kclj.si

Disclosure: No potential conflicts of interest were disclosed.

Background. *JAK2* V617F (*JAK2*) mutation is associated with clonal hemopoiesis in myeloproliferative neoplasms as well as with faster progression of cardiovascular diseases. Little is known about the relationship between allele burden and the degree of atherosclerotic alteration of coronary vasculature. We previously reported that carotid artery stiffness progressed faster in patients with *JAK2* positive essential thromocythemia (ET) patients. After a four-year follow-up we investigated whether mutation burden of a *JAK2* allele correlates with a higher coronary calcium score.

Patients and methods. Thirty-six patients with *JAK2* positive ET and 38 healthy matched control subjects were examined twice within four years. At each visit clinical baseline characteristics and laboratory testing were performed, *JAK2* mutation burden was determined, and coronary calcium was measured.

Results. *JAK2* allele burden decreased in 19 patients, did not change in 5 patients, and increased in 4 patients. The coronary calcium Agatston score increased slightly in both groups. Overall, there was no correlation between *JAK2* allele burden and calcium burden of coronary arteries. However, in patients with the *JAK2* mutation burden increase, the coronary calcium score increased as well.

Conclusions. The average *JAK2* allele burden decreased in our patients with high-risk ET during the four-year period. However, in the small subgroup whose *JAK2* mutation burden increased the Agatston coronary calcium score increased as well. This finding, which should be interpreted with caution and validated in a larger group, is in line with emerging evidence that *JAK2* mutation accelerates atherosclerosis and can be regarded as a non-classical risk factor for cardiovascular disease.

Key words: essential thrombocythemia; *JAK2* V617F mutation; *JAK2* V617F allele burden; coronary calcium score

Introduction

Essential thrombocythemia (ET) is one of the classic Philadelphia chromosome negative chronic myeloproliferative neoplasms (MPN), along with polycythemia vera and primary myelofibrosis.[1] MPNs are characterized by clonal expansion of abnormal hematopoietic stem cells.[1] In about 50–

60% of patients with ET, *JAK2* V617F mutation is identified, followed by *CALR* and *MPL* mutations[2] The *JAK2* V617F mutation causes constitutive activation of the JAK2-STAT tyrosine kinase signal transducers that mediate intracellular signals from different cytokine receptors and affect gene transcription, cell cycle regulation, cell differentiation and apoptosis.[3] In about 20% patients no mutation is identified which does not preclude ET diagnosis, the so-called triple-negative patients.[4]

JAK2 V617F mutation is associated with clonal hemopoiesis in MPN leading to development of the hematologic disease. However, cell clones with *JAK2* V617F are associated with multiple cardiovascular diseases: atherosclerosis and aortic thrombosis leading to ischemic stroke, coronary artery disease and heart failure, pulmonary hypertension, venous thrombosis, and aortic aneurysm.[5] Furthermore, clonal hematopoiesis of indeterminate potential, defined as the presence of an expanded somatic blood-cell clone in persons without any hematologic abnormalities, is common among older persons and is associated with nearly a doubling in the risk of coronary heart disease in humans and with accelerated atherosclerosis in mice.[6]

We have previously reported that the increase in carotid artery stiffness and pulse wave velocity over the four-year observation period was much more pronounced in high-risk patients with *JAK2* V617F ET than in the control group.[7] In the same cohort, we further determined the burden of the *JAK2* V617F mutation at the beginning and at the end of the four-year observation period and correlated changes in the mutation burden with the coronary artery calcium score. Our hypothesis was that the *JAK2* V617F mutation burden would be correlated with the coronary calcium score.

Patients and methods

Study design

The study design was described previously.[7,8] Briefly, among 61 patients with *JAK2 V617F* positive ET who did not have clinically evident atherosclerotic disease, 40 participated at the first visit and of these 36 at the second visit after four-year time period. The control group consisted of 42 healthy control subjects participated at the first visit and 38 at the second visit. The study was approved by the Committee of Medical Ethics of the Republic of Slovenia (No. 154/05/12 and No. 0120-428/2017/4). The study has been registered at ClinicalTrials.gov PRS: Protocol Section NCT03828422.

Baseline characteristics

At the first visit and at the fourth-year follow-up visit we physically examined the participants, measured their height, weight, waist circumference and blood pressure. The participants completed a structured questionnaire about personal and family medical history, medication and risk factors for cardiovascular disease.

Blood was drawn at the first and at the fourth-year follow-up visit for blood cell count, electrolytes, urea, creatinine, liver function tests and lipid profile. Inflammatory markers, i.e., high sensitivity C-reactive protein, interleukins IL-1, IL-6, IL-8, IL-10, tumor necrosis factor -alpha (TNF-α), P-selectin, vascular adhesion molecule -1 (VCAM-1) and von Willebrand factor (VWF-A2) were measured at the second visit.

JAK2 V617F mutation burden

JAK2 V617F allele burden was determined in DNA extracted from granulocytes in peripheral blood, from samples collected at the Hematology Department, UMC Ljubljana at the time of the first visit, and from samples and the four-year follow-up visit. Real-time quantitative polymerase chain reaction (qPCR) was done with double-dye oligonucleotide hydrolysis, using Ipsogen JAK2 MutaQuant Kit, Qiagen (ZDA).[9] Allele burden was calculated from the standard curves and was defined as the percentage of *JAK2* V617F mutated alleles in total *JAK2*.

At the first visit we analyzed 28 blood samples, as eight patients did not have their blood samples collected for allele burden determination. Blood samples were collected from all patients at the second visit. In total, we had 28 pairs of samples taken four years apart.

Coronary calcium

The Biograph M 128-row PET-CT scanner (Siemens, Erlangen, Germany) was used for coronary artery calcium scanning. Scanning was done in sustained breath hold, from the carina to the base of the heart. We used a non-contrast protocol with sequential, prospective ECG triggering. Rotation time was 0.33 sec, tube voltage 120 kV, CARE Dose 4D and slice thickness 3 mm, with no slice overlap. Post-processing was done on a Syngo Leonardo workstation. The coronary calcium burden was expressed as the Agatston score.[10] Measurements were done tree times for each visit and the average value was used for analysis.

TABLE 1. Baseline characteristics of patients with *JAK2* V617F positive essential thromocythemia (ET) and of control group at the first visit and at the second visit (body mass index, BMI)

	FIRST VISIT			SECOND VISIT			Patient group	Control group
							First vs. second visit	First vs. second visit
	Patient group	Control group	p-value	Patient group	Control group	p-value	p-value	p-value
Age (years)	55.11 (13.40)	59.07 (12.02)	0.186	58.36 (13.44)	62.08 (11.99)	0.214	-	-
Sex (M/F)	12/24	14/24	0.811	12/24	14/24	0.754	-	-
BMI (kg/m2)	25.22 (3.65)	27.27 (4.64)	0.038	26.13 (4.66)	27.54 (4.60)	0.195	0.021	0.184
Waist (cm)								
Male	94.6 (11.1)	102.2 (10.4)	0.086	98.4 (11.2)	104.0 (12.7)	0.260	0.014	0.201
Female	89.5 (9.1)	89.3 (14.2)	0.965	93.1 (11.1)	93.6 (15.0)	0.899	0.086	0.005
Systolic blood pressure (mmHg)	140 (22)	134 (14)	0.219	144 (19)	141 (20)	0.615	0.134	0.018
Diastolic blood pressure (mmHg)	81 (9)	82 (11)	0.870	86 (12)	89 (10)	0.247	0.044	< 0.001
Smoking			0.267			0.403	0.892	0.924
Current	5/36	3/38		4/36	3/38			
Former	10/36	6/38		12/36	8/38			

BMI = body mass index; M/F = male/fimale

Statistical analysis

Variables were presented as mean and standard deviation (SD) or as median and interquartile range (IQR) when asymmetrically distributed. Paired versions of statistical tests were used when comparing study group in time. Counts were used for discrete variables, and differences between groups were assessed by Fisher exact test. Spearman correlation coefficient was used to calculate monotonic correlation between different parameters. All *p*-values were two-sided and *p*-values of < 0.05 were considered statistically significant.

Results

Patients and baseline characteristics

We included 36 subjects (12 male and 24 female) with ET and 38 control subjects (14 male and 24 female). The patient baseline characteristics are shown in Table 1.

Laboratory tests at the second visit are shown in Table 2. No correlation of the laboratory parameters with *JAK2* V617F mutation burden was found.

JAK2 V617F allele burden

The average *JAK2* V617F allele burden at the first visit (n = 28) was 28.57% (SD 20.45%) and at the four-year follow-up visit (n = 36) 15.92% (SD 15.42%); p = 0.001. Over the four-year observation period *JAK2* V617F allele burden decreased in 19 patients, did not change in five patients and increased in four patients. Overall, the allele burden decreased significantly.

In the subgroup of patients where the allele burden decreased, the average *JAK2* V617F allele burden at the first visit was 37.93% (SD 15.57%) and at the fourth-year follow-up visit 19.65% (SD 14.86%), p < 0.001. In the subgroup of patients where allele burden increased or stayed the same, the median *JAK2* V617F allele burden at the first visit was 0.00% (0.00 – 15.93) and at the four-year follow-up visit 0.00% (0.0 – 31.55), p = 0.068.

In the control group *JAK2* V617F allele burden was measured only at the four-year follow-up visit (median 0.00% (IQR 0.00–0.00)).

Coronary calcium

Table 3 presents coronary calcium burden of patents and control subjects at the first and at the

TABLE 2. Laboratory parameters of patients with *JAK2* V617F positive essential thromocythemia (ET) and of the control group at the second visit after 4-year follow-up. Means and standard deviations are given for the normally distributed data, medians and interquartile range are given for non-normally distributed data

THE SECOND VISIT	ET PATIENTS (n = 36)	CONTROL GROUP (n = 38)	COMPARISON BETWEEN GROUPS (p-value)
[2]Glucose (mmol/l)	5.00 (4.60–5.40)	5.00 (4.70–5.60)	0.565
[2]Creatinine (µmol/l)	76.10 (63.85–85.85)	71.30 (62.45–83.55)	0.351
[1]Total cholesterol (mmol/l)	5.00 (1.05)	5.33 (0.93)	0.163
[1]HDL-cholesterol (mmol/l)	1.45 (0.59)	1.66 (0.53)	0.118
[1]LDL-cholesterol (mmol/l)	2.66 (0.89)	2.94 (0.82)	0.168
[1]Triglycerides (mmol/l)	1.97 (0.89)	1.61 (0.80)	0.850
[1]Leukocytes (10^9/L)	7.86 (2.83)	6.54 (1.63)	0.016
[1]Red blood cells (10^{12}/L)	4.42 (0.69)	4.84 (0.42)	0.002
[1]Haemoglobinb	133 (15)	145 (12)	0.001
[1]Platelets (10^9/L)	524.56 (218.67)	250.38 (60.05)	< 0.001
[1]Lymphocytes (10^9/L)	1.88 (0.90)	2.02 (0.72)	0.195
[1]Mixed cells (10^9/L)	0.71 (0.29)	0.59 (0.20)	0.067
[1]Neutrophils (10^9/L)	4.81 (1.97)	3.93 (1.31)	0.031
[1]IL-1 (ng/L)	43.26 (4.98)	34.59 (6.48)	< 0.001
[1]IL-8 (ng/L)	28.89 (8.45)	20.64 (9.51)	< 0.001
[1]P-selectin (ug/L)	76.24 (19.54)	43.33 (13.36)	< 0.001
[1]VCAM-1 (mg/L)	1.17 (0.52)	0.72 (0.26)	< 0.001
[2]IL-6 (ng/L)	8.70 (7.70–9.38)	6.80 (6.28–7.40)	< 0.001
[2]IL-10 (ng/L)	5.65 (0.33–9.35)	5.25 (0.00–7.90)	0.417
[1]TNFa (ng/L	43.90 (7.34)	37.60 (9.15)	0.002
[2]VWF-A2 (ng/L)	231.50 (199.25–256.25)	195.00 (167.50–213.00)	< 0.001
[2]hs-CRP (mg/L)	0.87 (0.50–2.16)	0.91 (0.55–4.43)	0.314

Comparisons between groups were tested by Student's t-test[1]or the Mann-Whitney test[2]

HDL = high-density lipoprotein; IL = interkeucin; Idl = low-density lipoprotein; TNF-a = tumor necrosis factor –alpha; VCAM-1 = vascular adhesion molecule -1; VWF-A2 = von Willebrand factor -A2

four-year follow-up visit. The ET and control group did not differ in the Agatston score at both visits (p = 0.252 at the first visit and p = 0.954 at the four-year follow-up visit). The coronary calcium Agatston score increased slightly, but significantly in both groups: in the ET group from 0 (IQR 0–8.6) to 0.6 (IQR 0–40.3), p = 0.009 and in the control group from 0 (0–8.6) to 2.6 (0–30.1), p < 0.001. Overall, there was no correlation between the *JAK2* V617F allele burden and the calcium burden of coronary arteries (at the first visit r_s = 0.182, p = 0.355 and at the fourth-year follow-up visit r_s = 0.161, p = 0.355).

In the subgroup of patients with ET, in which the *JAK2 V617F* mutation burden decreased, the coronary calcium score remained low without a change. However, in the patients in whom the *JAK2 V617F* mutation burden increased, the coronary calcium score also increased (Figure 1).

No differences were found in inflammatory parameters between the subgroup with increased and the one with decreased *JAK2 V617F* mutation burden. All measured inflammatory parameters (IL-1, IL-8, P-selectin, VCAM-1, IL-6, TNFα and VWF-A2) were elevated in both subgroups of patients with ET. On the other hand, IL-10 which is an anti-inflammatory parameter, was in normal range in both subgroups.

Discussion

JAK2 V617F mutation is the predominant mutation in MPNs and also the mutation most strongly

TABLE 3. Coronary calcium burden expressed as Agatston score of patients with *JAK2* V617F positive essential thromocythemia (ET) and control subjects at the first visit and at the fourth-year follow-up visit and the correlation with *JAK2* V617F allele burden for the ET patient group

	FIRST VISIT			SECOND VISIT			Patient group First *vs.* second visit	Control group First *vs.* second visit	Correlation with *JAK2* V617F allele burden, p-value	
	Patient group	Control group	p-value	Patient group	Control group	p-value	p-value	p-value	First visit	Second visit
Agatston score	0 (0–8.6)	0 (0–8.6)	0.525	0.6 (0–40.3)	2.6 (0–30.1)	0.954	0.009	< 0.001	0.191	0.069
Calcium burden LM	0 (0–0)	0 (0–0)	0.359	0 (0–1.2)	0 (0–0)	0.274	0.014	0.953	0.700	0.657
Calcium burden LAD	0 (0–2.7)	0 (0–2.68)	0.581	0 (0–32.5)	0 (0–21.3)	0.861	0.435	< 0.001	0.243	0.069
Calcium burden LCX	0 (0–0)	0 (0–0)	0.630	0 (0–0)	0 (0–0)	0.825	0.208	0.204	0.433	0.074
Calcium burden RCA	0 (0–0)	0 (0–0)	0.245	0 (0–0.8)	0 (0–0)	0.676	0.074	0.012	0.700	0.045

LAD = left anterior descending artery; LCX = left circumflex artery; LM = the left main coronary artery; RCA = right coronary artery

associated with cardiovascular disease risk.[11] It causes constitutive activation of JAK/STAT signaling which promotes expression of inflammatory cytokines, reactive oxygen species, production of oxidative low-density lipoproteins and formation of foam cells. This creates a chronic inflammatory state as a driving force for atherosclerosis.[12,13]

It is known that patients with *JAK2* V617F positive MPNs have accelerated atherosclerosis, higher incidence of acute coronary syndrome and other cardiovascular events.[14] Experimental studies on animal models elucidated the pathophysiologic mechanisms that underlie increased cardiovascular disease risk in MPNs. Wang *et al*., experimenting on mice, showed that *JAK2* V617F mutation promotes neutrophil infiltration and leukocytes attachment to the vascular wall, impairs macrophage function, accelerates atherosclerotic lesion formation with larger plaques which have unstable necrotic cores.[15,16] In rabbits, Yang *et al*. found that JAK2 inhibitor blocks upregulation of inflammatory mediators, decreases plasma triglycerides, total cholesterol, and LDL, enhances HDL-C and reduces formation of atheromatous plaque.

Association between *JAK2* V617F mutation and atherosclerosis is being more thoroughly investigated in the last decade, however, little is known about correlation between allele burden and CVS risk. Our study examined the *JAK2* V617F allele burden in correlation with coronary artery calcium burden and inflammatory mediators in patients with high-risk ET. We found no overall correlation between the *JAK2* V617F mutation burden and the coronary artery calcium score. On the contrary, the recent publication by Nordheim Solli *et al*. showed

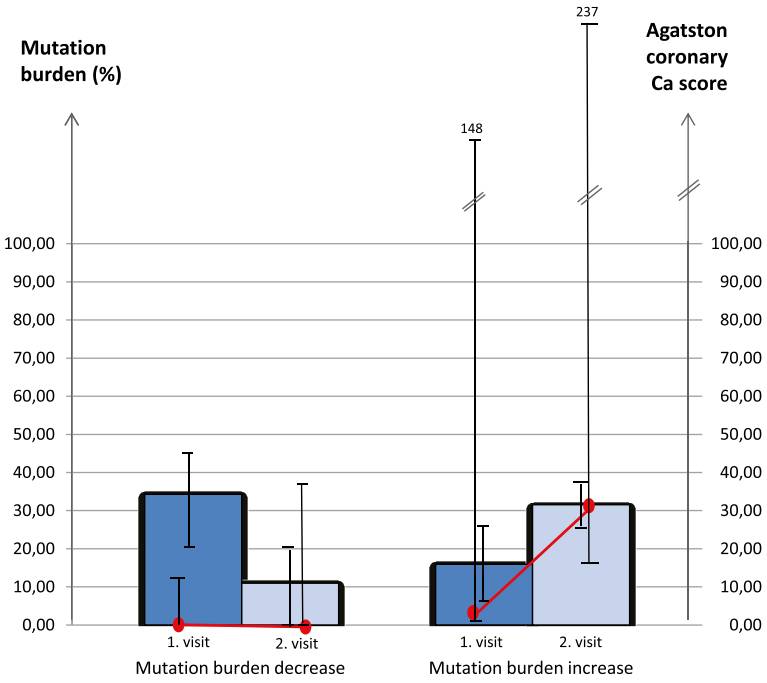

FIGURE 1. Change in *JAK2* V617F mutation burden and Agatston coronary calcium score over the 4-year observation period in patients whose *JAK2* V617F mutation burden increased (left-side columns) and in patients whose mutation burden decreased (right-side columns). Bar charts represent the mean mutation burden (%), and line graphs represent the median Agatston coronary calcium score.

that there is a significant association between the variant allele fraction in the upper quartile (≥ 52%) and severe coronary calcifications in patients with MPNs. The study had limited statistical power to focus on MPN subgroups, though, and it did not specifically address patients with ET.[17] However,

in our study with high-risk ET patients coronary calcium burden increased during the four-year follow-up in the small subgroup of patients whose mutation burden increased as well. This, though not statistically significant, was to our knowledge observed for the first time in the developing field of research in MPN, atherosclerosis and coronary calcium burden. Conversely, in the subgroup of our patients where mutation burden decreased during the observation time, there was no progression in coronary artery calcium burden.

In the subgroup of patients where mutation burden increased, the average *JAK2* allele burden at the first visit was lower in comparison to the subgroup where allele burden decreased However, they reached comparable levels at the second visit (Figure 1). Six out of 19 patients (32%) whose allele burden decreased and three out of nine patients (33%) whose allele burden increased or stayed the same had undergone a change in hematologic therapy. Changes in therapy were all different and overall did not seem to have any influence on allele burden. An uneven change in kinetics of the *JAK2* V617F allele burden over time was observed also by Antonioli *et al*.[19]

The mutation burden was independent of patients' age which was previously observed by Kittur *et.al*.[20] Also, consistent with previous data[19-21], we found no correlation of *JAK2* V617F mutation burden with levels of erythrocytes, leukocytes or platelets. Previous research found an association of *JAK2* V617F allele burden with increased CRP levels in patients with ET.[22] In contrast, we did not find any correlation between allele burden, CRP and other inflammatory mediators. Yet, there was a negative correlation between *JAK2* V617F allele burden and IL-10 ($r = -0.333$, $p = 0.047$), which is an anti-inflammatory factor.

Among chronic myeloproliferative disorders, ET is characterized by the greatest heterogeneity in clinical profile, as well as in cellular and molecular levels.[19] Autonomous activation of the JAK-STAT pathway in ET patients is progressively increased with the amount of mutant allele.[19] Splenomegaly was significantly more frequent when the mutation burden was over 50%, and symptoms due to microvascular disease were present when the mutant allele level was over 25%. Also, a 3-fold greater risk of arterial thrombosis was found in those patients.[19] In our study group, the overall *JAK2* V617F mutation burden was relatively low. Therefore, a lack of correlation between overall allele burden and coronary artery calcium burden or inflammatory mediators might be accounted for by confounding factors overshadowing the relatively low burden of mutant alleles.

JAK2 V617F associated abnormalities are more common in patients with polycythemia vera or primary myelofibrosis where allele burden is much higher than in ET.[23,24] Correlations between *JAK2* V617F allele burden and clinical features in ET are not as definite. Available data about the clinical and prognostic importance of the *JAK2* V617F mutation in patients with ET are still incomplete and sometimes even controversial.[21,25]

In some reports, higher mutated *JAK2* allele burden was associated with increased blood counts and hemoglobin[26,27] but this was not confirmed by others.[28-30] Thrombotic risk was elevated in patients with ET.[26,31] Also, higher mutant allele burden together with histology classification was associated with disease progression to primary myelofibrosis.[32]

All ET patients in our study were identified as high risk for thrombotic complications and were treated accordingly. Acetylsalicylic acid (ASA) was started in all except if they had an indication for anticoagulation therapy. Low-dose ASA significantly reduces thrombotic complications in ET patients[33] and may have some anti-inflammatory effect in the setting of atherosclerosis.[34] Anagrelide was the most common choice of drug for platelet reduction, followed by hydroxyurea. Anagrelide successfully achieves hematologic response in ET[35,36], however, it does not have any impact on *JAK2* allele burden.[37] Hydroxyurea is a preferable choice to anagrelide in older patient population with similar effectiveness as anagrelide but with less cardiovascular side effects[33,36], also not affecting the *JAK2* allele burden.[38,39] Interferon is a second line treatment choice, that can prolong the time to disease progression, may prolong survival in MPNs and ET and often significantly reduces the *JAK2* allele burden.[40-42] However, we used interferon for a short period in only two patients, in whom it did not lead to a significant change in *JAK2* burden. Ruxolitinib, a *JAK1/2* inhibitor, though not a standard of care in ET, was used in two patients. Ruxolitinib was shown to affect *JAK2* burden in patients with ET and could lead to molecular remissions.[43,44] However, again as in patients on interferon, we could not draw any conclusions due to the low patient numbers. Thus, the treatment landscape of patients in our study was very heterogenous and primarily focused on hematologic responses with most probably no impact on *JAK2* allele burden.

Study limitations

The main limitation of our study is the small number of participants. As we decided to determine *JAK2* V617F allele burden after our initial study, blood samples from eight participants were not collected at the first visit and we were unable to determine their initial *JAK2* V617F allele burden.

A minor limitation is that all participants were not examined at the exact time interval between both visits, however, the time difference varied at most for a few weeks.

In conclusion, our study, contrary to expectation, showed a decrease of the average *JAK2* V617F allele burden in patients with high-risk ET during four-year observation period. However, in the small subgroup of four patients whose *JAK2* V617F mutation burden increased the Agatston coronary calcium score increased as well but the significance of this finding cannot be calculated due to the small sample. This preliminary finding, which should be interpreted with caution and validated in a larger study, is in line with the emerging evidence that the *JAK2* V617F mutation is a non-classical risk factor for cardiovascular disease.

Acknowledgement

This study was funded by the Research Program P3-0308 of the Slovenian Research Agency, and the Tertiary Research Project TP 20180038 of the University Medical Centre Ljubljana.

References

1. Tefferi A, Pardanani A. Myeloproliferative neoplasms: a contemporary review. *JAMA Oncol* 2015; **1:** 97-105. doi: 10.1001/jamaoncol.2015.89
2. Chuzi S, Stein BL. Essential thrombocythemia: a review of the clinical features, diagnostic challenges, and treatment modalities in the era of molecular discovery. Leuk Lymphoma 2017; **58:** 2786-2798. doi: 10.1080/10428194.2017.1312371
3. Bousoik E, Montazeri Aliabadi H. "Do we know Jack" about JAK? A closer look at JAK/STAT signaling pathway. *Front Oncol* 2018; **8:** 287. doi: 10.3389/fonc.2018.00287
4. Babakhanlou R, Masarova L, Verstovsek S. A review of essential thrombocythemia and its complications. *Clin Adv Hematol Oncol* 2023; **21:** 76-84. PMID: 36780473
5. Misaka T, Kimishima Y, Yokokawa T, Ikeda K, Takeishi Y. Clonal hematopoiesis and cardiovascular diseases: role of JAK2V617F. *J Cardiol* 2023; **81:** 3-9. doi: 10.1016/j.jjcc.2022.02.001
6. Jaiswal S, Natarajan P, Silver AJ, Gibson CJ, Bick AG, Shvartz E, et al. Clonal hematopoiesis and risk of atherosclerotic cardiovascular disease. *N Engl J Med* 2017; **377:** 111-21. doi: 10.1056/NEJMoa1701719
7. Anžič Drofenik A, Vrtovec M, Božič Mijovski M, Sever M, Preložnik Zupan I, Kejžar N, et al. Progression of coronary calcium burden and carotid stiffness in patients with essential thrombocythemia associated with JAK2 V617F mutation. *Atherosclerosis* 2020; **296:** 25-31. doi: 10.1016/j.atherosclerosis.2020.01.001
8. Vrtovec M, Anzic A, Preložnik Zupan I, Zaletel K, Blinc A. Carotid artery stiffness, digital endothelial function, and coronary calcium in patients with essential thrombocytosis, free of overt atherosclerotic disease. *Radiol Oncol* 2017; **51:** 203-10. doi: 10.1515/raon-2017-0006
9. *Ipsogen JAK2 MutaQuant Kit Handbook.* Version 1(Catalog no. 673523). Hilden, Germany: QIAGEN GmbH. 2013. p. 1-48.
10. Agatston AS, Janowitz WR, Hildner FJ, Zusmer NR, Viamonte M Jr, Detrano R. Quantification of coronary artery calcium using ultrafast computed tomography. *J Am Coll Cardiol* 1990; **15:** 827-32. doi: 10.1016/0735-1097(90)90282-t
11. Leiva O, Gabriela Hobbs G, Ravid K, Libby P. Cardiovascular disease in myeloproliferative neoplasms. JACC CardioOncology state-of-the-art review. *JACC CardioOncol* 2022; **4:** 166-82. doi: 10.1016/j.jaccao.2022.04.002
12. Lussana F, Rambaldi A. Inflammation and myeloproliferative neoplasms. *J Autoimmun* 2017; **85:** 58-63. doi: 10.1016/j.jaut.2017.06.010
13. Genovese E, Mirabile M, Rontauroli S, Sartini S, Fantini S, Tavernari L, et al. The response to oxidative damage correlates with driver mutations and clinical outcome in patients with myelofibrosis. *Antioxidants* 2022; **11:** 113. doi: 10.3390/antiox11010113
14. Malak S, Labopin M, Saint-Martin C, Bellanne-Chantelot C, Najman A. Long term follow up of 93 families with myeloproliferative neoplasms: life expectancy and implications of JAK2V617F in the occurrence of complications. *Blood Cells Mol Dis* 2012; **49:** 170-6. doi: 10.1016/j.bcmd.2012.06.004
15. Wang W, Liu W, Fidler T, Wang Y, Tang Y, Woods B, et al. Macrophage inflammation, erythrophagocytosis, and accelerated atherosclerosis in Jak2 (V617F) mice. *Circ Res* 2018; **123:** e35-47. doi: 10.1161/CIRCRESAHA.118.313283
16. Edelmann B, Gupta N, Schnoeder TM, Oelschlegel AM, Shahzad K, Goldschmidt J, et al. JAK2-V617F promotes venous thrombosis through β1/β2 integrin activation. *J Clin Invest* 2018; **128:** 4359-71. doi: 10.1172/JCI90312
17. Yang X, Jia J, Yu Z, Duanmu Z, He H, Chen S, et al. Inhibition of JAK2/STAT3/SOCS3 signaling attenuates atherosclerosis in rabbit. *BMC Cardiovasc Disord* 2020; **20:** 133. doi: 10.1186/s12872-020-01391-7
18. Solli CN, Chamat-Hedemand S, Elming H, Ngo A, Kjaer L, Skov V, et al. High JAK2V617F variant allele frequency is associated with coronary artery but not aortic valve calcifications in patients with Philadelphia-negative myeloproliferative neoplasms. *Eur J Haematol* 2023; **111:** 400-6. doi: 10.1111/ejh.14019
19. Antonioli E, Guglielmelli P, Poli G, Bogani C, Pancrazzi A, Longo G, et al. Influence of JAK2V617F allele burden on phenotype in essential thrombocythemia. *Haematologica* 2008; **93:** 41-8. doi: 10.3324/haematol.11653
20. Kittur J, Knudson RA, Lasho TL, Finke CM, Gangat N, Wolanskyj AP, et al. Clinical correlates of JAK2V617F allele burden in essential thrombocythemia. *Cancer* 2007; **109:** 2279-84. doi: 10.1002/cncr.22663
21. Antonioli E, Guglielmelli P, Pancrazzi A, Bogani C, Verrucci M, Ponziani V, et al. Clinical implications of the JAK2 V617F mutation in essential thrombocythemia. *Leukemia* 2005; **19:** 1847-9. doi: 10.1038/sj.leu.2403902
22. Barbui T, Carobbio A, Finazzi G, Vannucchi AM, Barosi G, Antonioli E, et al. Inflammation and thrombosis in essential thrombocythemia and polycythemia vera: different role of C-reactive protein and pentraxin 3. *Haematologica* 2011; **96:** 315-8. doi: 10.3324/haematol.2010.031070
23. Campbell PJ, Griesshammer M, Dohner K, Dohner H, Kusec R, Hasselbalch HC, et al. V617F mutation in JAK2 is associated with poorer survival in idiopathic myelofibrosis. *Blood* 2006; **107:** 2098-100. doi: 10.1182/blood-2005-08-3395
24. Vannucchi AM, Antonioli E, Guglielmelli P, Longo G, Pancrazzi A, Ponziani V, et al. Prospective identification of high-risk polycythemia vera patients based on JAK2(V617F) allele burden. *Leukemia* 2007; **21:** 1952-9. doi: 10.1038/sj.leu.2404854

25. Wolanskyj AP, Lasho TL, Schwager SM, McClure RF, Wadleigh M, Lee SJ, et al. JAK2 mutation in essential thrombocythaemia: clinical associations and long-term prognostic relevance. *Br J Haematol* 2005; **131:** 208-13. doi: 10.1111/j.1365-2141.2005.05764.x

26. Zhao S, Zhang X, Xu Y, Feng Y, Sheng W, Cen J, et al. Impact of JAK2V617F mutation burden on disease phenotype in chinese patients with JAK2V617F-positive polycythemia vera (PV) and essential thrombocythemia (ET). *Int J Med Sci* 2016; **13:** 85-91. doi: 10.7150/ijms.10539

27. Lee AJ, Kim SG, Nam JY, Yun J, Ryoo HM, Bae SH. Clinical features and outcomes of JAK2 V617F-positive polycythemia vera and essential thrombocythemia according to the JAK2 V617F allele burden. *Blood Res* 2021; **56:** 259-65. doi: 10.5045/br.2021.2021089

28. Yow KS, Liu X, Chai CN, Tung ML, Yan B, Christopher D, et al. Relationship of JAK2 (V617F) allelic burden with clinico- haematological manifestations of Philadelphia-negative myeloproliferative neoplasms. *Asian Pac J Cancer Prev* 2020; **21:** 2805-10. doi: 10.31557/APJCP.2020.21.9.2805

29. Popova-Labachevska M, Panovska-Stavridis I, Eftimov A, Kapedanovska NA, Cevreska L, Ivanovski M, et al. Evaluation of the JAK2V617F mutational burden in patients with Philadelphia chromosome negative myeloproliferative neoplasms: a single-center experience. *Balkan J Med Genet* 2019; **22:** 31-6. doi: 10.2478/bjmg-2019-0021

30. Ha JS, Kim YK, Jung SI, Jung HR, Chung IS. Correlations between Janus kinase 2 V617F allele burdens and clinicohematologic parameters in myeloproliferative neoplasms. *Ann Lab Med* 2012; **32:** 385-91. doi: 10.3343/alm.2012.32.6.385

31. Trifa AP, Bănescu C, Voina CM, Popa Ş, Török-Vistai T, Bojan AS, et al. Modest contribution of JAK2 V617F allele burden to the occurrence of major thrombosis in polycthemia vera and essential thrombocythemia. *Blood Cells Mol Dis* 2018; **73:** 45-6. doi: 10.1016/j.bcmd.2018.09.003

32. Latagliata R, Polverelli N, Tieghi A, Palumbo GA, Breccia M, Sabattini E, et al. Comparison of JAK2 V617 -positive essential thrombocythaemia and early primary myelofibrosis: the impact of mutation burden and histology. *Hematol Oncol* 2018; **36:** 269-75. doi: 10.1002/hon.2430

33. Tefferi A, Vannucchi AM, Barbui T. Essential thrombocythemia treatment algorithm 2018. *Blood Cancer J* 2018; **8:** 2. doi: 10.1038/s41408-017-0041-8

34. Morris T, Stables M, Hobbs A, de Souza P, Colville-Nash P, Warner T, et al. Effects of low-dose aspirin on acute inflammatory responses in humans. *J Immunol* 2009; **183:** 2089-96. doi: 10.4049/jimmunol.0900477

35. Gisslinger H, Gotic M, Holowiecki J, Penka M, Thiele J, Kvasnicka HM, et al. Anagrelide compared with hydroxyurea in WHO-classified essential thrombocythemia: the ANAHYDRET Study, a randomized controlled trial. *Blood* 2013; **121:** 1720-8. doi: 10.1182/blood-2012-07-443770

36. Birgegård G, Besses C, Griesshammer M, Gugliotta L, Harrison CN, Hamdani et al. Treatment of essential thrombocythemia in Europe: a prospective long-term observational study of 3649 high-risk patients in the Evaluation of Anagrelide Efficacy and Long-term Safety study. *Haematologica* 2018; **103:** 51-60. doi: 10.3324/haematol.2017.174672

37. Cascavilla N, De Stefano V, Pane F, Pancrazzi A, Iurlo A, Gobbi M, et al. Impact of JAK2(V617F) mutation status on treatment response to anagrelide in essential thrombocythemia: an observational, hypothesis-generating study. *Drug Des Devel Ther* 2015; **9:** 2687-94. doi: 10.2147/DDDT.S79576

38. Antonioli E, Carobbio A, Pieri L, Pancrazzi A, Guglielmelli P, Delaini F, et al. Hydroxyurea does not appreciably reduce JAK2 V617F allele burden in patients with polycythemia vera or essential thrombocythemia. *Haematologica* 2010; **95:**1435-8. doi: 10.3324/haematol.2009.021444

39. Zalcberg IR, Ayres-Silva J, de Azevedo AM, Solza C, Daumas A, Bonamino M. Hydroxyurea dose impacts hematologic parameters in polycythemia vera and essential thrombocythemia but does not appreciably affect JAK2-V617F allele burden. *Haematologica* 2011; **96:** e18-20. doi: 10.3324/haematol.2010.037846

40. Quintás-Cardama A, Kantarjian H, Manshouri T, Luthra R, Estrov Z, Pierce S, et al. Pegylated interferon alfa-2a yields high rates of hematologic and molecular response in patients with advanced essential thrombocythemia and polycythemia vera. *J Clin Oncol* 2009; **27:** 5418-24. doi: 10.1200/JCO.2009.23.6075

41. Quintás-Cardama A, Abdel-Wahab O, Manshouri T, Kilpivaara O, Cortes J, Roupie AL, et al. Molecular analysis of patients with polycythemia vera or essential thrombocythemia receiving pegylated interferon α-2a. *Blood* 2013; **122:** 893-901. doi: 10.1182/blood-2012-07-442012

42. Verger E, Cassinat B, Chauveau A, Dosquet C, Giraudier S, Schlageter MH, et al. Clinical and molecular response to interferon-α therapy in essential thrombocythemia patients with CALR mutations. *Blood* 2015; **126:** 2585-91. doi: 10.1182/blood-2015-07-659060

43. Deininger M, Radich J, Burn TC, Huber R, Paranagama D, Verstovsek S. The effect of long-term ruxolitinib treatment on JAK2p.V617F allele burden in patients with myelofibrosis. *Blood* 2015; **126:** 1551-4. doi: 10.1182/blood-2015-03-635235

44. Verstovsek S, Passamonti F, Rambaldi A, Barosi G, Rumi E, Gattoni E, et al. Ruxolitinib for essential thrombocythemia refractory to or intolerant of hydroxyurea: long-term phase 2 study results. *Blood* 2017; **130:** 1768-71. doi: 10.1182/blood-2017-02-765032

research article

Late intervention for type II endoleak is not determined by early sac diameter or volume changes after EVAR

Bernard Sneyers[1], Viktor Verbraeken[1], Annouschka Laenen[2], Walter Coudyzer[1], Hozan Mufty[3], Sabrina Houthoofd[3], Inge Fourneau[3], Geert Maleux[1]

[1] Department of Radiology, University Hospitals KU Leuven, Leuven, Belgium and Department of Imaging & Pathology, KU Leuven, Leuven, Belgium

[2] Department of Public Health and Primary Care, Leuven Biostatistics and Statistical Bioinformatics Centre, Leuven, Belgium

[3] Department of Vascular Surgery, University Hospitals KU Leuven, Leuven, Belgium

Radiol Oncol 2024; 58(4): 573-579.

Received 26 April 2024
Accepted 29 August 2024

Correspondence to: Prof. Geert Maleux, M.D., University Hospitals KU Leuven, Herestraat 49, 3000 Leuven, Belgium. E-mail: geert.maleux@uzleuven.be

Disclosure: No potential conflicts of interest were disclosed.

Background. To compare the diagnostic accuracy and predictive value of aneurysm sac volume measurement versus maximum diameter measurement of abdominal aortic aneurysm sac after endovascular aneurysm repair (EVAR) in patients with type II endoleak.

Patients and methods. Retrospective study on a cohort of 103 patients who presented with a type II endoleak after EVAR for infrarenal abdominal aortic aneurysm. Maximum diameter and volumetric measurements were calculated on computed tomography follow-up scans at 3 months and 1 year after index surgery. Pearson correlation coefficient was used to determine linear association between diameter and volume; Mann-Whitney U test was used to compare patients with and without later intervention for type II endoleak with regard to diameter and volume change.

Results. The correlation between diameter and volume measurement was high (Rho: 0.890–0.980 with $P < 0.0001$). In 38 out of 103 patients (37%) with type II endoleak, a later intervention for endoleak management was performed; early diameter ($P = 0.097$), or volume ($P = 0.387$) change could not predict risk for later intervention.

Conclusions. Both diameter and volume measurements can be used in the imaging follow-up of patients with endoleak type II after EVAR; however early changes in diameter or volume of the aneurysm sac cannot predict late intervention for type II endoleak.

Key words: endovascular aneurysm repair; type II endoleak; diameter; volume; changes in measurement

Introduction

Endovascular aneurysm repair (EVAR) for infrarenal abdominal aortic aneurysms (AAA's) has become the preferred treatment option related to the reduced risk of peri- and postoperative morbidity and mortality compared to open surgical repair.[1] However, persistent growth of the aneurysm sac after EVAR, associated with endoleak, is a risk factor for rupture and further management, including characterisation of the underlying endoleak and subsequent treatment, are mandatory.[2] Malignant endoleaks, including type I and type III endoleaks, should be promptly treated, once detected; type II endoleaks most probably need additional treatment if associated with persistent sac growth; if not, these endoleaks are considered as benign endoleaks and only need further imaging follow-up.[3] In case treatment is mandatory, mean time interval between initial EVAR and type II endoleak

treatment is > 3 years.[4] Predictive imaging factors for future need to treat a type II endoleak include endoleak volume, endoleak diameter, number of patent aortic side branch vessels before EVAR and a complex type endoleak pattern.[5,6] Furthermore, repeated tri-phasic contrast-enhanced computed tomography angiography (CTA) including a high cumulative, radiation dose and intravenous iodized contrast medium administration is needed in case a type II endoleak is detected.

Early detection of volumetric changes in the excluded aneurysm sac in patients with a type II endoleak could be a potential alternative for a better, earlier and more accurate selection of patients with malignant type II endoleak.

However, it is still unclear whether volume measurement or maximum diameter measurement of the excluded aneurysm sac is the most accurate for monitoring sac growth[7-9]; in addition, most of imaging studies comparing volume to maximum diameter measurement are dealing with patients with and without endoleaks. In this study, we analyzed the concordance between changes in maximum diameter compared to changes in volume measurement of the excluded aneurysm sac in patients presenting with type II endoleak after EVAR. Finally, we evaluated if early diameter and/or volume changes might be predictive for type II endoleaks associated with later persistent and substantial growth, ultimately requiring treatment.

Patients and methods

Study design and inclusion criteria

Patients who underwent an elective EVAR procedure to treat an AAA in the authors' institution between January 2002 and August 2019 and presenting with a type II endoleak on follow-up CT-imaging at 3 months and 1 year after the index EVAR-procedure, were included in this retrospective study. Patients with concomitant type I and/or type III endoleak were excluded. Patients gave informed consent for the EVAR-procedure and the follow-up CT-imaging and this retrospective study, with number MP11800, was approved by the local Ethics Committee (No. MP11800) from the University Hospitals Leuven, Belgium. Demographics and clinical follow-up data were collected from the patients' electronic medical records and CT-imaging analysis was performed on a dedicated imaging workstation, connected to the institutional Picture and Archiving Communication System (PACS, Agfa Gevaert, Mortsel, Belgium).

Computed tomography angiography scan protocol

All CTA-studies were performed on 16-, 64- or 256-row multidetector computed tomography (MDCT) scanners depending on the time period of performing the study. Briefly, patients underwent triphasic MDCT protocol, consisting of unenhanced, arterial and venous phase acquisitions at 3 months and 1 year after the index EVAR-procedure. The contrast-enhanced phases were performed after intravenous injection of a bolus of 100 ml nonionic, iomeprol iodinated contrast medium (Iomeron 350, Bracco, Milano, Italy) at a flow rate of 3 ml/second followed by 25 ml of saline flush at a flow rate of 3 ml/second into an antecubital vein. The start of the arterial phase scan was defined by bolus tracking technique with an attenuation threshold of 130 Hounsfield Units (HU) at the level of the supracoeliac portion of the abdominal aorta. Data acquisition started 6 seconds for the arterial and 80 seconds for the venous phase respectively after reaching the 130 HU threshold. Other scan parameters included: detector collimation of 128 x 0.6 mm, tube kilovoltage of 120 kV, reference mAs of 180 mAs with active CareDose, gantry rotation time of 0.5 seconds and a pitch 0.9, 0.5 for reconstructions 1mm and 3 mm respectively.

Image reconstructions and measurements were performed on a dedicated workstation with postprocessing software (Syngo.via, Siemens Healthcare, Forchheim, Germany). Axial (Ax) diameter is defined as the maximum distance between both outer borders of the aneurysm sac as measured on an axial image; perpendicular (Per) diameter is defined as the maximum distance between the outer border of the aneurysm sac as measured on a reconstructed image, perpendicular on the central lumen line of the abdominal aorta. Aortic sac volume measurements were calculated by semi-automated segmentation from the lowest renal artery to the aortic bifurcation. All measurements were performed in consensus by 2 radiologists with 5 and 25 years of experience in vascular radiology respectively.

Patients' follow-up protocol

Patients were followed-up by physical examination and triphasic CTA at 3 months, 1 year after index EVAR and yearly by CTA afterwards, in line with the EUROSTAR follow-up protocol.[10] Indication for type II endoleak treatment was made in consensus after multidisciplinary discussion, by vascular sur-

geons and interventional radiologists, involved in the institutional EVAR-program. Treatment was advised if the type II endoleak persist and the maximum diameter of the aneurysm sac increased with > 1 cm compared to the pre-EVAR sac diameter.

Statistical analysis

Statistical methodology included the Pearson correlation coefficient (ρ), which was used to determine the strength of the linear association between two continuous variables (Ax / Per diameter and volume); a reliability coefficient less than 0.40 was considered as poor, 0.40–0.59 as fair, 0.60–0.74 as good and 0.75–1.00 as excellent. The Mann-Whitney U test was used to compare patients with and without late intervention for type II endoleak with regards to aneurysm sac diameter and volume change at 3 months and 1 year of follow-up after EVAR. Diameter and volume changes were calculated as both absolute and relative changes. The absolute change was calculated as the second value minus the first value, with a positive number indicating increase and a negative number indicating decrease in sac diameter / volume. The relative change was calculated as the percentage increase or decrease with respect to the first value; e.g. a relative change of 10 indicates a 10% increase. All tests are two-sided and assumed a 5% significance level.

The Kappa coefficient (κ) was calculated as a measure of agreement between two binary variables. Both diameter cut-off values were associated with volume cut-off values. A Kappa-value of 0 indicates no agreement, a value 0.01–0.20 as none to slight, 0.21–0.40 as fair, 0.41–0.60 as moderate, 0.61–0.80 as substantial and 0.81–1.00 as almost excellent agreement.

Analyses have been performed using SAS-software, version 9.4 of the SAS System for Windows (Cary, N-Y, US)

Data availability

The data associated with the paper are available from the corresponding author on reasonable request.

Results

Demographic and clinical results

Overall, 505 patients underwent an EVAR-procedure between January 2002 and August 2019; in 103 patients (20.4 %) a type II endoleak was identified on both 3 months and 1-year follow-up CTA. The vast majority of the study population were men (n = 98, 95%) with mean age 74 years who underwent EVAR with use of an Excluder stent-graft (W.L. Gore and Associates, Flagstaff, AZ, USA) (n = 41, 40%) as summarized in Table 1.

In the follow-up period, 38 out of 103 patients (37%) with a persistent type II endoleak underwent treatment, including percutaneous embolization

TABLE 1. Patients' and procedural characteristics

Clinical characteristic	
Age (years)	
Mean age	74 (min 58; max 92)
Sex	
Female	n = 5 (5%)
Male	n = 98 (95%)
Risk factors for atherosclerotic aortic disease according to Doyle *et al.*[11]	
ASA-classification	
ASA 1	n = 4 (3.8%)
ASA 2	n = 18 (17.3%)
ASA 3	n = 75 (72.1%)
ASA 4	n = 6 (5.7%)
Cardiac disease	n = 49 (47.1%)
Carotid disease	n = 16 (15.4%)
Hyperlipidemia	n = 84 (80.7%)
Renal insufficiency	n = 43 (41.3%)
Diabetes mellitus	n = 26 (25%)
Arterial hypertension	
Controlled	n = 83 (79.8%)
Uncontrolled	n = 8 (7.7%)
Pulmonary disease	n = 38 (36.5%)
Smoking	
Active	n = 9 (8.6%)
Previous	n = 74 (71.1%)
Stent-graft for EVAR	
Excluder	n = 41 (40%)
Endurant	n = 20 (19%)
Ovation	n = 23 (22%)
Zenith	n = 13 (13%)
Quantum	n = 4 (4%)
Other	n = 2 (2%)

ASA = American Society of Anesthesiology; EVAR = endovascular aortic repair

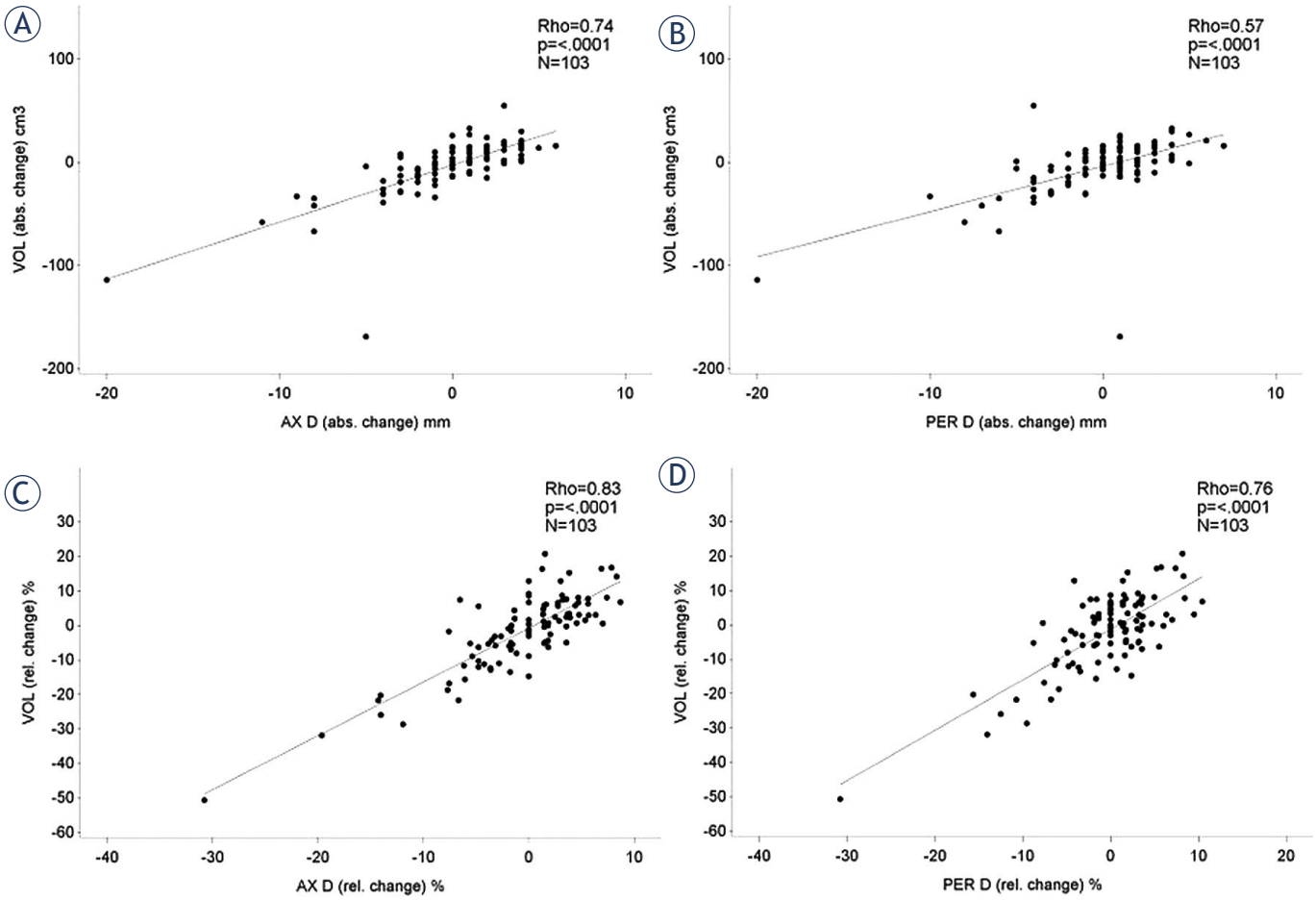

FIGURE 1. Correlation between aneurysm sac maximum axial or perpendicular diameter and volume at 3 months and 1 year with ρ -values of 0.89, 0.90 and 0.91, 0.92 respectively; correlations between absolute differences are 0.74 **(A)**, 0.57 **(B)** and 0.83 **(C)**, 0.76 **(D)** respectively.

TABLE 2. Diameter and volume measurements of the excluded aneurysm sac of 103 patients

Maximum diameter / volume	
Axial diameter (mm) at 3 months	63.7 (min 36.0; max 138.0)
Axial diameter (mm) at 1 year	63.4 (min 37.0; max 133.0)
Perpendicular diameter (mm) at 3 months	63.2 (min 35.0; max 141.0)
Perpendicular diameter (mm) at 1 year	63.0 (min 36.0; max 142.0)
Volume aneurysm sac (cm^3) at 3 months	213.8 (min 67.0; max 1316.0)
Volume aneurysm sac (cm3) at 1 year	209.3 (min 72.0; max 1147.0)
Axial diameter absolute change (mm)	-0.3 (min -20.0; max -7.0)
Axial diameter relative change (%)	-0.51 (min -30.8; max 8.7)
Perpendicular diameter absolute change (mm)	-0.2 (min -20.0; max -7.0)
Perpendicular diameter relative change (%)	-0.2 (min -30.8; max 10.5)
Volume absolute change (cm^3)	-4.5 (min -169.0; max -55.0)
Volume relative change (%)	-1.6 (min -50.7; max 20.8)

(n = 37; 97.3%), conversion to open repair (n = 1; 2.7%). The mean time interval between the index EVAR procedure and the treatment for persistent type II endoleak, associated to aneurysm sac expansion was 1370 days (range: 236–4173 days).

Computed tomography angiography data

Maximum Ax and Per diameter and volume of the excluded aneurysm sac at 3 months and 1 year after EVAR as well as absolute and relative changes in Ax and Per diameter and volume between measurements on CTA at 3 months and 1 year after EVAR are summarized in Table 2.

Correlation between Ax / Per diameter and volume measurements at 3 months and 1 year of follow-up are summarized in Table 3 and Figure 1, showing excellent correlation between aneurysm sac maximum Ax or Per diameter and volume at 3 months and 1 year with ρ values of 0.89, 0.90 and 0.91, 0.92 respectively; correlations between abso-

TABLE 3. Correlation between axial / perpendicular diameter and volume at 3 months and 1 year

At 3 months of follow-up			
Association of sac volume (cm^3) with	**Rho**	**95% CI**	**P-value**
Axial diameter (mm)	0.89	(0.84; 0.92)	< 0.0001
Perpendicular diameter (mm)	0.90	(0.86; 0.93)	< .0001
At 1 year of follow-up			
Association of sac volume (cm^3) with			
Axial diameter (mm)	0.91	(0.87; 0.93)	< 0.0001
Perpendicular diameter (mm)	0.92	(0.89; 0.95)	< 0.0001
Association of volume (absolute changes) (cm^3) with			
Axial diameter (mm)	0.74	(0.64; 0.82)	< 0.0001
Perpendicular diameter (mm)	0.57	(0422; 0.69)	< 0.0001
Association of volume (relative changes) (cm^3) with			
Axial diameter (mm)	0.83	(076; 0.89)	< 0.0001
Perpendicular diameter (mm)	0.76	(0.66; 083)	< 0.0001

lute differences are 0.74, 0.57 and 0.83, 0.76 respectively.

Finally, the potential agreement between diameter increase and volume increase above a threshold of 5 mm and 12% respectively, as proposed by Quan *et al.*,[12] were tested and summarized in Table 4. In patients with an underlying type II endoleak, we did not find evidence of agreement between a diameter increase > 5 mm and a sac volume increase > 12% with a κ-value of 0.032 and 0.121 respectively between volume and Ax diameter and volume and Per diameter.

Correlations between computed tomography angiography data and later intervention for type II endoleak

Ax / Per diameter and volume changes in patient subgroup with and without later intervention for type II endoleak management are summarized in Table 5, showing no evidence of an association between the diameter or volume change and later need for intervention.

Discussion

In this study on 103 patients presenting with a type II endoleak after EVAR as identified by follow-up CTA, an excellent agreement between maximum aneurysm sac axial and perpendicular diameter measurement and sac volume measurement was found, with ρ-values in between 0.84 and 0.95. This observation is in line with several studies[8,9,13], but in contradiction to other studies.[7,14,15] In the presented study, we tested the hypothesis by Quan *et al.* [12], showing a diameter increase cut-off of 5 mm correlates to a volume increase of 12%; however, this observation could not be confirmed by this study. In the presented study, we only included patients with type II endoleaks as this subgroup of patients is at higher risk for late adverse outcomes after EVAR.[2] However we did not perform a comparative study between patients with and without type II endoleak. In addition, a good correlation was found between change in maximum Ax / Per diameter and volume measurement between 3 months and 1 year of follow-up after EVAR with

TABLE 4. Agreement between axial (Ax)/ perperdicular (Per) sac diameter and sac volume

Diameter	statistic volume change < 12%	volume change > 12%
Ax diameter		
< 5 mm change	n/N (%) 93/95 (97.9%)	8/8 (100%)
> 5 mm change	n/N (%) 2/95 (2.1%)	0/8 (0%)
Per diameter		
< 5 mm change	n/N (%) 92/95 (96.8%)	7/8 (87.5%)
> 5 mm change	n/N (%) 3/95 (3.2%)	1/8 (12.5%)

TABLE 5. Diameter and volume changes in patients with (n = 27) and without (n = 76) later intervention for type II endoleak

Diameter / volume changes between 3 months and 1 year of follow-up			
	no intervention	**intervention**	**P-value**
Ax diameter absolute change (mm)	-0.22 (min -9.0; max 6.0)	-0.48 (min -20.0; max 5.0)	0.37
Ax diameter relative change (%)	-0.43 (min -14.3; max 8.7)	-0.74 (min -30.8; max 7.8)	0.37
Per diameter absolute change (mm)	0.05 (min -10.0; max 7.0)	-0.85 (min -20.0; max 5.0)	0.91
Per diameter relative change (%)	0.15 (min -15.6; max 10.4)	-1.3 (min -30.8; max 8.2)	0.79
Volume absolute change (cm^3)	-2.22 (min -67.0; max 55.0)	-10.89 (min -169.0; max 33.0)	0.96
Volume relative change (%)	-1.4 (min -28.6; max 14.2)	-2.2 (min -10.3; max 7.4)	0.92

Ax = axial; Per = perpendicular

ρ-values 0.57 and 0.83. Here a better correlation for Ax diameter versus Per diameter to volume measurement was observed. Adversely, Boos *et al*., including both patients with and without type II endoleaks, found an increase in centreline diameter (= perpendicular diameter) and volume (measured from the lowest renal artery to the iliac bifurcation) as most sensitive criteria for detecting endoleaks.[8] Schnitzbauer *et al*. found a low to moderate sensitivity for the detection of volume increase compared to diameter measurements with cut-off values of > 5 mm and > 5%; however these authors did not analyze absolute or relative changes in diameter versus volume as predictors for type II endoleak.[7]

This study could not demonstrate differences in early changes in aneurysm sac diameter nor volume in patients who needed or did not need endoleak-related re-intervention in a later phase. Therefore, continued follow-up including contrast-enhanced CTA is still mandatory to identify endoleak volume or diameter growth or changes in endoleak pattern as demonstrated by Dudeck *et al*.[5] In addition, combined findings of type II endoleak associated with clear growth of the sac diameter > 1 cm are mostly found later than 1 year after index EVAR procedure.[4]

Limitations of this study are multiple. First, different CT-scanners with different scan protocols were used, related to the long-time interval included patients were scanned after their EVAR procedure. However, scan and injection protocols did not change significantly between 16-, 64- and 256-row MDCT.[16] Second, no intra- nor interobserver variability studies on diameter and volume measurements were performed and all measurements were performed in consensus by two radiologists. However, acceptable intra- and interobserver variability of aortic aneurysm volume measurement with or without semi-automated tools has been demonstrated by van Prehn *et al*..[17] Third, various types of endografts were used; nevertheless, sac measurements on CTA or indications for re-intervention are independent of the type of endograft. Fourth, only two sets of early follow-up CTA were included in the study; potentially, inclusions of measurements on CTA's at two or more years of follow-up after EVAR might better select patients with type II endoleak for re-intervention as indication for type II-related intervention is made after a mean of 3 years postoperatively.[4]

In conclusion, this study demonstrates an excellent correlation of diameter and volume measurements of the aneurysm sac in patients with type II endoleak early after EVAR. However, these early changes in sac diameter or volume on CTA at 3 months and 1 year after initial EVAR cannot predict patients at later risk for type II endoleak-related re-intervention. Continued CTA is still needed to further monitor patients with type II endoleak after EVAR and eventually to select patients at risk for re-intervention.

References

1. Chaikof E, Dalman R, Eskandari M, Jackson BM, Lee WA, Mansour MA, et al. The Society of Vascular Surgery practice guidelines on the care of patients with an abdominal aortic aneurysm. *J Vasc Surg* 2018; **67:** 2-77. doi: 10.1016/j.jvs.2017.10.044

2. Jones J, Atkins M, Brewster D, Chung TK, Kwolek CJ, LaMuraglia GM, et al. Persistent type 2 endoleak after endovascular repair of abdominal aortic aneurysm is associated with adverse late outcomes. *J Vasc Surg* 2007; **46:** 1-8. doi: 10.1016/j.jvs.2007.02.073

3. Rokosh R, Wu W, Dalman R, Chaikof EL. Society of Vascular Surgery implementation of clinical practice guidelines for patients with an abdominal aortic aneurysm: endoleak management. *J Vasc Surg* 2021; **74:** 1792-4. doi: 10.1016/j.jvs.2021.04.042

4. Vandenbulcke R, Houthoofd S, Laenen A, Buyck PJ, Mufty H, Fourneau I, et al. Embolisation therapy for type 2 endoleaks after endovascular aortic aneurysm repair: imaging-based predictive factors and clinical outcome on long-term follow-up. *Diagn Intervent Radiol* 2023; **29:** 331-41. doi: 10.4274/dir.2022.22352

5. Dudeck O, Schnapauff D, Herzog L, Loventhal D, Bulla K, Halloul Z, et al. Can early computed tomography angiography after endovascular aortic aneurysm repair predict the need for reintervention in patients with type II endoleak? *Cardiovasc Intervent Radiol* 2015; **38:** 45-52. doi: 10.1007/s00270-014-0901-6

6. Löwenthal D, Herzog L, Rogits B, Bulla K, Weston S, Meyer F, et al. Identification of predictive CT angiographic factors in the development of high-risk type 2 endoleaks after endovascular aneurysm repair in patients with infrarenal aortic aneurysms. *Forschr Röntgenstr* 2015; **187:** 49-55. doi: 10.1055/s-0034-1385123

7. Schnitzbauer M, Günther O, Wohlgemuth W, Zeman F, Haimerl M, Stroszczynski C, et al. CT after endovascular repair of abdominal aortic aneurysms: diagnostic accuracy of diameter measurements for the detection of aneurysm sac enlargement. *J Vasc Intervent Radiol* 2018; **29:** 178-87. doi: 10.1016/j.jvir.2017.09.012

8. Boos J, Brook O, Fang J, Temin N, Brook A, Raptopoulos. What is the optimal abdominal aortic sac measurement on CT images during follow-up after endovascular repair? *Radiology* 2017; **285:**1032-41. doi: 10.1148/radiol.2017161424

9. Hahne J, Arndt C, Herrmann J, Schonnagel B, Adam G, Habermann CR. Follow-up of abdominal aortic aneurysm after endovascular aortic repair: comparison of volumetric and diametric measurement. *Eur J Radiol* 2012; **81:** 1187-91. doi: doi.org/10.1016/j.ejrad.2011.03.065

10. Laheij R, van Marrewijk C. Endovascular stenting of abdominal aortic aneurysm in patients unfit for elective open surgery. Eurostar group. EUROpean collaborators registry on stent-graft techniques for abdominal aortic aneurysm repair. *Lancet* 2000; **356:** 832. doi: 10.1016/s0140-6736(00)02662-3

11. Doyle D, Hendrix J, Garmon E. American Society of Anesthesiologists Classification. In: *StatPearls* [Internet]. Tresure Island (FL, USA): StatPearls Publishing; 2024. [cited 2024 Mar 15]. Available at: https://www.ncbi.nlm.nih.gov/books/NBK441940/

12. Quan C, Oh Y, Park S, Won YS, Yun SS, Suh YJ, et al. Efficacy of volumetric analysis of aorta as surveillance tool after EVAR. *Asian J Surg* 2019; **42:** 746-54. doi: 10.1016/j.asjsur.2018.12.006

13. Baumueller S, Nguyen T, Goetti R, Lachat M, Seifert B, Pfammatter T, et al. Maximum diameter measurements of aortic aneurysms on axial CT images after endovascular aneurysm repair: sufficient for follow-up? *Cardiovasc Intervent Radiol* 2011; **34:** 1182-9. doi: 10.1007/s00270-010-9992-x

14. Kritpracha B, Beebe H, Comerota A. Aortic diameter is an insensitive measurement of early aneurysm expansion after endografting. *J Endovasc Ther* 2004; **11:** 184-90. doi: 10.1583/03-976.1

15. Van Keulen J, van Prehn J, Prokop M, Moll FL, van Herwaarden JA. Potential value of aneurysm sac volume measurements in addition to diameter measurements after endovascular aneurysm repair. *J Endovasc Ther* 2009; **16:** 506-13. doi: 10.1583/09-2690.1

16. Müller-Wille R, Schötz S, Zeman F, Uller W, Guntner O, Pfister K, et al. CT features of early type II endoleaks after endovascular repair of abdominal aortic aneurysms help predict aneurysm sac enlargement. *Radiology* 2015; **274:** 906-16. doi: 10.1148/radiol.14140284

17. Van Prehn J, van der Wal M, Vincken K, Bartels LW, Moll FL, van Herwaarden JA, et al. Intra- and interobserver variability of aortic aneurysm volume measurement with fast CTA postprocessing software. *J Endovasc Ther* 2008; **15:** 505-10. doi: 10.1583/08-2478.1

research article

Inter-observer variation in gross tumour volume delineation of oesophageal cancer on MR, CT and PET/CT

Ajra Secerov-Ermenc[1,2], Primoz Peterlin[1], Franc Anderluh[1], Jasna But-Hadzic[1,2], Ana Jeromen-Peressutti[1], Vaneja Velenik[1,2], Barbara Segedin[1,2]

[1] Department of Radiation Oncology, Institute of Oncology Ljubljana, Ljubljana, Slovenia
[2] Faculty of Medicine, University of Ljubljana, Ljubljana, Slovenia

Radiol Oncol 2024; 58(4): 580-587.

Received 11 May 2024
Accepted 25 July 2024

Correspondence to: Assist. Ajra Šečerov-Ermenc, M.D., M.Sc., Department of Radiation Oncology, Institute of Oncology Ljubljana, Zaloska 2, SI-1000 Ljubljana, Slovenia. E-mail: asecerov@onko-i.si

Disclosure: No potential conflicts of interest were disclosed.

Background. The aim of our study was to assess the inter-observer variability in delineation of the gross tumour volume (GTV) of oesophageal cancer on magnetic resonance (MR) in comparison to computed tomography (CT) and positron emission tomography and CT (PET/CT).

Patients and methods. Twenty-three consecutive patients with oesophageal cancer treated with chemo-radiotherapy were enrolled. All patients had PET/CT and MR imaging in treatment position. Five observers independently delineated the GTV on CT alone, MR alone, CT with co-registered MR, PET/CT alone and MR with co-registered PET/CT. Volumes of GTV were measured per patient and imaging modality. Inter-observer agreement, expressed in generalized conformity index (CIgen), volumetric conformity index (VCI), planar conformity index (PCI) and inter-delineation distance (IDD) were calculated per patient and imaging modality. Linear mixed models were used for statistical analysis.

Results. GTV volume was significantly lower on MR (33.03 cm3) compared to CT (37.1 cm^3; p = 0.002) and on PET/CT MR (35.2 cm^3; p = 0.018) compared to PET/CT (39.1 cm^3). The CIgen was lowest on CT (0.56) and highest on PET/CT MR (0.67). The difference in CIgen between MR (0.61) and CT was borderline significant (p = 0.048). The VCI was significantly higher on MR (0.71; p = 0.007) and on CT MR (0.71; p = 0.004) compared to CT (0.67). The PCI was significantly higher on CT MR (0.67; p = 0.031) compared to CT (0.64). The largest differences were observed in the craniocaudal direction.

Conclusions. The highest inter-observer agreement was found for PET/CT MR and the lowest for CT. MR could reduce the difference in delineation between observers and provide additional information about the local extent of the tumour.

Key words: oesophageal cancer; gross tumour volume; positron emission tomography; magnetic resonance

Introduction

Oesophageal cancer is the 11th most common cancer and the 7th leading cause of cancer death worldwide.[1] It is characterised by high mortality, poor prognosis and a variable geographical distribution.[2] Surgery and radiotherapy play an important role in both limited and locally advanced

disease.[3-7] Accurate tumour delineation is crucial in radiotherapy planning to ensure adequate target coverage and local control of the disease, which can also impact on disease free survival and overall survival.[8] Computed tomography (CT) is the standard imaging modality for radiotherapy treatment planning in oesophageal cancer. However, it can overestimate the length of the tumour.[9] Other imaging modalities could therefore have a role in radiotherapy treatment planning, in particular, positron emission tomography (PET) and magnetic resonance imaging (MR).[8,10,11]

18-F-fluorodeoxyglucose (FDG)-PET/CT is considered an essential diagnostic method for the initial staging of oesophageal cancer, because of its ability to detect metastatic disease, including lymph node metastases (LNM), with 66% sensitivity and 96% specificity.[12,13] FDG-PET/CT seems superior to CT, especially in the detection of LNM, consequently, it is essential when determining nodal clinical target volume (CTV) in the elective or involved-field irradiation.[14-16] On the other hand, PET-based segmentation algorithms or PET manual contouring of the primary tumour did not show a good correlation compared to CT imaging after clipping the cranial and caudal border of the tumour.[17] However, studies comparing the length of the tumour on preoperative FDG-PET/CT scans with histopathological specimens after surgery showed a good correlation.[18-20] Some studies showed improved inter-observer variability in the delineation of gross tumour volume (GTV) on PET/CT, while others did not confirm it. [21-26] GTV delineation on FDG-PET/CT imaging thus remains controversial.

MR is not yet an established method for radiotherapy treatment planning for oesophageal cancer, but it is promising because of its excellent soft tissue contrast. Over the past decade, several technical innovations have reduced image artefacts, such as the use of automatic gating navigators or multi-channel receiver coils.[27] The longitudinal length of GTV measured on diffusion-weighted MR (DWI) correlated more precisely with the length of the histopathological specimen compared to CT or T2-weighted MRI (T2 MRI).[28] MR-based GTV delineation of oesophageal cancer was feasible, with inter-observer variability comparable to FDG-PET/CT.[29] However, further studies are needed.

The aim of our study was to assess the inter-observer variability in delineation of the GTV in oesophageal cancer on MRI in comparison to CT and PET/CT.

Patients and methods

The study was approved by the National Medical Ethics Committee of Slovenia (No. 0120-620/2019/3) on 21 January 2020 and in accordance with the Declaration of Helsinki. The study was registered in the ClinicalTrials.gov database (NCT05611658). Written informed consent was obtained from all patients.

Patients

We prospectively enrolled 23 patients with locally advanced oesophageal cancer from April 2020 to May 2021. Patients had to meet the following inclusion criteria: locally advanced oesophageal cancer, Siewert I or II for distal oesophageal tumours, planned preoperative or definitive chemoradiotherapy, no contraindications for MR. We included

TABLE 1. Characteristics of the patients with oesophageal cancer enrolled in the study

Case	Location – third	Histology	Treatment	Stage	Gender	Age
1	Proximal	SCC	definitive	T3N0M0	M	62
2	Proximal	SCC	definitive	T3N0M0	M	66
3	Distal	AC	preoperative	T3N1M0	M	64
4	Middle	SCC	definitive	T3N1M0	M	68
5	Proximal	SCC	definitive	T3N2M0	F	60
6	Proximal	SCC	definitive	T3N1M0	M	57
7	Distal	AC	preoperative	T3N1M0	M	66
8	Proximal	SCC	definitive	T3N1M0	M	64
9	Distal	AC	definitive	T2N0M0	M	81
10	Distal	AC	preoperative	T3N2M0	M	35
11	Proximal	SCC	definitive	T3N0M0	M	58
12	Distal	SCC	preoperative	T3N1M0	M	61
13	Proximal	SCC	definitive	T3N0M0	M	63
14	Middle	SCC	preoperative	T3N0M0	M	54
15	Distal	AC	preoperative	T3N0M0	M	64
16	Middle	SCC	definitive	T3N1M0	F	83
17	Distal	AC	preoperative	T3N1M0	M	58
18	Proximal	SCC	definitive	T3N0M0	M	42
19	Distal	AC	preoperative	T3N0M0	M	75
20	Proximal	SCC	definitive	T3N0M0	M	70
21	Proximal	SCC	definitive	T3N2M0	F	46
22	Middle	SCC	preoperative	T3N0M0	M	53
23	Middle	SCC	preoperative	T2N2M0	M	67

AC = adenocarcinoma; F = female; M = male; SCC = squamous cell carcinoma

20 men and 3 women with an average age of 61 years.

Patient characteristics are listed in Table 1.

Image acquisition

FDG-PET CT

All patients underwent a planning FDG-PET/CT scan in treatment position on Siemens BiographTM mCT 40 PET-CT simulator after standard preparation protocol. The activity of the intravenously administered 18F-FDG was 3.7 MBq/kg. After about 60 minutes, the CT scan was performed with the following settings: 120 kV, 200 mAs, 1 second rotation time, pitch of 0.8 and 3 mm slice thickness. An iodine intravenous contrast agent was administered before the CT scan. After CT, a PET scan was acquired 3-dimesionally with duration of 2 minutes per bed position.

MR

MR imaging was performed on a 1.5T Optima™ MR450w GE MR simulator (General Electric). Patients were scanned prior to radiotherapy in treatment position without intravenous contrast. We acquired T2-weighted images in the transverse plane with a slice thickness of 3 mm and diffusion-weighted images (DWI) for each patient.

Target volume delineation and observers

Five radiation oncologists with at least 5 years of experience in the treatment of oesophageal cancer delineated the gross tumour volume (GTV). Contouring was performed using the Eclipse™ planning system (Palo Alto, California, USA). Initially, a meeting was organised with the aim of familiarising the observers with MR images of oesophageal cancer. Under the guidance of an experienced radiologist, they delineated the GTV on MR images of two pilot cases. The observers received relevant information about the location and characteristics of the tumour. GTV was contoured separately on different imaging modalities, as follows: CT, PET/CT, MR, CT with MR fusion and PET/CT with MR fusion. All the images in the study were anonymised.

GTV was defined as the visible tumour on imaging as the whole circumference of the oesophagus. Regional pathological lymph nodes were not included in the GTV. Contouring on different imaging modalities was performed after an interval of at least two weeks to minimise recollection of the previous images.

When contouring on the PET CT images, the observers delineated the GTV on the CT and corrected it according to the PET images if necessary. The GTVPET corresponded to 20% of the maximum standardized uptake value (SUV). The PET and CT images were then fused. The visible tumour was contoured as GTV and, if necessary, corrected taking into account the GTVPET. When contouring on the MR images, the observers delineated the GTV on the T2 MR and modified it using the DWI if necessary.

Observers were instructed to record the delineation time, image quality (good, moderate, poor) and difficulty of contouring the GTV in all imaging modalities (five-point scale: very difficult – very easy).

Data analysis

GTV volumes were measured per observer, per patient and per imaging modality and average volumes were calculated per patient and per imaging modality. In order to assess contouring uncertainties, we calculated the generalized conformity index (CIgen), which is independent of the number of volumes analysed.[30] The CIgen was calculated per patient and averaged over all patients per imaging modality.

$$CI\text{gen}=\frac{\sum \text{pairs} ij[Ai \cap Aj]}{\sum \text{pairs} ij[Ai \cup Aj]}$$

In order to quantify the accuracy of the contouring, the deviations of the observers from the reference contours were analysed. The Contour analysis tool 2 (CAT 2) software and the associated methodology were used for the volumetric and distance-based calculations. The reference contour was calculated using the Simultaneous Truth and Performance Level Estimation (STAPLE) algorithm from the collection of the contours from all observers per patient and per imaging modality.[31] Using the STAPLE delineations as a reference, the volumetric conformity index (VCI) - the ratio of the intersection and union of the test and reference volumes - of the pairs between the reference and each test delineation were averaged for each imaging modality. In addition, the planar conformity index (PCI) was calculated as the ratio between the intersection and union surface of the test and reference contours on each image slice and presented as a function of slice number for each patient.[32,33] To assess cranio-caudal variation, we evaluated the mean distance of the caudal and cranial borders of the tumour for all observers between CT and MR,

CT and MR CT, and PET/CT and PET CT MR. We recorded the number of slices and multiplied it by the slice thickness (3 mm).

For the analysis in the transverse plane, we calculated the inter-delineation distance (IDD), which is the shortest distance between the reference and test contours from the centre of mass in 72.5° angular segments, expressed in millimetres. Using the centre of mass as the origin, a coordinate system was defined and divided into 12 angular segments (6 on the right and 6 on the left) that were separated on each transverse slice of all imaging modalities: on the right (0–25°, 30–55°, 60–85°, 90–115°, 120–145° and 150–175°) and on the left (180–205°, 210–235°, 240–265°, 270–295°, 300–325° and 330–355°) (Figure 1).

We calculated the average IDD for all slices of the imaging methods, all observers and all test cases for each target volume. This method has been previously used and described in detail.[32-34]

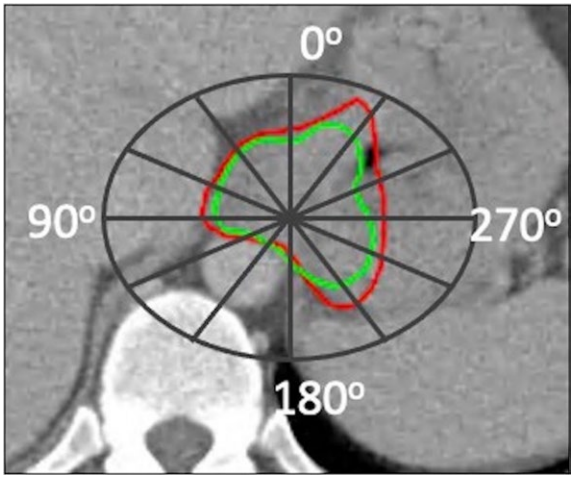

FIGURE 1. The coordinate system for spatial assessment of inter-delineation distances is projected on a single slice of imaging modality containing an example of GTV and divided in 12 angular segments (6 on the left and 6 on the right). Green line represents the reference contour, red line is the test contour.

Statistic analysis

Before starting the analysis, we calculated the sample size. Taking into account the data from previous studies, we calculated that we would need about 21 patients at a significance level of 0.05 and a statistical power of 0.8.[21,29,35]

The numerical variables were presented as means and standard deviations (SD). The correlation between CIgen and imaging modalities was tested with linear mixed models, patients were included as a random factor. When analyzing the association between VCI, PCI, GTV volume and imaging modalities observers were included as a random factor in addition to patients. The analysis was performed with R 4.3.2 using the libraries *lme4*, *lmerTest*, *emmeans* and *forestplot*.

Results

The results are presented in Table 2.

The mean GTV volume is lowest in MR (33.03 cm^3) and highest in PET/CT (44.12 cm^3). The difference in mean GTV volume between MR and CT ($p = 0.002$) and between PET/CT MR and PET/CT is statistically significant ($p = 0.018$).

The mean CIgen is lowest on CT (0.56) and highest for PET/CT MRI (0.67). The difference in mean CIgen between MR and CT is borderline significant ($p = 0.048$).

The VCI is on average the lowest on CT (0.67) and the highest on PET/CT MR (0.77). The differ-

TABLE 2. Mean volume of gross tumor volume (GTV), CIgen, VCI, PCI, IDD and standard deviation

	CT (SD)	MR (SD)	CT MR (SD)	PET/CT (SD)	PET/CT MR (SD)
Volume (cm^3)	37.14 (35.66)	33.03 (30.40)	35.04 (32.58)	44.12 (39.10)	40.94 (35.16)
CIgen	0.56 (0.18)	0.61 (0.14)	0.61 (0.14)	064 (0.13)	0.67 (0.12)
VCI	0.67 (0.18)	0.71 (0.15)	0.71 (0.14)	0.74 (0.14)	0.77 (0.12)
PCI	0.64 (0.17)	0.67 (0.16)	0.67 (0.15)	0.71 (0.14)	0.73 (0.13)
IDD (mm)	1.39 (1.47)	1.44 (1.44)	1.70 (1.50)	1.68 (1.50)	1.60 (1.66)

CIgen = generalized conformity index; CT = computed tomography; ; CT MR = fusion of CT and MR; MR = magnetic resonance imaging; IDD = inter-delineation distance; PET/CT = positron emission tomography and CT; PET/CT MR = fusion of PET/CT and MR; VCI = volumetric conformity index; PCI = planar conformity index; SD = standard deviation

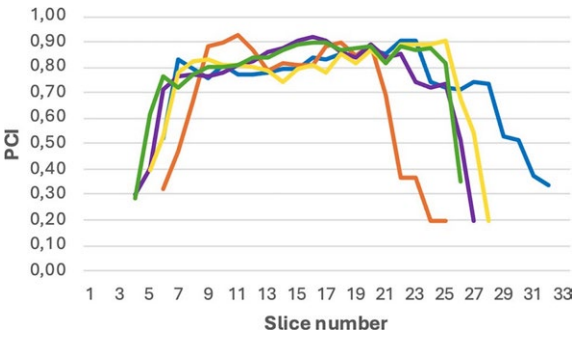

FIGURE 2. Mean planar conformity index (PCI) for the GTV as a function of slice number for all imaging modalities for case 22.

Blue = computed tomography (CT); Green = fusion of PET/CT and MR; Red = magnetic resonance imaging (MR); Violet = positron emission tomography and CT (PET/CT); Yellow = fusion of CT and MR (CT MR); 1= most caudal slice; 33= most cranial slice.

ence in mean VCI between MR and CT (p = 0.007) and between CT and MR is statistically significant (p = 0.008). The PCI is on average the lowest in CT (0.64) and the highest in PET/CT MR (0.70). The difference in mean PCI between CT MR and CT is statistically significant (p = 0.031). We analysed the PCI per imaging modality as a function of the number of slices for each patient. In all imaging modalities, the variations were greatest caudally and cranially, while agreement was high in the middle of the target volumes. An example is shown in Figure 2 and 3.

The mean distance between the caudal border of the GTV on CT and MR, CT and CT MR, and PET/CT and PET/CT MR was 12.00 mm, 10.96 mm, and 4.57 mm, respectively. The mean distance between the cranial border of the GTV on CT and MR, CT and CT MR and PET/CT and PET/CT MR was 12.26 mm, 6.22 mm, 3.56 mm, respectively.

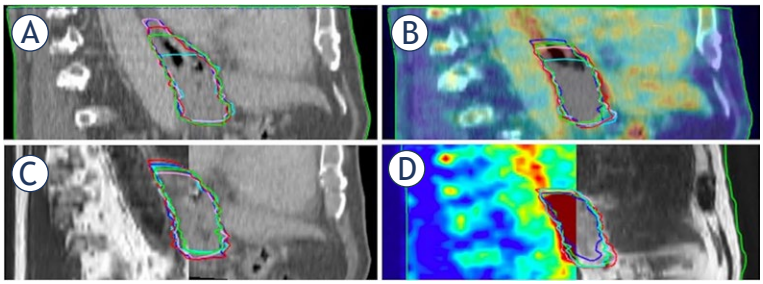

FIGURE 3. Delineation of the gross tumour volume (GTV) of all five observers of case 22, sagittal view. The variation in cranial border is highest on computed tomography (CT) and lowest on positron emission tomography (PET/CT) magnetic resonance (MR).

(A) CT; **(B)** PET/CT; **(C)** fusion of CT and MR; **(D)** fusion of PET/CT and MR.

In the analysis in the transverse plane, we found that the IDD is smallest on CT and largest on CT-MR. Comparing the average values between the imaging modalities for each angular segment, CT has the lowest values at 0–25°, 30–55°, 60–85°, 90–115°, 150–175°, 180–205° and 330–355°, which is predominantly on the right lateral side, while MR has the lowest values in all other angular segments, predominantly on the left side. We recorded larger mean IDDs when delineation was performed using fused imaging modalities. The cases were divided into groups of patients according to the tumour location in the oesophagus (upper, middle and lower third). We found that IDDs were small in tumours in the upper and middle third of the oesophagus, in the range of 2 mm. In tumours in the lower third of the oesophagus, the IDDs were larger, especially in the angular segments on the left lateral side, up to 4 mm (Figure 4).

We also compared the difference in IDD between CT and MR, CT and MR CT, and PET CT and PET CT MR. Statistically significantly higher IDDs were observed mainly when comparing MR CT with CT sequences, at angular segments 180–205° (p = 0.030), 120–145° (p = 0.005), 60–85° (p = 0.009) and 30–55° (p = 0.003).

Image quality was rated good in 66%, 59%, 51%, 43% in 41% in PET/CT MR, PET/CT, CT MR, MR and CT, respectively. The difficulty of contouring was rated as easiest for PET CT MR (22% very easy and 5% very difficult) and most difficult for CT, with the highest rating of being very difficult (23%). In terms of contouring time, MR tends to have the lowest values compared to the other modalities with a median (Me) of 4.6 minutes (interquartile range (IQR) 4.1–5), followed by PET CT (Me 6.4; IQR 4.7–6.8), CT MR (Me 6.6; IQR 5.2–7.6), PET CT MR (Me 7; IQR 5.3–7.9) and CT (Me 7.2; IQR 6–8.4).

Discussion

In our study, five observers contoured the GTV of oesophageal tumours of 23 patients treated with preoperative or definitive chemoradiotherapy on CT, PET/CT, MR, CT MR fusion and PET/CT MRI fusion.

The results showed that the mean GTV volume was smallest on MR and largest on PET/CT. MR significantly reduced the volume compared to CT and when fused with PET/CT compared to PET/CT alone. Similarly, Vollenbrock *et al.* compared GTV contouring of oesophageal cancer on PET/CT, MR

and MR with DWI sequences and reported statistically significantly smaller volumes on MR with DWI compared to PET/CT and MR.[29] Furthermore, the tumour length in the histopathological specimen correlated better with the length of the GTV contoured on DWI than with target volumes on CT or T2-MR, so we can assume that MR images with DWI sequences are closest to the "ground truth" of tumour length.[28] One of the possible reasons for larger GTV volumes on PET/CT is that FDG is not tumour specific and high FDG uptake could also be due to inflammation. Patients with oesophageal cancer often have erosive oesophagitis caused by alcohol consumption or gastro-oesophageal reflux. The inflammation of the oesophagus detected by FDG PET/CT correlates with the endoscopic findings.[36] The inclusion of the FDG-avid area in the GTV may not represent only the tumour. Observers tend to delineate larger volumes on CT as well, mainly because of poor soft tissue contrast, especially in the cranio-caudal direction, as confirmed by histopathological correlation.[9] Poor differentiation of tumour borders could lead to large cranio-caudal variation between observers. Fusion of MR with CT or PET/CT reduced the variation. However, even when the imaging modalities were fused, the cranio-caudal deviation remained large.

On the other hand, the uncertainty in contouring in the transverse plane in oesophageal cancer was low and probably not clinically significant. We analysed the IDD as a function of the angles in the transverse plane in relation to the thirds of the oesophagus due to the different anatomical conditions. In the upper and middle third, we observed small differences of less than 2 mm in all angular segments, while in the lower third the differences were up to 4 mm mainly in the left lateral angular segments. The oesophagus merges into the stomach in the distal part to the left side and it is more difficult to define the tumour borders in this area. Different fused imaging modalities did not reduce this uncertainty. Two other studies confirmed small variations in the transverse plane.[21,29]

Our study has some limitations. Firstly, the observers had no experience in contouring on MR for oesophageal cancer before the start of the study, which could explain the lower CIgen on MR compared to PET/CT. We tried to overcome this problem by organising a meeting with an experienced radiologist and contouring on two pilot cases. However, this probably remained a disadvantage as the observers had several years of experience with delineation on PET/CT. Vollenbrock *et al*. concluded that contouring on MR images is feasible despite lack of experience as they found similar inter-observer variability between MR and PET/CT.[29] Secondly, the observers delineated the same cases multiple times, starting with CT and ending with PET/CT MR, so they could recall the anatomical features of the cases to some extent, which could represent bias. All the metrics of overlap, image quality and contouring difficulty were lowest/worst for CT and highest/best for PET/CT MR. To minimise recall of the images, at least 14 days (usually more) had elapsed between delineations, but this was probably not enough to overcome it

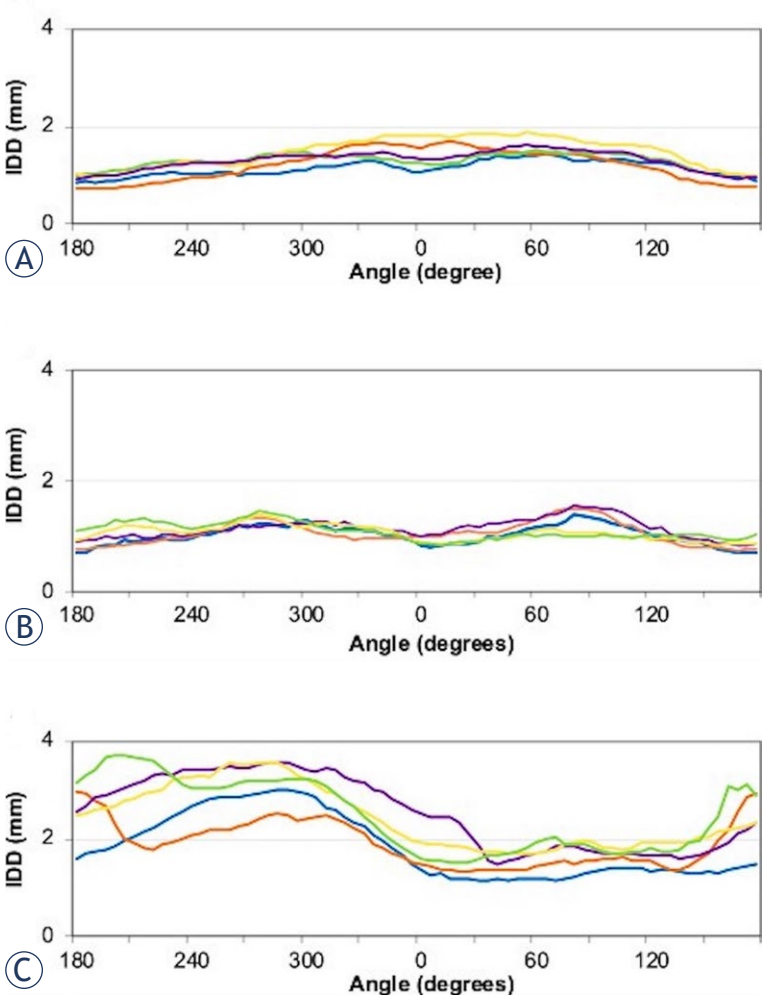

FIGURE 4. Mean inter-delineation distance (IDD) curves of the gross tumour volume (GTV) delineated on different imaging modalities as a function of the angle. The IDD is largest in tumours of the lower third and similar in upper and thirds. **(A)** Upper third of the oesophagus; **(B)** Middle third of the oesophagus; **(C)** Lower third of the oesophagus.

Blue = computed tomography; Green = fusion of PET CT and MR.Red = magnetic resonance imaging; Violet = positron emission tomography and CT; Yellow = fusion of CT and MR

completely. Thirdly, all observers come from the same institution. All had at least five years of experience, but some have learnt from others over the years, which could be the reason for the similarity of the contours and does not represent all real-life scenarios.

Conclusions

In conclusion, the lowest inter-observer agreement was found for CT and the highest for PET/CT MR. The improvement in inter-observer agreement with fused imaging modalities is mainly due to the reduction of differences in the cranio-caudal direction, which may affect dose distribution and thus local control and side effects of radiotherapy treatment. MR and CT MR imaging reduced inter-observer variability compared to CT imaging alone, but not compared to PET/CT. Therefore, the use of MR for delineation could be recommended, especially for non-FDG-avid tumours or for patients with marked inflammation of the oesophagus, which can be assessed in scans prior to treatment. MR imaging provides additional information about the local extent of the tumour. As the number of patients with oesophageal cancer is not high, additional MR simulation would not represent a major financial burden, but optimisation of imaging protocols and further studies are required. Its use can minimise cranio-caudal variation, but more experience and appropriate training programmes are needed.

References

1. World Health Organization International Agency for Research on Cancer (IARC). GLOBOCAN 2020: Estimated cancer incidence, mortality and prevalence worldwide in 2020. [internet]. [cited 2024 Jan 20]. Available at: http://globocan.iarc.fr/
2. Uhlenhopp DJ, Then EO, Sunkara T, Gaduputi V. Epidemiology of esophageal cancer: update in global trends, etiology and risk factors. *Clin J Gastroenterol* 2020; **13:** 1010-21. doi: 10.1007/s12328-020-01237-x
3. Stahl M, Mariette C, Haustermans K, Cervantes A, Arnold D. ESMO Guidelines Working Group. Oesophageal cancer: ESMO Clinical Practice Guidelines for diagnosis, treatment and follow-up. *Ann Oncol* 2013; **24(Suppl 6):** vi51-6. doi: 10.1093/annonc/mdt342
4. Eyck BM, Van Lanschot JJB, Hulshof MCCM, van der Wilk BJ, Shapiro J, van Hagen P, et al. Ten-year outcome of neoadjuvant chemoradiotherapy plus surgery for esophageal cancer: the randomized controlled CROSS Trial. *J Clin Oncol* 2021; **39:** 1995-2004. doi: 10.1200/JCO.20.03614
5. van Hagen P, Hulshof MC, van Lanschot JJ, Steyerberg EW, van Berge Henegouwen MI, Wijnhoven BP, et al. Preoperative chemoradiotherapy for esophageal or junctional cancer. *N Engl J Med* 2012; **366:** 2074-84. doi: 10.1056/NEJMoa1112088
6. Chan KKW, Saluja R, Santos KD, Lien K, Shah K, Cramarossa G, et al. Neoadjuvant treatments for locally advanced, resectable esophageal cancer: a network meta-analysis. *Int J Cancer* 2018; **143:** 430-37. doi: 10.1002/ijc.31312
7. Mariette C, Piessen G, Triboulet JP. Therapeutic strategies in oesophageal carcinoma: role of surgery and other modalities. *Lancet Oncol* 2007; **8:** 545-53. doi: 10.1016/S1470-2045(07)70172-9
8. Beaton L, Bandula S, Gaze MN, Sharma RA. How rapid advances in imaging are defining the future of precision radiation oncology. *Br J Cancer* 2019; **120:** 779-90. doi: 10.1038/s41416-019-0412-y
9. Sillah K, Williams LR, Laasch HU, Saleem A, Watkins G, Pritchard SA, et al. Computed tomography overestimation of esophageal tumor length: Implications for radiotherapy planning. *World J Gastrointest Oncol* 2010; **2:** 197-204. doi: 10.4251/wjgo.v2.i4.197
10. Decazes P, Hinault P, Veresezan O, Thureau S, Gouel P, Vera P. Trimodality PET/CT/MRI and radiotherapy: a mini-review. *Front Oncol* 2021; **10:** 1-9. doi: 10.3389/fonc.2020.614008
11. Lambrecht M, Haustermans K. Clinical evidence on PET-CT for radiation therapy planning in gastro-intestinal tumors. *Radiother Oncol* 2010; **96:** 339-46. doi: 10.1016/j.radonc.2010.07.019
12. Lu J, Sun XD, Yang X, Ang XY, Qin Q, Zhu HC, et al. Impact of PET/CT on radiation treatment in patients with esophageal cancer: a systematic review. *Crit Rev Oncol Hematol* 2016; **107:** 128-37. doi: 10.1016/j.critrevonc.2016.08.015
13. Jiang C, Chen Y, Zhu Y, Xu Y. Systematic review and meta-analysis of the accuracy of 18F-FDG PET/CT for detection of regional lymph node metastasis in esophageal squamous cell carcinoma. *J Thorac Dis* 2018; **10:** 6066-76. doi: 10.21037/jtd.2018.10.57
14. Garcia B, Goodman KA, Cambridge L, Dunphy M, Wu AJ. Distribution of FDG-avid nodes in esophageal cancer: Implications for radiotherapy target delineation. *Radiat Oncol* 2016; **11:** 1-8. doi: 10.1186/s13014-016-0731-6
15. Machiels M, Wouterse SJ, Geijsen ED, van Os RM, Bennink RJ, van Laarhoven HW, et al. Distribution of lymph node metastases on FDG-PET/CT in inoperable or unresectable oesophageal cancer patients and the impact on target volume definition in radiation therapy. *J Med Imaging Radiat Oncol* 2016; **60:** 520-27. doi: 10.1111/1754-9485.12474
16. Münch S, Marr L, Feuerecker B, Dapper H, Braren R, Combs SE, et al. Impact of 18F-FDG-PET/CT on the identification of regional lymph node metastases and delineation of the primary tumor in esophageal squamous cell carcinoma patients. *Strahlentherapie Onkol* 2020; **196:** 787-94. doi: 10.1007/s00066-020-01630-y
17. Thomas L, Lapa C, Bundschuh RA, Polat B, Sonke JJ, Guckenberger M. Tumour delineation in oesophageal cancer – a prospective study of delineation in PET and CT with and without endoscopically placed clip markers. *Radiother Oncol* 2015; **116:** 269-75. doi: 10.1016/j.radonc.2015.07.007
18. Mamede M, El Fakhri G, Abreu-E-Lima P, Andler W, Nosé V, Gerbaudo VH. Pre-operative estimation of esophageal tumor metabolic length in FDG-PET images with surgical pathology confirmation. *Ann Nucl Med* 2007; **21:** 553-62. doi: 10.1007/s12149-007-0040-0
19. Han D, Yu J, Yu Y, Zhang G, Zhong X, Lu J, et al. Comparison of 18F-Fluorothymidine and 18F-Fluorodeoxyglucose PET/CT in delineating gross tumor volume by optimal threshold in patients with squamous cell carcinoma of thoracic esophagus. *Int J Radiat Oncol Biol Phys* 2010; **76:** 1235-41. doi: 10.1016/j.ijrobp.2009.07.1681
20. Zhong X, Yu J, Zhang B, Mu D, Zhang W, Li D, et al. Using 18F-Fluorodeoxyglucose positron emission tomography to estimate the length of gross tumor in patients with squamous cell carcinoma of the esophagus. *Int J Radiat Oncol Biol Phys* 2009; **73:** 136-41. doi: 10.1016/j.ijrobp.2008.04.015
21. Nowee ME, Voncken FEM, Kotte ANTJ, Goense L, van Rossum PSN, van Lier ALHMW, et al. Gross tumour delineation on computed tomography and positron emission tomography-computed tomography in oesophageal cancer: a nationwide study. *Clin Transl Radiat Oncol* 2018; **14:** 33-9. doi: 10.1016/j.ctro.2018.10.003
22. Toya R, Matsuyama T, Saito T, Imuta M, Shiraishi S, Fukugawa Y, et al. Impact of hybrid FDG-PET/CT on gross tumor volume definition of cervical esophageal cancer: reducing interobserver variation. *J Radiat Res* 2019; **60:** 348-52. doi: 10.1093/jrr/rrz004

23. Vesprini D, Ung Y, Dinniwell R, Breen S, Cheung F, Grabarz D, et al. Improving observer variability in target delineation for gastro-oesophageal cancer – the role of 18Fluoro-2-deoxy-d-glucose positron emission tomography/computed tomography. *Clin Oncol* 2008; **20:** 631-38. doi: 10.1016/j.clon.2008.06.004

24. Schreurs LM, Busz DM, Paardekooper GM, Beukema JC, Jager PL, Van der Jagt EJ, et al. Impact of 18-fluorodeoxyglucose positron emission tomography on computed tomography defined target volumes in radiation treatment planning of esophageal cancer: reduction in geographic misses with equal inter-observer variability. *Dis Esophagus* 2010; **23:** 493-501. doi: 10.1111/j.1442-2050.2009.01044.x

25. Li F, Li Y, Wang X, Zhang Y, Liu X, Liu S, et al. Inter-observer and Intra-observer variability in gross tumor volume delineation of primary esophageal carcinomas based on different combinations of diagnostic multimodal images. *Front Oncol* 2022; **12:** 1-10. doi: 10.3389/fonc.2022.817413

26. Shi J, Li J, Li F, Zhang Y, Guo Y, Wang W, et al. Comparison of the gross target volumes based on diagnostic PET/CT for primary esophageal cancer. *Front Oncol* 2021; **11:** 1-10. doi: 10.3389/fonc.2021.550100

27. van Rossum PSN, Van Lier ALHMW, Lips IM, Meijer GJ, Reerink O, van Vulpen M, et al. Imaging of oesophageal cancer with FDG-PET/CT and MRI. *Clin Radiol* 2015; **70:** 81-95. doi: 10.1016/j.crad.2014.07.017

28. Hou DL, Shi GF, Gao XS, Asaumi J, Li XY, Liu H, et al. Improved longitudinal length accuracy of gross tumor volume delineation with diffusion weighted magnetic resonance imaging for esophageal squamous cell carcinoma. *Radiat Oncol* 2013; **8:** 169. doi: 10.1186/1748-717X-8-169

29. Vollenbrock SE, Nowee ME, Voncken FEM, Kotte ANTJ, Goense L, van Rossum PSN, et al. Gross tumor delineation in esophageal cancer on MRI compared with 18F-FDG-PET/CT. *Adv Radiat Oncol* 2019; **4:** 596-604. doi: 10.1016/j.adro.2019.04.004

30. Kouwenhoven E, Giezen M, Struikmans H. Measuring the similarity of target volume delineations independent of the number of observers. *Phys Med Biol* 2009; **54:** 2863-73. doi: 10.1088/0031-9155/54/9/018

31. Warfield SK, Zou KH, Wells WM. Simultaneous truth and performance level estimation (STAPLE): an algorithm for the validation of image segmentation. *IEEE Trans Med Imaging* 2004; **23:** 903-21. doi: 10.1109/TMI.2004.828354

32. Petrič P, Hudej R, Rogelj P, Blas M, Tanderup K, Fidarova E, et al. Uncertainties of target volume delineation in MRI guided adaptive brachytherapy of cervix cancer: a multi-institutional study. *Radiother Oncol* 2013; **107:** 6-12. doi: 10.1016/j.radonc.2013.01.014

33. Rogelj P, Hudej R, Petric P. Distance deviation measure of contouring variability. *Radiol Oncol* 2013; **47:** 86-96. doi: 10.2478/raon-2013-0005

34. Šegedin B. *[Objective evaluation of the impact of learning on differences in the contouring of target volumes in radiotherapy].* [Slovenian]. Doctoral thesis. Ljubljana: University of Ljubljana. Medical Faculty; 2016.

35. Machiels M, Jin P, van Hooft JE, Gurney-Champion OJ, Jelvehgaran P, Geijsen ED, et al. Reduced inter-observer and intra-observer delineation variation in esophageal cancer radiotherapy by use of fiducial markers. *Acta Oncol* 2019; **58:** 943-50. doi: 10.1080/0284186X.2019.1588991

36. Wu YW, Tseng PH, Lee YC, Wang SY, Chiu HM, Tu CH, et al. Association of esophageal inflammation, obesity and gastroesophageal reflux disease: From FDG PET/CT perspective. *PLoS One* 2014; **9:** e92001. doi: 10.1371/journal.pone.0092001

Radiol Oncol 2024; 58(4): 459-568.
doi: 10.2478/raon-2024-0051

Značilnosti izpostavljenosti radioaktivnemu jodu med jedrsko nesrečo

Zaletel K, Mihovec A, Gaberšček S

Izhodišča. Med jedrsko nesrečo se sprostijo številni produkti jedrske cepitve, tudi izotopi radioaktivnega joda. Med njimi je jod-131 z razpolovno dobo 8,02 dni, ki oddaja sevanje β. Že desetletja ga učinkovito in varno uporabljamo v medicini. V primeru jedrske nesreče pa ima lahko nenadzorovana izpostavljenost škodljive biološke učinke. Glavni viri notranje kontaminacije z jodom-131 so kontaminirani zrak, hrana in voda. Najbolj izpostavljen organ je ščitnica, ki kopiči radioaktivni jod s pomočjo Na^+/I^--simporterja (NIS). NIS ne razlikuje med izotopi radioaktivnega joda in stabilnim izotopom joda-127, ki je nujen za sintezo ščitničnih hormonov. Izpostavljenost radioaktivnemu joda med jedrsko nesrečo je povezana predvsem s papilarnim rakom ščitnice, katerega pojavnost začne naraščati nekaj let po izpostavljenosti. Največjemu tveganju so izpostavljeni otroci in mladostniki, tveganje pa je še zlasti pomembno za posameznike, ki živijo na področjih s pomanjkanjem joda.

Zaključki. Na nivoju populacije je za zmanjšanje tveganja škodljivih učinkov izpostavljenosti radioaktivnemu jodu zato ključno zagotoviti ustrezno preskrbo z jodom. Zaščita ščitnice s tabletami kalijevega jodida bistveno zmanjša izpostavljenost sevanju, saj stabilni jod prepreči vstop radiokativnega joda v ščitnico. Takšna zaščita je učinkovita le v ozkem časovnem oknu – nekaj ur pred izpostavljenostjo in nekaj ur po njej in je priporočena le za mlajše od 40 let, saj so pri starejših posameznikih tveganja čezmernega vnosa joda večja od možnih koristi.

Radiol Oncol 2024; 58(4): 469-479.
doi: 10.2478/raon-2024-0061

Trenutni operativni postopek (COP) za elektroskleroterapijo z bleomicinom (BEST) pri žilnih malformacijah z nizkim pretokom

Muir T, Wohlgemuth WA, Cemazar M, Bertino G, Groselj A, Ratnam L, McCafferty I, Wildgruber M, Gebauer B, de Terlizzi F, Zanasi A, Sersa G

Izhodišča. Bleomicinska elektroskleroterapija (BEST) je nov pristop k zdravljenju žilnih malformacij. Po vnosu bleomicina v malformacijo na ciljno območje nanesemo električne impulzi, ki povečajo učinkovitost bleomicina. Način delovanja je primerljiv z učinkom elektrokemoterapije na tumorsko ožilje. Za širšo in varnejšo uporabo metode BEST pri kliničnem zdravljenju malformacij z nizkim žilnim pretokom smo pripravili opisani trenutni operativni postopek (*angl. Current Operating Procedure*, COP). Predlagamo klinično standardizacijo metode BEST z uporabo naprave Cliniporator® kot generatorja električnih impulzov s pripadajočimi elektrodami. V protokolu smo upoštevali električne parametre, ki so potrjeni z Evropskimi standardnimi operativnimi postopki za elektrokemoterapijo in elektrogensko terapijo (ESOPE) z napravo Cliniporator®.

Zaključki. Predlagamo splošne zahteve in glede na vrsto lezije, lokalne sposobnosti in razpoložljivost radiološke opreme opišemo dva tehnična pristopa BEST. Temeljita na ultrazvočno vodenem ali pa kombiniranem ultrazvočnem in fluoroskopskem vodenem posegu.

Radiol Oncol 2024; 58(4): 480-485.
doi: 10.2478/raon-2024-0041

Poškodba posteriornega interosalnega živca zaradi lipoma. Pregled literature s prikazom primera

Rojc B, Golob P

Izhodišča. Okvare posteriornega interosalnega živca predstavljajo redko mononevropatijo zgornjega uda. Najpogostejši vzrok nepoškodbene okvare tega živca je lipom proksimalne podlakti. Značilna simptomatika nastopi postopno.

Bolniki in metode. Opravili smo sistematični pregled literature z namenom poiskati opise bolnikov z okvaro posteriornega interosalnega živca, ki je nastala kot posledica lipoma. Sledili smo smernicam PRISMA. Osrednji interes pregleda je bil poiskati časovni presek nastanka simptomov. Predstavljamo tudi redek primer bolnika s klinično sliko akutne okvare posteriornega interosalnega živca zaradi lipoma.

Rezultati. Po pregledu literature smo izsledili 30 bolnikov z okvaro posteriornega interosalnega živca, ki je bila posledica lipoma. Pri 28 bolnikih so se simptomi pojavili postopoma, v obdobju od 1 meseca do največ 240 mesecev. Našli smo le en primer bolnika z akutnim nastankom težav ter en primer bolnika z akutnim poslabšanjem kronične okvare živca zaradi poškodbe podlakti.

Zaključki. Nepoškodbene okvare posteriornega interosalnega živca so najpogosteje posledica lipoma proksimalne podlakti. Pri teh bolnikih pričakujemo postopno razvijajočo klinično sliko. Čeprav redke, so možne tudi akutne okvare posteriornega interosalnega živca zaradi lipoma, kar prikazuje naš primer.

Radiol Oncol 2024; 58(4): 486-493.
doi: 10.2478/raon-2024-0058

Primerjava preiskav PET/CT z [^{18}F]fluoroholinom ter scintigrafije [^{99m}Tc]sestamibi za ugotavljanje in lociranje prekomerno delujočih obščitničnih žlez pri bolnikih s primarnim hiperparatiroidizmom. Učinkovitost in končni izid obravnave bolnikov

Rep S, Širca K, Maček Ležaić E, Zaletel K, Hočevar M, Ležaić L

Izhodišča. Minimalno invazivna paratiroidektomija je zdravljenje izbire pri bolnikih s primarnim hiperparatiroidizmom, vendar pa temelji na zanesljivi predoperativni metodi lociranja prekomerno delujočega obščitničnega tkiva. Višjo občutljivost in nižjo izpostavljenost ionizirajočemu sevanju so dokazali pri uporabi PET/CT z [^{18}F]fluoroholinom v primerjavi s scintigrafijo obščitnic z [^{99m}Tc]sestamibi. Namen raziskave je bil določiti učinkovitost obeh metod in končni izid obravnave bolnikov, ker so podatki o tem pičli.

Bolniki in metode. Skupino 234 bolnikov, ki smo jih operirali na podlagi izvida scintigrafije z [^{99m}Tc]sestamibi, smo primerjali s skupino 163 bolnikov, ki smo jih operirali na podlagi izvida PET/CT z [^{18}F]fluoroholinom. Analizirali smo celoten delovni proces od izvajanja slikanja do zaključka kirurškega zdravljenja. Ekonomsko obremenitev smo izrazili v času, ki je bil potreben za izvedene postopke.

Rezultati. Čas, potreben za izvedbo slikanja, se je pri uporabi PET/CT z [^{18}F]fluoroholinom zmanjšal za 83 % v primerjavi s scintigrafijo z [^{99m}Tc]sestamibi. Čas, potreben za izvedbo operativnega posega se je zmanjšal za 41 %, če med posegom nismo določali vrednosti paratiroidnega hormona. Sicer pa ni bilo časovne razlike, ali smo operirali na podlagi izvidov ene ali druge metode.

Zaključki. PET/CT z [^{18}F]fluoroholinom skrajša čas slikanja, čas operativnega posega in potencialno zmanjša število ponovnih operativnih posegov zaradi vztrajajoče bolezni.

Radiol Oncol 2024; 58(4): 494-500.
doi: 10.2478/raon-2024-0062

PET/MRI celega telesa za odkrivanje kostnih metastaz. Primerjava diagnostične učinkovitosti zaporedij

Ulusoy OL, Server S, Yesilova M, Inan N

Izhodišča. Pozitronska emisijska tomografija/slikanje z magnetno resonanco (PET/MRI) celega telesa vse pogosteje uporabljamo pri začetni oceni onkoloških bolnikov. Namen raziskave je bil primerjati diagnostično učinkovitost sekvenc celega telesa MRI, pozitronsko-emisijske tomografije s korigiranimi neobdelanimi podatki (AC PET) in spojenih slik PET/MRI za odkrivanje kostnih metastaz.

Bolniki in metode. Vključili smo 765 zaporednih onkoloških bolnikov, pri katerih smo naredili PET/MRI celega telesa od januarja 2017 do septembra 2023. Prisotnost kostnih metastaz sta s pomočjo posameznih sekvenc ocenila dva radiologa. Izračunali smo ujemanje med opazovalcema. Za oceno učinkovitosti vsakega posameznega zaporedja in združenih slik smo naredili analizo ROC.

Rezultati. Ujemanje med opazovalcema za odkrivanje kostnih metastaz na vseh sekvencah je bilo v razponu od dobrega do zelo dobrega. Diagnostika s pomočjo kombinacije sekvenc MRI s slikami PET je pokazalo statistično značilno boljše rezultate kot diagnostika s pomočjo posameznih sekvenc MRI in samo komponente PET. Zaporedje T1obteženo (T1 W) z volumsko interpolirano preiskavo zadrževanja dihanja (*angl. contrast enhanced* [CE] T1 W *volume-interpolated breath-hold examination* [VIBE]) je bilo boljše od PET za odkrivanje kostnih metastaz, vendar statistična pomembnost ni bila tako visoka kot pri spojenih slikah T1W-PET in CE T1W-PET. Najvišjo učinkovitost smo dosegli s spojenimi slikami CE T1W-PET, kjer je bila občutljivost 100 %, specifičnost 92 %, pozitivna napovedna vrednost 96 % in negativna napovedna vrednost 100 %.

Zaključki. Kombinacija sekvenc CE T1W VIBE s slikami PET ima največjo diagnostično učinkovitost pri odkrivanju kostnih metastaz pri onkoloških bolnikih. Zato bi bilo to zaporedje potrebno vključiti v preiskave PET/MRI celega teles za začetno diagnosticiranje napredovanja raka.

Radiol Oncol 2024; 58(4): 501-508.
doi: 10.2478/raon-2024-0060

Začetni rezultati fuzijske biopsije prostate z magnetno resonanco in transrektalnim ultrazvokom (MRI-TRUZ) v večji terciarni ustanovi

Smrkolj T, Taskovska M, Ditz I, Černelč K, Hawlina S

Izhodišča. Multiparametrično slikanje z magnetno resonanco (mpMRI) omogoča ciljano biopsijo prostate. Namen pričujoče raziskave je bil oceniti učinkovitost in učno krivuljo postopka biopsije s fuzijo slik mpMRI in transrektalnega ultrazvoka (MRI-TRUS fuzija) v prvem letu po njeni uvedbi na našem urološkem oddelku.

Bolniki in metode. Fuzijsko biopsijo MRI-TRUS smo izvedli pri 293 bolnikih, pri katerih je bila prisotna vsaj ena lezija ≥ 3 po sistemu poročanja podatkov o slikanju prostate (*angl. Prostate Imaging-Reporting and Data System*, PI-RADS). Analizirali smo delež bolnikov in lezij s pozitivnim histopatološkim izvidom za rak prostate. Učno krivuljo za MRI-TRUS fuzijsko biopsijo smo ocenili na ravni oddelka in na ravni posameznega urologa. Pozitivne lezije smo dodatno analizirali glede na PI-RADS in oceno po Gleasonu.

Rezultati. Delež bolnikov s pozitivnim histopatološkim izvidom pri ciljani biopsiji, sistematični biopsiji in kombinirani biopsiji je bil 53,9 %, 47,9 % in 63,5 %. Chi-kvadrat test za delež bolnikov, ki so bili pozitivni za rak prostate ni pokazal pomembne razlike med časovnimi skupinami bolnikov na oddelčni ravni niti pomembne razlike med posameznimi urologi. Pri analizi posameznih lezij so bili ocena PI-RADS ($p < 0,001$), koncentracija celotnega prostatičnega specifičnega antigena (PSA) ($p = 0,05$), volumen prostate ($p < 0,001$) in število vzorcev na lezijo ($p = 0,034$) pomembni napovedni dejavniki pozitivnega histopatološkega izvida. Klinično pomemben rak prostate (*angl. clinically significant prostate cancer*, csPCa) je bil potrjen pri 34,7 % od 412 lezij in pri 76,4 % od 187 pozitivnih lezij za rak prostate.

Zaključki. Fuzijska biopsija MRI-TRUS je bistveno izboljšala stopnjo odkrivanja raka prostate v primerjavi s sistematično biopsijo. Pri analizi rezultatov posameznih urologov nismo ugotovili izrazite učne krivulje. Delež lezij s klinično nepomembnim rakom prostate je bil nizek, kar zmanjšuje prekomerno diagnosticiranje raka prostate

Radiol Oncol 2024; 58(4): 509-516.
doi: 10.2478/raon-2024-0063

Volumetrija jeter izboljša oceno odgovora na kemoterapevtsko zdravljenje, ki ga izvajamo z infuzijo jetrne arterije pri bolnikih z uvealnim melanomom in metastazami v jetrih

Zensen S, Steinberg-Vorhoff HL, Milosevic A, Richly H, Siveke JT, Opitz M, Haubold J, Li Y, Forsting M, Schaarschmidt BM

Izhodišča. Pri bolnikih z uvealnim melanomom je kratkoročno ocenjevanje odgovora na kemoterapevtsko zdravljenje z infuzijo v jetrno arterijo po merilih RECIST 1.1 (*angl. Response Evaluation Criteria in Solid Tumors*) težavno, ker so metastaze razpršene. Pogosto opazimo povečana jetra, zato je bil namen pričujoče raziskave primerjati merila RECIST 1.1 in volumetrijo jeter pri ocenjevnjui odgovora na zdravljenje.

Bolniki in metode. Pri 143 bolnikih (povprečna starost 65,1 ± 10,9 let, 54 % žensk), ki smo jih zdravili s kemoterapijo v jetrno arterijo, smo ocenili odgovor na zdravljenje z merili RECIST 1.1 in jetrno volumetrijo na podlagi slik računalniške tomografije (CT), ki smo jih naredili pred in po zdravljenju. Z jetrno volumetrijo smo ocenili različna povečanja volumna jeter, da bi določili učinkovit prag za razlikovanje med stabilno boleznijo in napredujočo boleznijo. Celokupno preživetje smo opredelili kot čas od prve aplikacije kemoterapije z infuzijo v jetrno arterijo do smrti bolnika in za izračun uporabili Kaplan-Meierjev test, pri merilih RECIST 1.1 in jetrni volumetriji pa smo naredili multivariatno analizo.

Rezultati. V celotni preiskovani skupini je bilo srednje celokupno preživetje 13,5 meseca (95 % interval zaupanja [IZ] 11,2-15,8 meseca). Pri jetrni volumetriji je bil prag 10-odstotnega povečanja volumna jeter primeren za prepoznavanje bolnikov s pomembno zmanjšanim celokupnim preživetjem (pri stabilni bolezni: 103 od 143 [103/143] bolnikov, srednje celokupno preživetje 15,9 meseca; pri napredujoči bolezni: 40/143 bolnikov, srednje celokupno preživetje 6,6 meseca; $p < 0,001$). V primerjavi s standardom RECIST 1.1 je bila jetrna volumetrija edini pomemben napovedni dejavnik, ki je lahko opredelil zmanjšano celokupno preživetje.

Zaključki. Pri bolnikih z uvealnim melanomom in metastazami v jetrih je bila jetrna volumetrija s pragom za 10-odstotno povečanje volumna jeter primerna za oceno odziva na zdravljenje in bi se lahko uporabljala kot dragocen dodatek ali celo alternativa merilom RECIST 1.1.

Radiol Oncol 2024; 58(4): 517-526.
doi: 10.2478/raon-2024-0052

Transarterijska kemoembolizacija z idarubicinom pri bolnikih z jetrnoceličnim karcinomom v srednjem stadiju bolezni. Varnost, učinkovitost in farmakokinetika

Koršič Š, Osredkar J, Šmid A, Steblovnik K, Popović M, Locatelli I, Trontelj J, Popović P

Izhodišča. Transarterijska kemoembolizacija (*angl. transarterial chemoembolization*, TACE) je metoda izbora za zdravljenje bolnikov z jetrnoceličnim karcinomom v srednjem stadiju bolezni. Najpogosteje uporabljen kemoterapevtik pri TACE je doksorubicin, v *in vitro* raziskavi pa se je za najbolj citotoksičnega proti jetrnoceličnem karcinomu pokazal idarubicin. Z raziskavo smo želeli proučiti varnost, učinkovitost in farmakokinetiko uporabe idarubicina pri TACE z mikrodelci (*angl. idarubicin-loaded drug-eluting microspheres* TACE, DEMIDA-TACE).

Bolniki in metode. V prospektivno raziskavo smo med januarjem 2019 in decembrom 2021 vključili 31 bolnikov z jetrnoceličnim karcinomom v srednjem stadiju bolezni. Bolnike smo zdravili z mešanico 10 mg (1 mg/mL) idarubicina in 2 mL mikrodelcev velikosti 100 µm. Beleženi smo neželene dogodke, odgovor na zdravljenje, izračunali srednji čas preživetja brez napredovanja bolezni, srednji čas do napredovanja bolezni, po katerem zdravljenje s TACE ni bilo več mogoče in srednje celokupno preživetje. Proučili smo farmakokinetiko idarubicina in metabolita idarubicinola ter analizirali morebitne povezave farmakokinetičnih parametrov s kliničnimi izidi zdravljenja.

Rezultati. Opravili smo 68 posegov. Neželene dogodke ≥ 3. stopnje smo zabeležili pri 29,4 % posegov. Objektivni odgovor na zdravljenje je bil dosežen pri 83,9 % bolnikov. Srednje preživetje brez napredovanja bolezni je bilo 10,5 mesecev (95% IZ: 6,8–14,3 mesecev), srednji čas do napredovanja bolezni, po katerem zdravljenje s TACE ni bilo več mogoče 24,6 mesecev (95% IZ: 11.6–37,6 mesecev) in srednje celokupno preživetje 36,0 mesecev (95% IZ: 21,1–50,9 mesecev). Plazemska koncentracija idarubicinola in vsota plazemskih koncentracij idarubicin-idarubicinol 72 ur po posegu sta bili statistično značilno povezani z objektivnim odgovorom na zdravljenje (za obe p = 0,014; mejni vrednosti 1,2 ng/mL za idarubicinol in 1,29 ng/mL za vsoto).

Zaključki. DEMIDA-TACE je varna in učinkovita metoda zdravljenja bolnikov z jetrnoceličnim karcinomom v srednjem stadiju bolezni. Ima malo neželenih dogodkov ob ugodnem odgovoru na zdravljenje in preživetju. Plazemska koncentracija in vsota koncentracij idarubicin-idarubicinol 72 ur po posegu bi lahko služili kot napovedna dejavnika za objektivni odgovor na zdravljenje.

Radiol Oncol 2024; 58(4): 527-534.
doi: 10.2478/raon-2024-0049

Ocena kemičnega premika in difuzijsko obteženega slikanja z magnetno resonanco za razlikovanje malignih in benignih sprememb v vretencih pri onkoloških bolnikih. Izkušnje terciarne ustanove

Mijaljević MB, Milošević ZC, Lavrnić SĐ, Joković ZM, Ninković DI, Tubić RM, Janković RR

Izhodišča. Namen raziskave je bil analizirati prispevka dveh nestandardnih tehnik slikanja z magnetno resonanco (MR), slike kemičnega premika in difuzijsko obteženega slikanja, pri razlikovanju malignih in benignih sprememb kostnega mozga vretenc.

Bolniki in metode. Uporabili smo konvencionalni protokol slikanja za MR hrbtenice, nato pa slike kemičnega premika in difuzijsko obteženo slikanje. Preiskave smo naredili z napravo 1,5 T pri 102 onkoloških bolnikih med januarjem 2020 in decembrom 2023. Ugotovili smo 325 lezij kostnega mozga in med njimi izbrali 102 reprezentativnih (po eno na bolnika). Lezije kostnega mozga so bile na podlagi histopatologije ali slikovnega spremljanja razdeljene na maligne (n = 74) in benigne (n = 28). Kvantitativna parametra za oceno lezij sta bila razmerje med intenzivnostjo signala, pridobljeno s slikami kemičnega premika, in difuzijskim koeficientom, pridobljenim z difuzijsko obteženim slikanjem.

Rezultati. Maligne lezije so imele pomembno višje vrednosti intenzivnosti signala ($p < 0,05$) in nižje vrednosti difuzijskega koeficienta v primerjavi z benignimi lezijami kostnega mozga ($p < 0,05$). Površina pod krivuljo (AUC) je bila 0,953 ($p < 0,001$) za intenzivnost signala in 0,894 za difuzijski koeficient ($p < 0,001$) (meja pri > 0,82 oziroma ≤ 1,57 x 10^{-3} mm^2/s). Občutljivost in specifičnost za intenzivnost signala sta bili 93,6 % in 88,5 %, za difuzijski koeficient pa 88,2 % in 92,3 %. Kombinirana uporaba intenzivnosti signala in difuzijskega koeficienta je izboljšala diagnostično natančnost (AUC 0,988 [$p < 0,001$, meja pri > 0,19]), občutljivost in specifičnost sta bili 100,0 % in 90,9 %.

Zaključki. Kvantitativna parametra, intenzivnost signala in difuzijski koeficient, pridobljena iz dveh nestandardnih tehnik MR, slikami kemičnega premika in difuzijsko obteženim slikanjem so pokazali diagnostično moč pri razlikovanju malignih in benignih lezij kostnega mozga. V klinični praksi lahko kombinacija obeh metod izboljša diagnostično učinkovitost in natančnost preiskave MR za lezije v hrbtenici.

Radiol Oncol 2024; 58(4): 535-543.
doi: 10.2478/raon-2024-0059

Vpliv dopolnilne radioterapije na jetra pri desnostranskem raku dojke

Hanedan Uslu G, Taşçı F

Izhodišča. Pri bolnicah z desnostranskim rakom dojke lahko med dopolnilno radioterapijo (RT) delno obsevamo jetra. Zato smo z magnetnoresonančno elastografijo (MRE) in biološkimi vrednostmi želeli ugotoviti učinke RT na dele jetr pri obsevanju zaradi raka dojke.

Bolniki in metode. V retrospektivno raziskavo smo vključili 34 bolnic z diagnozo desnostranskega raka dojke, ki smo jih zdravili z dopolnilno RT. Pri vseh udeleženkah smo ocenili jetrne segmente z MRE. Pri vsaki bolnici smo naredili tudi osnovno analizo krvi in določili vrednosti jetrnih encimov. Vse meritve somo opravili pred začetkom in po koncu RT.

Rezultati. Pred in po RT smo ugotovili statistično pomembno razliko v vrednostih ALT (p = 0,015), ALP (p = 0,026), celokupnih beljakovin (p = 0,037) in albuminov (p = 0,004). Najvišjo povprečno vrednost togosti jeter (kPa) smo zabeležili v 8. segmentu, najnižjo pa v 6. segmentu. Ugotovili smo šibko, vendar statistično pomembno pozitivno korelacija med togostjo segmenta 5 in prostornino jetr (p = 0,039). Ugotovili smo tudi statistično pomembno pozitivno korelacijo med vrednostmi ALP in vrednostmi togosti v 4A segmentu (p = 0,020) in 6. segmentu (p = 0,003). Nasprotno pa smo opazili šibko negativno korelacijo med vrednostmi togosti v 8. segmentu in vrednostmi celokupnih beljakovin po RT (p = 0,031).

Zaključki. MRE nam lahko pomaga določiti stopnjo fibroznih sprememb v jetrnih segmentih znotraj območja RT brez ugotavljanja kliničnih simptomov. MRE je lahko kliniku v pomoč pri ocenjevanju delovanja jetr pri bolnicah z rakom desne dojke, ki smo jih obsevali. Predvidevamo, da bodo ti rezultati spodbudili nove raziskave z velikim številom bolnic ob slikanju z MRE v določenih časovnih presledkih. Na ta način bi lahko spremljali bolnice z rakom desne dojke, ki smo jih zdravili z RT in ugotavljali spremembe še pred razvojem bolezni jetr, povzročene z obsevanjem.

Radiol Oncol 2024; 58(4): 544-555.
doi: 10.2478/raon-2024-0046

Analiza zgodnje obravnave bolnikov z rakom prostate v družinski medicini v Sloveniji

Kokalj Kokot M, Miroševič Š, Bric N, Petek D

Izhodišča. Rak prostate je najpogostejši rak pri moških v Sloveniji in tudi v Evropi. Obolevnost za rakom prostate pri nas in v svetu raste. Podaljšani diagnostični časovni intervali so povezani s slabšimi izidi, kar poudarja potrebo po optimizaciji tega procesa. Namen raziskave je bil ovrednotiti časovni interval obravnave na primarni zdravstveni ravni, raziskati vpliv na preživetje bolnikov in preučiti možnosti za izboljšanje diagnostične poti za rak prostate v primarni oskrbi.

Bolniki in metode. Naredili smo retrospektivno kohortno raziskavo in uporabili anonimizirane podatke o bolnikih z rakom prostate iz primarnega zdravstvenega varstva in podatke iz Registra raka Slovenije.

Rezultati. V raziskavi smo ugotovili, da je bilo povprečno trajanje zdravnikovega intervala 0 dni (interkvartilni razpon [IQR] 0–6), intervala primarne ravni pa povprečno 5 dni (IQR 0–58). Daljše časovne intervale smo opazili pri bolnikih z več kot dvema pridruženima boleznima, kadar osebni izbrani zdravniki niso imeli dostopa do laboratorijskih diagnostičnih preiskav v svojem zdravstvenem centru in kadar so bolnike pričeli obravnavati zaradi simptomov (poročani simptomi ob prvem obisku so bili dizurija, simptomi spodnjih sečil, bolečine v trebuhu). Ugotovili smo tudi statistično pomembno povezavo med nižjo petletno stopnjo preživetja in slabšo dostopnostjo laboratorijske in ultrazvočne diagnostike v primarnih zdravstvenih centrih ter krajše petletno preživetje simptomatskih bolnikov v primerjavi z bolniki, ki smo jih pričeli obravnavati zaradi povišane ravni prostatičnega specifičnega antigena (PSA).

Zaključki. Raziskava je pokazala, da obravnava suma na rak prostate v primarnem zdravstvenem varstvu pomembno vpliva na petletno preživetje. K boljšemu preživetju prispeva več dejavnikov, vključno z enostavnim dostopom do laboratorijske diagnostike in dostopnostjo abdominalnega ultrazvoka v centrih primarnega zdravstvenega varstva. Raziskava poudarja zapleteno paleto dejavnikov, ki vplivajo na obravnavo suma na rak prostate, ki poleg veščin posameznih zdravnikov zajemajo tudi razpoložljivost testov in storitev.

Radiol Oncol 2024; 58(4): 556-564.
doi: 10.2478/raon-2024-0034

Traheotomija pred in med COVID-19 pandemijo

Jensterle S, Benedik J, Šifrer R

Izhodišča. Namen raziskave je bil ugotoviti vpliv pandemije COVID-19 na pogostost in značilnosti nujnih in urgentnih traheotomij s primerjavo podatkov, zbranih pred in med pandemijo. Naši dve hipotezi sta bili, (1) da je bilo med COVID-19 opravljenih več urgentnih traheotomij in (2) da je bilo med COVID-19 več traheotomij opravljenih v splošni anesteziji.

Bolniki in metode. Raziskava je bila retrospektivna. Raziskovalno obdobje je zajemalo dve leti pred in dve leti po izbruhu pandemije COVID-19 v Sloveniji. V vsakem obdobju je 41 bolnikov izpolnjevalo merila za vključitev. Pregledali smo njihove zdravstvene kartone. Zbrali smo anamnestične, klinične, kirurške in anesteziološke podatke. Skupini bolnikov iz različnih časovnih obdobij smo med seboj statistično primerjali.

Rezultati. Večinoma so moški potrebovali kirurško reševanje akutne zapore zgornjih dihal (76 % bolnikov). Vzroki za akutno dihalno stisko so bili rak glave in vratu (62 %), okužbe (20 %), paraliza glasilk (16 %) in stenoza (2 %). Statistično značilnih razlik ni bilo niti v urgentni/nujni izvedbi traheotomij niti v vrsti anestezije. Obe hipotezi sta bili zavrnjeni. Poročali smo o statistično pomembnem porastu uporabe laringoskopa C-MAC med COVID-19 (s 3 % na 15 %).

Zaključki. Izbruh COVID-19 ni imel statistično pomembnega vpliva na pogostost izvajanja urgentnih in nujnih traheotomij niti na uporabo splošne ali lokalne anestezije. Povzročil pa je spremembo tehnike intubacije. Posledično smo opazili znaten porast uporabe laringoskopa C-MAC.

Radiol Oncol 2024; 58(4): 565-572.
doi: 10.2478/raon-2024-0036

Povezava med alelnim bremenom *JAK2* V617F in koronarno kalcifikacijo pri bolnikih z esencialno trombocitemijo

Drofenik A, Blinc A, Božič Mijovski, Pajić T, Vrtovec M, Sever M

Izhodišča. Mutacija *JAK2* V617F (*JAK2*) je povezana s klonalno hemopoezo pri mieloproliferativnih novotvorbah in s hitrejšim napredovanjem srčno-žilnih bolezni. Malo je znanega o razmerju med *JAK2* alelnim bremenom in stopnjo napredovanja ateroskleroze koronarnega žilja. Predhodno smo že dokazali, da togost karotidne arterije hitreje napreduje pri bolnikih z *JAK2* pozitivno esencialno trombocitemijo. Po štiriletnem spremljanju smo pogledali, ali je alelno breme *JAK2* sorazmerno z višjo koronarno kalcifikacijo.

Bolniki in metode. V razponu štirih let smo pregledali 36 bolnikov z *JAK2* pozitivno esencialno trombocitemijo in 38 zdravih kontrolnih prostovoljcev. Ob obiskih smo zbrali klinične značilnosti preiskovancev, laboratorijske teste, določili alelno breme mutacije *JAK2* in izmerili koronarno kalcifikacijo.

Rezultati. Alelno breme *JAK2* se je zmanjšalo pri 19 bolnikih, pri 5 bolnikih se ni spremenilo, pri 4 bolnikih pa se je povečalo. Koronarna kalcifikacija po Agatstonu se je v obeh skupinah rahlo povečala. Na splošno ni bilo korelacije med alelnim bremenom *JAK2* in koronarno kalcifikacijo, vendar pa se je pri bolnikih z povečanjem alelnega bremena *JAK2* mutacije povečala tudi koronarna kalcifikacija.

Zaključki. Povprečno alelno breme *JAK2* se je pri bolnikih z visokim tveganjem esencialne trombocitemije v štiriletnem obdobju zmanjšalo. Vendar pa se je pri bolnikih, pri katerih se je povečalo alelno breme mutacije *JAK2*, povečala tudi koronarna kalcifikacija po Agatstonu. Naše opažanje, ki ga je potrebno razlagati previdno in ga tudi potrditi v večji raziskavi, je v skladu z najnovejšimi dokazi, da mutacija *JAK2* pospešuje aterosklerozo in se zato lahko uvršča med neklasične dejavnike tveganja za kardiovaskularne bolezni.

Radiol Oncol 2024; 58(4): 573-579.
doi: 10.2478/raon-2024-0056

Pozna intervencija pri zatekanju v anevrizmatsko vrečo tipa II ni določena s spremembami premera ali volumna vreče v zgodnjem obdobju po endovaskularnem zdravljenju anevrizme

Sneyers B, Verbraeken V, Laenen A, Coudyzer W, Mufty H, Houthoofd S, Inge Fourneau, Maleux G

Izhodišča. Diagnostično natančnost in napovedno vrednost izmerjenega volumna anevrizmatske vreče smo želeli primerjati z izmerjenim največjim premerom anevrizmatske vreče abdominalne aorte po endovaskularnem zdravljenju anevrizme pri bolnikih z zatekanjem v anevrizmatsko vrečo tipa II.

Bolniki in metode. Retrospektivna raziskavo smo izvedeli na kohorti 103 bolnikov, kjer smo ugotovili zatekanje v anevrizmatsko vrečo tipa II po endovaskularnem zdravljenju infrarenalne anevrizme abdominalne aorte. Največji premer in volumetrične meritve smo izvedli na kontrolnih posnetkih CT tri mesece in leto dni po osnovni operaciji. Pearsonov korelacijski koeficient smo uporabili za določitev linearne povezave med premerom in volumnom; Mann-Whitney U test pa za primerjavo bolnikov z in brez pozne intervencije zaradi zatekanja v anevrizmatsko vrečo tipa II.

Rezultati. Korelacija med merjenjem premera in volumna je bila visoka (ρ: 0,890–0,980 s $P < 0,0001$). Pri 38 od 103 bolnikov (37 %) z zatekanjem v anevrizmatsko vrečo tipa II smo naredili pozno intervencijo zaradi obvladovanja zatekanja; zgodnji spremembi premera ($P = 0,097$) ali volumna ($P = 0,387$) se nista izkazali kot napovedna dejavnika tveganja za pozno intervencijo.

Zaključki. Merjenje premera in volumna lahko uporabljamo pri slikovnem spremljanju bolnikov z zatekanjem v anevrizmatsko vrečo tipa II po endovaskularnem zdravljenju, vendar zgodnje spremembe v premeru ali volumnu anevrizmatske vreče ne napovedujejo poznejše intervencije.

Radiol Oncol 2024; 58(4): 580-587.
doi: 10.2478/raon-2024-0043

Primerjava razlik med vrisovalci pri določanju tumorskega tarčnega volumna pri raku požiralnika ob uporabi MR, CT in PET/CT

Šečerov-Ermenc A, Peterlin P, Anderluh F, But-Hadžić J, Jeromen-Peressutti A, Velenik V, Šegedin B

Izhodišča. Z raziskavo smo želeli oceniti razlike med vrisovalci pri določanju tumorskega tarčnega volumna (*angl. gross tumour volume, GTV)* pri raku požiralnika ob uporabi magnetne resonance (MR) v primerjavi z računalniško tomografijo (CT) ter primerjavi s pozitronsko emisijsko tomografijo in CT-jem (PET/CT)

Bolniki in metode. Vključili smo 23 zaporednih bolnikov z rakom požiralnika, pri katerih smo na Onkološkem inštitutu Ljubljana načrtovali predoperativno ali definitivno kemoradioterapijo. Sodelovalo je 5 izkušenih vrisovalcev, vrisali so GTV samo na CT, samo na MR, na CT s sočasno opravljeno MR, samo na PET/CT in na MR s sočasno opravljeno PET/CT. Ocenjevali smo razlike med vrisovalci in naredili prostorsko analizo vseh razlik med konturami. Določili smo generaliziran indeks konformnosti (*angl. generalised conformity index,* CIgen), volumski indeks konformnosti (*angl. volumetric conformity index,* VCI), planarni indeks konformnosti (*angl. planar conformity index*, PCI) in povprečne razdalje med referenčno in testno konturo (*angl. inter-delineation distance*, IDD). Razlike med vrisovalci smo testirali z metodo linearnih mešanih modelov.

Rezultati. Prostornina GTV je bila statistično značilno nižja pri vrisovanju na MR (33.03 cm^3) v primerjavi s CT (37.1 cm^3; p = 0.002) in pri PET/CT MR (35.2 cm^3; p = 0.018) v primerjavi s PET/CT (39.1 cm^3). CIgen je bil najnižji pri CT (0.56) in najvišji pri PET/CT MR (0.67). Razlika v CIgen med MR (0.61) in CT je bila mejno statistično značina (p = 0.048). VCI je bil višji pri MR (0.71; p = 0,007) in pri CT MR (0,71; p = 0.004) v primerjavi s CT (0,67). PCI je bil višji na CT MR (0,67; p = 0.031) v primerjavi s CT (0,64). Največje razlike smo opazili v kranio-kavdalni smeri.

Zaključki. Največje ujemanje med vrisovalci smo opažali pri vrisovanju na PET/CT MR, najmanjše pa na CT. MR lahko zmanjša razlike med vrisovalci in nam lahko poda dodatne informacije o lokalni razširjenosti tumorja požiralnika.

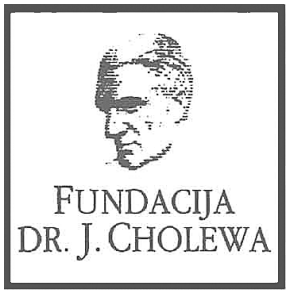

Fundacija ''Docent dr. J. Cholewa''
je neprofitno, neinstitucionalno in nestrankarsko
združenje posameznikov, ustanov in organizacij, ki želijo
materialno spodbujati in poglabljati raziskovalno
dejavnost v onkologiji.

Dunajska 106
1000 Ljubljana
IBAN: SI56 0203 3001 7879 431

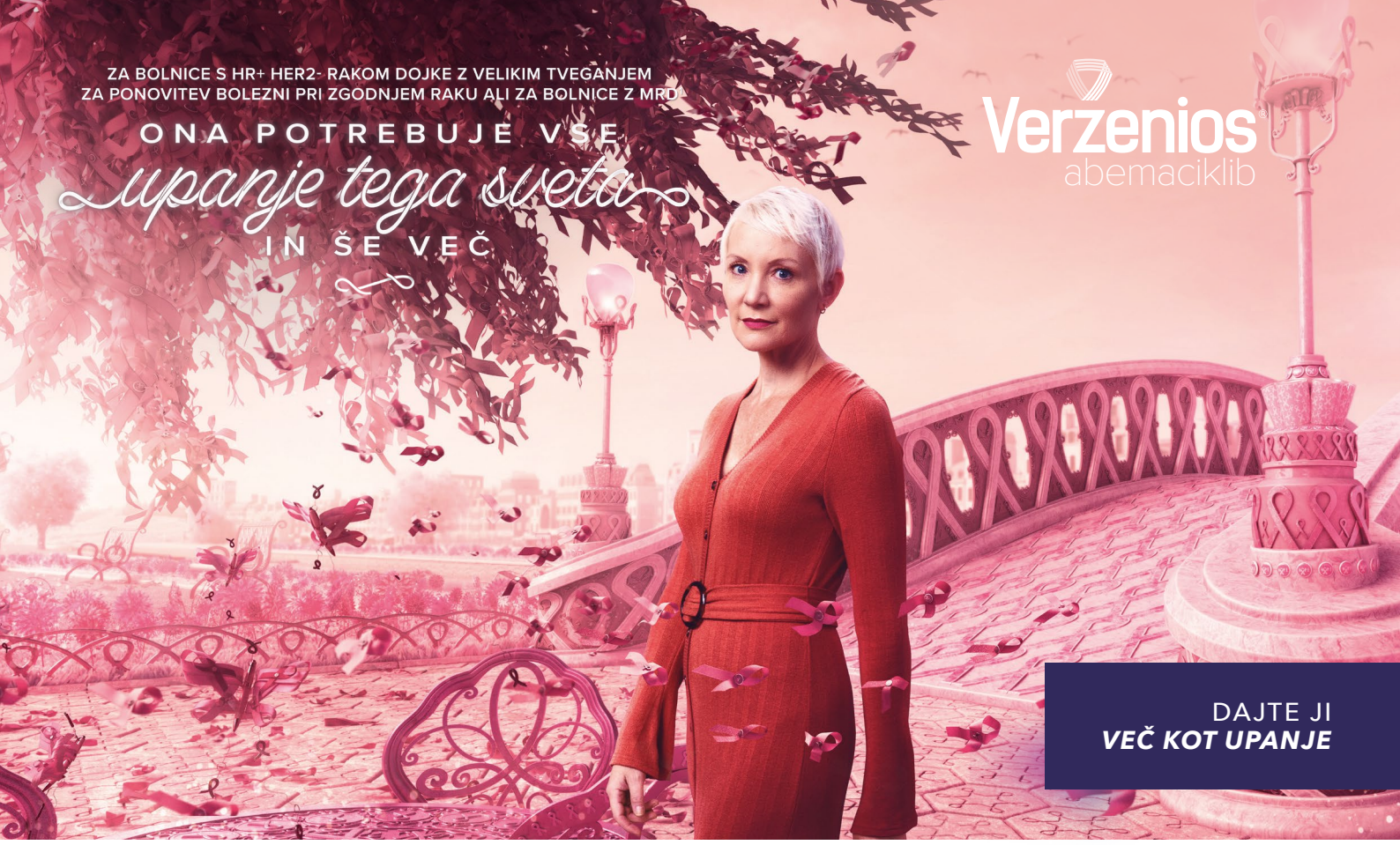

SKRAJŠAN POVZETEK GLAVNIH ZNAČILNOSTI ZDRAVILA

IME ZDRAVILA: Verzenios 50 mg/100 mg/150 mg filmsko obložene tablete **KAKOVOSTNA IN KOLIČINSKA SESTAVA:** Ena filmsko obložena tableta vsebuje 50 mg/100 mg/150 mg abemacikliba. Ena filmsko obložena tableta vsebuje 14 mg/28 mg/42 mg laktoze (v obliki monohidrata). **Terapevtske indikacije**: Zgodnji rak dojk: Zdravilo Verzenios je v kombinaciji z endokrinim zdravljenjem indicirano za adjuvantno zdravljenje odraslih bolnikov z na hormonske receptorje (HR) pozitivnim, na receptorje humanega epidermalnega rastnega faktorja 2 (HER2) negativnim zgodnjim rakom dojk s pozitivnimi bezgavkami, pri katerih obstaja veliko tveganje za ponovitev. Pri ženskah v pred- ali perimenopavzi je treba endokrino zdravljenje z zaviralcem aromataze kombinirati z agonistom gonadoliberina LHRH – luteinizing hormone-releasing hormone). Napredovali ali metastatski rak dojk: Zdravilo Verzenios je indicirano za zdravljenje žensk z lokalno napredovalim ali metastatskim, na hormonske receptorje (HR) pozitivnim in na receptorje humanega epidermalnega rastnega faktorja 2 (HER2) negativnim rakom dojk v kombinaciji z zaviralcem aromataze ali s fulvestrantom kot začetnim endokrinim zdravljenjem ali pri ženskah, ki so prejele predhodno endokrino zdravljenje. Pri ženskah v pred- ali perimenopavzi je treba endokrino zdravljenje kombinirati z agonistom LHRH. **Odmerjanje in način uporabe**: Zdravljenje z zdravilom Verzenios mora uvesti in nadzorovati zdravnik, ki ima izkušnje z uporabo zdravil za zdravljenje rakavih bolezni. Priporočeni odmerek abemacikliba je 150 mg dvakrat na dan, kadar se uporablja v kombinaciji z endokrinim zdravljenjem. *Zgodnji rak dojk:* Zdravilo Verzenios je treba jemati neprekinjeno dve leti, ali do ponovitve bolezni ali pojava nesprejemljive toksičnosti. *Napredovali ali metastatski rak dojk:* Zdravilo Verzenios je treba jemati, dokler ima bolnica od zdravljenja klinično korist ali do pojava nesprejemljive toksičnosti. Če bolnica bruha ali izpusti odmerek zdravila Verzenios, ji je treba naročiti, da naj naslednji odmerek vzame ob predvidenem času; dodatnega odmerka ne sme vzeti. Obvladovanje nekaterih neželenih učinkov lahko zahteva prekinitev in/ali zmanjšanje odmerka. Zdravljenje z abemaciklibom prekinite v primeru povišanja vrednosti AST in/ali ALT >3 x ZMN SKUPAJ s celokupnim bilirubinom > 2,0 x ZMN v odsotnosti holestaze ter pri bolnicah z intersticijsko pljučno boleznijo (ILD)/pnevmonitis stopnje 3 ali 4. Sočasni uporabi močnih zaviralcev CYP3A4 se je treba izogibati. Če se uporabi močnih zaviralcev CYP3A4 ni mogoče izogniti, je treba odmerek abemaciklibа znižati na 100 mg dvakrat na dan. Pri bolnicah, pri katerih je bil odmerek znižan na 100 mg abemaciklibа dvakrat na dan in pri katerih se sočasnemu dajanju močnega zaviralca CYP3A4 ni mogoče izogniti, je treba odmerek abemaciklibа dodatno znižati na 50 mg dvakrat na dan. Pri bolnicah, pri katerih je bil odmerek znižan na 50 mg abemaciklibа dvakrat na dan in pri katerih se sočasnemu dajanju močnega zaviralca CYP3A4 ni mogoče izogniti, je mogoče z odmerkom abemaciklibа nadaljevati ob natančnem spremljanju znakov toksičnosti. Alternativno je mogoče odmerek abemaciklibа znižati na 50 mg enkrat na dan ali prekiniti dajanje abemaciklibа. Če je uporaba zaviralca CYP3A4 prekinjena, je treba odmerek abemaciklibа povečati na odmerek, kakršen je bil pred uvedbo zaviralca CYP3A4 (po 3-5 razpolovnih časih zaviralca CYP3A4). Prilagajanje odmerka glede na starost in pri bolnicah z blago ali zmerno ledvično okvaro ter z blago (Child Pugh A) ali zmerno (Child Pugh B) jetrno okvaro ni potrebno. Pri dajanju abemaciklibа bolnicam s hudo ledvično okvaro sta potrebna previdnost in skrbno spremljanje glede znakov toksičnosti. Način uporabe: Zdravilo Verzenios je namenjeno za peroralno uporabo. Odmerek se lahko vzame s hrano ali brez nje. Zdravila se ne sme jemati z grenivko ali grenivkinim sokom. Bolnice naj odmerke vzamejo vsak dan ob približno istem času. Tableto je treba pogoltniti celo (bolnice tablet pred zaužitjem ne smejo gristi, drobiti ali deliti). **Kontraindikacije**: Preobčutljivost na učinkovino ali katero koli pomožno snov. **Posebna opozorila in previdnostni ukrepi**: Pri bolnicah, ki so prejemale abemaciklib, so poročali o nevtropeniji, o večji pogostnosti okužb kot pri bolnicah, zdravljenih s placebom in endokrinim zdravljenjem, o povečanih vrednostih ALT in AST. Pri bolnicah, pri katerih se pojavi nevtropenija stopnje 3 ali 4, je priporočljivo prilagoditi odmerek. Do primerov nevtropenične sepse s smrtnim izidom je prišlo pri < 1 % bolnic z metastatskim rakom dojk. Bolnicam je treba naročiti, naj o vsaki epizodi povišane telesne temperature poročajo zdravstvenemu delavcu. Bolnice je treba spremljati za znake in simptome globoke venske tromboze (VTE) in pljučne embolije ter jih zdraviti, kot je medicinsko utemeljeno. Glede na stopnjo VTE bo morda treba spremeniti odmerek abemaciklibа. Pri bolnikih, pri katerih se pojavi resni arterijski trombembolični dogodek (ATE), je treba oceniti koristi in tveganja nadaljnjega zdravljenja z abemaciklibom. Glede na povečanje vrednosti ALT ali AST je mogoče potrebna prilagoditev odmerka. Driska je najpogostejši neželeni učinek. Bolnice je treba ob prvem znaku tekočega blata začeti zdraviti z antidiaroiki, kot je loperamid, povečati vnos peroralnih tekočin in obvestiti zdravnika. Sočasni uporabi induktorjev CYP3A4 se je treba izogibati zaradi tveganja za zmanjšano učinkovitost abemaciklibа. Bolnice z redkimi dednimi motnjami, kot so intoleranca za galaktozo, popolno pomanjkanje laktase ali malapsorpcija glukoze/galaktoze, tega zdravila ne smejo jemati. Bolnice je treba spremljati glede pljučnih simptomov, ki kažejo na ILD/pnevmonitis, in jih ustrezno zdraviti. Glede na stopnjo ILD/pnevmonitisa je morda potrebno prilagajanje odmerka abemaciklibа. **Medsebojno delovanje z drugimi zdravili in druge oblike interakcij**: Abemaciklib se primarno presnavlja s CYP3A4. Sočasna uporaba abemaciklibа in zaviralcev CYP3A4 lahko poveča plazemsko koncentracijo abemaciklibа. Uporabi močnih zaviralcev CYP3A4 sočasno z abemaciklibom se je treba izogibati. Če je močne zaviralce CYP3A4 treba dajati sočasno, je treba odmerek abemaciklibа zmanjšati, nato pa bolnico skrbno spremljati glede toksičnosti. Pri bolnicah, zdravljenih z zmernimi ali šibkimi zaviralci CYP3A4, ni potrebno prilagajanje odmerka, vendar jih je treba skrbno spremljati za znake toksičnosti. Sočasni uporabi močnih induktorjev CYP3A4 (vključno, vendar ne omejeno na: karbamazepin, fenitoin, rifampicin in šentjanževko) se je treba izogibati zaradi tveganja za zmanjšano učinkovitost abemaciklibа. Abemaciklib in njegovi glavni aktivni presnovki zavirajo prenašalce v ledvicah, in sicer kationski organski prenašalec 2 (OCT2) ter prenašalca MATE1. *In vivo* lahko pride do medsebojnega delovanja abemaciklibа in klinično pomembnih substratov teh prenašalcev, kot je dofelitid ali kreatinin. Trenutno ni znano, ali lahko abemaciklib zmanjša učinkovitost sistemskih hormonskih kontraceptivov, zato se ženskam, ki uporabljajo sistemske hormonske kontraceptive, svetuje, da hkrati uporabljajo tudi mehansko metodo. **Neželeni učinki**: Najpogostejši neželeni učinki so driska, okužbe, nevtropenija, levkopenija, anemija, utrujenost, navzea, bruhanje in zmanjšanje apetita. *Zelo pogosti:* okužbe, nevtropenija, levkopenija, anemija, trombocitopenija, limfopenija, zmanjšanje apetita, glavobol, disgevzija, omotica, driska, bruhanje, navzea, stomatitis, alopecija, pruritus, izpuščaj, pireksija, utrujenost, povečana vrednost alanin-aminotransferaze, povečana vrednost aspartat-aminotransferaze *Pogosti:* povečano solzenje, venska trombembolija, ILD/pnevmonitis, dispepsija, spremembe na nohtih, suha koža, mišična šibkost *Občasni:* febrilna nevtropenija, fotopsija **Rok uporabnosti**: 3 leta **Posebna navodila za shranjevanje** Za shranjevanje zdravila niso potrebna posebna navodila. **Imetnik dovoljenja za promet z zdravilom**: Eli Lilly Nederland B.V., Papendorpseweg 83, 3528BJ, Utrecht, Nizozemska. Datum prve odobritve dovoljenja za promet: 27. september 2018. Datum zadnjega podaljšanja: 23. junij 2023. **Datum zadnje revizije besedila**: 4. 7. 2024 **Režim izdaje:** Rp/Spec - Predpisovanje in izdaja zdravila je le na recept zdravnika specialista ustreznega področja medicine ali od njega pooblaščenega zdravnika.

Reference: 1. Povzetek glavnih značilnosti zdravila Verzenios, zadnja odobrena verzija.

Pomembno: Predpisovanje in izdaja zdravila je le na recept zdravnika specialista ustreznega področja medicine ali od njega pooblaščenega zdravnika. Pred predpisovanjem zdravila Verzenios si preberite zadnji veljavni Povzetek glavnih značilnosti zdravil. Podrobne informacije o zdravilu so objavljene na spletni strani Evropske agencije za zdravila http://www.ema.europa.eu

Eli Lilly farmacevtska družba, d.o.o., Dunajska cesta 167, 1000 Ljubljana, telefon 01 / 580 00 10, faks 01 / 569 17 05

PP-AL-SI-0306, 24.9.2024. Samo za strokovno javnost.

PR/BSI/BEN/2024/008

TANTUM VERDE®

benzidaminijev klorid

Za lajšanje bolečine in oteklin v ustni in žrelu, ki so posledica radiomukozitisa

Bistvene informacije iz Povzetka glavnih značilnosti zdravila

Tantum Verde 1,5 mg/ml oralno pršilo, raztopina
Tantum Verde 3 mg/ml oralno pršilo, raztopina

Sestava: 1,5 mg/ml: 1 ml raztopine vsebuje 1,5 mg benzidaminijevega klorida, kar ustreza 1,34 mg benzidamina. V enem razpršku je 0,17 ml raztopine. En razpršek vsebuje 0,255 mg benzidaminijevega klorida, kar ustreza 0,2278 mg benzidamina. **Sestava 3 mg/ml:** 1 ml raztopine vsebuje 3 mg benzidaminijevega klorida, kar ustreza 2,68 mg benzidamina. V enem razpršku je 0,17 ml raztopine. En razpršek vsebuje 0,51 mg benzidaminijevega klorida, kar ustreza 0,4556 mg benzidamina. **Terapevtske indikacije:** Samozdravljenje: Lajšanje bolečine in oteklin pri vnetju v ustni votlini in žrelu, ki so lahko posledica okužb in stanj po operaciji. Po nasvetu in navodilu zdravnika: Lajšanje bolečine in oteklin v ustni votlini in žrelu, ki so posledica radiomukozitisa. **Odmerjanje in način uporabe:** Uporaba: 2- do 6-krat na dan (vsake 1,5 do 3 ure). Odmerjanje 1,5 mg/ml: Odrasli: 4 do 8 razprškov 2- do 6-krat na dan. Pediatrična populacija: Mladostniki, stari od 12 do 18 let: 4-8 razprškov 2- do 6-krat na dan. Otroci od 6 do 12 let: 4 razprški 2- do 6-krat na dan. Otroci, mlajši od 6 let: 1 razpršek na 4 kg telesne mase; do največ 4 razprške 2- do 6-krat na dan. Odmerjanje 3 mg/ml: Odrasli: 2 do 4 razprški 2- do 6-krat na dan. Pediatrična populacija: Mladostniki, stari od 12 do 18 let: 2 do 4 razprški 2- do 6-krat na dan. Otroci od 6 do 12 let: 2 razprška 2- do 6-krat na dan. Otroci, mlajši od 6 let: 1 razpršek na 8 kg telesne mase; do največ 2 razprška 2- do 6-krat na dan. Starejši bolniki, bolniki z jetrno okvaro in bolniki z ledvično okvaro: niso potrebni posebni previdnostni ukrepi. Trajanje zdravljenja ne sme biti daljše od 7 dni. Način uporabe: Za orofaringealno uporabo. Zdravilo se razprši v usta in žrelo. **Kontraindikacije:** Preobčutljivost na učinkovino ali katero koli pomožno snov. **Posebna opozorila in previdnostni ukrepi:** Pri nekaterih bolnikih lahko resne bolezni povzročijo ustne/žrelne ulceracije. Če se simptomi v treh dneh ne izboljšajo, se mora bolnik posvetovati z zdravnikom ali zobozdravnikom, kot je primerno. Uporaba benzidamina ni priporočljiva za bolnike s preobčutljivostjo na salicilno kislino ali druga nesteroidna protivnetna zdravila. Pri bolnikih, ki imajo ali so imeli bronhialno astmo, lahko pride do bronhospazma. Pri takih bolnikih je potrebna previdnost. To zdravilo vsebuje 13,6 mg alkohola (etanola) v enem razpršku (0,17 ml), kar ustreza manj kot 0,34 ml piva oziroma 0,14 ml vina. Majhna količina alkohola v zdravilu ne bo imela nobenih opaznih učinkov. To zdravilo vsebuje metilparahidroksibenzoat (E218). Lahko povzroči alergijske reakcije (lahko zapoznele). To zdravilo vsebuje manj kot 1 mmol (23 mg) natrija v enem razpršku (0,17 ml), kar v bistvu pomeni 'brez natrija'. Zdravilo vsebuje aromo poprove mete z benzilalkoholom, cinamilalkoholom, citralom, citronelolom, geraniolom, izoevgenolom, linalolom, evgenolom in D-limonen, ki lahko povzročijo alergijske reakcije. Zdravilo z jakostjo 3 mg/ml vsebuje makrogolglicerol hidroksistearat 40. Lahko povzroči želodčne težave in drisko. **Medsebojno delovanje z drugimi zdravili in druge oblike interakcij:** Študij medsebojnega delovanja niso izvedli. **Nosečnost in dojenje:** O uporabi benzidamina pri nosečnicah in doječih ženskah ni zadostnih podatkov. Uporaba zdravila med nosečnostjo in dojenjem ni priporočljiva. **Vpliv na sposobnost vožnje in upravljanja strojev:** Zdravilo v priporočenem odmerku nima vpliva na sposobnost vožnje in upravljanja strojev. **Neželeni učinki:** Neznana pogostnost (ni mogoče oceniti iz razpoložljivih podatkov): anafilaktične reakcije, preobčutljivostne reakcije, odrevenelost, laringospazem, suha usta, navzea in bruhanje, oralna hipestezija, angioedem, fotosenzitivnost, pekoč občutek v ustih. Neposredno po uporabi se lahko pojavi občutek odrevenelosti v ustih in v žrelu. Ta učinek se pojavi zaradi načina delovanja zdravila in po kratkem času izgine. **Način in režim izdaje zdravila:** BRp-Izdaja zdravila je brez recepta v lekarnah in specializiranih prodajalnah. **Imetnik dovoljenja za promet:** Aziende Chimiche Riunite Angelini Francesco – A.C.R.A.F. S.p.A., Viale Amelia 70, 00181 Rim, Italija **Datum zadnje revizije besedila:** 05. 04. 2022

Pred svetovanjem ali izdajo preberite celoten Povzetek glavnih značilnosti zdravila.

Samo za strokovno javnost.

Datum priprave informacije: julij 2024

Odgovoren za trženje: Bonifar d.o.o.

ANGELINI

IMFINZI™
durvalumab
50 mg/ml koncentrat za raztopino za infundiranje

AKTIVIRA IMUNSKI SISTEM.
PREPOZNA. **REAGIRA.**

5-LETNO CELOKUPNO PREŽIVETJE BOLNIKOV Z LOKALNO NAPREDOVALIM, NEOPERABILNIM NSCLC S PDL-1 ≥ 1%[1]

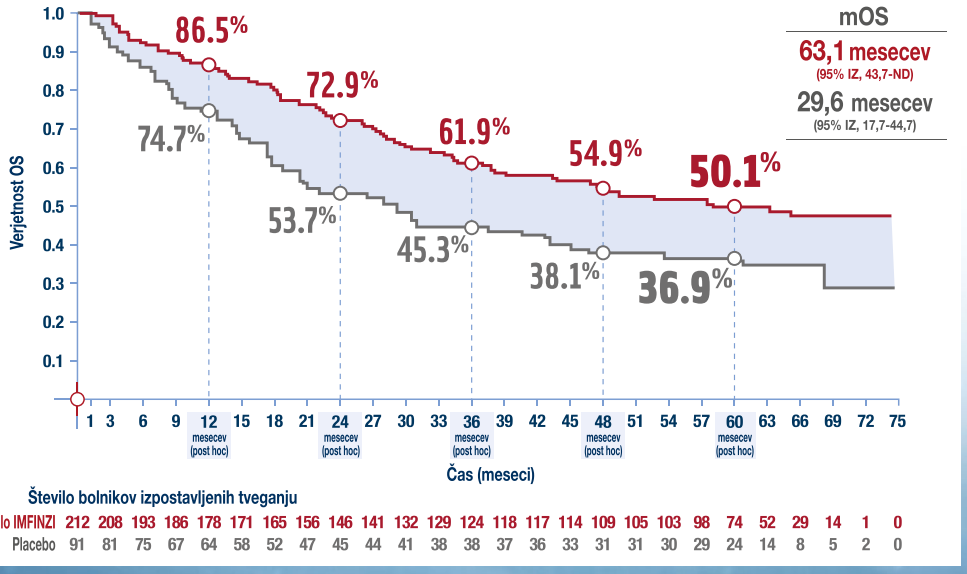

Po petih letih je bilo živih še 50% bolnikov zdravljenih z zdravilom Imfinzi po zaključeni sočasni kemoradioterapiji na osnovi platine.

NSCLC... nedrobnocelični rak pljuč (non small cell lung cancer), mOS...mediano celokupno preživetje

SKRAJŠAN POVZETEK GLAVNIH ZNAČILNOSTI ZDRAVILA

Imfinzi 50 mg/ml koncentrat za raztopino za infundiranje

SESTAVA: 1 ml koncentrata za raztopino za infundiranje vsebuje 50 mg durvalumaba. Ena viala z 2,4 ml koncentrata vsebuje 120 mg durvalumaba. Ena viala z 10 ml koncentrata vsebuje 500 mg durvalumaba. **INDIKACIJE:** *Neoperabilni nedrobnocelični rak pljuč (NSCLC).* Zdravilo IMFINZI je kot samostojno zdravljenje indicirano za zdravljenje lokalno napredovalega, neoperabilnega nedrobnoceličnega raka pljuč (NSCLC – non small cell lung cancer) pri odraslih, ki imajo tumorje z ≥ 1 % izraženostjo PD L1 na tumorskih celicah in pri katerih bolezen ni napredovala po kemoradioterapiji na osnovi platine. Zdravilo IMFINZI je v kombinaciji s tremelimumabom in kemoterapijo na osnovi platine indicirano za prvo linijo zdravljenja odraslih z metastatskim NSCLC brez senzibilizirajočih mutacij EGFR ali pozitivnih mutacij ALK. *Drobnocelični rak pljuč (SCLC).* Zdravilo IMFINZI je v kombinaciji z etopozidom in bodisi karboplatinom bodisi cisplatinom indicirano za prvo linijo zdravljenja odraslih z razsejanim drobnoceličnim rakom pljuč (ES SCLC – extensive stage small cell lung cancer). *Rak biliarnega trakta (RBT).* Zdravilo IMFINZI je v kombinaciji z gemcitabinom in cisplatinom indicirano za prvo linijo zdravljenja odraslih z neoperabilnim ali metastatskim rakom biliarnega trakta (RBT). *Hepatocelularni karcinom (HCK).* Zdravilo IMFINZI je kot samostojno zdravljenje indicirano za prvo linijo zdravljenja odraslih z napredovalim ali neoperabilnim hepatocelularnim karcinomom (HCK). Zdravilo IMFINZI je v kombinaciji s tremelimumabom indicirano za prvo linijo zdravljenja odraslih z napredovalim ali neoperabilnim karcinomom jetrnih celic (hepatocelularnim karcinomom – HCK). **ODMERJANJE IN NAČIN UPORABE:** Zdravljenje mora uvesti in nadzorovati zdravnik, ki ima izkušnje na področju zdravljenja raka. Bolnike z lokalno napredovalim nedrobnoceličnim rakom pljuč je treba za zdravljenje izbrati na podlagi izraženosti PD-L1, ugotovljene z validirano testno metodo. Odmerjanje: Priporočeni odmerek zdravila Imfinzi pri samostojnem zdravljenju pri lokalno napredovalem NSCLC je 10 mg/kg na 2 tedna ali 1500 mg na 4 tedne do napredovanja bolezni, nesprejemljivih toksičnih učinkov ali največ 12 mesecev. Pri HCK je priporočeni odmerek zdravila Imfinzi 1500 mg na 4 tedne do napredovanja bolezni ali do nesprejemljivih toksičnih učinkov. Priporočeni odmerek zdravila Imfinzi pri kombinaranem zdravljenju pri metastatskem NSCLC je med kemoterapijo s platino: 1500 mg v kombinaciji s 75 mg tremelimumaba in kemoterapijo na osnovi platine na 3 tedne (21 dni) 4 cikle (12 tednov), po kemoterapiji s platino: 1500 mg na 4 tedne kot monoterapija in vzdrževalno zdravljenje s pemetreksedom (na podlagi histologije) na 4 tedne, peti odmerek 75 mg tremelimumaba je treba dati 16. teden skupaj z zdravilom Imfinzi. Trajanje zdravljenja je do napredovanja bolezni ali nesprejemljivih toksičnih učinkov. Pri ES-SCLC je priporočeni odmerek zdravila Imfinzi 1500 mg v kombinaciji s kemoterapijo na 3 tedne (21 dni) 4 cikluse in nato 1500 mg na 4 tedne kot samostojno zdravljenje do napredovanja bolezni ali nesprejemljivih toksičnih učinkov. Pri RBT je priporočeni odmerek zdravila Imfinzi 1500 mg v kombinaciji s kemoterapijo na 3 tedne (21 dni) do 8 ciklusov, nato po 1500 mg na 4 tedne kot samostojno zdravljenje do napredovanja bolezni ali nesprejemljivih toksičnih učinkov. Pri HCK je priporočeni odmerek 1500 mg zdravila IMFINZI v kombinaciji s 300 mg tremelimumaba v enem odmerku 1. dan 1. cikla, nato zdravilo Imfinzi kot monoterapija na 4 tedne do napredovanja bolezni ali nesprejemljivih toksičnih učinkov. Povečevanje ali zmanjševanje odmerka ni priporočljivo. Glede na individualno varnost in prenašanje je lahko potrebna odložitev zdravljenja ali trajno prenehanje uporabe zdravila. V primeru domnevnih imunsko pogojenih neželenih učinkov je treba opraviti ustrezno ovrednotenje za potrditev etiologije ozioroma izključitev druge etiologije. Glede na resnost neželenega učinka je treba prenehati uporabljati zdravilo Imfinzi in/ali tremelimumab in pričeti z dajanjem kortikosteroidov. Če se stanje ne izboljša ali se poslabša, pride v poštev povečanje odmerka kortikosteroidov in/ali dodatna uporaba sistemskih imunosupresivov. Po izboljšanju na ≤ 1. stopnjo je treba začeti s postopnim zmanjševanjem kortikosteroida in ga zmanjševati v obdobju vsaj 1 meseca. Po odložitvi uporabe je mogoče zdravilo Imfinzi in/ali tremelimumab znova začeti uporabljati v času 12 tednov, če se neželeni učinki izboljšajo na ≤ 1. stopnjo in je odmerek kortikosteroida zmanjšan na ≤ 10 mg prednizona ali ekvivalenta na dan. Zdravilo Imfinzi in tremelimumab je treba dokončno ukiniti, če se imunsko pogojeni neželeni učinki 3. stopnje (močno izraženi) ponavljajo in pri katerih koli imunsko pogojenih neželenih učinkih 4. stopnje (življenjsko nevarni), razen pri endokrinopatijah, ki jih nadziramo z nadomestnimi hormoni. Način uporabe: Zdravilo Imfinzi je namenjeno za intravensko uporabo. Dati ga je treba kot raztopino za intravensko infundiranje v obdobju 1 ure. Če je zdravilo Imfinzi uporabljeno v kombinaciji s kemoterapijo, je treba dati zdravilo Imfinzi pred kemoterapijo na isti dan. Če je zdravilo Imfinzi uporabljeno v kombinaciji s tremelimumabom in kemoterapijo na osnovi platine, je treba najprej dati tremelimumab, ki mu v istem dnevu sledita zdravilo Imfinzi in nato kemoterapija na osnovi platine. Če je zdravilo Imfinzi uporabljeno v kombinaciji s petim odmerkom tremelimumaba in vzdrževalnim zdravljenjem s pemetreksedom 16. teden, je treba najprej dati tremelimumab, ki mu v istem dnevu sledita zdravilo Imfinzi in potem vzdrževalno zdravljenje s pemetreksedom. Zdravilo Imfinzi, tremelimumab in kemoterapijo na osnovi platine je treba dati v ločenih intravenskih infuzijah. Dajanje zdravila Imfinzi in tremelimumaba vsako traja po 1 uro. Če je zdravilo Imfinzi uporabljeno v kombinaciji s tremelimumabom, je treba dati tremelimumab pred zdravilom Imfinzi na isti dan. Zdravilo Imfinzi in tremelimumab je treba dati v ločenih intravenskih infuzijah. **KONTRAINDIKACIJE:** Preobčutljivost na učinkovino (učinkovine) ali katero koli pomožno snov. **OPOZORILA IN PREVIDNOSTNI UKREPI:** Za izboljšanje sledljivosti bioloških zdravil je treba jasno zabeležiti lastniško ime in številko serije uporabljenega zdravila. Imunsko pogojeni pnevmonitis: Pri bolnikih, ki so prejemali zdravilo Imfinzi ali zdravilo Imfinzi v kombinaciji s tremelimumabom, sta se pojavila imunsko pogojeni pnevmonitis ali intersticijska bolezen pljuč, opredeljeno kot potreba po uporabi sistemskih kortikosteroidov in brez jasne druge etiologije. Pnevmonitis in radiacijski pnevmonitis: Pri bolnikih, zdravljenih z radioterapijo pljuč, je pogost radiacijski pnevmonitis in klinična slika pnevmonitisa in radiacijskega pnevmonitisa je zelo podobna. V študiji PACIFIC sta se pri bolnikih, ki so opravili zdravljenje z najmanj 2 cikloma sočasne kemoradioterapije od 1 do 42 dni pred začetkom preskušanja, pnevmonitis ali radiacijski pnevmonitis pojavila pri 161 (33,9 %) bolnikih v skupini z zdravilom Imfinzi in pri 58 (24,8 %) bolnikih v skupini s placebom, vključno s 3. stopnjo (3,4 % in 3,0 %) in 5. stopnjo (1,1 % in 1,7 %). Bolnike je treba spremljati glede znakov in simptomov pnevmonitisa ali radiacijskega pnevmonitisa. Imunsko pogojeni hepatitis: Pri bolnikih, ki so prejemali zdravilo Imfinzi ali zdravilo Imfinzi v kombinaciji s tremelimumabom, se je pojavil imunsko pogojeni hepatitis, opredeljen kot potreba po sistemskih kortikosteroidih in brez jasne druge etiologije. Alanin-aminotransferazo, aspartat-aminotransferazo, celokupni bilirubin in alkalno fosfatazo kontrolirajte pred začetkom zdravljenja in pred vsako nadaljnjo infuzijo. Dodaten nadzor pride v poštev na podlagi klinične ocene. Imunsko pogojeni kolitis: Pri bolnikih, ki so prejemali zdravilo Imfinzi ali zdravilo Imfinzi v kombinaciji s tremelimumabom, sta se pojavila imunsko pogojeni kolitis ali driska, opredeljeno kot potreba po sistemskih kortikosteroidih in brez jasne druge etiologije. Pri bolnikih, ki so prejemali zdravilo Imfinzi v kombinaciji s tremelimumabom, so poročali o neželenih učinkih perforacije črevesa in perforacije debelega črevesa. Imunsko pogojene endokrinopatije: Imunsko pogojeni hipotiroidizem, hipertiroidizem in tiroiditis: Pri bolnikih, ki so prejemali zdravilo Imfinzi ali zdravilo Imfinzi v kombinaciji s tremelimumabom, so se pojavili imunsko pogojeni hipotiroidizem, hipertiroidizem in tiroiditis; hipertiroidizmu lahko sledi hipotiroidizem. Bolnike je treba spremljati glede nenormalnih izvidov delovanje ščitnice pred zdravljenjem in redno med zdravljenjem ter kot je potrebno glede na klinično oceno. Imunsko pogojena adrenalna insuficienca: Pri bolnikih, ki so prejemali zdravilo Imfinzi ali zdravilo Imfinzi v kombinaciji s tremelimumabom, se je pojavila imunsko pogojena adrenalna insuficienca. Bolnike je treba spremljati glede kliničnih znakov in simptomov adrenalne insuficience. Imunsko pogojena sladkorna bolezen tipa 1: Pri bolnikih, ki so prejemali zdravilo Imfinzi ali zdravilo Imfinzi v kombinaciji s tremelimumabom, se je pojavila imunsko pogojena sladkorna bolezen tipa 1, ki se lahko najprej kaže kot diabetična ketoacidoza, ki je lahko smrtno nevarna, če je dovolj zgodaj ne odkrijemo. Bolnike je treba spremljati glede kliničnih znakov in simptomov sladkorne bolezni tipa 1. Imunsko pogojeni hipofizitis/hipopituitarizem: Pri bolnikih, ki so prejemali zdravilo Imfinzi ali zdravilo Imfinzi v kombinaciji s tremelimumabom, sta se pojavila imunsko pogojena hipofizitis ali hipopituitarizem. Bolnike je treba spremljati glede kliničnih znakov in simptomov hipofizitisa ali hipopituitarizma. Imunsko pogojeni nefritis: Pri bolnikih, ki so prejemali zdravilo Imfinzi ali zdravilo Imfinzi v kombinaciji s tremelimumabom, se je pojavil imunsko pogojeni nefritis, opredeljen kot potreba po sistemskih kortikosteroidih in brez jasne druge etiologije. Imunsko pogojeni izpuščaj: Pri bolnikih, ki so prejemali zdravilo Imfinzi ali zdravilo Imfinzi v kombinaciji s tremelimumabom, se je pojavil imunsko pogojeni izpuščaj ali dermatitis (vključno s pemfigoidom), opredeljen kot potreba po sistemskih kortikosteroidih in brez jasne druge etiologije. Pri bolnikih, ki so bili zdravljeni z zaviralci PD-1, so poročali o pojavljanju Stevens-Johnsonovega sindroma ali toksične epidermalne nekrolize. Imunsko pogojeni miokarditis: Pri bolnikih, ki so prejemali zdravilo Imfinzi ali zdravilo Imfinzi v kombinaciji s tremelimumabom, se je pojavil imunsko pogojeni miokarditis, ki je lahko usoden. Imunsko pogojeni pankreatitis: Pri bolnikih, ki so prejemali zdravilo Imfinzi v kombinaciji s tremelimumabom in kemoterapijo, se je pojavil imunsko pogojeni pankreatitis. Drugi imunsko pogojeni neželeni učinki: Glede na mehanizem delovanja zdravila Imfinzi ali zdravila Imfinzi v kombinaciji s tremelimumabom se lahko pojavijo še drugi potencialno imunsko pogojeni učinki. Naslednji imunsko pogojeni neželeni učinki so bili opaženi pri bolnikih, ki so prejemali samostojno zdravljenje z zdravilom Imfinzi ali zdravilo Imfinzi v kombinaciji s tremelimumabom: miastenija gravis, transverzni mielitis, miozitis, polimiozitis, meningitis, encefalitis, Guillain Barréjev sindrom, imunska trombocitopenija, neinfektivni cistitis. Z infundiranjem povezane reakcije: Bolnike je treba spremljati glede znakov in simptomov z infundiranjem povezanih reakcij. Pri bolnikih, ki so prejemali zdravilo Imfinzi ali zdravilo Imfinzi v kombinaciji s tremelimumabom, so bile opisane hude z infundiranjem povezane reakcije. Za bolezen specifični previdnostni ukrepi (RBT): Holangitis in okužbe biliarnega trakta pri bolnikih z napredovalim RBT niso redke. V študiji TOPAZ-1 so o primerih holangitisa poročali v obeh terapevtskih skupinah (14,5 % v skupini z zdravilom Imfinzi + kemoterapijo, 8,2 % v skupini s placebom + kemoterapijo); ti primeri so bili večinoma povezani z biliarnimi opornicami in niso imeli imunsko posredovane etiologije. Bolnike z RBT (zlasti tiste z biliarno opornico) je treba natančno nadzorovati glede holangitisa ali okužb biliarnega trakta tako pred uvedbo zdravljenja kot redno med zdravljenjem. Metastatski NSCLC: Podatkov o starejših bolnikih (≥ 75 let), zdravljenih z zdravilom Imfinzi v kombinaciji s tremelimumabom in kemoterapijo na osnovi platine, je malo. Morebitno korist/tveganje te sheme je priporočljivo skrbno pretehtati za vsakega bolnika posebej. Bolniki, ki niso bili vključeni v klinične študije: V klinične študije niso bili vključeni bolniki z naslednjimi značilnostmi: izhodiščno oceno zmogljivosti ECOG ≥ 2; aktivno ali predhodno dokumentirano avtoimunsko boleznijo v 2 letih pred začetkom študije; anamnezo imunske pomanjkljivosti; anamnezo hudih imunsko pogojenih neželenih učinkov; boleznimi, ki so zahtevale sistemsko imunosupresijo, razen fiziološkega odmerka sistemskih kortikosteroidov (≤ 10 mg na dan prednizona ali ekvivalenta); neobvladanimi sočasnimi boleznimi; aktivno tuberkulozo ali okužbo s hepatitisom B ali C ali HIV; bolniki, ki so prejeli živo oslabljeno cepivo v 30 dneh pred začetkom zdravljenja z zdravilom Imfinzi ali v 30 dneh po začetku. Dokler takšnih podatkov ni, je treba durvalumab v teh skupinah bolnikov uporabljati previdno ter po skrbnem individualnem pretehtanju možnih koristi in tveganj za posameznega bolnika. Varnost sočasnega profilaktičnega kranialnega obsevanja obenem z zdravilom Imfinzi pri bolnikih z ES SCLC ni znana. **MEDSEBOJNO DELOVANJE Z DRUGIMI ZDRAVILI:** Razen fizioloških odmerkov sistemskih kortikosteroidov (≤ 10 mg na dan prednizona ali ekvivalenta) pred uvedbo durvalumaba ni priporočljivo uporabljati sistemskih kortikosteroidov ali imunosupresivov, ker lahko vplivajo na farmakodinamično aktivnost in učinkovitost durvalumaba. Vendar pa je mogoče kortikosteroide ali druge imunosupresive uporabiti po začetku zdravljenja z durvalumabom za zdravljenje imunsko pogojenih neželenih učinkov. Z durvalumabom niso izvedli formalnih farmakokinetičnih (PK) študij medsebojnega delovanja zdravil. Primarni poti odstranjevanja durvalumaba sta katabolizem beljakovin preko retikuloendotelijskega sistema oziroma tarčno posredovano odstranjevanje, zato ni pričakovati presnovnih medsebojnih delovanj med zdravili. Farmakokinetična medsebojna delovanja med durvalumabom in kemoterapijo so ocenjevali v študiji CASPIAN; izkazalo se je, da sočasno zdravljenje z durvalumabom ne vpliva na farmakokinetiko etopozida, karboplatina ali cisplatina. Poleg tega populacijska farmakokinetična analiza kaže, da sočasno zdravljenje s kemoterapijo ne vpliva pomembno na farmakokinetiko durvalumaba. Farmakokinetična medsebojna delovanja med durvalumabom v kombinaciji s tremelimumabom in kemoterapijo na osnovi platine so ocenili v študiji POSEIDON. Izkazalo se je, da med sočasnim zdravljenjem ni bilo klinično pomembnih farmakokinetičnih medsebojnih delovanj med tremelimumabom, durvalumabom, nab-paklitakselom, gemcitabinom, pemetreksedom, karboplatinom ali cisplatinom. **PLODNOST, NOSEČNOST IN DOJENJE:** Ženske v rodni dobi morajo med zdravljenjem z durvalumabom in vsaj še 3 mesece po zadnjem odmerku durvalumaba uporabljati učinkovito kontracepcijo. Podatkov o uporabi durvalumaba pri nosečnicah ni. Glede na mehanizem delovanja durvalumab lahko vpliva na vzdrževanje nosečnosti; v alogenskem modelu nosečnosti pri miših je bilo ugotovljeno, da moteno signaliziranje PD-L1 poveča izgubo plodov. Pri nosečnici uporabljeni durvalumab lahko škoduje plodu in ga ni priporočljivo uporabljati med nosečnostjo in pri ženskah v rodni dobi, ki ne uporabljajo učinkovite kontracepcije med zdravljenjem in vsaj še 3 mesece po zadnjem odmerku. Ni znano, ali se durvalumab pri človeku izloča v materinem mleku. Pri človeku protitelesa lahko prehajajo v materino mleko, a možnost absorpcije in škode za novorojenčka ni znana. Toda možnega tveganja za dojenega otroka ni mogoče izključiti. Odločiti se je treba, ali naj ženska prekine z dojenjem ali naj prekine zdravljenje z durvalumabom oziroma sploh ne začne zdravljenja z njim, pri čemer je treba upoštevati koristi dojenja za otroka in koristi zdravljenja za žensko. Podatkov o možnih vplivih durvalumaba na plodnost pri človeku ali živalih ni. **NEŽELENI UČINKI:** Ugotovitve o varnosti zdravila Imfinzi pri samostojnem zdravljenju temeljijo na kumulativnih podatkih 4045 bolnikov z več vrstami tumorjev. Zdravilo Imfinzi so uporabljali v odmerku 10 mg/kg na 2 tedna, 20 mg/kg na 4 tedne ali 1500 mg/kg na 4 tedne. Najpogostejši neželeni učinki (> 10 %) so bili kašelj/produktiven kašelj (18,7 %), driska (16,1 %), izpuščaj (15,5 %), artralgija (13,8 %), zvišana telesna temperatura (13,0 %), bolečine v trebuhu (13,0 %), okužbe zgornjih dihal (12,1 %), srbenje (11,4 %) in hipotiroidizem (10,9 %). Podatki o varnosti zdravila Imfinzi v kombinaciji s kemoterapijo temeljijo na kumulativnih podatkih 603 bolnikov iz 2 študij (TOPAZ-1 in CASPIAN). Najpogostejši (> 10 %) neželeni učinki so bili nevtropenija (53,1 %), anemija (43,9 %), navzea (37,5 %), utrujenost (36,8 %), trombocitopenija (28,0 %), zaprtje (25,4 %), zmanjšan apetit (22,6 %), bolečine v trebuhu (18,4 %), alopecija (18,4 %), levkopenija (17,2 %), bruhanje (16,9 %), zvišana telesna temperatura (15,1 %), izpuščaj (14,8 %), driska (13,8 %), zvišana aspartat-aminotransferaza ali zvišana alanin-aminotransferaza (10,9 %), kašelj/produktiven kašelj (10,8 %) in srbenje (10,4 %). Izsledki o varnosti zdravila Imfinzi v kombinaciji s 75 mg tremelimumaba in kemoterapijo temeljijo na podatkih 330 bolnikov z metastatskim NSCLC. Najpogostejši (> 20 %) neželeni učinki so bili anemija (49,7 %), navzea (41,5 %), nevtropenija (41,2 %), utrujenost (36,1 %), izpuščaj (25,8 %), trombocitopenija (24,5 %) in driska (21,5 %). Izsledki o varnosti zdravila Imfinzi v kombinaciji z enkratnim odmerkom 300 mg tremelimumaba temeljijo na združenih podatkih 462 bolnikov v HCK iz študije HIMALAYA in še ene študije pri bolnikih s HCK, študija 22. Najpogostejši neželeni učinki (> 10 %) so bili izpuščaj (32,5 %), srbenje (25,5 %), driska (25,3 %), bolečine v trebuhu (19,7 %), zvišana aspartat aminotransferaza/zvišana alanin aminotransferaza (18,0 %), zvišana telesna temperatura (13,9 %), hipotiroidizem (13,0 %), kašelj/produktiven kašelj (10,8 %), periferni edemi (10,4 %) in zvišana lipaza (10,0 %). **VRSTA IN VSEBINA OVOJNINE:** 2,4 ml (skupno 120 mg durvalumaba) koncentrata v stekleni viali iz stekla tipa 1 z elastomernim zamaškom in sivo snemno aluminijsko zaporo. Pakiranje vsebuje 1 vialo. 10 ml (skupno 500 mg durvalumaba) koncentrata v stekleni viali iz stekla tipa 1 z elastomernim zamaškom in belo snemno aluminijsko zaporo. Pakiranje vsebuje 1 vialo. **NAČIN IZDAJANJA ZDRAVILA:** H - Predpisovanje in izdaja zdravila je le na recept. **DATUM REVIZIJA BESEDILA:** 14.12.2023 (ŠI-3708). **IMETNIK DOVOLJENJA ZA PROMET:** AstraZeneca AB, S-151 85, Sodertalje, Švedska

Pred predpisovanjem, prosimo, preberite celoten povzetek glavnih značilnosti zdravila.
Dodatne informacije so na voljo pri družbi AstraZeneca UK Limited, Podružnica v Sloveniji, Verovškova 55, Ljubljana, telefon +386 1 51 35 600.

Samo za strokovno javnost. Informacija pripravljena januarja 2024.

Reference: 1.Spigel DR, Faivre-Finn C, Gray JE, et al. Five-year survival outcomes from the PACIFIC trial: durvalumab after chemoradiotherapy in stage III non-small-cell lung cancer. J Clin Oncol. Forthcoming 2021.

AstraZeneca

SI-3715

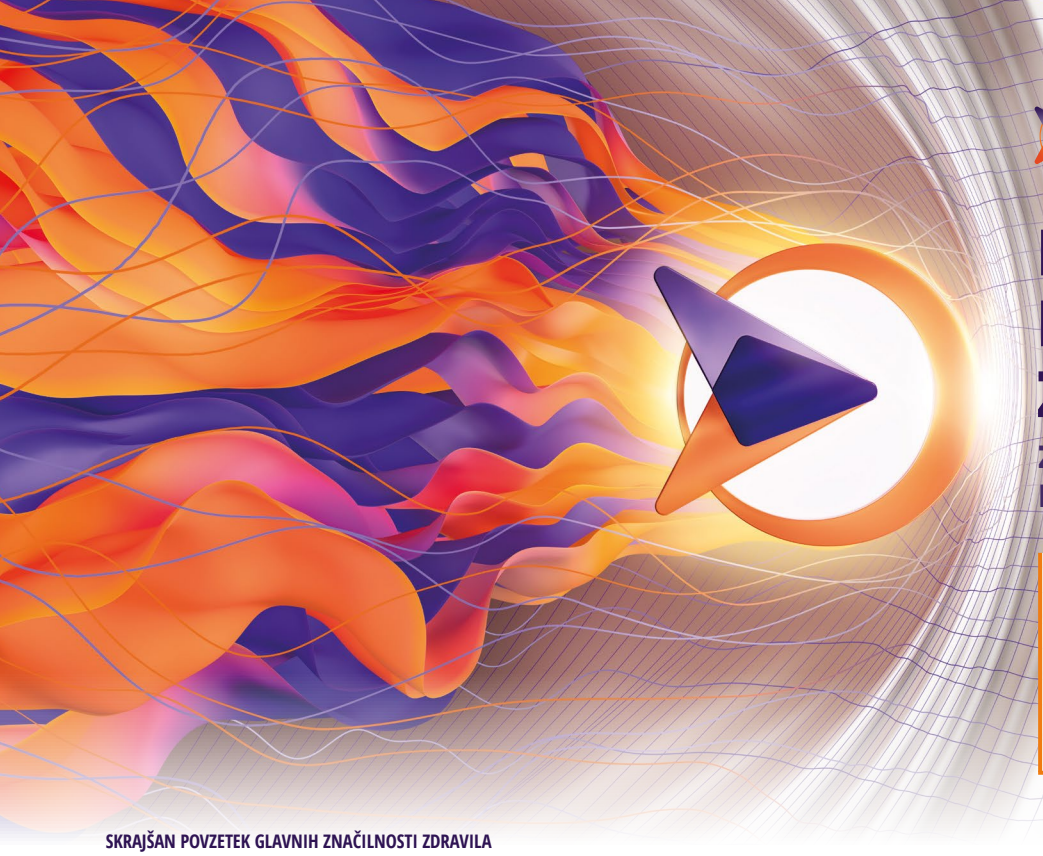

ENHERTU®
trastuzumab derukstekan

PREMIKAMO MEJE ZDRAVLJENJA

Z UČINKOVITOSTJO, KI PRESEGA PRIČAKOVANJA

- Terapija izbora v smernicah za 2L HER2+ raka dojk[1-5]
- Prvo in edino zdravljenje proti HER2, ki je učinkovito tudi pri bolnikih z nizkim izražanjem HER2*.[1,3-6]

SKRAJŠAN POVZETEK GLAVNIH ZNAČILNOSTI ZDRAVILA

▼Za to zdravilo se izvaja dodatno spremljanje varnosti. Tako bodo hitreje na voljo nove informacije o njegovi varnosti. Zdravstvene delavce naprošamo, da poročajo o katerem koli domnevnem neželenem učinku zdravila.

ENHERTU 100 mg prašek za koncentrat za raztopino za infundiranje

SESTAVA: Ena viala praška za koncentrat za raztopino za infundiranje vsebuje 100 mg trastuzumab derukstekana. Po rekonstituciji ena viala s 5 ml raztopine vsebuje 20 mg/ml trastuzumab derukstekana. Trastuzumab derukstekan je konjugat protitelesa in zdravila, ki vsebuje humanizirano monoklonsko protitelo IgG1 proti HER2 z istim zaporedjem aminokislin, kot ga ima trastuzumab. Proizvajajo ga sesalske celice (ovarij kitajskega hrčka) in je prek razcepljivega veznika na tetrapeptidni bazi kovalentno vezan na DXd, ki je derivat eksatekana in zaviralec topoizomeraze I. Na vsako molekulo protitelesa je vezanih približno 8 molekul derukstekana. *Pomožne snovi*: L-histidin, L-histidinijev klorid monohidrat, saharoza, polisorbat 80. **TERAPEVTSKE INDIKACIJE:** ***Rak dojk:*** *HER2-pozitiven rak dojk:* Zdravilo Enhertu kot monoterapija je indicirano za zdravljenje odraslih bolnikov z neresektabilnim ali metastatskim HER2-pozitivnim rakom dojk, ki so pred tem že prejeli eno ali več shem zdravljenja na podlagi anti-HER2. *Rak dojk z nizkim statusom HER2:* Zdravilo Enhertu kot monoterapija je indicirano za zdravljenje odraslih bolnikov z neresektabilnim ali metastatskim rakom dojk z nizkim statusom HER2, ki so pred tem že prejeli kemoterapijo v prisotnosti metastaz ali pa se je pri njih bolezen ponovila med adjuvantno kemoterapijo ali znotraj 6 mesecev po njenem zaključku. ***Nedrobnocelični rak pljuč*** (NSCLC - non-small cell lung cancer): Zdravilo Enhertu kot monoterapija je indicirano za zdravljenje odraslih bolnikov z napredovalim NSCLC, ki imajo tumorje z aktivirajočo mutacijo HER2 (ERBB2) in potrebujejo sistemsko terapijo po kemoterapiji na podlagi platine z imunoterapijo ali brez nje. ***Rak želodca:*** Zdravilo Enhertu v obliki monoterapije je indicirano za zdravljenje odraslih bolnikov z napredovalim HER2-pozitivnim adenokarcinomom želodca ali gastroezofagealnega prehoda, ki so pred tem že prejeli shemo na podlagi trastuzumaba. **ODMERJANJE IN NAČIN UPORABE:** Zdravilo Enhertu mora predpisati zdravnik in njegovo dajanje nadzorovati zdravstveni delavec, ki sta izkušena v uporabi zdravil proti raku. Za preprečitev napak, povezanih z zdravili, je pomembno, da preverite nalepke na vialah in se prepričate, da je zdravilo, ki se pripravlja in daje, res zdravilo Enhertu (trastuzumab derukstekan), in ne trastuzumab ali trastuzumab emtanzin. Zdravilo Enhertu se ne sme zamenjati s trastuzumabom ali trastuzumab emtanzinom. Bolniki, ki se zdravijo s trastuzumab derukstekanom zaradi *HER2-pozitivnega raka dojk, raka želodca ali gastroezofagealnega prehoda*, morajo imeti dokumentiran HER2-pozitiven status tumorja, ki je opredeljen kot ocena 3 + na podlagi imunohistokemije (IHC) ali razmerje ≥ 2,0 na podlagi *in situ* hibridizacije (ISH) ali fluorescenčne *in situ* hibridizacije (FISH), ocenjeno z *in vitro* diagnostičnim (IVD) medicinskim pripomočkom z oznako CE. Bolniki, ki se zdravijo s trastuzumab derukstekanom zaradi *raka dojk z nizkim statusom HER2*, morajo imeti dokumentiran nizek status HER2 tumorja, ki je opredeljen kot ocena IHC 1+ ali IHC 2+/ISH-, ocenjeno z IVD z oznako CE. Bolniki, ki se zdravijo s trastuzumab derukstekanom zaradi napredovalega NSCLC, morajo imeti aktivirajočo mutacijo HER2 (ERBB2), odkrito z *in vitro* diagnostičnim (IVD) medicinskim pripomočkom, označenim s CE. Če IVD z oznako CE ni na voljo, je treba status HER2 in status mutacije HER2 oceniti z drugim potrjenim testom. Odmerjanje: *Rak dojk in NSCLC:* Priporočeni odmerek zdravila Enhertu je 5,4 mg/kg, ki se daje z intravensko infuzijo enkrat vsake 3 tedne (21-dnevni cikel) do napredovanja bolezni ali nesprejemljive toksičnosti. *Rak želodca:* Priporočeni odmerek zdravila Enhertu je 6,4 mg/kg, ki se daje z intravensko infuzijo enkrat vsake 3 tedne (21-dnevni cikel) do napredovanja bolezni ali nesprejemljive toksičnosti. Začetni odmerek je treba dati z 90-minutno intravensko infuzijo. Če bolnik prejšnjo infuzijo dobro prenaša, se lahko naslednji odmerki zdravila Enhertu dajejo kot 30-minutne infuzije. Hitrost infundiranja zdravila Enhertu je treba zmanjšati ali infundiranje prekiniti, če se pri bolniku razvijejo simptomi, povezani z infuzijo. V primeru hudih reakcij na infuzijo je treba zdravilo Enhertu trajno ukiniti. Premedikacija: Zdravilo Enhertu je emetogeno, kar vključuje zapoznelo navzeo in/ali bruhanje. Pred vsakim odmerkom zdravila Enhertu je treba bolnike premedicirati s kombiniranim režimom dveh ali treh zdravil (npr. deksametazon z antagonistom receptorjev 5-HT3 in/ali antagonistom receptorjev NK1 ter drugimi zdravili, kot je indicirano) za preprečevanje navzee in bruhanja zaradi kemoterapije. Prilagajanje odmerka: Obvladovanje neželenih učinkov lahko zajema začasno prekinitev uporabe, zmanjšanje odmerka ali ukinitev zdravljenja z zdravilom Enhertu, skladno s smernicami, podanimi v povzetku glavnih značilnosti zdravila (preglednici 1 in 2). Po zmanjšanju odmerka zdravila Enhertu se odmerek ne sme več ponovno povečati. Načrt zmanjševanja odmerka: Priporočeni začetni odmerek je 5,4 mg/kg pri raku dojk in NSCLC oz. 6,4 mg/kg pri raku želodca; prvo zmanjšanje odmerka (4,4 mg/kg oz. 5,4 mg/kg), drugo zmanjšanje odmerka (3,2 mg/kg oz. 4,4 mg/kg), pri potrebi po nadaljnjem zmanjšanju odmerka ukinite zdravljenje. *Prosimo, glejte celoten povzetek glavnih značilnosti zdravila Enhertu za prilagajanje odmerka zaradi neželenih učinkov: intersticijska pljučna bolezen (IPB)/pnevmonitis* (asimptomatska IPB/asimptomatski pnevmonitis (stopnja 1), simptomatska IPB/simptomatski pnevmonitis (stopnja 2 ali višja)), *nevtropenija* (stopnja 3 (manj kot 1,0-0,5 × 10^9/l), stopnja 4 (manj kot 0,5 × 10^9/l)), *febrilna nevtropenija* (absolutno število nevtrofilcev manj kot 1,0 × 10^9/l in telesna temperatura, višja od 38,3 °C, ali telesna temperatura 38 °C ali višja, ki vztraja več kot eno uro), *zmanjšan iztisni delež levega prekata* (LVEF) (LVEF več kot 45 % in absolutno zmanjšanje glede na izhodiščno vrednost za 10 % do 20 %; LVEF 40 % do 45 %; LVEF manj kot 40 % ali absolutno zmanjšanje glede na izhodiščno vrednost za več kot 20 %; simptomatično kongestivno srčno popuščanje). Zakasnjen ali izpuščen odmerek: Če se načrtovani odmerek zakasni ali izpusti, ga je treba dati takoj, ko je mogoče, brez čakanja na naslednji načrtovani cikel. Časovni načrt dajanja je treba prilagoditi, da se ohrani 3-tedenski razmik med odmerki. Infuzijo je treba dati s hitrostjo in odmerkom, ki ga je bolnik prenašal pri zadnji infuziji. Posebne populacije: *Starejši:* Pri bolnikih, starih 65 let ali starejših, prilagajanje odmerka zdravila Enhertu ni potrebno. Podatki pri bolnikih, starih ≥ 75 let, so omejeni. *Okvara ledvic:* Prilagajanje odmerka pri bolnikih z blago (očistek kreatinina [CLcr] ≥ 60 in < 90 ml/min) ali zmerno (CLcr ≥ 30 in < 60 ml/min) okvaro ledvic ni potrebno. Morebitne potrebe po prilagajanju odmerka pri bolnikih s hudo okvaro ledvic ali končno ledvično odpovedjo ni mogoče opredeliti, ker je bila huda okvara ledvic v kliničnih študijah izključitveni kriterij. Pri bolnikih z zmerno okvaro ledvic so opazili višjo pogostnost IPB stopnje 1 in 2/pnevmonitisa, ki sta vodila do zvečanja števila prekinitev zdravljenja. Pri bolnikih z zmerno okvaro ledvic v izhodišču, ki so prejemali zdravilo Enhertu 6,4 mg/kg, so ugotovili večjo pogostnost resnih neželenih učinkov kot pri tistih z normalnim delovanjem ledvic. Bolnike z zmerno ali hudo okvaro ledvic je treba natančno spremljati glede neželenih učinkov, vključno z IPB/pnevmonitisom. *Okvara jeter:* Pri bolnikih, ki imajo celokupni bilirubin ≤ 1,5-kratnik zgornje meje normalnih vrednosti (ZMN), ne glede na vrednost aspartat transaminaze (AST), odmerka ni treba prilagajati. Morebitne potrebe po prilagajanju odmerka pri bolnikih, ki imajo celokupni bilirubin > 1,5-kratnik ZMN, ne glede na vrednost AST, ni mogoče opredeliti zaradi omejenih podatkov. Zato je treba te bolnike natančno spremljati. Način uporabe: Zdravilo Enhertu je za intravensko uporabo. Zdravstveni delavec ga mora rekonstituirati in razredčiti. Treba ga je dati z intravenskim infundiranjem. Zdravilo Enhertu se ne sme dati kot hitro intravensko injekcijo ali bolus. **KONTRAINDIKACIJE:** Preobčutljivost na učinkovino ali katero koli pomožno snov. **POSEBNA OPOZORILA IN PREVIDNOSTNI UKREPI:** Intersticijska pljučna bolezen/pnevmonitis: Pri zdravilu Enhertu so poročali o primerih intersticijske pljučne bolezni (IPB) in/ali pnevmonitisa. Nekateri primeri so bili smrtni. Bolnikom je treba naročiti, naj takoj poročajo o kašlju, dispneji, zvišani telesni temperaturi in/ali katerih koli novih dihalnih simptomih ali poslabšanju obstoječih. Bolnike je treba spremljati glede znakov in simptomov IPB/pnevmonitisa. Dokaze za IPB/pnevmonitis je treba takoj proučiti. Bolnike s sumom na IPB/pnevmonitis je treba oceniti z radiografskimi posnetki, najbolje z računalniško tomografijo (CT). Treba je razmisliti o posvetu s pulmologom. Nevtropenija: V kliničnih študijah z zdravilom Enhertu so poročali o primerih nevtropenije, vključno s primeri febrilne nevtropenije s smrtnim izidom. Pred uvedbo zdravila Enhertu in pred vsakim odmerkom ter vsakič, ko je klinično indicirano, je treba preveriti celotno krvno sliko. Morda bo treba začasno prekiniti dajanje zdravila Enhertu ali zmanjšati odmerek, odvisno od tega, kako huda je nevtropenija. Zmanjšanje iztisnega deleža levega prekata: Pri zdravljenjih anti-HER2 so poročali o zmanjšanem iztisnem deležu levega prekata (LVEF). Pred uvedbo zdravljenja z zdravilom Enhertu in v rednih intervalih med njim (v skladu s kliničnimi indikacijami) je treba izvesti standardne preiskave delovanja srca (ehokardiografija ali slikanje MUGA) za oceno LVEF. Zmanjšanje LVEF je treba obvladovati s prekinitvami zdravljenja. Zdravljenje z zdravilom Enhertu je treba trajno ukiniti, če se potrdi LVEF manj kot 40 % ali absolutno zmanjšanje glede na izhodiščno vrednost za več kot 20 %. Zdravilo Enhertu je treba trajno ukiniti pri bolnikih s simptomatskim kongestivnim srčnim popuščanjem. Embrio-fetalna toksičnost: Zdravilo Enhertu lahko ima škodljiv vpliv na plod, če se da nosečnici. Pri ženskah v rodni dobi je treba pred uvedbo zdravljenja z zdravilom Enhertu preveriti status nosečnosti. Bolnice je treba seznaniti z možnimi tveganji za plod. Ženskam v rodni dobi je treba svetovati, da uporabljajo učinkovito kontracepcijo med zdravljenjem in še vsaj 7 mesecev po zadnjem odmerku zdravila Enhertu. Moškim bolnikom s partnerkami v rodni dobi je treba svetovati, da uporabljajo učinkovito kontracepcijo med zdravljenjem z zdravilom Enhertu in še vsaj 4 mesece po zadnjem odmerku zdravila Enhertu. Bolniki z zmerno ali hudo okvaro jeter: Zdravilo Enhertu je treba pri bolnikih z zmerno in hudo okvaro jeter dajati previdno. **MEDSEBOJNO DELOVANJE Z DRUGIMI ZDRAVILI IN DRUGE OBLIKE INTERAKCIJ:** Pri sočasnem dajanju trastuzumab derukstekana z zdravili, ki so zaviralci CYP3A ali OATP1B ali prenašalcev P-gp, odmerka ni treba prilagajati. **PLODNOST, NOSEČNOST IN DOJENJE:** Nosečnost: Dajanje zdravila Enhertu nosečnicam se ne priporoča. Bolnice je treba seznaniti z možnimi tveganji za plod, preden zanosijo. Ženske, ki zanosijo, se morajo takoj obrniti na zdravnika. Če ženska zanosi med zdravljenjem z zdravilom Enhertu ali v obdobju 7 mesecev po zadnjem odmerku zdravila Enhertu, se priporoča natančno spremljanje. Dojenje: Ni znano, ali se trastuzumab derukstekan izloča v materino mleko. Humani IgG se izloča v materino mleko in potencial za absorpcijo in resne neželene učinke na dojenčka ni znan. Zato ženske ne smejo dojiti med zdravljenjem z zdravilom Enhertu in še 7 mesecev po zadnjem odmerku. Odločiti se je treba med prenehanjem dojenja in prenehanjem zdravljenja z zdravilom Enhertu, pri čemer je treba pretehtati prednosti dojenja za otroka in prednosti zdravljenja za mater. Plodnost: Namenskih študij plodnosti s trastuzumab derukstekanom niso izvedli. Ni znano, ali so trastuzumab derukstekan ali njegovi presnovki prisotni v semenski tekočini. Pred začetkom zdravljenja je treba moškim bolnikom svetovati, da se posvetujejo o možnosti shranjevanja semena. Moški bolniki v celotnem obdobju zdravljenja in še najmanj 4 mesece po zadnjem odmerku zdravila Enhertu ne smejo zamrzniti ali darovati semena. **NEŽELENI UČINKI:** *Zdravilo Enhertu 5,4 mg/kg:* Združeno varnostno populacijo so ocenili pri bolnikih, ki so v kliničnih študijah dobili vsaj en odmerek 5,4 mg/kg zdravila Enhertu (N = 1449) zaradi različnih vrst tumorjev. Mediani čas trajanja zdravljenja v tej združeni populaciji je bil 9,8 meseca (razpon: 0,7-45,1 meseca). *Zelo pogosti:* okužba zgornjih dihal, anemija, nevtropenija, trombocitopenija, levkopenija, limfopenija, hipokaliemija, zmanjšan apetit, glavobol, omotica, intersticijska pljučna bolezen, dispneja, kašelj, epistaksa, navzea, bruhanje, zaprtje, driska, bolečina v trebuhu, stomatitis, dispepsija, zvišane transaminaze, alopecija, mišično-skeletna bolečina, utrujenost, pireksija, zmanjšan iztisni delež, zmanjšanje telesne mase. *Pogosti:* pljučnica, dehidracija, disgevzija, suhe oči, zamegljen vid, abdominalna distenzija, gastritis, flatulenca, izpuščaj, pruritus, hiperpigmentacija kože, perifermni edem, zvišana alkalna fosfataza v krvi, zvišan bilirubin v krvi, zvišan kreatinin v krvi, reakcije, povezane z infuzijo. *Zdravilo Enhertu 6,4 mg/kg:* Združeno varnostno populacijo so ocenili za bolnike, ki so v kliničnih študijah dobili vsaj en odmerek 6,4 mg/kg zdravila Enhertu (N = 669) zaradi različnih vrst tumorjev. Mediani čas trajanja zdravljenja v tej združeni populaciji je bil 5,7 meseca (razpon: 0,7-41,0 meseca). *Zelo pogosti:* pljučnica, okužba zgornjih dihal, anemija, nevtropenija, trombocitopenija, levkopenija, limfopenija, hipokaliemija, zmanjšan apetit, glavobol, disgevzija, intersticijska pljučna bolezen, dispneja, kašelj, navzea, bruhanje, driska, zaprtje, bolečina v trebuhu, stomatitis, zvišane transaminaze, alopecija, mišično-skeletna bolečina, utrujenost, pireksija, perifermni edem, zmanjšan iztisni delež, zmanjšanje telesne mase. *Pogosti:* febrilna nevtropenija, dehidracija, omotica, suhe oči, zamegljen vid, epistaksa, dispepsija, abdominalna distenzija, gastritis, flatulenca, izpuščaj, pruritus, hiperpigmentacija kože, zvišana alkalna fosfataza v krvi, zvišan bilirubin v krvi, zvišan kreatinin v krvi, reakcije, povezane z infuzijo. **IMETNIK DOVOLJENJA ZA PROMET Z ZDRAVILOM:** Daiichi Sankyo Europe GmbH, Zielstattstrasse 48, 81379 München, Nemčija **DATUM ZADNJE REVIZIJE BESEDILA:** 11. 1. 2024 (SI-3585) **REŽIM PREDPISOVANJA IN IZDAJE:** H **Prosimo, da pred predpisovanjem preberete celoten povzetek glavnih značilnosti zdravila.** Dodatne informacije so na voljo pri podjetju AstraZeneca UK Limited, Podružnica v Sloveniji, Verovškova 55, 1000 Ljubljana, telefon: 01/51 35 600.

Literatura: 1. Povzetek glavnih značilnosti zdravila ENHERTU, 11. 1. 2024, **2.** Cortes J et al; Trastuzumab Deruxtecan versus Trastuzumab Emtansine for Breast Cancer; NEJM 2022;386(12):1143-1154, **3.** Gennari A et al: Ann Oncol 2021;32(12): 1475-1495 **4.** Curigliano G et al. ESMO Metastatic Breast Cancer Living Guidelines, v1.1 May 2023, https://www.esmo.org/living-guidelines/esmo-metastatic-breast-cancer-living-guideline, dostopano 12. 3. 2024 **5.** NCCN guidelines Breast Cancer, v1.2024, https://www.nccn.org/professionals/physician_gls/pdf/breast.pdf, dostopano 12. 3. 2024. **6.** Hurvitz SA. DESTINY-changing results for advanced breast cancer. N Engl J Med. 2022;387(1):75-76.

* rak dojk z nizkim izražanjem HER2 je definiran kor IHK1+ ali IHK2+/ISH-

Datum priprave materiala: marec 2024. Samo za strokovno javnost. SI-3868

Daiichi-Sankyo | AstraZeneca

KEYTRUDA® je odobrena za zdravljenje več kot 30 indikacij rakavih obolenj[1]

Referenca: 1. Keytruda EU SmPC

SKRAJŠAN POVZETEK GLAVNIH ZNAČILNOSTI ZDRAVILA • Pred predpisovanjem, prosimo, preberite celoten Povzetek glavnih značilnosti zdravila! • Ime zdravila: KEYTRUDA 25 mg/ml koncentrat za raztopino za infundiranje vsebuje pembrolizumab. **• Terapevtske indikacije:** Zdravilo KEYTRUDA je kot samostojno zdravljenje indicirano za zdravljenje: odraslih in mladostnikov, starih 12 let ali več, z napredovalim (neoperabilnim ali metastatskim) melanomom; za adjuvantno zdravljenje odraslih in mladostnikov, starih 12 let ali več, z melanomom v stadiju IIB, IIC ali III, in sicer po popolni kirurški odstranitvi; za adjuvantno zdravljenje odraslih z nedrobnoceličnim pljučnim rakom, ki imajo visoko tveganje za ponovitev bolezni po popolni kirurški odstranitvi in kemoterapiji na osnovi platine; metastatskega nedrobnoceličnega pljučnega raka (NSCLC) v prvi liniji zdravljenja pri odraslih, ki imajo tumorje z ≥ 50 % izraženostjo PD-L1 (TPS) in brez pozitivnih tumorskih mutacij EGFR ali ALK; lokalno napredovalega ali metastatskega NSCLC pri odraslih, ki imajo tumorje z ≥ 1 % izraženostjo PD-L1 (TPS) in so bili predhodno zdravljeni z vsaj eno shemo kemoterapije, bolniki s pozitivnimi tumorskimi mutacijami EGFR ali ALK so pred prejemom zdravila KEYTRUDA morali prejeti tudi tarčno zdravljenje; odraslih in pediatričnih bolnikov, starih 3 leta ali več, s ponovljenim ali neodzivnim klasičnim Hodgkinovim limfomom (cHL), pri katerih avtologna presaditev matičnih celic (ASCT) ni bila uspešna, ali po najmanj dveh predhodnih zdravljenjih kadar ASCT ne pride v poštev kot možnost zdravljenja; lokalno napredovalega ali metastatskega urotelijskega raka pri odraslih, predhodno zdravljenih s kemoterapijo, ki je vključevala platino; lokalno napredovalega ali metastatskega urotelijskega raka pri odraslih, ki niso primerni za zdravljenje s kemoterapijo, ki vsebuje cisplatin in imajo tumorje z izraženostjo PD-L1 ≥ 10, ocenjeno s kombinirano pozitivno oceno (CPS); ponovljenega ali metastatskega ploščatoceličnega raka glave in vratu (HNSCC) pri odraslih, ki imajo tumorje z ≥ 50 % izraženostjo PD-L1 (TPS), in pri katerih je bolezen napredovala med zdravljenjem ali po zdravljenju s kemoterapijo, ki je vključevala platino; za adjuvantno zdravljenje odraslih z rakom ledvičnih celic s povišanim tveganjem za ponovitev bolezni po nefrektomiji, ali po nefrektomiji in kirurški odstranitvi metastatskih lezij, za zdravljenje odraslih z MSI-H (microsatellite instability-high) ali dMMR (mismatch repair deficient) kolorektalnim rakom v naslednjih terapevtskih okoliščinah: prva linija zdravljenja metastatskega kolorektalnega raka; zdravljenje neoperabilnega ali metastatskega kolorektalnega raka po predhodnem kombiniranem zdravljenju, ki je temeljilo na fluoropirimidinu; in za zdravljenje MSI-H ali dMMR tumorjev pri odraslih z: napredovalim ali ponovljenim rakom endometrija, pri katerih je bolezen napredovala med ali po predhodnem zdravljenju, ki je vključevalo platino, v katerih koli terapevtskih okoliščinah, in ki niso kandidati za kurativno operacijo ali obsevanje; neoperabilnim ali metastatskim rakom želodca, tankega črevesa ali biliarnega trakta, pri katerih je bolezen napredovala med ali po vsaj enem predhodnem zdravljenju. Zdravilo KEYTRUDA je kot samostojno zdravljenje ali v kombinaciji s kemoterapijo s platino in 5-fluorouracilom (5-FU) indicirano za prvo linijo zdravljenja metastatskega ali neoperabilnega ponovljenega ploščatoceličnega raka glave in vratu pri odraslih, ki imajo tumorje z izraženostjo PD-L1 s CPS ≥ 1. Zdravilo KEYTRUDA je v kombinaciji s kemoterapijo, ki vključuje platino, indicirano za neoadjuvantno zdravljenje, in v nadaljevanju kot samostojno zdravljenje za adjuvantno zdravljenje odraslih z operabilnih nedrobnoceličnim pljučnim rakom, ki imajo visoko tveganje za ponovitev bolezni; v kombinaciji s pemetreksedom in kemoterapijo na osnovi platine je indicirano za prvo linijo zdravljenja metastatskega neploščatoceličnega NSCLC pri odraslih, pri katerih tumorji nimajo pozitivnih mutacij EGFR ali ALK; v kombinaciji s karboplatinom in bodisi paklitakselom bodisi nab-paklitakselom je indicirano za prvo linijo zdravljenja metastatskega ploščatoceličnega NSCLC pri odraslih; v kombinaciji z enfortumab vedotinom je indicirano za prvo linijo zdravljenja neoperabilnega ali metastatskega urotelijskega raka pri odraslih; v kombinaciji z aksitinibom ali v kombinaciji z lenvatinibom je indicirano za prvo linijo zdravljenja napredovalega raka ledvičnih celic (RCC) pri odraslih; v kombinaciji s kemoterapijo s platino in fluoropirimidinom je indicirano za prvo linijo zdravljenja lokalno napredovalega neoperabilnega ali metastatskega raka požiralnika pri odraslih, ki imajo tumorje z izraženostjo PD-L1 s CPS ≥ 10; v kombinaciji s kemoterapijo za neoadjuvantno zdravljenje, in v nadaljevanju kot samostojno adjuvantno zdravljenje po kirurškem posegu, je indicirano za zdravljenje odraslih z lokalno napredovalim trojno negativnim rakom dojk ali trojno negativnim rakom dojk v zgodnjem stadiju z visokim tveganjem za ponovitev bolezni; v kombinaciji s kemoterapijo je indicirano za zdravljenje lokalno ponovljenega neoperabilnega ali metastatskega trojno negativnega raka dojk pri odraslih, ki imajo tumorje z izraženostjo PD-L1 s CPS ≥ 10 in predhodno niso prejeli kemoterapije za metastatsko bolezen; v kombinaciji s karboplatinom in paklitakselom je indicirano za prvo linijo zdravljenja primarno napredovalega ali ponovljenega raka endometrija (EC) pri odraslih, ki so kandidati za sistemsko zdravljenje; v kombinaciji z lenvatinibom je indicirano za zdravljenje napredovalega ali ponovljenega raka endometrija pri odraslih z napredovalo boleznijo med ali po predhodnem zdravljenju s kemoterapijo, ki je vključevala platino, v katerih koli terapevtskih okoliščinah, in ki niso kandidati za kurativno operacijo ali obsevanje; v kombinaciji s kemoradioterapijo (zdravljenje z zunanjim obsevanjem, ki mu sledi brahiterapija) je indicirano za zdravljenje lokalno napredovalega raka materničnega vratu v stadiju III - IVA po FIGO 2014 pri odraslih, ki niso prejeli predhodne definitivne terapije; v kombinaciji s kemoterapijo, z bevacizumabom ali brez njega, je indicirano za zdravljenje persistentnega, ponovljenega ali metastatskega raka materničnega vratu pri odraslih bolnicah, ki imajo tumorje z izraženostjo PD-L1 s CPS ≥ 1; v kombinaciji s trastuzumabom, fluoropirimidinom in kemoterapijo, ki vključuje platino, je indicirano za prvo linijo zdravljenja lokalno napredovalega neoperabilnega ali metastatskega HER2-pozitivnega adenokarcinoma želodca ali gastroezofagealnega prehoda pri odraslih, ki imajo tumorje z izraženostjo PD-L1 s CPS ≥ 1; v kombinaciji s fluoropirimidinom in kemoterapijo, ki vključuje platino, je indicirano za prvo linijo zdravljenja lokalno napredovalega neoperabilnega ali metastatskega HER2-negativnega adenokarcinoma želodca ali gastroezofagealnega prehoda pri odraslih, ki imajo tumorje z izraženostjo PD-L1 s CPS ≥ 1; v kombinaciji z gemcitabinom in cisplatinom je indicirano za prvo linijo zdravljenja lokalno napredovalega neoperabilnega ali metastatskega raka biliarnega trakta pri odraslih. **• Odmerjanje in način uporabe:** Testiranje PD-L1: Če je navedeno v indikaciji, je treba izbiro bolnika za zdravljenje z zdravilom KEYTRUDA na podlagi izraženosti PD-L1 tumorja potrditi z validirano preiskavo. Testiranje MSI/MMR: Če je navedeno v indikaciji, je treba izbiro bolnika za zdravljenje z zdravilom KEYTRUDA na podlagi MSI-H/dMMR statusa tumorja potrditi z validirano preiskavo. Odmerjanje: Priporočeni odmerek zdravila KEYTRUDA pri odraslih je bodisi 200 mg na 3 tedne ali 400 mg na 6 tednov, apliciran z intravensko infuzijo v 30 minutah. Priporočeni odmerek zdravila KEYTRUDA za samostojno zdravljenje pri pediatričnih bolnikih s cHL, starih 3 leta ali več, ali bolnikih z melanomom, starih 12 let ali več, je 2 mg/kg telesne mase (do največ 200 mg) na 3 tedne, apliciran z intravensko infuzijo v 30 minutah. Za uporabo v kombinaciji glejte povzetke glavnih značilnosti zdravil sočasno uporabljenih zdravil. Če se zdravilo KEYTRUDA uporablja kot del kombiniranega zdravljenja skupaj z intravensko kemoterapijo, je treba zdravilo KEYTRUDA aplicirati prvo. Če se zdravilo KEYTRUDA uporablja kot del kombiniranega zdravljenja skupaj z enfortumab vedotinom, je treba zdravilo KEYTRUDA aplicirati po enfortumab vedotinu, kadar sta uporabljena na isti dan. Bolnike je treba zdraviti do napredovanja bolezni ali nesprejemljivih toksičnih učinkov (in do maksimalnega trajanja zdravljenja, če je le to določeno za indikacijo). Pri adjuvantnem zdravljenju melanoma, NSCLC ali RCC je treba zdravilo uporabljati do ponovitve bolezni, pojava nesprejemljivih toksičnih učinkov oziroma mora zdravljenje trajati do enega leta. Za neoadjuvantno in adjuvantno zdravljenje operabilnega NSCLC morajo bolniki neoadjuvantno prejeti zdravilo KEYTRUDA v kombinaciji s kemoterapijo, in sicer 4 odmerke po 200 mg na 3 tedne ali 2 odmerka po 400 mg na 6 tednov ali do napredovanja bolezni, ki izključuje definitivni kirurški poseg, ali do pojava nesprejemljivih toksičnih učinkov, čemur sledi adjuvantno zdravljenje z zdravilom KEYTRUDA kot samostojnim zdravljenjem, in sicer 13 odmerkov po 200 mg na 3 tedne ali 7 odmerkov po 400 mg na 6 tednov ali do ponovitve bolezni ali do pojava nesprejemljivih toksičnih učinkov. Bolniki, pri katerih pride do napredovanja bolezni, ki izključuje definitivni kirurški poseg, ali do nesprejemljivih toksičnih učinkov, povezanih z zdravilom KEYTRUDA kot neoadjuvantnim zdravljenjem v kombinaciji s kemoterapijo, ne smejo prejeti zdravila KEYTRUDA kot samostojnega zdravljenja za adjuvantno zdravljenje. Za neoadjuvantno in adjuvantno zdravljenje TNBC morajo bolniki neoadjuvantno prejeti zdravilo KEYTRUDA v kombinaciji s kemoterapijo, in sicer 8 odmerkov po 200 mg na 3 tedne ali 4 odmerke po 400 mg na 6 tednov, ali do napredovanja bolezni, ki izključuje definitivni kirurški poseg, ali do pojava nesprejemljivih toksičnih učinkov, čemur sledi adjuvantno zdravljenje z zdravilom KEYTRUDA kot samostojnim zdravljenjem, in sicer 9 odmerkov po 200 mg na 3 tedne ali 5 odmerkov po 400 mg na 6 tednov ali do ponovitve bolezni ali pojava nesprejemljivih toksičnih učinkov. Bolniki, pri katerih pride do napredovanja bolezni, ki izključuje definitivni kirurški poseg, ali do nesprejemljivih toksičnih učinkov povezanih z zdravilom KEYTRUDA kot neoadjuvantnim zdravljenjem v kombinaciji s kemoterapijo, ne smejo prejeti zdravila KEYTRUDA kot samostojnega zdravljenja za adjuvantno zdravljenje. Za lokalno napredovalega raka materničnega vratu morajo bolnice prejeti zdravilo KEYTRUDA sočasno s kemoradioterapijo, čemur sledi samostojno zdravljenje z zdravilom KEYTRUDA. Zdravilo KEYTRUDA se lahko daje v odmerku 200 mg na 3 tedne ali 400 mg na 6 tednov do napredovanja bolezni, pojava nesprejemljivih toksičnih učinkov ali do 24 mesecev. Če je aksitinib uporabljen v kombinaciji s pembrolizumabom, se lahko razmisli o povečanju odmerka aksitiniba nad začetnih 5 mg v presledkih šest tednov ali več. V primeru uporabe v kombinaciji z lenvatinibom je treba zdravljenje z enim ali obema zdraviloma prekiniti, kot je primerno. Uporabo lenvatiniba je treba zadržati, odmerek zmanjšati ali prenehati z uporabo, v skladu z navodili v povzetku glavnih značilnosti zdravila za lenvatinib, in sicer za kombinacijo s pembrolizumabom. Pri bolnikih starih ≥ 65 let, bolnikih z blago do zmerno okvaro ledvic, bolnikih z blago ali zmerno okvaro jeter prilagoditev odmerka ni potrebna. Odložitev odmerka ali ukinitev zdravljenja: Zmanjšanje odmerka zdravila KEYTRUDA ni priporočljivo. Za obvladovanje neželenih učinkov je treba uporabo zdravila KEYTRUDA zadržati ali ukiniti, prosimo, glejte celoten Povzetek glavnih značilnosti zdravila. **• Kontraindikacije:** Preobčutljivost na učinkovino ali katero koli pomožno snov. **• Povzetek posebnih opozoril, previdnostnih ukrepov, interakcij in neželenih učinkov:** Imunsko pogojeni neželeni učinki (pnevmonitis, kolitis, hepatitis, nefritis, endokrinopatije, neželeni učinki na kožo in drugi): Pri bolnikih, ki so prejemali pembrolizumab, so se pojavili imunsko pogojeni neželeni učinki, vključno s hudimi in smrtnimi primeri. Večina imunsko pogojenih neželenih učinkov, ki so se pojavili med zdravljenjem s pembrolizumabom, je bila reverzibilnih in so jih obvladali s prekinitvami uporabe pembrolizumaba, uporabo kortikosteroidov in/ali podporno oskrbo. Pojavijo se lahko tudi po zadnjem odmerku pembrolizumaba in hkrati prizadanejo več organskih sistemov. V primeru suma na imunsko pogojene neželene učinke je treba poskrbeti za ustrezno oceno za potrditev etiologije oziroma izključitev drugih vzrokov. Glede na izrazitost neželenega učinka je treba zadržati uporabo pembrolizumaba in uporabiti kortikosteroide – za natančna navodila, prosimo, glejte Povzetek glavnih značilnosti zdravila Keytruda. Zdravljenje s pembrolizumabom lahko poveča tveganje za zavrnitev pri prejemnikih presadkov čvrstih organov. Pri bolnikih, ki so prejemali pembrolizumab, so poročali o hudih z infuzijo povezanih reakcijah, vključno s preobčutljivostjo in anafilaksijo. Pembrolizumab se iz obtoka odstrani s katabolizmom, zato presnovnih medsebojnih delovanj zdravil ni pričakovati. Uporabi sistemskih kortikosteroidov ali imunosupresivov pred uvedbo pembrolizumaba se je treba izogibati, ker lahko vplivajo na farmakodinamično aktivnost in učinkovitost pembrolizumaba. Vendar pa je kortikosteroide ali druge imunosupresive mogoče uporabiti za zdravljenje imunsko pogojenih neželenih učinkov. Kortikosteroide je mogoče uporabiti tudi kot premedikacijo, če je pembrolizumab uporabljen v kombinaciji s kemoterapijo, kot antiemetično profilakso in/ali za ublažitev neželenih učinkov, povezanih s kemoterapijo. Ženske v rodni dobi morajo med zdravljenjem s pembrolizumabom in vsaj še 4 mesece po zadnjem odmerku pembrolizumaba uporabljati učinkovito kontracepcijo, med nosečnostjo in dojenjem se ga ne sme uporabljati. Varnost pembrolizumaba pri samostojnem zdravljenju so v kliničnih študijah ocenili pri 7631 bolnikih, ki so imeli različne vrste raka, s štirimi odmerki (2 mg/kg telesne mase na 3 tedne, 200 mg na 3 tedne in 10 mg/kg telesne mase na 2 ali 3 tedne). V tej populaciji bolnikov je mediani čas opazovanja znašal 8,5 meseca (v razponu od 1 dneva do 39 mesecev), najpogostejši neželeni učinki zdravljenja s pembrolizumabom pa so bili utrujenost (31 %), driska (22 %) in navzea (20 %). Večina poročanih neželenih učinkov pri samostojnem zdravljenju je bila po izrazitosti 1. ali 2. stopnje. Najresnejši neželeni učinki so bili imunsko pogojeni neželeni učinki in hude z infuzijo povezane reakcije. Pojavnost imunsko pogojenih neželenih učinkov pri uporabi pembrolizumaba samega za adjuvantno zdravljenje je znašala 37 % za vse stopnje in 9 % od 3. do 5. stopnje, pri metastatski bolezni pa 25 % za vse stopnje in 6 % od 3. do 5. stopnje. Pri adjuvantnem zdravljenju niso zaznali nobenih novih imunsko pogojenih neželenih učinkov. Varnost pembrolizumaba pri kombiniranem zdravljenju s kemoterapijo ali kemoradioterapijo (CRT) so ocenili pri 6093 bolnikih z različnimi vrstami raka, ki so v kliničnih študijah prejemali pembrolizumab v odmerkih 200 mg, 2 mg/kg telesne mase na vsake 3 tedne. V tej populaciji bolnikov so bili najpogostejši neželeni učinki naslednji: anemija (53 %), navzea (52 %), diareja (36 %), utrujenost (35 %), zaprtost (32 %), bruhanje (28 %), zmanjšano število nevtrofilcev (28 %) in zmanjšanje apetita (27 %). Pojavnost neželenih učinkov 3. do 5. stopnje je pri bolnikih z NSCLC pri kombiniranem zdravljenju s pembrolizumabom znašala 69 % in pri zdravljenju samo s kemoterapijo 61 %, pri bolnikih s HNSCC pri kombiniranem zdravljenju s pembrolizumabom 85 % in pri zdravljenju s kemoterapijo v kombinaciji s cetuksimabom 84 %, pri bolnikih z rakom požiralnika pri kombiniranem zdravljenju s pembrolizumabom 86 % in pri zdravljenju samo s kemoterapijo 83 %, pri bolnikih s TNBC pri kombiniranem zdravljenju s pembrolizumabom 80 % in pri zdravljenju samo s kemoterapijo 77 %, pri bolnicah z rakom materničnega vratu pri kombiniranem zdravljenju s pembrolizumabom (kemoterapija z ali brez bevacizumaba ali v kombinaciji s CRT) 77 % in pri zdravljenju s kemoterapijo z ali brez bevacizumaba ali samostojno s CRT 71 %, pri bolnikih z rakom želodca pri kombiniranem zdravljenju s pembrolizumabom (kemoterapija z ali brez trastuzumaba) 74 % in pri kemoterapiji v kombinaciji z ali brez trastuzumaba 68 %, pri bolnikih z rakom biliarnega trakta pri kombiniranem zdravljenju s pembrolizumabom 85 % in pri samostojni kemoterapiji 84 %, in pri bolnicah z EC pri kombiniranem zdravljenju s pembrolizumabom 59 % in pri samostojni kemoterapiji 46 %. Varnost pembrolizumaba v kombinaciji z aksitinibom ali lenvatinibom pri napredovalem RCC in v kombinaciji z lenvatinibom pri napredovalem EC so ocenili pri skupno 1456 bolnikih z napredovalim RCC ali napredovalim EC, ki so v kliničnih študijah prejemali 200 mg pembrolizumaba na 3 tedne skupaj s 5 mg aksitiniba dvakrat na dan ali z 20 mg lenvatiniba enkrat na dan, kot je bilo ustrezno. V teh populacijah bolnikov so bili najpogostejši neželeni učinki diareja (58 %), hipertenzija (54 %), hipotiroidizem (46 %), utrujenost (41 %), zmanjšan apetit (40 %), navzea (40 %), artralgija (30 %), bruhanje (28 %), zmanjšanje telesne mase (28 %), disfonija (28 %), bolečine v trebuhu (28 %), proteinurija (27 %), sindrom palmarno-plantarne eritrodizestezije (26 %), izpuščaj (26 %), stomatitis (25 %), zaprtost (25 %), mišično-skeletna bolečina (23 %), glavobol (23 %) in kašelj (21 %). Neželenih učinkov od 3. do 5. stopnje je bilo pri bolnikih z RCC med uporabo pembrolizumaba v kombinaciji z aksitinibom ali lenvatinibom 80 % in med uporabo sunitiniba samega 71 %. Pri bolnicah z EC je bilo neželenih učinkov od 3. do 5. stopnje med uporabo pembrolizumaba v kombinaciji z lenvatinibom 89 % in med uporabo kemoterapije same 73 %. Varnost pembrolizumaba v kombinaciji z enfortumab vedotinom so ocenili pri 564 bolnikih z neoperabilnim ali metastatskim urotelijskim rakom, ki so prejemali 200 mg pembrolizumaba 1. dan in 1,25 mg/kg enfortumab vedotina 1. in 8. dan vsakega 21-dnevnega ciklusa. Na splošno so opazili, da je bila pojavnost neželenih učinkov za pembrolizumab v kombinaciji z enfortumab vedotinom višja kot pri samostojnem zdravljenju s pembrolizumabom, kar odraža prispevek enfortumab vedotina in daljšega trajanja kombiniranega zdravljenja. Neželeni učinki so bili na splošno podobni neželenim učinkom, ki so jih opazili pri bolnikih, ki so prejemali pembrolizumab ali enfortumab vedotin kot samostojno zdravljenje. Pojavnost makulopapuloznega izpuščaja vseh stopenj je bila 36 % (10 % od 3. do 4. stopnje), kar je višje, kot je bilo opaženo pri samostojnem zdravljenju s pembrolizumabom. Na splošno so bile pogostnosti neželenih učinkov višje pri bolnikih, starih ≥ 65 let, v primerjavi z bolniki, starimi < 65 let, predvsem za resne neželene učinke (56,3 % pri bolnikih, starih ≥ 65 let, in 35,3 % pri bolnikih, starih < 65 let) in učinke ≥ 3. stopnje (80,3 % pri bolnikih, starih ≥ 65 let, in 64,2 % pri bolnikih, starih < 65 let), podobno kot opažanja pri primerjalni kemoterapiji. Za celoten seznam neželenih učinkov, prosimo, glejte celoten Povzetek glavnih značilnosti zdravila. Za dodatne informacije o varnosti v primeru uporabe pembrolizumaba v kombinaciji glejte povzetke glavnih značilnosti zdravila za posamezne komponente kombiniranega zdravljenja. **• Način in režim izdaje zdravila:** H – Predpisovanje in izdaja zdravila je le na recept, zdravilo se uporablja samo v bolnišnicah. **• Imetnik dovoljenja za promet z zdravilom:** Merck Sharp & Dohme B.V. , Waarderweg 39, 2031 BN Haarlem, Nizozemska.

Merck Sharp & Dohme inovativna zdravila d.o.o.
Ameriška ulica 2, 1000 Ljubljana; tel: +386 1/ 520 42 01, fax: +386 1/ 520 43 50

Samo za strokovno javnost

H - Predpisovanje in izdaja zdravila je le na recept, zdravilo pa se uporablja samo v bolnišnicah. Pred predpisovanjem, prosimo, preberite celoten Povzetek glavnih značilnosti zdravila Keytruda, ki je na voljo pri naših strokovnih sodelavcih ali na lokalnem sedežu družbe.

Zdravilo TECENTRIQ (atezolizumab) 1875 mg raztopina za injiciranje je prvi in edini v EU odobren zaviralec PD-(L)1 za zdravljenje raka v obliki podkožne injekcije[1,2]

TECENTRIQ® SC
subkutani atezolizumab

Možnost hitrejšega odmerjanja atezolizumaba za vas in vaše bolnike[2]

Zdravilo TECENTRIQ 1875 mg raztopina za injiciranje je v EU odobreno za iste indikacije kot intravenski obliki zdravila Tecentriq (Tecentriq 840 mg koncentrat za raztopino za infundiranje ter Tecentriq 1200 mg koncentrat za raztopino za infundiranje)[2]

Zdravilo TECENTRIQ 1875 mg raztopina za injiciranje nudi prednosti za bolnike, zdravstvene delavce in celoten zdravstveni sistem[2–5]

Bolniki

Bolnikom omogoča, da prejmejo zdravljenje v približno **7 minutah**, medtem ko intravenske oblike zdravila TECENTRIQ trajajo od 30 do 60 minut[2,3]

Zdravstveni delavci

Večina zdravstvenih delavcev (75–90 %) je menila, da je podkožna oblika zdravila TECENTRIQ **enostavna za uporabo** in zdravstvenemu osebju **prihrani čas**[3]

Zdravstveni sistem

Pri uporabi podkožnih oblik zdravil so se pokazali **pomembni časovni in stroškovni prihranki**[5]

Zdravilo Tecentriq 1875 mg raztopina za injiciranje še ni krito iz obveznega zdravstvenega zavarovanja.

Reference: 1. Roche sporočilo za javnost: European Commission approves Roche's Tecentriq SC, the EU's first PD-(L)1 cancer immunotherapy subcutaneous injection for multiple cancer types. Dostopno na: https://www.roche.com/media/releases/med-cor-2024-01-16 (datum dostopa: november 2024). 2. Povzetek glavnih značilnosti zdravila Tecentriq: https://www.ema.europa.eu/sl/documents/product-information/tecentriq-epar-product-information_sl.pdf. 3. Burotto M et al. Presented at ESMO 2023, Madrid, Spain, 20–24 October 2023 (Poster 1447). 4. Burotto M et al. Ann Oncol 2023;34(8):693–702. 5. McCloskey C et al. Pharmacoecon Open. 2022;23:1–34.

Skrajšan povzetek glavnih značilnosti zdravila Tecentriq

Ime zdravila: Tecentriq 840 mg koncentrat za raztopino za infundiranje, Tecentriq 1200 mg koncentrat za raztopino za infundiranje in Tecentriq 1875 mg raztopina za injiciranje. **Kakovostna in količinska sestava:** 840 mg i.v.: ena 14-ml viala s koncentratom vsebuje 840 mg atezolizumaba. 1200 mg i.v.: ena 20-ml viala s koncentratom vsebuje 1200 mg atezolizumaba. Po redčenju je končna koncentracija razredčene raztopine med 3,2 mg/ml in 16,8 mg/ml. 1875 mg s.c.: ena viala s 15 ml raztopine za injiciranje vsebuje 1875 mg atezolizumaba. 1 ml raztopine vsebuje 125 mg atezolizumaba. **Terapevtske indikacije:** Urotelijski karcinom (UC): Zdravilo Tecentriq je kot monoterapija indicirano za zdravljenje odraslih bolnikov z lokalno napredovalim ali razsejanim UC, ki: so bili predhodno zdravljeni s kemoterapijo na osnovi platine ali niso primerni za zdravljenje s cisplatinom in katerih tumorji izražajo PD-L1 v ≥ 5 %. Zgodnji stadij nedrobnoceličnega raka pljuč (NDRP): Zdravilo Tecentriq je kot monoterapija indicirano za adjuvantno zdravljenje po popolni resekciji in kemoterapiji na osnovi platine za odrasle bolnike z NDRP in velikim tveganjem za ponovitev, katerih tumorji izražajo PD-L1 na ≥ 50 % tumorskih celic (TC) in nimajo EGFR mutiranega ali ALK pozitivnega NDRP. Napredovali NDRP: Zdravilo Tecentriq je v kombinaciji z bevacizumabom, paklitakselom in karboplatinom indicirano v prvi liniji zdravljenja odraslih bolnikov z razsejanim neploščatoceličnim NDRP. Pri bolnikih z EGFR mutiranim ali ALK pozitivnim NDRP je zdravilo Tecentriq v kombinaciji z bevacizumabom, paklitakselom in karboplatinom indicirano le, ko so izčrpana ustrezna tarčna zdravljenja. Zdravilo Tecentriq je v kombinaciji z nab-paklitakselom in karboplatinom indicirano v prvi liniji zdravljenja odraslih bolnikov z razsejanim neploščatoceličnim NDRP, ki ni EGFR mutiran ali ALK pozitiven. Zdravilo Tecentriq je kot monoterapija indicirano v prvi liniji zdravljenja odraslih bolnikov z razsejanim NDRP, pri katerih je PD-L1 izražen na ≥ 50 % TC ali ≥ 10 % imunskih celic (IC), ki infiltrirajo tumor, ter nimajo EGFR mutiranega ali ALK pozitivnega NDRP. Zdravilo Tecentriq je kot monoterapija indicirano v prvi liniji zdravljenja odraslih bolnikov z napredovalim NDRP, ki niso primerni za zdravljenje s kemoterapijo na osnovi platine. Zdravilo Tecentriq je kot monoterapija indicirano za zdravljenje odraslih bolnikov z lokalno napredovalim ali razsejanim NDRP, ki so bili predhodno zdravljeni s kemoterapijo. Bolniki z EGFR mutiranim ali ALK pozitivnim NDRP morajo pred uvedbo zdravila Tecentriq prejeti tudi tarčna zdravljenja. Drobnocelični rak pljuč (DRP): Zdravilo Tecentriq je v kombinaciji s karboplatinom in etopozidom indicirano v prvi liniji zdravljenja odraslih bolnikov z razsejanim DRP. Trojno negativni rak dojk (TNRD): Zdravilo Tecentriq je v kombinaciji z nab-paklitakselom indicirano za zdravljenje odraslih bolnikov z inoperabilnim lokalno napredovalim ali razsejanim TNRD, katerih tumorji izražajo PD-L1 v ≥ 1 % in predhodno še niso prejemali kemoterapije zaradi razsejane bolezni. Hepatocelularni karcinom (HCC): Zdravilo Tecentriq je v kombinaciji z bevacizumabom indicirano za zdravljenje odraslih bolnikov z napredovalim ali neresektabilnim HCC, ki predhodno še niso prejemali sistemskega zdravljenja. **Odmerjanje in način uporabe:** Zdravilo Tecentriq morajo uvesti in nadzorovati zdravniki z izkušnjami pri zdravljenju raka. Bolniki, ki trenutno prejemajo intravensko obliko atezolizumaba, lahko preidejo na zdravilo Tecentriq v obliki raztopine za injiciranje. Odmerjanje: 840 mg in 1200 mg i.v.: priporočeni odmerek zdravila Tecentriq je 840 mg, danega intravensko na dva tedna, ali 1200 mg, danega intravensko na tri tedne, ali 1680 mg, danega intravensko na štiri tedne. 1875 mg s.c.: priporočeni odmerek je 1875 mg, dan na tri tedne. Kadar zdravilo Tecentriq dajete v kombinaciji, glejte tudi celotne informacije za predpisovanje zdravil, ki se uporabljajo v kombinaciji. *Prilagoditev odmerka med zdravljenjem:* odmerkov zdravila Tecentriq ni priporočljivo zmanjševati. *Zapoznitev odmerka ali prenehanje uporabe* glede na neželeni učinek je opisano v SmPC. Način uporabe: Pomembno je preveriti nalepke zdravila in se tako prepričati, da bo bolnik dobil pravo obliko zdravila (intravensko ali subkutano), kot je predpisano. Intravenska oblika zdravila Tecentriq ni namenjena za subkutano uporabo in se jo sme injicirati le intravensko. Infuzij se ne sme dajati kot hiter intravenski odmerek ali bolus. Začetni odmerek zdravila Tecentriq je treba dati v 60 minutah. Če bolnik prvo infuzijo dobro prenese, je mogoče vse nadaljnje infuzije dati v 30 minutah.Zdravilo Tecentriq 1875 mg raztopina za injiciranje ni namenjeno za intravensko uporabo in se ga sme injicirati le subkutano (v približno 7 minutah v stegno). **Kontraindikacije:** Preobčutljivost na atezolizumab ali katero koli pomožno snov. **Posebna opozorila in previdnostni ukrepi:** Sledljivost: Z namenom izboljšanja sledljivosti bioloških zdravil je treba jasno zabeležiti ime in številko serije uporabljenega zdravila. Imunsko pogojeni neželeni učinki: Večina imunsko pogojenih neželenih učinkov, ki so se pojavili med zdravljenjem, je bila po prekinitvi atezolizumaba in uvedbi kortikosteroidov in/ali podpornega zdravljenja reverzibilna. Imunsko pogojeni neželeni učinki, povezani z atezolizumabom, se lahko pojavijo po zadnjem odmerku atezolizumaba. Pri sumu na imunsko pogojene neželene učinke je treba opraviti temeljito oceno za potrditev etiologije oziroma izključitev drugih vzrokov. Glede na izrazitost neželenega učinka je treba uporabo atezolizumaba odložiti in uvesti kortikosteroide. Atezolizumab je treba trajno prenehati uporabljati pri vseh imunsko pogojenih neželenih učinkih 3. stopnje, ki se ponovijo, in pri vseh imunsko pogojenih neželenih učinkih 4. stopnje, z izjemo endokrinopatij, ki jih je mogoče nadzorovati z nadomestnimi hormoni. Podatki iz opazovalnih študij kažejo, da imajo bolniki z obstoječo avtoimunsko boleznijo po zdravljenju z zaviralci imunskih kontrolnih točk lahko povečano tveganje imunsko pogojenih neželenih učinkov v primerjavi z bolniki brez obstoječe avtoimunske bolezni. Bolnike je treba spremljati glede znakov in simptomov pnevmonitisa ter izključiti druge možne vzroke. Bolnike je treba spremljati glede znakov in simptomov hepatitisa. Vrednosti AST, ALT in bilirubina je treba spremljati pred začetkom zdravljenja z atezolizumabom, redno med zdravljenjem in kot je potrebno glede na klinično oceno. Bolnike je treba spremljati glede znakov in simptomov kolitisa in endokrinopatij, meningitisa ali encefalitisa, motoričnе in senzorične nevropatije. Bolnike je treba nadzorovati glede znakov in simptomov, ki kažejo na mielitis, akutni pankreatitis, miokarditis, miozitis. Imunsko pogojeni nefritis: bolnike je treba nadzorovati glede sprememb v delovanju ledvic. Bolnike je treba spremljati glede sumov na hude kožne neželene učinke in izključiti druge vzroke. V primeru suma na hude kožne neželene učinke je treba bolnike napotiti k specialistu po nadaljnjo diagnozo in zdravljenje. Pri zdravljenju z atezolizumabom so opažali perikardialne motnje. Pri bolnikih, ki so prejemali atezolizumab, so poročali o hemofagocitni limfohistiocitozi. Pri sumu na HLH je treba trajno prenehati zdravljenje z atezolizumabom in bolnike napotiti k specialistu po nadaljnjo diagnozo in zdravljenje. Z infundiranjem povezane reakcije: pri zdravljenju z atezolizumabom so opažali z infundiranjem povezane reakcije. Pri bolnikih, ki imajo z infundiranjem povezane reakcije 1. ali 2. stopnje, je treba hitrost infundiranja/injiciranja zmanjšati ali zdravljenje/injiciranje prekiniti. Pri bolnikih, ki imajo z infundiranjem povezane reakcije 3. ali 4. stopnje, je treba zdravljenje z atezolizumabom trajno ukiniti. Kartica za bolnika: Zdravnik, ki predpiše zdravilo, se mora z bolnikom pogovoriti o tveganjih zdravljenja z zdravilom Tecentriq. Bolniku je treba dati kartico za bolnika in mu naročiti, naj jo ima vedno pri sebi. **Medsebojno delovanje z drugimi zdravili in druge oblike interakcij:** Formalnih farmakokinetičnih študij medsebojnega delovanja z atezolizumabom niso izvedli. Ker se atezolizumab odstrani iz obtoka s katabolizmom, ni pričakovati presnovnih medsebojnih delovanj med zdravili. Uporabi sistemskih kortikosteroidov ali imunosupresivov se je pred uvedbo atezolizumaba treba izogibati, ker lahko vplivajo na farmakodinamično aktivnost in učinkovitost atezolizumaba. Vendar pa se sistemske kortikosteroide ali druge imunosupresive lahko uporabi po začetku zdravljenja z atezolizumabom za zdravljenje imunsko pogojenih neželenih učinkov. **Neželeni učinki:** *Informacije o varnosti atezolizumaba v monoterapiji:* najpogostejši neželeni učinki (> 10 %) so bili utrujenost, zmanjšan apetit, izpuščaj, navzea, kašelj, diareja, zvišana telesna temperatura, dispneja, artralgija, srbenje, astenija, bolečina v hrbtu, bruhanje, okužba sečil in glavobol. *Varnost intravenske oblike atezolizumaba v kombinaciji z drugimi učinkovinami:* najpogostejši neželeni učinki (≥ 20 %) so bili anemija, nevtropenija, navzea, utrujenost, alopecija, izpuščaj, diareja, trombocitopenija, zaprtost, zmanjšan apetit in periferna nevropatija. Varnostni profil zdravila Tecentriq raztopina za injiciranje je bil na splošno podoben znanemu varnostnemu profilu intravenske oblike; dodaten neželeni učinek so bile reakcije na mestu injiciranja. Poročanje o domnevnih neželenih učinkih: Poročanje o domnevnih neželenih učinkih zdravila po izdaji dovoljenja za promet je pomembno. Omogoča namreč stalno spremljanje razmerja med koristmi in tveganji zdravila. Od zdravstvenih delavcev se zahteva, da poročajo o katerem koli domnevnem neželenem učinku zdravila na: Javna agencija Republike Slovenije za zdravila in medicinske pripomočke, Sektor za farmakovigilanco, Nacionalni center za farmakovigilanco, Slovenčeva ulica 22, SI-1000 Ljubljana, Tel: +386 (0)8 2000 500, Faks: +386 (0)8 2000 510, e-pošta: h-farmakovigilanca@jazmp.si, spletna stran: www.jazmp.si. Za zagotavljanje sledljivosti zdravila je pomembno, da pri izpolnjevanju obrazca o domnevnih neželenih učinkih zdravila navedete številko serije biološkega zdravila. **Režim izdaje zdravila:** H. **Imetnik dovoljenja za promet:** Roche Registration GmbH, Emil-Barell-Strasse 1, 79639 Grenzach-Wyhlen, Nemčija. Za podrobnejše informacije glejte celoten Povzetek glavnih značilnosti zdravila. **Verzija: 5.0/24**

Roche

Samo za strokovno javnost.

DODATNE INFORMACIJE SO NA VOLJO PRI: Roche farmacevtska družba d.o.o., Stegne 13G, Ljubljana.

M-SI-00001267(v2.0) | Datum priprave informacije: november 2024.

Širimo obzorja v 3. liniji zdravljenja metastatskega kolorektalnega raka (mCRC)

VEČ KOT 10-MESEČNO CELOKUPNO PREŽIVETJE

Lonsurf® v kombinaciji z bevacizumabom je pokazal edinstvene rezultate pri zdravljenju mCRC v 3. liniji, saj je bila prvič dosežena mediana celokupnega preživetja (mOS) 10,8 meseca, s skoraj polovico živih bolnikov po enem letu in v dobri kondiciji za nadaljnje zdravljenje.[1]

Lonsurf®
trifluridin/tipiracil

Usmerjen v prihodnost

Literatura: 1. Prager GW et al. N Engl J Med 2023;388:1657-67.
Družba Servier ima licenco družbe Taiho za zdravilo Lonsurf®. Pri globalnem razvoju zdravila sodelujeta obe družbi in ga tržita na svojih določenih področjih.

Skrajšan povzetek glavnih značilnosti zdravila: Lonsurf 15 mg/6,14 mg filmsko obložene tablete in Lonsurf 20 mg/8,19 mg filmsko obložene tablete

SESTAVA*: Lonsurf 15 mg/6,14 mg: Ena filmsko obložena tableta vsebuje 15 mg trifluridina in 6,14 mg tipiracila (v obliki klorida). **Lonsurf 20 mg/8,19 mg**: Ena filmsko obložena tableta vsebuje 20 mg trifluridina in 8,19 mg tipiracila (v obliki klorida). **TERAPEVTSKE INDIKACIJE*:** V kombinaciji z bevacizumabom za zdravljenje odraslih bolnikov z metastatskim kolorektalnim rakom (KRR), ki so prejeli dva predhodna režima zdravljenja raka, vključno s kemoterapijo na osnovi fluoropirimidina, oksaliplatina in irinotekana, zdravljenje z zaviralci žilnega endotelijskega rastnega dejavnika (VEGF – Vascular Endothelial Growth Factor) in/ali zaviralci receptorjev za epidermalni rastni dejavnik (EGFR – Epidermal Growth Factor Receptor). V monoterapiji za zdravljenje odraslih bolnikov z metastatskim kolorektalnim rakom, ki so bili predhodno že zdravljeni ali niso primerni za zdravljenja, ki so na voljo. Ta vključujejo kemoterapijo na osnovi fluoropirimidina, oksaliplatina in irinotekana, zdravljenje z zaviralci VEGF in zaviralci EGFR. V monoterapiji za zdravljenje odraslih bolnikov z metastatskim rakom želodca, vključno z adenokarcinomom gastro-ezofagealnega prehoda, ki so bili predhodno že zdravljeni z najmanj dvema sistemskima režimoma zdravljenja za napredovalo bolezen. **ODMERJANJE IN NAČIN UPORABE*:** Priporočeni začetni odmerek zdravila Lonsurf pri odraslih je 35 mg/m^2/odmerek peroralno dvakrat dnevno na 1. do 5. dan in 8. do 12. dan vsakega 28dnevnega cikla zdravljenja, najpozneje 1 uro po zaključku jutranjega in večernega obroka (20 mg/m^2/odmerek dvakrat dnevno pri bolnikih s hudo ledvično okvaro). Odmerek, izračunan glede na telesno površino, ne sme preseči 80 mg/odmerek. Možne prilagoditve odmerka glede na varnost in prenašanje zdravila pri posameznem bolniku: dovoljena so zmanjšanja odmerka na najmanjši odmerek 20 mg/m^2 dvakrat dnevno (oz. 15 mg/m^2/odmerek dvakrat dnevno pri bolnikih s hudo ledvično okvaro). Potem ko je bil odmerek zmanjšan, povečanje ni dovoljeno. Kadar se zdravilo Lonsurf uporablja v kombinaciji z bevacizumabom za zdravljenje metastatskega KRR, je odmerek bevacizumaba 5 mg/kg telesne mase enkrat na 2 tedna. **KONTRAINDIKACIJE*:** Preobčutljivost na učinkovini ali katero koli pomožno snov. **OPOZORILA IN PREVIDNOSTNI UKREPI*:** Supresija kostnega mozga: Pred uvedbo zdravljenja in po potrebi za spremljanje toksičnosti zdravila, najmanj pred vsakim ciklom zdravljenja, je treba pregledati celotno krvno sliko. Zdravljenja ne smete začeti, če je absolutno število nevtrofilcev < 1,5 x 10^9/l, če je število trombocitov < 75 x 10^9/l ali če se je pri bolniku zaradi predhodnih zdravljenj pojavila klinično pomembna nehematološka toksičnost 3. ali 4. stopnje, ki še traja. Bolnike je treba skrbno spremljati zaradi morebitnih okužb, uvesti je treba ustrezne ukrepe, kot je klinično indicirano. Toksičnost za prebavila: Potrebna je uporaba antiemetikov, antidiaroikov ter drugih ukrepov, kot je klinično indicirano. Če je potrebno, prilagodite odmerke. Ledvična okvara: Uporaba zdravila ni priporočljiva pri bolnikih s končno stopnjo ledvične bolezni. Bolnike z ledvično okvaro je potrebno med zdravljenjem skrbno spremljati; bolnike z zmerno ali hudo ledvično okvaro je treba zaradi hematološke toksičnosti bolj pogosto spremljati. Jetrna okvara: Uporaba zdravila Lonsurf pri bolnikih z obstoječo zmerno ali hudo jetrno okvaro ni priporočljiva. Proteinurija: Pred začetkom zdravljenja in med njim je priporočljivo spremljanje proteinurije z urinskimi testnimi lističi. Pomožne snovi: Zdravilo vsebuje laktozo. **INTERAKCIJE*:** Previdnost: Zdravila, ki medsebojno delujejo z nukleozidnimi prenašalci CNT1, ENT1 in ENT2, zaviralci OCT2 ali MATE1, substrati humane timidin-kinaze (npr. zidovudin), hormonski kontraceptivi. **PLODNOST*.** Bolnikom, ki želijo spočeti otroka, je treba svetovati, da se odločijo za svetovanje o reprodukciji ter shranjevanje jajčnih celic oz. sperme z zamrzovanjem pred začetkom zdravljenja z zdravilom Lonsurf. **NOSEČNOST IN DOJENJE*:** Ni priporočljivo. **KONTRACEPCIJA*:** Ženske in moški morajo uporabljati zelo učinkovite metode kontracepcije med zdravljenjem in do 6 mesecev po zaključku zdravljenja. **VPLIV NA SPOSOBNOST VOŽNJE IN UPRAVLJANJA STROJEV*:** Med zdravljenjem se lahko pojavijo utrujenost, omotica ali splošno slabo počutje. **NEŽELENI UČINKI*:** *Zelo pogosti:* nevtropenija, levkopenija, anemija, trombocitopenija, zmanjšan apetit, diareja, navzea, bruhanje, utrujenost, stomatitis. *Pogosti:* okužba spodnjih dihal, okužba, febrilna nevtropenija, limfopenija, hipoalbuminemija, disgevzija, omotica, glavobol, hipertenzija, dispneja, bolečina v trebuhu, zaprtje, razjede v ustih, bolezni ustne votline, hiperbilirubinemija, izpuščaj, artralgija, mialgija, alopecija, pruritus, suha koža, proteinurija, pireksija, edem, vnetje sluznice, splošno slabo počutje, zvišanje jetrnih encimov, zvišanje alkalne fosfataze v krvi, zmanjšanje telesne mase. *Občasni:* okužba žolčevoda, gripa, okužba sečil, gingivitis, herpes zoster, okužba s kandido, bakterijska okužba, nevtropenična sepsa, okužba zgornjih dihal, konjunktivitis, bolečina zaradi raka, pancitopenija, monocitopenija, eritropenija, levkocitoza, monocitoza, dehidracija, hiperglikemija, hiperkaliemija, hipokaliemija, hipofosfatemija, hiponatriemija, hipokalciemija, anksioznost, nespečnost, periferna nevropatija, nevrotoksičnost, parestezija, letargija, vrtoglavica, angina pektoris, aritmija, palpitacije, hipotenzija, vročinski oblivi, pljučna embolija, disfonija, epistaksa, izcedek iz nosu, kašelj, krvavitev v prebavilih, ileus, kolitis, gastritis, moteno praznjenje želodca, abdominalna distenzija, analno vnetje, dispepsija, gastroezofagealna refluksna bolezen, glositis, bolezen zob, siljenje na bruhanje, flatulenca, hepatotoksičnost, sindrom palmarne-plantarne eritrodisestezije, urtikarija, akne, hiperhidroza, bolezni nohtov, bolečina v kosteh, mišična oslabelost, mišični krči, bolečina v okončinah, ledvična odpoved, motnje mikcije, hematurija, motnje menstruacije, poslabšanje splošnega zdravstvenega stanja, bolečina, občutek spremembe telesne temperature, neugodje v okončinah, zvišanje kreatinina v krvi, povečanje mednarodnega umerjenega razmerja (INR), zvišanje sečnine v krvi, zvišanje laktatne dehidrogenaze v krvi, zvišanje C-reaktivnega proteina, zmanjšan hematokrit. *Redki:* infekcijski enteritis, tinea pedis, septični šok, granulocitopenija, putika, hipernatriemija, pekoč občutek, disestezija, hiperestezija, hipoestezija, sinkopa, katarakta, suho oko, zamegljen vid, diplopija, zmanjšana ostrina vida, neugodje v ušesu, embolija, orofaringealna bolečina, plevralni izliv, ascites, akutni pankreatitis, subileus, slab zadah, bukalni polip, hemoragični enterokolitis, krvavitev dlesni, ezofagitis, parodontalna bolezen, proktalgija, refluksni gastritis, razširitev žolčnih vodov, mehur, eritem, preobčutljivostne reakcije na svetlobo, luščenje kože, otekanje sklepov, neinfektivni cistitis, levkociturija, kseroza, podaljšanje aktiviranega parcialnega tromboplastinskega časa, podaljšanje intervala QT na elektrokardiogramu, znižanje celokupnih proteinov. *Post-marketinške izkušnje:* intersticijska bolezen pljuč. **PREVELIKO ODMERJANJE*:** Neželeni učinki, o katerih so poročali v povezavi s prevelikim odmerjanjem, so bili v skladu z uveljavljenim varnostnim profilom. Glavni pričakovani zaplet prevelikega odmerjanja je supresija kostnega mozga. **FARMAKODINAMIČNE LASTNOSTI*:** *Farmakoterapevtska skupina:* zdravila z delovanjem na novotvorbe, antimetaboliti, oznaka ATC: L01BC59. Zdravilo Lonsurf sestavljata antineoplastični timidinski nukleozidni analog, trifluridin, in zaviralec timidin-fosforilaze (TPaze), tipiracilijev klorid. Po privzemu v rakave celice timidin-kinaza fosforilira trifluridin. Ta se v celicah nato presnovi v substrat deoksiribonukleinske kisline (DNA), ki se vgradi neposredno v DNA ter tako preprečuje celično proliferacijo. TPaza hitro razgradi trifluridin in njegova presnova po peroralni uporabi je hitra zaradi učinka prvega prehoda, zato je v zdravilo vključen zaviralec TPaze, tipiracilijev klorid. **PAKIRANJE*:** 20 filmsko obloženih tablet. **NAČIN PREDPISOVANJA IN IZDAJE ZDRAVILA:** Rp/Spec - Predpisovanje in izdaja zdravila je le na recept zdravnika specialista ustreznega področja medicine ali od njega pooblaščenega zdravnika. **Imetnik dovoljenja za promet:** Les Laboratoires Servier, 50, rue Carnot, 92284 Suresnes cedex, Francija. Številka dovoljenja za promet z zdravilom: EU/1/16/1096/001 (Lonsurf 15 mg/6,14 mg), EU/1/16/1096/004 (Lonsurf 20 mg/8,19 mg). **Datum zadnje revizije besedila: julij 2023. *Pred predpisovanjem preberite celoten povzetek glavnih značilnosti zdravila. Celoten povzetek glavnih značilnosti zdravila in podrobnejše informacije so na voljo pri: Servier Pharma d.o.o., Podmilščakova ulica 24, 1000 Ljubljana, www.servier.si.**

LON AD1 C1 2023-24. Samo za strokovno javnost. Datum priprave informacije: avgust 2023.

SERVIER
moved by you

Instructions for authors

The editorial policy

Radiology and Oncology is a multidisciplinary journal devoted to the publishing original and high-quality scientific papers and review articles, pertinent to oncologic imaging, interventional radiology, nuclear medicine, radiotherapy, clinical and experimental oncology, radiobiology, medical physics, and radiation protection. Papers on more general aspects of interest to the radiologists and oncologists are also published (no case reports).

The Editorial Board requires that the paper has not been published or submitted for publication elsewhere; the authors are responsible for all statements in their papers. Accepted cannot be published elsewhere without the written permission of the editors.

Submission of the manuscript

The manuscript written in English should be submitted to the journal via online submission system Editorial Manager available for this journal at: www.radioloncol.com.

In case of problems, please contact Sašo Trupej at saso.trupej@computing.si or the Editor of this journal at gsersa@onko-i.si

All articles are subjected to the editorial review and when the articles are appropriated they are reviewed by independent referees. In the cover letter, which must accompany the article, the authors are requested to suggest 3-4 researchers, competent to review their manuscript. However, please note that this will be treated only as a suggestion; the final selection of reviewers is exclusively the Editor's decision. The authors' names are revealed to the referees, but not vice versa.

Manuscripts which do not comply with the technical requirements stated herein will be returned to the authors for the correction before peer-review. The editorial board reserves the right to ask authors to make appropriate changes of the contents as well as grammatical and stylistic corrections when necessary. Page charges will be charged for manuscripts exceeding the recommended length, as well as additional editorial work and requests for printed reprints.

Articles are published printed and on-line as the open access:

(https://content.sciendo.com/raon).

All articles are subject to 1500 EUR + VAT publication fee. Exceptionally, waiver of payment may be negotiated with editorial office, at the time of article submission.

Manuscripts submitted under multiple authorship are reviewed on the assumption that all listed authors concur in the submission and are responsible for its content; they must have agreed to its publication and have given the corresponding author the authority to act on their behalf in all matters pertaining to publication. The corresponding author is responsible for informing the co-authors of the manuscript status throughout the submission, review, and production process.

Preparation of manuscripts

Radiology and Oncology will consider manuscripts prepared according to the Uniform Requirements for Manuscripts Submitted to Biomedical Journals by International Committee of Medical Journal Editors (www.icmje.org). The manuscript should be written in grammatically and stylistically correct language. Abbreviations should be avoided. If their use is necessary, they should be explained at the first time mentioned. The technical data should conform to the SI system. The manuscript, excluding the references, tables, figures and figure legends, must not exceed 5000 words, and the number of figures and tables is limited to 8. Organize the text so that it includes: Introduction, Materials and methods, Results and Discussion. Exceptionally, the results and discussion can be combined in a single section. Start each section on a new page, and number each page consecutively with Arabic numerals. For ease of review, manuscripts should be submitted as a single column, double-spaced text. The template for preparation of the manuscript is available in the editorial manager.

The Title page should include a concise and informative title, followed by the full name(s) of the author(s); the institutional affiliation of each author; the name and address of the corresponding author (including telephone, fax and E-mail), and an abbreviated title (not exceeding 60 characters). This should be followed by the abstract page, summarizing in less than 250 words the reasons for the study, experimental approach, the major findings (with specific data if possible), and the principal conclusions, and providing 3-6 key words for indexing purposes. Structured abstracts are required. Slovene authors are requested to provide title and the abstract in Slovene language in a separate file. The text of the research article should then proceed as follows:

Introduction should summarize the rationale for the study or observation, citing only the essential references and stating the aim of the study.

Materials and methods should provide enough information to enable experiments to be repeated. New methods should be described in details.

Results should be presented clearly and concisely without repeating the data in the figures and tables. Emphasis should be on clear and precise presentation of results and their significance in relation to the aim of the investigation.

Discussion should explain the results rather than simply repeating them and interpret their significance and draw conclusions. It should discuss the results of the study in the light of previously published work.

Charts, Illustrations, Images and Tables

Charts, Illustrations, Images and Tables must be numbered and referred to in the text, with the appropriate location indicated. Charts, Illustrations and Images, provided electronically, should be of appropriate quality for good reproduction. Illustrations and charts must be vector image, created in CMYK color space, preferred font "Century Gothic", and saved as .AI, .EPS or .PDF format. Color charts, illustrations and Images are encouraged, and are published without additional charge. Image size must be 2.000 pixels on the longer side and saved as .JPG (maximum quality) format. In Images, mask the identities of the patients. Tables should be typed double-spaced, with a descriptive title and, if appropriate, units of numerical measurements included in the column heading. The files with the figures and tables can be uploaded as separate files.

References

References must be numbered in the order in which they appear in the text and their corresponding numbers quoted in the text. Authors are responsible for the accuracy of their references. References to the Abstracts and Letters to the Editor must be identified as such. Citation of papers in preparation or submitted for publication, unpublished observations, and personal communications should not be included in the reference list. If essential, such material may be incorporated in the appropriate place in the text. References follow the style of Index Medicus, DOI number (if exists) should be included.

All authors should be listed when their number does not exceed six; when there are seven or more authors, the first six listed are followed by "et al.". The following are some examples of references from articles, books and book chapters:

Dent RAG, Cole P. In vitro maturation of monocytes in squamous carcinoma of the lung. *Br J Cancer* 1981; **43:** 486-95. doi: 10.1038/bjc.1981.71

Chapman S, Nakielny R. *A guide to radiological procedures*. London: Bailliere Tindall; 1986.

Evans R, Alexander P. Mechanisms of extracellular killing of nucleated mammalian cells by macrophages. In: Nelson DS, editor. *Immunobiology of macrophage.* New York: Academic Press; 1976. p. 45-74.

Authorization for the use of human subjects or experimental animals

When reporting experiments on human subjects, authors should state whether the procedures followed the Helsinki Declaration. Patients have the right to privacy; therefore, the identifying information (patient's names, hospital unit numbers) should not be published unless it is essential. In such cases the patient's informed consent for publication is needed, and should appear as an appropriate statement in the article. Institutional approval and Clinical Trial registration number is required. Retrospective clinical studies must be approved by the accredited Institutional Review Board/Committee for Medical Ethics or other equivalent body. These statements should appear in the Materials and methods section.

The research using animal subjects should be conducted according to the EU Directive 2010/63/EU and following the Guidelines for the welfare and use of animals in cancer research (Br J Cancer 2010; 102: 1555 – 77). Authors must state the committee approving the experiments, and must confirm that all experiments were performed in accordance with relevant regulations.

These statements should appear in the Materials and methods section (or for contributions without this section, within the main text or in the captions of relevant figures or tables).

Transfer of copyright agreement

For the publication of accepted articles, authors are required to send the License to Publish to the publisher on the address of the editorial office. A properly completed License to Publish, signed by the Corresponding Author on behalf of all the authors, must be provided for each submitted manuscript.

Conflict of interest

When the manuscript is submitted for publication, the authors are expected to disclose any relationship that might pose real, apparent or potential conflict of interest with respect to the results reported in that manuscript. Potential conflicts of interest include not only financial relationships but also other, non-financial relationships. In the Acknowledgement section the source of funding support should be mentioned. The Editors will make effort to ensure that conflicts of interest will not compromise the evaluation process of the submitted manuscripts; potential editors and reviewers will exempt themselves from review process when such conflict of interest exists. The statement of disclosure must be in the Cover letter accompanying the manuscript or submitted on the form available on www.icmje.org/coi_disclosure.pdf

The use and explanation of AI and AI-assisted technologies in scientific writing

When authors use artificial intelligence (AI) and AI-assisted technologies in the writing process, they should consider that:

- These technologies should only be used to improve readability and language and to assist in the investigation of data. They should not replace researchers' primary tasks of explaining, the interpretation of data and drawing valid scientific conclusions.
- Apply the technology under human supervision and control, and carefully review and edit the result, because AI can produce authoritative-sounding results that may be incorrect, incomplete, or biased.
- Do not list AI or AI-assisted technologies as authors or co-authors, and do not cite AI as an author. Authorship carries with it responsibilities and tasks that only humans can perform.
- Disclose in your manuscript the use of AI and AI-enabled technologies in the writing process by following the instructions below. An appropriate statement should appear in the published paper. Please note that authors are ultimately responsible and accountable for the content of the paper.

Disclosure notes

Authors must disclose the use of AI and AI-assisted technologies in the writing process by adding a statement at the end of their manuscript in the main manuscript file before the bibliography, at the time of manuscript submission. The statement should be included in a new section titled 'Statement on the Use of AI and AI-Assisted Technologies in the Writing Process'.

Statement: during the preparation of this paper, the author(s) used [NAME TOOL / SERVICE] to create [REASON]. After using this tool/service, the author(s) have reviewed and edited the content as required and take full responsibility for the content of the publication.

This statement does not apply to the use of basic tools to check grammar, spelling, references, etc. If there is nothing to disclose, it is not necessary to add a statement.

Page proofs

Page proofs will be sent by E-mail to the corresponding author. It is their responsibility to check the proofs carefully and return a list of essential corrections to the editorial office within three days of receipt. Only grammatical corrections are acceptable at that time.

Open access

Papers are published electronically as open access on https://content.sciendo.com/raon, also papers accepted for publication as E-ahead of print.

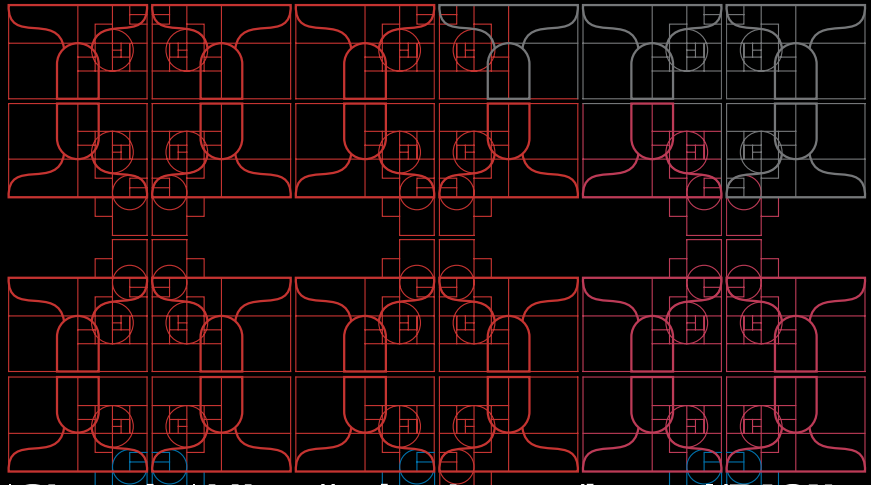

Radiology and Oncology | Ljubljana | Slovenia | https://sciendo.com/journal/RAON

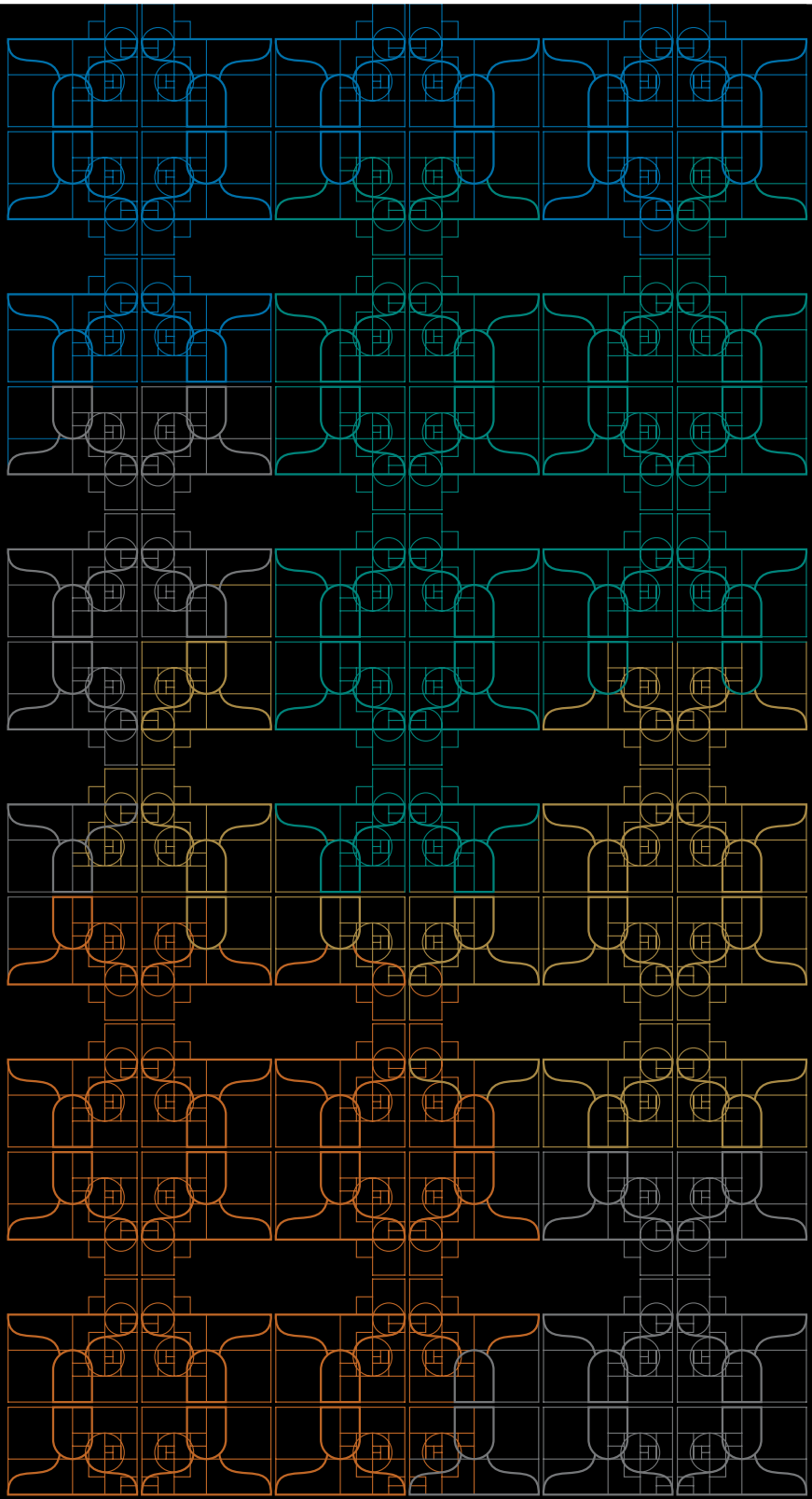

ISSN 1318 - 2099